Winter 1992

Measurement of deforestation in the Brazilian Amazon using satellite remote sensing

David Lewis Skole
University of New Hampshire, Durham

Order Number 9307358

Measurement of deforestation in the Brazilian Amazon using satellite remote sensing

Skole, David Lewis, Ph.D.

University of New Hampshire, 1992

U·M·I
300 N. Zeeb Rd.
Ann Arbor, MI 48106

MEASUREMENT OF DEFORESTATION IN THE BRAZILIAN AMAZON USING SATELLITE REMOTE SENSING

BY

DAVID LEWIS SKOLE
A.B., Biological Sciences, Indiana University, 1978
M.S., Environmental Science, Indiana University, 1980

DISSERTATION

Submitted to the University of New Hampshire
in Partial Fulfillment of
the Requirements for the Degree of

Doctor of Philosophy

in

Natural Resources

December, 1992

This dissertation has been examined and approved.

Dissertation director, Dr. John D. Aber,
Professor of Natural Resources

Dr. Berrien Moore III
Director, Institute for the Study of Earth, Oceans and Space

Dr. Robert C. Harriss
Professor of Earth Sciences

Dr. Jerry M. Melillo
Senior Scientist and Co-Director, the Ecosystems Center,
Marine Biological Laboratory

Dr. Richard W. England
Associate Professor of Economics

16 November 1992

Date

ACKNOWLEDGEMENTS

I acknowledge with pleasure the help, support, and guidance of my committee. I extend special appreciation to Berrien for his long-term support and mentorship since the O'Kane house days. I also wish to recognize the help of dozens of work study students, and particular thanks to Walter Chomentowski. Over the years I have had much support from friends and colleagues as I did this work. I can think of no one who deserves more thanks and gratitude than my friend and colleague Richard Houghton. Finally, thanks Janet, Jordan, and Benjamin, for without your support and understanding I would not have made it.

Financial support came from NASA grants NAGW 2294 and NAGW 2749.

PREFACE

The dissertation consists of seven chapters, each one written in the style of a published paper. Each chapter is meant to stand alone as a single paper. Hence, the reader will find some overlap in figures, tables, references, and text. Some of the chapters have already been submitted to journals. Taken together the chapters of this dissertation provide a train of logic in the development of a study of deforestation in one of the most important tropical forest regions of the world. Below, I briefly summarize the contents of this dissertation.

Chapter 1. ***Data on global land cover change: acquisition, assessment, and analysis.*** This first chapter is a general review of the issues. The manuscript lays out the basis for much of the remaining chapters. It includes some material presented in later chapters. It is now in press in Meyer, W.B. and B.L. Turner (eds.), *Global Land Use/Land Cover Change*, Office of Interdisciplinary Earth Studies, Boulder.

Chapter 2. ***Spatial analysis of land cover change and carbon flux associated with biomass burning in Brazil, 1970-1980.*** This manuscript develops a geographically referenced analysis of land cover change and carbon flux using tabular data (i.e., non-remote sensing data). It moves beyond spatially aggregate analyses used in the past.

It is in press in: Zepp, R. (ed.), *Climate-Biosphere Interactions: Biogenic Emissions and Environmental Effects of Climate Change*, Wiley Interscience, John Wiley and Sons, New York.

Chapter 3. ***Mapping deforestation in the Brazilian Amazon using a geographic information system.*** This manuscript extends the analysis of Chapter 2, but here remote sensing-derived data is used in place of the tabular data. The remote sensing approach is first explored using maps made available from a remote sensing study done in Brazil during the late 1970s, so that the time period is the same as Chapter 2.

Chapter 4. ***A comparison of methods for remote sensing of tropical deforestation.*** This chapter presents results of a detailed examination of remote sensing techniques for measurement of deforestation. It extends the work of Chapter 3 by looking very hard at the specific method one would use, focusing on a detailed study in a test site in the Amazon.

Chapter 5. ***Dynamics of deforestation and secondary succession in tropical forests.*** This manuscript measures the amount of secondary growth, an important and yet unmeasured type of land cover transition in the tropics. It is based on multi-temporal analysis of satellite data for the same test site as described in Chapter 4.

<u>Chapter 6</u>. ***Area deforested and rate of deforestation in the Brazilian Amazon, 1978-1988.*** Here the techniques developed in previous chapters are applied to the entire Brazilian Amazon, an area of $\sim 5 \times 10^6$ km^2, encompassing ~250 Landsat scenes.

<u>Chapter 7</u>. ***What is driving deforestation in the Brazilian Amazon?***. This chapter concludes the dissertation with an analysis of the underlying factors (as I hypothesize them) which cause deforestation in the Amazon. It was my attempt to explore some aspects of the "human dimensions" of global change, and begin to ask some fundamental questions about what I was measuring from space, and why it was happening.

TABLE OF CONTENTS

LIST OF TABLES

LIST OF FIGURES

FIGURE PAGE

ABSTRACT

MEASUREMENT OF DEFORESTATION IN THE BRAZILIAN AMAZON USING SATELLITE REMOTE SENSING

by

David Lewis Skole
University of New Hampshire, December 1992

A clear understanding of the role of the biota in the global carbon cycle is limited by an absence of accurate measurements of deforestation rates in the tropics. This study measures the rate and extent of deforestation in the Brazilian Amazon, a tropical forest biome approximately 5 x 10^6 km^2 in size and the largest extant tropical forest biome in the world. The study focuses on remote sensing measurements of deforestation rates and the area of secondary vegetation, but also utilizes tabular data to document deforestation when satellite data are not available. The analysis concludes: (1) Regression analysis of SPOT, TM, and AVHRR measurements suggests that the AVHRR will greatly overestimate deforestation and be highly variable; the use of a brightness temperature threshold is highly sensitive and unreliable. The upward bias of AVHRR is a function of the density of deforestation. (2) An accurate measurement of deforestation requires Landsat TM data, and can be accomplished using low cost visual interpretation of photographic products at 1:250,000 scale, with accuracies within 10% of that obtained using digital image processing techniques employing

supervised statistical classifiers. (3) Secondary growth in the Brazilian Amazon represents a large fraction of the total deforested area, and the abandonment of agricultural land is an important land cover transition. Abandonment rates were 70-83% of clearing rates from primary forests. At any one point in time, approximately 30% of the deforested area is in some stage of abandonment, and quite likely nearly all deforested land becomes abandoned after approximately 5 years. (4) Previous estimates of the total area deforested in the Amazon, as well as the rate of deforestation, have been too high by as much as 4-fold. A complete assessment of the entire Legal Amazon using over 200 Landsat images measures 251×10^3 km^2 deforestation as of 1988, or approximately 6% of the closed forests of the region. The average annual rate of deforestation between 1978 and 1988 was 18×10^3 km^2 yr^{-1}. These findings are important to carbon cycle research. They suggest the estimates of carbon emissions from the Amazon for the late 1980s have been too high, since the area of regrowth is large and rates of deforestation are lower than previously believed.

CHAPTER 1

DATA ON GLOBAL LAND COVER CHANGE: ACQUISITION, ASSESSMENT, AND ANALYSIS

Introduction

The global distribution of vegetative land cover presumably reflects large-scale variations in the distribution of temperature, precipitation, and various edaphic factors. This array of environmental factors results in a heterogeneous, but somewhat predictable, description of a potential global biogeography (cf. Holdridge 1947). However, climatic factors alone do not account for the varied and changing set of land cover types seen today. Absent from this view is consideration of phenology or any number of other functional attributes, including nutrient limitations or nutrient cycling rates. More importantly, humans have continually modified the landscape. Thus, the contemporary state of the world's land cover must be viewed as a constantly shifting mosaic of land cover types determined by both the physical environment and human transformations.

Human activities have transformed the natural landscape over the past 200 years in a variety of ways and to varying degrees. Often, human transformation of land cover is obvious, as when tropical forests are cut, burned and converted to pastures. But there are also more subtle forms. The forest decline phenomenon which exists in many industrialized, temperate zone countries is thought to be due to chronic deposition of atmospheric pollutants or excess nutrients (Aber et al. 1989). Whether directly or indirectly, it is clear that humans now play a major role in determining the state of land cover on a global scale.

Land cover conversion is an important historical and contemporary component of global change. Recent research suggests that the historical conversion of natural systems to agriculture and other human uses of the land has resulted in a net release of carbon dioxide to the atmosphere over the last 150 years roughly equivalent to the release from fossil fuel burning (Houghton et al. 1985b, Houghton et al. 1987, Houghton & Skole 1990). The conversion of forests and savannas is frequently accompanied by biomass burning, an important factor in atmospheric chemistry and the release of other radiatively important trace gases (Crutzen and Andreae 1990). Land cover conversion may also have an important influence on regional climatology and hydrology (Shukla et al. 1990). A clear understanding of the significance of these large-scale impacts to global change is now limited by the absence of well documented and quantitative datasets on both land cover and its conversion.

One limitation has been the paucity of spatial datasets or maps. Mueller-Dombois (1984) suggests three reasons for mapping land cover: (1) for outlining land cover patterns and developing inventories, (2) for extrapolating parallel field observations and measurements to an appropriate level of geographic and ecological generalization, and

(3) for attempting to develop predictive explanations of land cover distributions in terms of past, present, and future climate. These three objectives generally apply for all disciplines and at all scales. Specific requirements for global change research are now being identified. For instance, the spatial arrangement of land transformation is an important factor in estimating its influence on biogeochemistry and climate. One component of the current uncertainty in modeling the net flux of carbon between terrestrial ecosystems and the atmosphere is lack of information on the type of ecosystems which have been cleared for agriculture. Terrestrial ecosystems vary considerably in biomass, soil organic matter, moisture regimes, rates of recovery, and other characteristics. The conversion of high-biomass humid forest would produce significantly greater total net carbon flux than the conversion of tropical dry savanna. Biomass burning would also likely result in greater releases of reduced trace gases such as CO and CH_4 at the expense of CO_2.

Attempts to develop global budgets of important trace gases, such as nitrous oxide, have also suffered from the lack of spatial data. Regional extrapolation of trace gas fluxes has been based on representative, or average, in-situ measurements. Matson et al. (1989) have argued that global budgets could be improved by deriving functional relationships between fluxes and gradients in soils, climate and disturbance within land cover types.

The spatial arrangement of land cover conversion, particularly deforestation, will also influence results of model simulations of continental scale climate and energy balance. Deforestation distributed as a few large blocks may have greater influence on sensible and latent heat flux than the same area distributed as many small, widely scattered patches (Henderson-Sellers 1987, Henderson-Sellers and Gornitz 1984).

Finally, there is increasing concern that land cover conversion in humid tropical forests will result in the loss of a significant number of species (Ehrlich and Wilson 1991). The impact on biodiversity is related to the total area of forest conversion and the amount of forest fragmentation. Quantifying fragmentation requires an understanding of the spatial arrangement of cleared areas (Soule 1991, Wilson and Peter 1988).

These few examples demonstrate the importance of knowing more than just areas of land cover types or the magnitude of land cover conversion; we must know where it occurs and its spatial characteristics. Yet, at this time there is virtually nothing known about the coincident distribution of land cover, land cover attributes, and land cover conversion. We know even less about the geometry and spatial organization of land cover conversion. New initiatives must involve strategies which focus on spatial and temporal characteristics of both natural land cover and conversion activities.

In this paper we review current approaches to acquiring land cover and land cover conversion data sets. The review is not exhaustive. We focus on approaches to acquiring data on land cover conversion at continental to global scales. While we am ultimately concerned with land cover conversion, land use change, and various facets of land transformation, it must be noted that land cover itself--particularly natural land cover--is an important component of the issue.

Some Generalizations about Land Cover and its Transformation

Vegetation, Land Cover, and Land Use

In any discussion of land cover, a milieu of terms and concepts usually surfaces. In this section we wish to present the conceptual framework within which we will work for the remainder of this paper. There are four similar and overlapping components to this framework: (1) vegetation, (2) land cover, (3) land cover conversion and transformation, and (4) land use. Each of these is somewhat nebulous conceptually, and indeed there is a plethora of concepts which have been built into each by different disciplines. My goal is not to supplant concepts developed by biogeographers, ecologists, or social scientists. Instead, we wish to lay a useful framework for the global change research community.

Land surface classification has typically focused on mapping vegetation, with an emphasis on natural and potential vegetation. While it is common to think of vegetation interchangeably with land cover, it actually is only one sub-category of land cover. Not all the landscape is covered by natural vegetation. Where natural vegetation exists, it is not always the climatic potential vegetation. For instance, large areas of natural savanna exist in the center of the Amazon basin surrounded by extensive closed canopy rainforest. Their existence is due largely to edaphic factors, principally soil conditions (Marden dos Santos 1987). The concept of land cover is broader than vegetation, and is used to encompass: a) the actual distribution of natural vegetation, b) water, desert, ice, and other natural features which do not have a predominant vegetative cover, and c) vegetative and non-vegetative landscapes created by human activities, such as agricultural and urban land.

Land cover conversion is used to define changes from one cover type to another. For instance, the conversion of forests to pasture is an important land cover conversion in the tropics. This should be distinguished from land cover transformation, which is a significant modification within a cover type. The transformation of a closed canopy forest to a palm forest or woodlands, as a result of long-term degradation by humans, is a form of transformation. The transformation of forests due to climate change or through air pollution are other examples. Transformation involves alterations of structure or function without a wholesale change from one type to another. Such transformations could involve changes in biomass, productivity, or phenology. Indeed, long-term and chronic transformation would eventually result in complete conversion.

Land cover conversion operates through specific processes over time. For instance, deforestation is a process which converts forest to pasture. Site abandonment, where pasture regrows to a secondary forest, is also a process which converts pasture to forest. Thus, processes such as deforestation and desertification mediate the conversion or transformation of land cover from one type to another. These processes can be envisioned as forcing functions, which have both magnitude (rate of deforestation) and direction (forest usually becomes pasture).

Land use itself characterizes the human use of a land cover type. Forests, for instance could be used by foresters (selective logging), rubber tapers, or not at all. Grasslands can be used as grazing land. Land use change is frequently concomitant with land cover conversion. For instance, the conversion of forest to pasture occurs in an effort to convert the land use from rubber tapping to cattle ranching. One generalization which can be made is that land use change drives land cover conversion; land use change is the means by which human activity reappropriate the products of net primary productivity as determined by a complex set of socioeconomic factors. Land use often involves questions of scale, intensity, and tenure. These properties are not necessarily inherent in the land cover properties. Small scale, subsistence agriculture is not synonymous with large-scale commercial enterprises, even if the land cover type is the same.

Classification of Vegetation and Land Cover

Mapping the distribution of vegetation has a long tradition, dating to the beginning of this century. Clements (1916) proposed early classifications based on concepts of successional climax communities. Koppen (1936), Holdridge (1947), and Thornthwaite (1948) established classifications based on climatic factors. Kuchler (1949) developed a physiognomic system of classification. Later attempts to develop classification systems have essentially followed the conventions of these and other analysts. Generally speaking, the aim of vegetation mapping has been to delineate vegetation distribution using a system of classification based on observed structural or environmental factors. The focus has been on vegetation in its natural condition or potential vegetation. A typology of vegetation classification approaches is shown in Table 1.1 (after Mueller-Dombois 1984). This table presents the canonical approach, which has been to describe or map vegetation based on any one of three general criteria: (1) properties of the vegetation itself, which includes both physiognomic and floristic characteristics of natural vegetation, (2) properties of the environment which influence the type and distribution of potential natural vegetation, (3) properties which combine vegetation and environment.

Physiognomic classifications use vegatation structure and morphology. This approach might also include characteristics of periodicity, such as phenological development of vegetation between dry and wet seasons. In contrast, floristic systems use species composition as the basis for classification and delineation (Whittaker 1978). Either physiognomic or floristic classifications might be amenable to large scale delineation of vegetation, but physiognomic systems tend to be broader in scope and more suitable to remote sensing, particularly when the remote sensing data captures some characteristics of phenology. Environmentally determined classifications, such as those by Holdridge (1967) and others, predict the distribution of vegetation types in the broadest sense, often without consideration of species, over a range of climatic regimes. They are robust in the sense that they are useful for characterizing past and future potential vegetation at the climatic equilibrium. They are limited in that they do not capture edaphic factors which may determine actual vegetation.

Recently, systems which combine environmental and physiognomic approaches have been widely used recently. One approach has been to independently array vegetation by empirical relations between physiognomic or floristic characteristics and features of the physical environment. One way to make such a determination would be through map overlays (e.g., the UNESCO (1973) classification). A recent derivation of this approach is what Mueller-Dombois calls the ecological landscape map, which takes advantage of principles of ecology, incorporating climatic and edaphic gradients. This view is comprehensive and tends to be oriented to land cover rather than simply vegetation. An additional factor well known to ecologists is that of successional state. The incorporation of successional state carries with it two assumptions: a) the potential or natural vegetation of a region is determined and predicted in part by an understanding of what constitutes climax vegetation and the controls on the climax condition, b) pre-climax conditions can be determined at any point in time based on an understanding of the process of primary and secondary succession. To some extent an understanding of secondary succession implies consideration of disturbance and vegetation response to disturbance.

Few systems consider characteristics of vegetation which are not related to morphology, climate, or edaphic factors. A functional classification would integrate vegetation and environmental factors, taking into consideration variation along gradients and the dynamics of succession. However, instead of focusing on vegetation itself a functional classification would be based on ecosystem processes rather than physiognomy or floristics. Field and Mooney (1986) demonstrated a strong relationship between net photosynthesis and leaf nitrogen concentration across a range of plant genera. Similarly, Vitousek (1982) has demonstrated a functional relationship between nitrogen in litterfall and leaf nutrient content across a range of forest types around the world. Melillo et al. (1982) have shown a strong relationship between the lignin to nitrogen ratio in litter and first-year decomposition rate and nutrient cycling. In the first year climate plays has an important influence on the rate (Meentemyer 1978), but long term rates may be more simple functions of lignin (Aber et al. in press). These studies suggest functional differences between groups, and raises possibilities for delineating vegetation into groups which elucidate processes.

Historical Approaches Using Tabular Data

Recent historiographic analyses have demonstrated new techniques for documenting original land cover and its long term change. Most of these studies have been qualitative or limited in geographic scope; some have only focused on certain sub-categories of land cover, such as forests. These kinds of case-study analyses are important for elucidating the fundamental causes of land transformation. But as foundations for large scale datasets they are somewhat limited.

Flint and Richards (1991) have demonstrated a data-intensive approach in South and Southeast Asia. It relies on the availability of historical documents such as revenue records, gazetteers, land assessments, or forestry reports. In some cases direct evidence of the type of land cover present or predominant in a region can be found in these documents, particularly in former colonies of the British Empire. In these cases it is possible to obtain a direct assessment of land cover. However, in most cases, records of land use or agricultural area are more readily available than records of vegetation and land cover directly. Thus, estimates of land cover are indirectly derived from data on changes in agricultural area. A baseline delineation of natural land cover is established and these areas are reduced in proportion to the increase in agricultural area.

Changes in the area of cultivated land can be used to approximate land cover conversion rates since the most important form of land cover conversion has historically been agricultural expansion (Richards 1984, Tucker and Richards 1983). This assumption is generally accurate, but it must be noted that in some instances the omission of logging and other non-agricultural causes of land cover conversion could be significant. Certain areas in the tropics, such as Ivory Coast, Nigeria, Malaysia, and Thailand have experienced large-scale losses of forest in this way (Myers 1980, Lanly 1982, WRI 1990). Thus, this approach is necessarily limited in the absence of direct observations of land cover.

This approach to historical reconstruction of land cover conversion presents a number of difficulties. A review can be found in Houghton (1986). Two important problems are:

(1) sparse sampling in space and time can result in a variety of possible time series in a single dataset. Figure 1.1 shows an example of this. This example uses three data points of cultivated land which were used by Richards et al. (1983) to estimate historical changes in carbon stocks on land as a result of agricultural expansion. As shown, there are at least three different time-series which could be derived. These in turn would result in different histories of carbon flux when the data were coupled to a numerical model (Houghton 1986). To reduce this type of data aliasing, sampling at a finer temporal resolution would be required.

(2) data from the same source may vary considerably from year to year due to changes in methodology or terminology. Figure 1.2 presents an example. Time-series derived from later editions of the FAO Production Yearbooks, an important source of this kind

of data for recent history, are different from the same time-series derived from earlier editions.

It must also be noted that historical reconstruction does not actually document land cover transformations, such as closed forest to palm forest or woodland, due to human intervention. Instead they provide estimates of land cover replacement by agriculture, or land cover conversion. Moreover, land cover conversion estimates obtained this way are based on net changes in the amount of agricultural land. Being based on net change only, it is not possible to know how much abandonment there is at any point in time. This could be important for analyses of net fluxes of carbon since a large amount of abandonment would result in lower net releases to the atmosphere.

Historical reconstructions use tabular data only (e.g., the FAO/UNEP Forest Assessment which provides tabular data at the country level on forest area). There is no inherent spatial organization to the data. One way to develop digital maps of historical land cover conversion is to use geographic information systems (GIS). The GIS approach permits accurate spatial representation of data on agricultural area, which can then be merged with digital maps of land cover to estimate conversion rates by land cover type. The GIS also makes it possible to integrate a wide variety of other data, such as roads and other human-use features, hydrology, soils, and the like. Moreover the GIS approach makes it possible to link historical data to remote sensing data.

We have been developing a technique to study land cover conversion in Brazil utilizing geographic information systems in conjunction with reconstructions based on tabular data. Data are first tabulated by administrative district from agricultural census documents (IBGE 1960, 1970a, 1980a). These documents report the area in temporary crops, permanent crops, pasture and other categories for each of the approximately 4000 municipios (the smallest administrative unit in Brazil). Maps showing the borders of each of these municipios are also available and can be digitized into the GIS. Each municipio in the GIS can have associated with it a numerical identifier, which relates the digital map to the tabular database. In this way, we have been able to map the total area of land converted to agriculture for 1960, 1970, 1975, 1980, and 1985. Figures 1.3 through 1.5 present these results for 1970, 1975, and 1980. These data can then be compared with data derived from direct observations using satellite data during the period of overlap (Figure 1.6).

To determine the type of land cover which was converted, a digital vegetation or land cover map is created. Generally, sources of this data are maps or satellite imagery, which are encoded as another layer in the GIS. One conversion map can be subtracted from another to create a map showing areas converted between the two successive dates. This change map can then be overlaid on the vegetation or land cover map to determine the rate and type of land cover conversion. Figure 1.7 presents the results of this type of analysis.

Existing Digital Map Databases of Land Cover

Maps are the most frequent source of land cover information. Although land cover mapping and classification is a fundamental approach to understanding the global environment, there are very few sources compiled at the global level. There are even fewer sources compiled in digital form and readily available for quantitative analysis. Mueller-Dombois (1984) has argued that the two basic features of land cover which could be classified and mapped are its variation in space and its variation over time. If the former is sparse, the latter has been virtually non-existent.

There are only few global-scale land cover maps available. The ones which exist have been derived at very coarse scales. Some of the earliest formulations of digital datasets have been developed to support general circulation and atmospheric tracer models (e.g., Matthews 1983, Wilson and Henderson-Sellers 1985). The intention of these datasets has been to broadly map ecosystem classes around the globe as a way to define surface roughness, albedo, and other physical parameters mediated by vegetation. These data have also provided a means to estimate global distributions of primary productivity and water/energy balance. The formulation by Matthews (1983) is probably the most often utilized dataset. This grid-cell dataset was derived by combining approximately 100 individual map sources into a single, UNESCO-based vegetation classification scheme. The major vegetation type is defined for each $1^\circ \times 1^\circ$ (horizontal resolution of approximately 110 km at the equator) land surface grid cell.

Other datasets have been developed to support global ecosystem models, particularly for model analyses of the global carbon cycle. Olson et al. (1983) have developed a 1/2° x 1/2° degree grid cell map (50 km horizontal resolution) of vegetation types and associated carbon contents. Like the Matthews map, this dataset delineates both natural and disturbed land uses. Researchers at the University of New Hampshire, USA, have prepared a digital dataset of actual and natural land cover in vector form at a horizontal resolution of approximately 10 km. It differs from the previous datasets in its finer resolution, somewhat comparable to AVHRR-GAC, and its delineation of pre-disturbance vegetation.

A third type of digital dataset has been developed based on climatological parameters. Emanuel et al. (1985) have developed a 1/2° x 1/2° grid cell map of Holdridge Life Zones of the world, based on temperature, precipitation, and evapotranspiration. Being climate sensitive, the dataset has been used to make first-order projections of vegetation distributions under a 2 x CO_2 scenario.

These digital datasets have been the best available source of global cover maps. The fact that they portray land cover using some pre-defined nomenclature has its advantages in that it allows assignments of parameters, such as carbon or biomass, to categories with which ecologists are familiar, and because to some degree a type of land cover conveys a general sense of structure and function familiar to ecologists. Nonetheless, all of the datasets suffer certain critical problems:

(1) the nomenclature itself may be variable from one dataset to the next, and mean different things to different scientists.

(2) type-classifications require a modeler to make (somewhat arbitrary) parameterization assignments, usually from point measurements found scattered in the literature.

(3) the complete dataset may be derived from individual primary sources, each using different systems of nomenclature and from different points in time,

(4) the dataset represents some interpretation, generalization, or abstraction, of vegetation and vegetation boundaries, and thus does not necessarily portray actual distributions,

(5) most existing datasets are very coarse resolution (50 - 100 km),

(6) none of the existing datasets provide indications of phenology or intra-annual variation

(7) all are static generalizations, not able to provide indications of inter-annual changes.

Clearly, existing sources have proven to be useful first-order delineations of land cover, and these will likely to be useful for a few years to come. The shortcomings of these cartographic approaches suggests the strong need to develop remotely sensed land cover datasets.

Remote Sensing of Land Cover and Land Cover Conversion

Satellite remote sensing provides large-area, multi-temporal data over a range of spatial and spectral resolutions. Table 1.2 provides an overview of some of the major satellite sensor systems now in operation. There is considerable variability in terms of resolution and coverage. The Advanced Very High Resolution Radiometer (AVHRR) onboard the NOAA polar orbiting satellites provides daily but spatially coarse resolution data (1-4 km). The French SPOT and the American Landsat satellites provide high resolution (10-30 m), but infrequent, data. These characteristics influence the types of applications for which each sensor is suitable. A complete description of the characteristics of the AVHRR, Landsat, and SPOT sensors can be found in the various operations manuals and published literature (e.g., Kidwell 1991, 1990, CNES 1988, Colwell 1983).

The AVHRR's capability to cover large areas with frequent repeat intervals makes it useful for regional land cover mapping and deforestation detection (Townshend and Tucker 1984, Malingreau and Tucker 1987). Justice et al. (1985) discuss the use of a greenness index computed from the visible and near infrared channels of AVHRR data to map the distribution of vegetation and its phenology at very large scales. This greenness index, or normalized difference vegetation index (NDVI), is computed as:

$$NDVI = (Channel\ 2 - Channel\ 1) / (Channel\ 2 + Channel\ 1)$$

This ratio has been correlated with vegetation parameters such as green-leaf biomass, leaf area, and phenology, thereby making it valuable for multi-temporal analysis of vegetation dynamics as well as static vegetation classification. The NDVI has also been shown to reproduce the seasonal variation in the global concentration of atmospheric carbon dioxide (Fung et al. 1987). The NDVI also reduces the effect of topography and radiometric variations due to sun and view angle (Holben and Justice 1981). It has promise as a very important sensor for global vegetation monitoring, but much research remains to be done.

Analyzing data from the Brazilian Amazon region, Malingreau and Tucker (1987) have shown that seasonal, multi-temporal NDVI data can be used to discriminate tropical forest, semi-seasonal tropical forest, and cerrado ecosystems since differences in greenness increases as the season progresses into drier conditions (Figure 1.8). However it is sometimes difficult to separate natural savanna areas from deforested areas using the NDVI. Other radiometric relationships between bands of the AVHRR hold promise for discriminating types of natural vegetation and deforestation simultaneously. Malingreau and his colleagues (pers. comm.) have been studying the application of the computed difference between channel 3 and channel 4 along a radiometric transect in the tropics. In these studies, each of three forest types (moist evergreen, dry deciduous, and tropical montane) can be individually classified as well as the deforested areas (Figure 1.9). While the NDVI poorly discriminates deforested areas from dry deciduous systems, the channel 3-channel 4 difference seems to work well.

Tucker et al. (1991) have used the AVHRR data to monitor dynamic changes in the size and distribution of the Saharan desert zone in Africa. This case demonstrates the capability of remote sensing data to define inter- and intra-annual transformation of land cover. This kind of characterization would not be possible with the static depictions of land cover provided by conventional map classifications. As another example, Figure 1.10 presents a composite phenologically derived land cover delineation which we have derived from the AVHRR Global Vegetation Index (GVI). The GVI is a 16km resolution product of the NDVI derived from GAC data. We compiled 288 weekly composites of the GVI from 1985 to 1990 into a single monthly-averaged NDVI dataset. This dataset provides a 5-year average phenology as depicted by the NDVI greenness. Three months of the northern hemisphere growing season (June, July, and August) were used to define a classification based on growing season length. Different colors represent differential timing in the sequence of green-up, and also show the southern hemisphere just out of phase with the northern hemisphere. A similar application of AVHRR temporal sequences for a North American land cover classification has been reported by Loveland et al. (1991).

The potential of AVHRR for deforestation mapping has been noted recently by a number of investigators. Malingreau and Tucker (1989,1988) and Tucker et al. (1984) observed large scale deforestation in the southern fringe of the Amazonian forest using AVHRR. Woodwell et al. (1984) suggest AVHRR could provide the first stratification of a global sampling scheme. The appeal of AVHRR is that both the channel 3 signal and the NDVI seem to discriminate deforested areas from intact forest.

In addition to detecting deforested areas, thermal channels on the AVHRR are able to detect the occurrence of fires. Setzer and Pereira (1990) suggest a scheme by which fires can be detected and the corresponding deforested area calculated. However, the extrapolation of a thermal anomaly to an estimate of area requires several assumptions and much research remains to be done.

There has been considerable success using fine or medium scale remote sensing techniques to monitor land cover conversion and land cover distribution, mostly in case studies in selected areas (Woodwell et al. 1986, Nelson et al. 1987a, Nelson et al. 1987b, Nelson and Holben 1986). But because a global or regional-scale effort to monitor deforestation with fine resolution imagery such as SPOT or Landsat would be time consuming and require a large number of scenes at a relatively high cost, many investigators have looked favorably at the use of coarse resolution sensors such as the AVHRR. But it now appears that this gain in efficiency comes with a loss in accuracy. There is evidence that coarse resolution imagery tends to over-estimate the deforested area; for 1 km resolution data the overestimation might be 50-75%. This point is demonstrated by some inter-satellite comparisons we have been working on in the Brazilian Amazon (Figure 1.11). In a test site in the state of Rondonia we have simultaneously ($\pm$4 weeks) acquired digital and photoproduct data from SPOT, Landsat-TM, and AVHRR. The analysis of this data was done in conjunction with a field component which verified classification accuracies. A simple classification of forest/non-forest was made using several common methods: digital image processing of SPOT and Landsat TM, analysis of Landsat-TM single channel photoproducts using a vector-based GIS at 1:250,000 and 1:500,000 scale, a maximum likelihood classification of AVHRR channels 1 and 2, and a brightness temperature threshold classification of AVHRR channel 3. The results indicated that both AVHRR techniques over estimate deforestation. One of the most interesting results is the fact that the use of photoproducts, even at relatively coarse scales, seems accurate.

The overestimation bias of AVHRR has been further noted by Cross et al. (1991), who found that less than half a pixel needs to be deforested before it is detected as deforested. This upward bias of the AVHRR seems to be an edge effect and is very dependent on the geometry of clearing. It is minimized in areas where the clearing pattern results in patches with high area to perimeter ratios (e.g. large blocks in cerrado areas). Conversely, it is maximized where the deforestation pattern is highly variegated, having low area to perimeter ratios (e.g., the "fish bone" pattern in forests of Rondonia, Brazil). The classification of the AVHRR channel 3 signal for deforestation is also highly sensitive to the specific threshold value chosen to define the deforested areas (Tucker pers. comm.).

Townshend and Justice (1989) compared an series of degraded Landsat MSS scenes to analyze the amount of variance in datasets of various resolutions. They were interested in understanding the effect spatial resolution had on locating and quantifying land transformation at relatively coarse scales in an effort to determine the optimal resolution for MODIS. Their conclusion was that land transformation could not be assessed with any reasonable accuracy at resolutions above 1 km. They recommended an optimal resolution of 250 meters. The creation of two 214 m bands on the latest version of MODIS is a response to this analysis. One important effect of Townshend and Justice (1989) is the suggestion that high spatial resolution data is required to measure land transformations, a view different than some earlier conclusions (cf. Woodwell et al. 1986).

Another problem relates to the needs of global carbon models. These analyses need to know the fraction of all deforestation coming from primary forests and secondary forests, since the difference in biomass may be significant. Coarse resolution data may not be able to discriminate these two types of conversion and may not provide necessary insight into the dynamic pattern of clearing, regrowth, and re-clearing which is characteristic of developing areas.

An optimal approach to deforestation monitoring could be to utilize high resolution remote sensing data from the Landsat or SPOT sensors. We have used this approach, as has the Brazilian space agency (INPE), to map deforestation in the Legal Amazon region (Tardin et al. 1980, Tardin and Pereira da Cunha 1990). Results from the state of Rondonia, for instance, suggest that approximately 25 x 10^3 km^2 were deforested as of 1988 (Figure 1.6). This number compares well with estimates from INPE (Fernside et al. 1990). It also seems to confirm that AVHRR estimation of deforestation is biased on the high side, and that previous estimates of deforestation in the Amazon based on AVHRR analyses (e.g., Malingeau and Tucker 1987, Kaufman et al. 1990) are probably too high.

It is possible to develop a low-cost, low-technology approach by using photoproducts rather than digital data. In this method, photoproducts are visually interpreted for deforestation. The scale used could range from 1:250,000 to 1:500,000, which appears adequate for most large-scale regional analyses. Data could be acquired frequently--on the order of two to four year intervals. This would provide data on the rate and pattern of land cover conversion. The high resolution approach requires the acquisition of a large number of individual scenes (approximately 200 in the Brazilian Amazon). This approach must be coupled to the development of capabilities for data management in a spatial and relational context using GIS. The development of digital datasets using GIS methods has the advantage of making the data interchangeable with numerical models and provides the opportunity for detailed spatial analysis of land cover conversion.

Coupling Remote Sensing and Geographic Information Systems

Berry (1987) provides a simple, but functional description of GIS as a special class of information systems which have three general characteristics: (1) they process and manipulate geographically referenced, spatially coherent data, (2) they internally relate geographical location data and attribute information,and 3) they are computerized. In essence, these characteristics distinguish geographic information systems from other information systems by their ability to utilize spatial datasets, such as maps and remote sensing imagery, in digital formats suitable for computational or statistical analysis in both numeric and geographic space. They can perform difficult co-registration and re-projection computations enabling them to manipulate many kinds of data from difference sources in a single system. They store all coordinate and attribute information in the same system as well, thus enabling them to couple multiple layers of geographically referenced data with numeric models. Detailed reviews of GIS have been published by Burrough (1986), Smith et al. (1987), Bracken and Webster (1989), and Maguire et al. (1991).

Geographically referenced data are usually encoded in two components in a GIS: a) a cartographic component and b) an attribute, or feature component. The cartographic component provides location and coordinate information for each geographic element of the dataset (e.g., pixel, pixel cluster, point, line, or polygon). The attribute component provides basic information for each element of the cartographic component (e.g., land cover type). This information can be numerical or thematic (e.g., biomass vs. vegetation type). To encode these data in digital form, there are two general data models (Peuquet 1984). The first is the tessellated model. The grid is the simplest and most commonly used tessellation, but others may be used depending on the application. The second is the vector model. Points, lines, and polygons all constitute common forms in the vector model. There have been some recent theoretical arguments that better data models are needed for global scale work (e.g., Peuquet 1988), but to date there has been very little practical experience with GIS applications at the global scale, so most work being done has pragmatically chosen to use either the grid or vector model, and indeed these seem adequate if not sufficient.

Here we provide an example how large-area GIS can be used to map land cover conversion. Maps of deforestation for the period 1975-1978 which were prepared by the Brazilian Instituto Pesquisas Espaciais from Landsat imagery (Tardin et al. 1980) were digitized in a vector-based GIS. The entire dataset consisted of 28 individual map modules. Each module covered one UTM zone at 1:500,000 scale. Areas deforested as of 1975 and 1978 were vector encoded and joined to form a master database.

The master database was digitally combined (overlaid) with the map of municipalities described above to delineate deforestation and deforestation rates by individual political district. This created a second generation database which also permitted the relational linking of the satellite-based data with the tabular land use data described above. Figure 1.12 shows this database, although greatly reduced in scale. The deforestation database was also combined with a digital map of forest and cerrado (savanna) ecosystem distributions. The forest-cerrado map was derived from an multi-temporal analysis of the AVHRR GVI shown in Figure 1.10.

The development of geographically referenced land cover and land cover change databases, as described above, enables us to estimate the net flux of carbon between the atmosphere and the biota by coupling these data to a geographically referenced numerical model. Figure 1.13 shows the GIS-generated map of the net flux of carbon from deforestation between 1975 and 1978. The results portray the two-dimensional release of carbon dioxide in a form suitable for coupling the results to atmospheric circulation models.

The use of GIS also makes it possible to analyze the spatial distribution of land cover change. Remote sensing can provide the primary source of spatial data, while the GIS provides the computational environment for spatial analysis. The spatial arrangement of land cover change provides insights into land use. It has been shown (Lambin 1988) that the spatial patterns detected at a certain scale on remote sensed data area related to some key characteristics of farming systems. Knowing something about the spatial dynamics of land cover conversion, particularly over time, could also be important when developing models. As an example of the latter, we have used the GIS dataset on deforestation for 1975 and 1978 described above to analyze the spatial pattern of deforestation. Figure 1.14 shows the density of deforestation as a function of distance from settlement centers, averaged for the entire Amazon Basin. Inspection of this graph suggests two points: (1) the difference between 1975 and 1978 reflects the rate and pattern of spatial diffusion over time, and (2) the spatial arrangement is generally quite persistent from one time period to the next.

Deforestation as a Special Form of Land Cover Conversion

Tropical deforestation is an important component of global change; it has been shown to have an important influence on regional hydrology, large-scale and long term climate systems, and global biogeochemical cycles (Houghton and Skole 1990, Houghton et al. 1991a,b, Shukla et al. 1990, Crutzen and Andreae 1990, Salati and Vose 1984). However, while deforestation is important data for global change research, there is little known about it. Its precise rate and geographic distribution is poorly known at continental or global scales (Williams 1990a,b). Remote sensing provides perhaps the best method for obtaining geographically and temporally detailed estimates of changes to land cover.

Current Estimates of the Rate of Deforestation

In 1980 the U.S. National Academy of Sciences released one of the first surveys of tropical deforestation (Myers 1980). This survey was a broad examination of the best available literature (see also Melillo et al. 1985). The first comprehensive survey of tropical deforestation was conducted by the UNEP and FAO for 76 tropical countries (FAO/UNEP 1981, Lanly 1982). This study reported deforestation rates for two periods, 1975-1980 and 1980-1985, the latter being projections based on the best available data. The report relied primarily on national reports based on forest inventories, with some remote sensing surveys where they had been done. This study estimated an annual deforestation rate of 11.3×10^6 ha per year for the period 1975-80, of which 6.9×10^6 ha was in closed forests (Tables 1.1 and 1.2). Six countries comprise 54 percent of the global total (Brazil, Columbia, Indonesia, Ivory Coast, Mexico, and Thailand).

The FAO/UNEP data are represented in Figure 1.15, which shows the 1980 deforestation rate for each country plotted against the total area reported in closed broad-leaved forest. Also shown on the figure are isolines which depict turnover times for total forest conversion based on the 1980 deforestation rate, the 1980 area in closed broad-leafed forest, and assumptions on the rate of deforestation in the future. The solid isolines show how long the closed forests of each country would be expected to last if the net deforestation rate in 1980 continued. The dashed lines show the same, but are based on the assumption that the net deforestation rate increases exponentially and doubles in 20 years. The assumptions are simple and arbitrary, but are used for demonstrative purposes only, not as actual predictions. Estimates of deforestation on a country basis are difficult to compare; this chart puts each country's deforestation rate in a perspective relative to the pressure on the extant forest reservoirs. Points to the right of a particular isoline represent countries which would be expected to loose all their closed forests during that time interval.

Clearly, the rate of deforestation worldwide is not uniform. Rates of deforestation span several orders of magnitude, as do the areas of closed forest, when measured on a national basis. This kind of analysis provides a broad, geographical perspective on global deforestation. But it is also a simplified geographical depiction. An improved geographical analysis is needed.

The UNEP/FAO assessment provides a foundation for defining the rate of deforestation in the mid to late 1970s. Using the results from this survey, with modifications based on my own work, we report an updated estimate of the annual rate of deforestation during the mid 1970s (ca. 1975) in Table 1.4. This updated rate is slightly higher (11.9×10^6 ha total deforestation and 7.5×10^6 ha for closed forests).

Myers (1989) has compiled a country-by-country estimate of annual tropical deforestation rates in 1989. Myers estimates a global rate of 13.9 x 10^6 ha per year in closed forests only (Table 1.3). This estimate should be compared with the FAO/UNEP 1970s estimate (Lanly 1982) for closed forests only, or 6.9 x 10^6 ha. Thus the annual rate of deforestation appears to have increased by 100 percent by the late 1980s. Six countries (Brazil, Burma, Columbia, Indonesia, Mexico, and Thailand) account for 8.95 x 10^6 ha, or 65 percent, of the global rate of deforestation in the late 1980s.

The World Resources Institute (WRI 1990) has published global estimates of deforestation rates in closed and open forests for the late 1980s (ca. 1988). Their estimate is higher than Myers (1989) at 20.7 x 10^6 ha per year, of which 16.5 is in closed forests (Tables 1.3 and 1.4). This estimate could be compared with the FAO/UNEP 1970s estimate (Lanly 1982) for both closed and open forests, or 11.3 x 10^6 ha. By the WRI estimate, deforestation rates have increased 83 percent, slightly less than reported by Myers (1989). The increase in the conversion rate is estimated at 140% which is considerably higher than Myers (1989). Six countries (Brazil, Burma, Columbia, India, Indonesia, and Mexico) account for 13.7 x 10^6 ha, or 66 percent, of the global rate of deforestation in the late 1980s.

The global estimates by Myers (1989) and WRI (1990) are similar, although some exceptions exist regionally. For instance, the late 1980s deforestation rate for Thailand reported by Myers (1989) is higher than WRI relative to other countries. In absolute terms Myers' (1989) deforestation rate for Thailand is 50 percent higher. The WRI estimate for India, on the other hand is much higher than Myers (1989). In absolute terms, India is almost 4-fold higher in the WRI report compared to Myers (1.5×10^6 ha vs. 0.4×10^6 ha, respectively). This difference cannot be attributed to the fact that the WRI report includes open forests as well as closed forests since all the Indian deforestation reported by WRI is in closed forest.

Both Myers (1989) and The World Resources Institute (WRI 1990) suggest that rate of deforestation has nearly doubled since the mid 1970s (Table 1.4). The World Resources Institute report (WRI 1990) provides the most recent estimate on deforestation rates for the late 1980s, and provides and evaluation of clearing in both closed and open forests. The increase in the rate of deforestation reported by WRI is 9.4×10^6 ha (ca. 1980-1989). Approximately 80 percent of this increase in attributed to Brazil alone. A full 95 percent of the reported increase in the rate of deforestation in the 1980s is from just two countries, Brazil and India.

The Brazilian estimate given by WRI is probably too high (see below). It was derived from preliminary estimates based on the assessment of thermal anomalies in the NOAA polar orbital satellite's AVHRR sensor as discussed above. A more conservative figure has been published by Fearnside et al. (1990). This estimate is 2.1×10^6 ha per year averaged over the period 1978 to 1988. Fearnside et al. (1990) also report the rate of deforestation between 1988 and 1989 to be slightly higher at 2.6 x 10^6. If these estimates are used in place of the 8.0 x 10^6 figure reported by WRI, we get a new estimate of the deforestation rate in the late 1980s of approximately 15.3 x 10^6 ha per year, which yields only a 28 percent increase in the global rate of deforestation for the 1980s (see Table 1.4).

Brazil: A Regional Example

The Brazilian Amazon region is the largest contiguous tropical forest in the world. By best estimates, the largest deforestation rate worldwide is in Brazil, and accounts for a large fraction (12-20 %) of the global estimate. Current estimates of deforestation there range from 2.1 x 10^6 ha to 8.0 x 10^6 ha annually. A Brazilian space agency report forms the low end of the range (Fearnside et al. 1990) and a World Resources Institute report gives data at the high end (WRI 1990). Several other estimates fall in between: for instance, Myers (1989) reports 5.0 x 10^6 ha per year.

This wide range is of considerable interest. Understanding the details of issues surrounding these estimates generally, and the current state of knowledge about Brazil point out many important features of the problem of measuring deforestation. For illustration we review the state of knowledge for Brazilian deforestation. Such an examination provides insights into an approach to monitoring deforestation which could be implemented worldwide.

Satellite surveys of deforestation have been made in Brazil by the Instituto de Pesquisas Espaciais (INPE) since the late 1970s. The first study, conducted in 1979, used Landsat MSS imagery in the format of 1:500,000 scale photoproducts to produce estimates of the area deforested in the Legal Amazon for the years 1975 and 1978 (Tardin et al. 1980). This was one of the earliest studies of large forested regions using satellite remote sensing, and even today it serves as an example method for a global monitoring program. Results were published for each state in the Legal Amazon. This study estimated a deforestation rate of 15.7 x 10^6 ha per year between 1975 and 1978. Total area estimation was based on a dot-grid overlay.

There were no comprehensive studies of deforestation in the Amazon between 1978 and 1988, when the Brazilian Space Research Institute initiated new analyses for the years 1988 and 1989 (Fearnside et al. 1990). (Indeed, there have been isolated analyses of specific states, but no assessments for the entire region.) From this analysis it is possible to define with some degree of precision and objectivity the average annual rate of deforestation during the 1970s and 1980s. If the analysis is correct, the average annual rate of deforestation over the decade 1978-1988 was 2.2 x 10^6 ha, although it is possible that certain years could have been higher or lower than this ten-year average. The rate for 1988-1989 was 2.6 x 10^6 ha.

Deforestation studies in the Brazilian state of Rondonia using coarse resolution satellite remote sensing have further demonstrated the application of remote sensing for the timely and accurate monitoring of deforestation in the tropics (Malingreau and Tucker 1987, 1988, 1989). By coupling these estimates with estimates based on tabular land use statistics and high resolution remote sensing data, it is possible to construct a detailed, long-term record of deforestation in that state (Figure 1.6).

Other work in Brazil has attempted to use satellite remote sensing for monitoring biomass burning. The number and geographic distribution of fires in the Amazon region can be estimated using thermal sensors on polar orbital satellites (Kaufman et al. 1990). The work of Setzer and Periera (1990) also reported in Kaufman et al. (1990) used the location and number of thermal anomalies on the AVHRR channel 3 to estimate the area of deforestation in Brazil in 1987. The approach used factor analysis and a number of assumptions concerning: (a) the average duration of a fire, (b) the average size of a fire in pixels showing a thermal anomaly, (c) the fraction of fires associated with new deforestation and pasture maintenance and (d) the average number of fires per month during the dry season. These factors were applied to the total number of observations to estimate a deforestation rate of 8.0×10^6 ha for 1987. This number is now thought to be high. For instance the estimated rate of deforestation in Rondonia was higher than the <u>total</u> area deforested based on high resolution studies.

The work in Brazil represents the state-of-the-art in remote sensing monitoring of tropical deforestation. Yet most of this work contains a number of problems. The use of photoproducts interpreted onto 1:250K-1:500K scale maps represents a cost effective method for mapping deforestation, but it cannot readily distinguish secondary growth nor differentiate deforestation of primary vs. secondary forests. The simple approach to area estimation using dot grids probably underestimates deforestation. On the other hand, coarse scale mapping tends to generalize shapes and therefor is probably overestimating the areas of deforestation. The use of coarser-resolution sensors such as AVHRR probably suffer similar problems; for instance preliminary work suggest the coarse resolution sensor may have overestimated deforestation in the state of Rondonia.

Nonetheless, it is possible to somewhat resolve the wide range in estimates. It is unlikely that the estimate based on fires is correct. But because the official INPE results were specifically for 1988-1989, it is not possible to categorically rule out the 1987 estimate based on fires until an earlier date, such as 1985 is analyzed. The WRI(1990) estimate is probably too high since it was based on the fire data. Moreover, the estimate of Myers (1989), which appears to be based on loose accounts and trends rather than an objective assessment, is also too high. A better estimate for the current rate of deforestation in Brazil is probably close to the INPE estimate at 2.0-3.0 x 10^6 ha per year, but there has of yet been no independent appraisal of this estimate.

Analysis of Deforestation Using Social and Demographic Factors

Demographic Change and Deforestation

In recent years, researchers have analyzed the relationship between deforestation and population growth, mostly at the global level. This interest stems, we believe, from a general interest in population pressure on natural resources and the carrying capacity of the planet. Allen and Barnes (1985) surveyed population and deforestation data for 76 tropical countries using statistical correlation. They also examined multiple regressions of deforestation against other variables such as arable land, roundwood production, and GDP. Their analysis suggested a low, but significant, correlation between population growth rates in 1970-1978 and deforestation reported for the period 1975-1980 in the FAO Forest Assessment (Lanly 1982). They also showed low, but significant, correlation between arable land change and deforestation. GDP was not a significant variable. Their conclusion was that the cause of deforestation is population growth.

Reis and Margulis (1990) have made a cursory examination of economic explanations for large and increasing deforestation rates in the Legal Amazon during the mid-1980s. Their analysis is interesting in that they relate demographic <u>and</u> economic factors to the contribution of deforestation to emissions of carbon dioxide. One conclusion they draw is that population growth appears related to deforestation when one plots population density against "deforestation density" (fraction of an administrative district deforested). Yet, they also develop a multiple regression model ($r^2 = 0.8$) which relates deforestation to the spatial density of population and a set of other measurable economic factors:

$$D = 0.3p + 0.4a + 0.11c + 0.04w + 0.28r - 0.02d + 2.42$$

where D is the deforestation rate, p is population density, a is the area in arable land, c is the density of cattle, w is the wood harvest per sq km, r is the number of roads, and d is the distance from the state capital.

The approach by Reis and Margulis (1990) does not consider environmental factors such as soil type and fertility, topography, or temperature and precipitation to define spatial concentration of deforestation. In a GIS, these factors could be readily elucidated to supplement this kind of analysis.

Using data which we have compiled on deforestation from both statistical land use surveys (IBGE 1970a, 1980a, 1989) and satellite data (Tardin et al. 1980), it is possible to look at deforestation trends in Brazil in relation to population growth derived from data in IBGE (1970c, 1980b). In the first analysis, we have tabulated data from remote sensing data reported in Tardin et al. (1980) (see earlier discussion). Data on population for each municipio for 1970 and 1980, arranged by rural and urban populations, were encoded into a GIS along with deforestation rates. The remote sensing data were for the period 1975 and 1978/9. By simple change detection, an average annual rate can be computed. This rate was regressed against the 1980 rural population for each municipio in the Legal Amazon. The results are shown in Figure 1.16. The coefficient of determination, r^2, is low. The apparent relationship found by Allen and Barnes (1985) at the global level and Reis and Margulis is not clear in this analysis. It must be noted that although the correlation was weak, it was significantly different from zero (p less than 0.001).

Simple regressions of this kind are difficult since various regions could be behaving independently, but still be well correlated within the region. That is, different regions could have different, but internally consistent linear relationships and this would not show up when viewed collectively. Therefore, we performed a simple Rank (Spearman's) correlation. The results are shown in Table 1.5. Again there appears no strong correlation.

Explanations by Understanding Social and Economic Drivers

The regression approaches are straightforward, and present a promising approach for prediction over short time periods (cf. to design a remote sensing sampling scheme), but do not provide a causal explanation for the explosive rates of deforestation in the Amazon. Hect (1983, 1989) studied cattle ranching in the Amazon and concluded that government policies, fiscal incentives, and the nature of individual farmer decision-making in an inflationary economy (i.e., cattle are a good hedge against uncertain economic conditions) control deforestation rate more than demographic considerations. She argues that "it is ludicrous to describe environmental degradation in this situation as only a function of demographics." A similar view has come out of recent studies of declining wood stocks in sub-Saharan Africa (Anderson 1986). In these case studies population growth is seen as part of a multiple feedback system, where it is as much a consequence of poverty and land degradation as it is a cause.

Nonetheless, we believe it is useful to develop explanatory conceptual framework which links to demographic and "modernization" factors, some of which we have already discussed (i.e., rural to urban migration, increasing substitution of machinery for labor in a rapidly developing industrial economy). In this next section we present a conceptual model which relates deforestation, with demography and spatial organization. We focus on Rondonia, Brazil as a case study.

Deforestation in Rondonia, 1970-1980. The highest deforestation density in Brazil is in the state of Rondonia, where 13% of the forests have been cleared as of 1987. The state of Rondonia has experienced nearly exponential deforestation rates over the last 30 years as new colonization and settlement programs opened large tracts of forest. These settlement programs, as well as specific fiscal incentives were established in the 1970s as a way to encourage migration to the region from overpopulated, poverty-stricken, and drought-ridden regions in the south and northeast of the country. It was once suggested that Rondonia and other colonization "poles" in the state of Para were oriented for "people without land in a land without people" (Moran 1981). The vast Amazonia was seen by many as an empty frontier, which at once could be consolidated under Brazilian national sovereignty and provide opportunity for millions of poor and landless (Bunker 1984a, 1984b).

In my model, this trend can be explained by changing demographic and economic conditions in the south of Brazil, particularly the state of Parana, during the period. We will focus my discussion on changes in the state of Parana in the early 1970s and explore how changes in land tenure and land use there directly influenced land use in Rondonia. But first it is important to consider certain international activities which were taking place at the time, particularly related to world oil production, distribution, and price.

The Flood of Petrodollars. After the OPEC-stimulated increase in the price of oil in the mid 1970s, large amounts of what have been called petrodollars flooded international money markets. This is discussed by Pool and Stamos (1987). The price of oil went from $1.30 a barrel in 1970 to $10.72 per barrel in 1975 and to $28.67 by 1980. Most energy-dependent countries paid OPEC prices, resulting in a large net transfer of wealth from industrial economies to OPEC. OPEC, in turn, deposited these revenues in U.S. and European banks. Since banks must pay dividends or interest to depositors, U.S. commercial institutions were eager to find borrowers.

Developing countries such as Brazil were eager for foreign capital to fund economic development, modernization, and industrialization programs. Moreover they also needed dollars to pay for oil (since oil is bought and traded in dollars). Brazil's strategy appears to be twofold: (a) the amount of imported oil declined as they developed their own sources (discussed above), (b) Brazil borrowed heavily to finance domestic economic development programs. One important development program in the 1970s was agricultural modernization, since it was viewed that agricultural products could provide a profitable export industry, which in turn would help pay for loans to modernize agriculture and the rest of the country (Mahar 1989).

Agricultural Modernization in Brazil in the 1970s. Between 1970 and 1980 there was large-scale investment in agriculture. Figure 1.17 shows an index of crop credits in Brazil since 1970. It increases almost five-fold (World Bank 1982). We have no direct data which shows the amount of these credits derived from foreign loans. It is probably safe to suggest that the deployment of credits was an effort to build an active agricultural export system, this being done to balance foreign debt and offset the rising cost of petroleum (World Bank 1982). Such investment did however require large amounts of capital from abroad. Nonetheless, such investment programs resulted in some degree of success; rising crop credits occurred with increasing crop output; the net value of agricultural output increased 2.68-fold between 1970 and 1980 (IBGE 1989, 1980a, 1975, 1970b). By 1977 more than 50% of the total value of principal crops were accounted for by export crops.

Figure 1.18 shows the distribution of crop credits by crop type. Three general patterns emerge. First, the export crops of wheat, soybeans, and coffee consumed almost half of all crop credits. Second, the largest fraction was invested in soybean production. And third, very little of the credits were allocated to staple crops such as black beans and manioc.

Soybean production was a major success story. The area harvested increased 6-fold in the 1970s, ten times more than any other crop except oranges and wheat; yields increased five-fold. The combination of land, fertilizers, improved seeds, and government-sponsored fiscal credits and incentives resulted in producing an internationally competitive export program. Soybeans became one of Brazil's major export crop. Figure 1.19 shows Brazil's changing share of world trade in soybean meal. From a small producer at 10% of the international markets, Brazil was able to compete with the United States by 1980.

One reason for Brazil's competitiveness in the soybean market might be related to comparative costs of production. Table 1.6 shows production costs for soybean production in Brazil compared to the United States, the world's leading exporter in the early 1970s. As might be expected, the cost of fertilizers and pesticides in Brazil is higher than in the U.S., reflecting poorer growing conditions. In fact, total variable costs are higher for soybeans grown in Brazil. Contrary to popular belief, the comparative advantage does not lie in labor costs, since they are nearly the same. The key difference lies in fixed costs, particularly land. Land costs in the Brazilian soybean production system are half the land costs in the U.S. Thus, actual production costs are lower for Brazilian soybeans than U.S. beans. But because commercialization costs (the middle man) are much higher in Brazil, total port costs are slightly higher. The conclusion is that Brazilian soybeans could be produced at highly competitive prices, primarily because of Brazil's competitive advantage in land.

Most of the soybean production was concentrated in two states: Rio Grande do Sul and Parana. The history of soybean cultivation during this period is interesting. Figure 1.20 shows the trend in area planted in some important crops in Parana during this period. Soybean production (and wheat) replaced coffee as the major crop in the region. Unlike soybeans, the international market for coffee was highly variable and undependable. Government programs concentrated on replacing coffee fields with soybeans (World Bank 1982).

Agricultural Modernization and Demographic Change. Just as the industrial sector was modernizing, so was agriculture as discussed above. A labor-intensive agricultural system was being transformed into an important energy- and machinery-intensive component of the national economy, particularly in Parana. Land prices rose significantly (World Bank 1982), as it was consolidated into larger holdings. Coffee, a labor-intensive crop, was replaced by soybeans and wheat which utilize machinery. This transformation of land use changed land tenure. Figure 1.21 shows the change in farm size distribution in Parana. It shows a loss of small farms and an increase in very large, presumably, commercial farms.

It has already been noted that the period 1970-1980 saw increased migration from rural to urban areas. Part of this migration was in response to "pull" factors as industrial development created increased opportunities for wages in urban areas. As well, commercialization of agriculture in Parana shifted the mode of production from labor to machinery, creating a "push" factor. Looking at demographic data we see that large numbers of people left the state of Parana during this period, the out-migration rate was higher than any other state. Undoubtedly many, if not most, of the migrants left for urban areas, which would be in keeping with what we found earlier. But a large number also went to new opportunities in the Rondonia frontier (Hect 1989).

Effect on Deforestation in Rondonia State. Much has been made of the large-scale government programs to facilitate the opening of the frontier (e.g., Mahar 1989, Moran 1981, Bunker 1984b, Fernside 1990), and the various reasons for doing so, which range from the military-oriented view of the need to consolidate the hollow frontier to the need to provide a population safety valve. Indeed, there were a number of reasons for opening the Rondonia frontier. The long-term drought in the northeast certainly played prominently. Moreover, much has been made of the massive road building projects, suggesting it to be the key determinant of change in the region. All of these factors must be considered, but must be view largely as mechanisms which facilitated a transformation which had more fundamental underpinnings.

Clearly, migration to the region was largely a response to events and conditions far removed from Rondonia. They involve changes in land tenure in the south of Brazil, and changes in the structure of rapidly developing national economy which was fueled to a large degree by excess petro-dollars. The demographic trends discussed in the earlier sections, and which influence the nature of fossil fuel energy use are related to the processes which have also stimulated deforestation and biomass burning in the Amazon.

Conclusion

Land cover change is one of the most important components of global change. It might be argued that over the next 20 to 50 years the global effects on ecosystems and human habitability from land cover conversion will be much larger than any estimated to arise from climate change. And yet there is really very little known about land cover and its conversion. Only a few datasets exist, and these suffer from a number of technical and interpretive problems. There are three areas of uncertainty which need much better documentation and analysis: (1) the state (ie information on biomass, net primary production, etc.) and distribution of existing land cover, (2) the rate and distribution of land cover conversion, both historically and currently, and (3) the underlying driving forces which determine the rate and extent of land cover conversion. Clearly, some combination of historical reconstruction and remote sensing are needed to refine the first two areas. The third area of uncertainty will require closer linkages of physical and social analysis.

Coarse resolution remote sensing data could provide the basis for defining the distribution of current land cover. The advantages to this over existing maps is temporal consistency and an explicit definition of actual, rather than estimated, boundaries between cover types. The most straightforward approach would be to derive maps of current land cover types from remote sensing measurements along pre-defined classification system. It seems unlikely that a single classification will suite all needs, however. But much could be gained by initiating international efforts to collect the necessary datasets from existing satellite sensors, such as AVHRR, from which various classifications could be made on a case by case basis. A remote sensing-based map of current land cover could form the base from which a pre-disturbance land cover map could be created by correlating existing natural land cover with physical variables (e.g., temperature, precipitation, edaphic conditions), or through approximation based on simple assumptions of contiguity and spatial clustering. Having such maps of both current and pre-disturbance land cover, it might then be possible to reconstruct the history of land cover change with the addition of geographically referenced time-series of human use and conversion, such as maps of the expansion of deforestation. Since much of the analysis is spatial, a GIS would be used to organize the data and analysis.

Thematic classification of land cover from remote sensing data follows traditional cartographic approaches. For many aspects of global change research, in the fields of biogeochemistry and water/energy dynamics for instance, there is a need to parameterize land cover beyond basic classes such as forest, savanna, and the like. Here, the need is for parameters such as nitrogen status, biomass, primary productivity and other land cover-related parameters. Functional classifications, of the type mentioned in this paper, could be very important new approaches to classification of land cover. However, much more research must be conducted. Another approach would be to develop methods by which direct parameterization of the state of land cover could be derived from satellite data. Direct parameterization of canopy chemistry, albedo, surface roughness, NPP and other variables could be one feasible approach which circumvents the necessity for an a-priori system of nomenclature.

Land cover conversion rates are not well known. The comparison between current estimates of deforestation in the tropics presented in this paper demonstrate the need for new and objective information. One approach would be to couple historical reconstruction with remote sensing, as shown in Figures 1.3 through 1.6. Tabular data, national censuses, or historical documents in which data are reported geographically (e.g., by administrative district) could be mapped in a geographic information system. Remote sensing provide direct observations of land cover change, while historical reconstruction generally relies on indirect estimation from changes in various human-use categories. Nonetheless, the coupling of these two approaches provides a way to "calibrate" the historical assessment, since the historical trend should overlap with remotely sensed data--both in magnitude and space--during the years where both historical and remotely sensed data exist.

The use of coarse resolution remotely sensed data (1km or greater) to map deforestation and other forms of land cover conversion has frequently been considered the optimal approach for monitoring land cover change since it requires fewer data than high resolution sensors (less than 100 m). However, in cases where coarse resolution datasets have been used in the past, they tend to overestimate deforestation. This over estimation bias is partly related to the geometry of clearing, so a single conversion factor cannot readily be developed. Considerable work remains before mixture modeling and other techniques which could derive an accurate estimate from coarse sensors could be used. Meanwhile, the best approach appears to be one based on high resolution data from such satellite systems as Landsat. The use of photoproducts at scales ranging from 1:250,000 to 1:500,000 provides an efficient, low-cost alternative. These data can be interpreted for areas of deforestation and then encoded digitally in a geographic information system.

The fine-scale dynamics of clearing, abandonment, regrowth and re-clearing are completely unknown and understudied, yet could be important to analyses of the net flux of carbon. The use of high spatial resolution remote sensing data provides detailed information on regrowth and abandonment. There is very little quantitative information on the amount of secondary growth. Some preliminary results from on my own work and others suggests as much as 20% of the deforested land in the Amazon Basin is in some stage of regrowth at any point in time.

Documentation of land cover change is the first step toward understanding the underlying agents of land cover change. But is clear that documentation alone will not yield a complete explanation. Simple correlations between various factors are often facile but not fruitful, and may in fact be misleading or wrong. When it works, correlation between deforestation and some other social factor such as population might be useful for developing a sampling scheme or for making short term predictions, but such an approach lacks the ability to explain the phenomenon. In Brazil, for instance, the rapid increase in deforestation in the Amazon Basin in the late 1970s was more a response to changing social and economics conditions--in fact conditions far outside the Amazon itself--than population pressure. Other examples can be found; it could be reasonably argued that population growth in Sub-Saharan Africa is as much a response to land degradation as it is a driving factor. Population pressure has been frequently and been cited as the main driver of land cover change, yet there is little strong quantitative evidence to support this since there is paucity of hard data on land cover change.

It could be reasonably argued that if a correlation between population and land cover change exists, such a relationship could be used as a first-order, short term predictor of land cover change, both in terms of extent and spatial distribution. However it is not clear that for short term predictions, complex formulations based on population, economic variables, or social drivers are required to make reasonable predictions. In mapping studies of deforestation in the Amazon which we are developing now at the University of New Hampshire, it appears that the rate and spatial distribution of deforestation are somewhat persistent over short time periods (see for example Figure 1.14 which shows the spatial arrangement of deforestation as a function of distance from concentrated settlements at two dates, 1975 and 1978). The indication from these data are that spatial relationships are maintained from one date to the next in generally predictable ways. The conclusion one draws is that the best predictor of deforestation at time, t=n, is the deforestation at time, t=n-1. This, in turn, suggests that one of the highest priorities in deforestation prediction and analysis is an accurate base map of deforestation. Predictions on time horizons beyond one or two decades will require more sophisticated models which consider primary causal factors, and an understanding of the complex social and economic conditions which exist in a particular region.

Future research can be developed around three general areas: (a) acquisition and analysis of new data on existing and pre-disturbance land cover, using a combination of satellite data, historical reconstructions, and maps, (b) acquisition and analysis of mapped data on the distribution of primary agents of land cover change, such as deforestation or agricultural expansion using satellite data for the contemporary period (since 1978), and tabular census data for historical periods, (c) development of models, both explanatory and numerical, which are based on simple extrapolation for short term analyses and socio-economic factors for long term analyses.

Table 1.1. Methods for classification of vegetation and land cover (from Mueller-Dombois, 1984).

Properties of the vegetation

Physiognomic: life form, structure, periodicity

Floristic: dominant species, groups of species

Properties of the Environment

Environmental: potential vegetation, related to climate, topography, soil, human use

Geographical location

Combination of vegetation and environment

Correlation: by map overlay

Integration: into common units: ecosystems, landscape units

Functional: groups related by processes

Table 1.2. A comparison of different satellite remote sensing systems.

	LANDSAT -MSS	LANDSAT-TM	SPOT	AVHRR
Spatial Resolution	79 m	30 m	10 m (panchromatic) 20 m (multispectral)	1 km (LAC) 4 km (GAC) 16 km (GVI)
Number of Spectral Bands	4	7	1 pan 3 multispectral	5
Spectral Range (micro-meters)	0.5-0.6 0.6-0.7 0.7-0.8 0.8-1.1	0.45-0.53 0.52-0.60 0.63-0.69 0.76-0.90 1.55-1.75 2.08-2.35 10.4-12.50	0.51-0.73 (pan) 0.50-0.59 0.61-0.68 0.79-0.89	0.58-0.68 0.73-1.1 3.55-3.93 10.3-11.3 11.5-12.5
Frequency of Coverage	16 days	16 days	26 days (8-day sequence with variable-look angle)	twice daily
Data Cost	moderate	high (digital) low (photo)	high (new acquisitions) moderate (archival)	low
Processing Burden	low	low	low	high

Table 1.3. Estimates of deforestation (10^3 ha yr^{-1}).

	FAO/UNEP (1981)	Myers (1989)	WRI (1990)
Bolivia	65	150	87
Brazil	1,360	5,000	8,000
Cameroon	80	200	100
Columbia	800	650	820
Congo	22	70	22
Ecuador	300	300	340
Gabon	15	60	15
Guyanas	4	50	5
India	132	400	1,500
Indonesia	550	1,200	900
Ivory Coast	310	250	290
Kampuchea	15	50	25
Laos	120	100	100
Madagascar	165	200	150
Malaysia	230	480	255
Mexico	420	700	595
Myanmar	92	800	677
Nigeria	285	400	300
P. New Guinea	21	350	22
Paraguay	16-	-	190
Peru	245	350	270
Philippines	100	270	143
Thailand	325	600	397
Venezuela	125	150	125
Vietnam	60	350	173
Zaire	165	400	182
Other Africa	277	-	300
Other Asia	124	-	84
Other Cent. Amer.	328	330	477
TOTAL	6,893	13,860	16,544

Table 1.4. Summary of recent estimates of the rate of deforestation and the change in the rate from the late 1970s (10^3 ha yr^{-1}).

	Africa	Asia	C/S America	Total
FAO/UNEP Late 1970s	1,319	1,767	3,807	6,893
Myers Late 1980s (% increase)[1]	1,580 (20)	4,600 (160)	7,680 (101)	13,860 (101)
WRI Late 1980s (% increase)[1]	1,359 (3)	4,276 (142)	10,909 (187)	16,544 (140)
Our Update[2] Late 1970s			4,447	7,533
Our Update[3] Late 1980s (% increase)[4]			5,509 (45)	11,144 (48)

Notes:

[1]The percent increase over the FAO/UNEP report.

[2]Our update is computed from our GIS database on deforestation between 1975 and 1978, as remeasured from Tardin et al. (1980). These values were substituted in place of the Brazilian values reported by Myers and WRI.

[3]Our update based by substituting the rates given in Fearnside et al. (1990) and our analysis of the Amazon Basin instead of the values for Brazil reported by Myers and WRI.

[4]Percent increase over the 1975-78 rate.

Table 1.5. Correlation matrixes for population and deforestation variables.

(a) Simple Correlation

	POP	POPDEN	DEFOR	DELTA	DELDEN	DEDEN
POP	1.0000					
POPDEN	0.6695	1.0000				
DEFOR	0.2928	-0.0290	1.0000			
DELTA	0.2873	-0.0513	0.9679	1.0000		
DELDEN	0.0379	0.0965	0.3058	0.3241	1.0000	1.0000
DEDEN	0.1908	0.3011	0.3551	0.3208	0.8955	

(b) Spearman's Rank Correlation

	POP	POPDEN	DEFOR	DELTA	DELDEN	DEDEN
POP	1.0000					
POPDEN	0.6077	1.0000				
DEFOR	0.4463	0.2656	1.0000			
DELTA	0.3875	0.2497	0.9654	1.0000		
DELDEN	0.2151	0.5904	0.7170	0.7591	1.0000	
DEDEN	0.2817	0.6088	0.7805	0.7689	0.9646	1.0000

Legend:

POP = Total population in 1980
POPDEN = Population density in 1980
DEFOR = Total deforested area in 1980
DELTA = Deforestation rate 1975-1978
DELDEN = Deforestation rate expressed as a fraction of total area
DEDEN = Fraction of area forested (deforestation density)

Table 1.6. A comparison of the costs of crop production in Brazil and the United States: Soybeans. (Units are arbitrary but have been corrected for exchange rates.

	U.S.	**Brazil**
1. Variable Costs		
Machinery	737	672
Labor	457	241
Inputs	964	2,299
Other	62	404
Subtotal	2,220	3,617
2. Fixed Costs		
Depreciation	781	427
Interest on capital	293	141
Labor	449	170
Land	2,029	937
Other	365	51
Subtotal	3,315	1,727
3. Total Costs per ha	6,136	5,343
4. Yield (kg/ha)	1,900	1,920
5. Unit Costs (per ton)	3,229	2,783
6. Port Costs	3,368	3,882

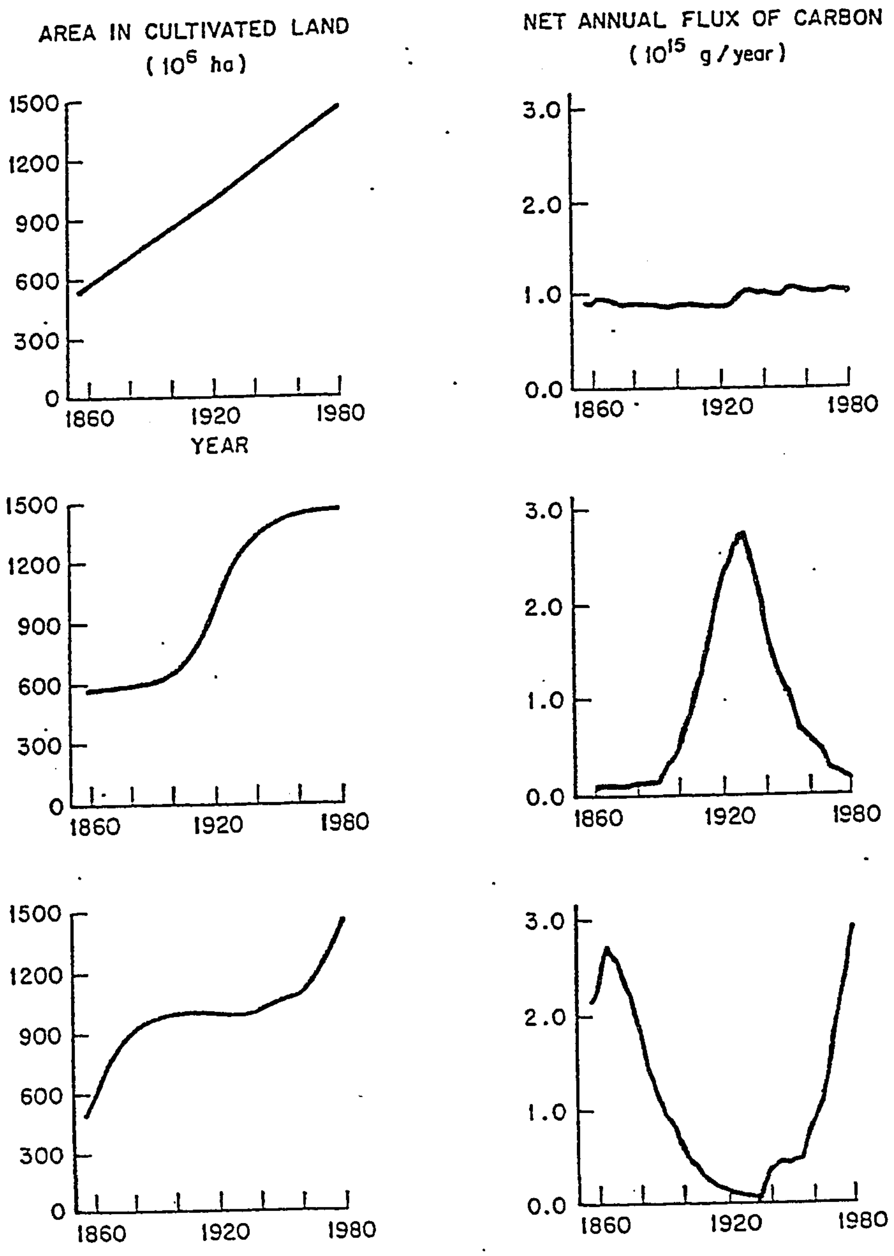

Figure 1.1. Three examples of the use of tabular historical data on cultivated land to estimate land cover conversion. Also shown is how each determines the net flux of carbon (from Houghton 1986).

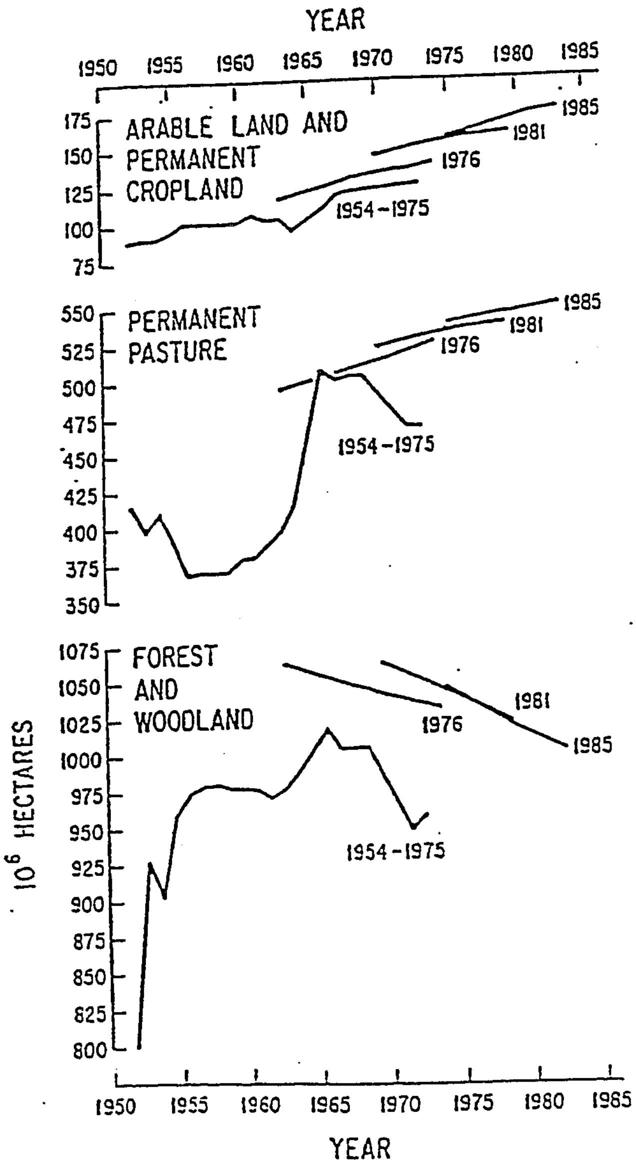

Figure 1.2. Different editions of the FAO Production Yearbook give different time series due to changes in methodology or terminology (from Houghton et al. 1991a).

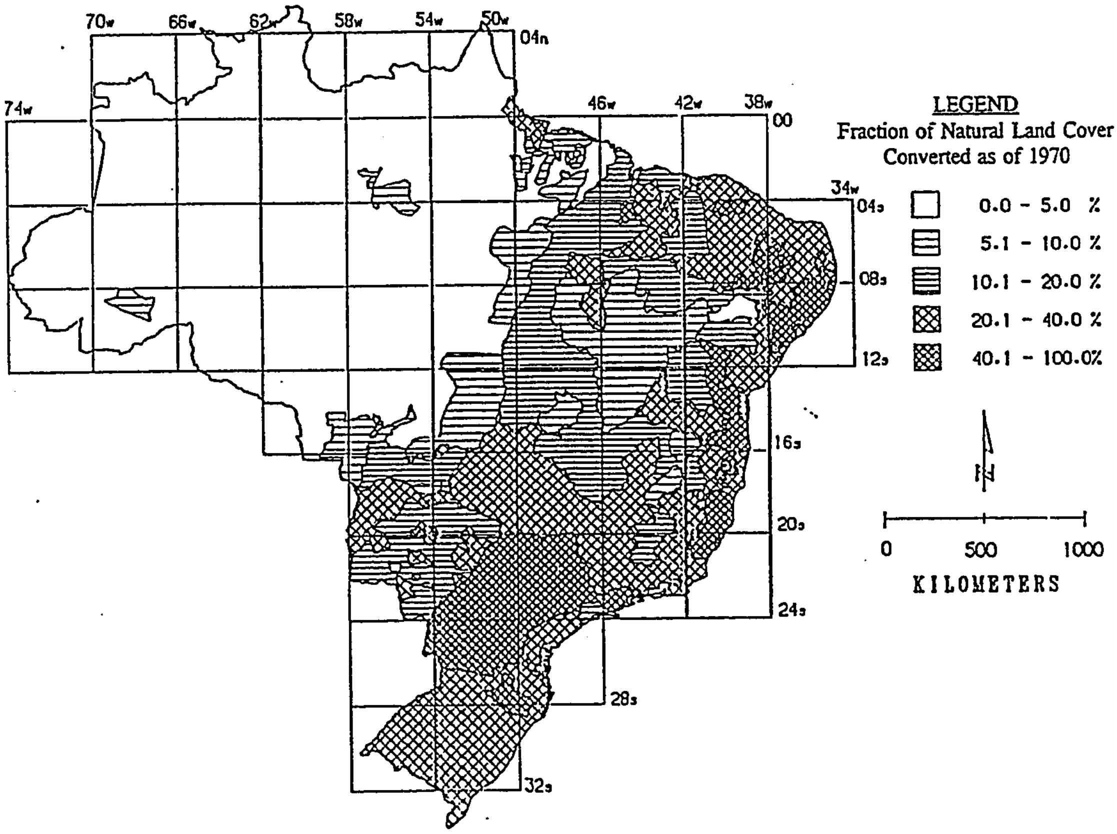

Figure 1.3. The results of mapping tabular data in a geographic information system to estimate the geographic extent of land cover conversion in Brazil in 1970. Legend shows the fraction (%) of natural land cover converted to human use as of 1970.

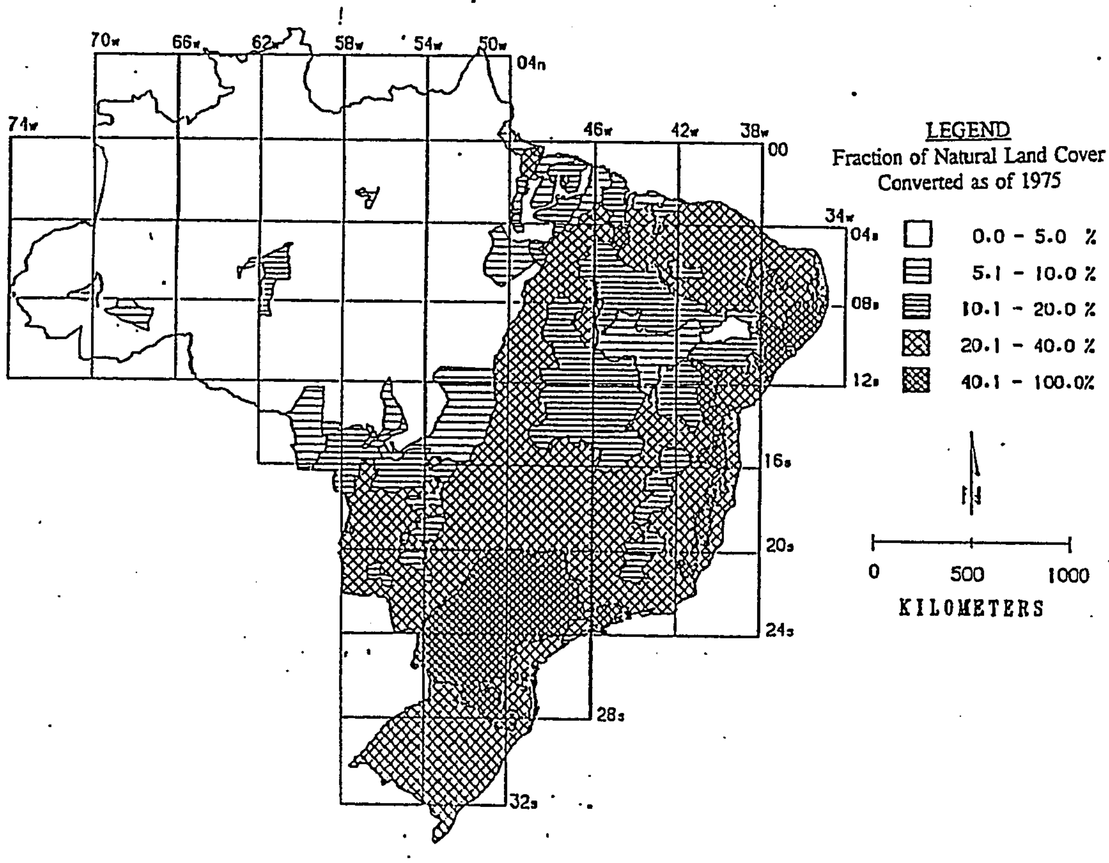

Figure 1.4. Land cover conversion derived from tabular documentary data mapped in a geographic information for 1975. Legend shows the fraction (%) of natural land cover coverted to human use as of 1975.

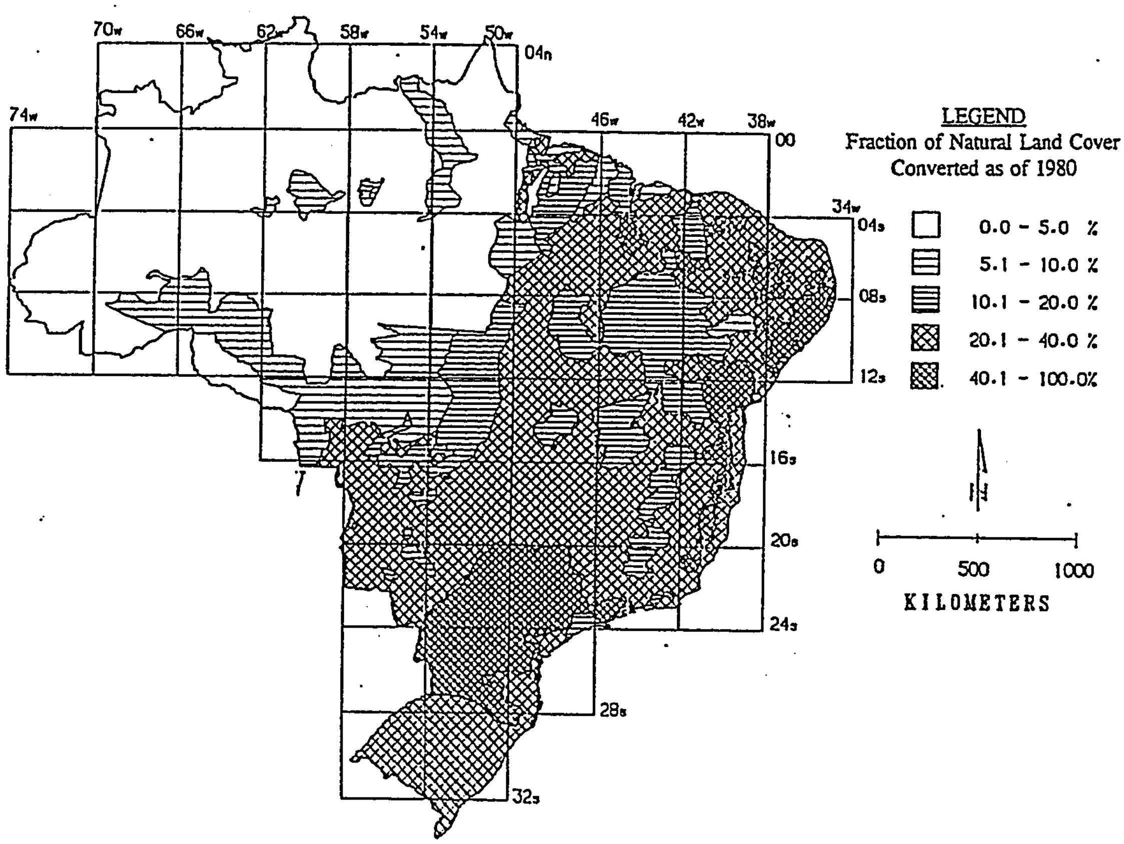

Figure 1.5. Land cover conversion derived from tabular documentary data mapped in a geographic information system for 1980. Legend shows the fraction (%) of natural land cover converted to human use as of 1980.

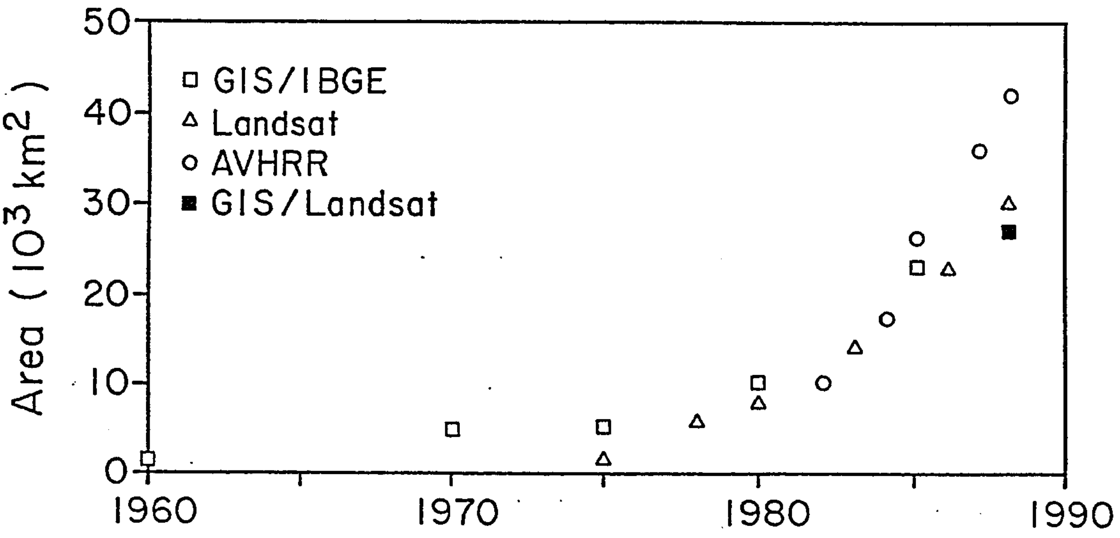

Figure 1.6. A comparison of different methods for estimating deforestation in the state of Rondonia, Brazil. The open squares represent data derived from agricultural statistics, which could be used to obtain long term deforestation prior to the availability of remote sensing data. The triangles show results from Landsat analyses. The triangle for 1988 is from the Brazilian space agency study. Circles show published results from AVHRR analyses. The closed square represents my analysis for 1988 using Landsat photoproducts.

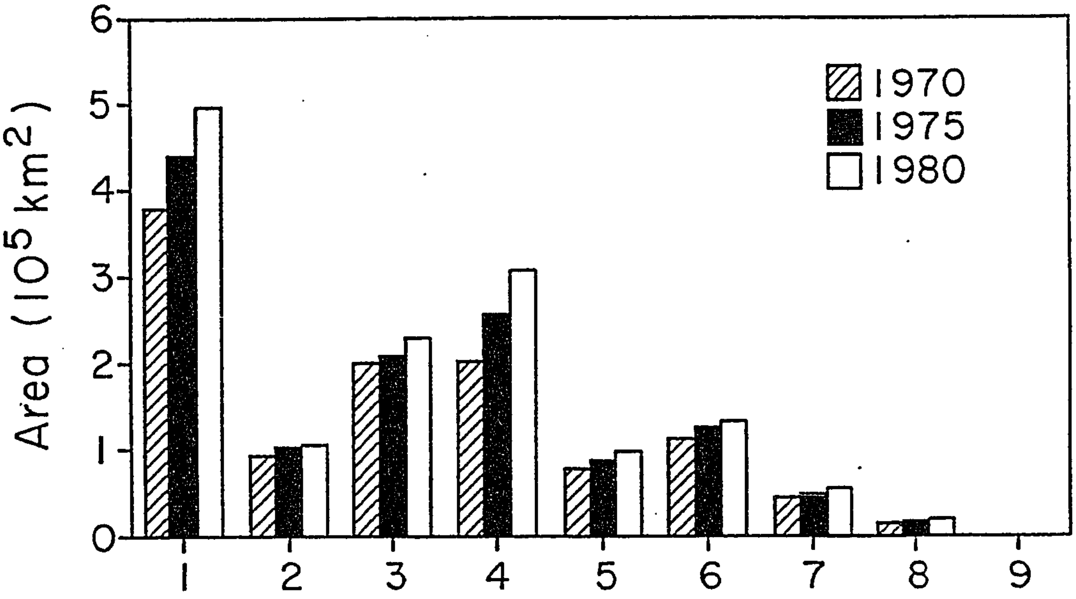

Figure 1.7. The total land cover conversion in Brazil distributed across cover types for different time periods (see also Figures 1.3-1.5). The cover types are 1: Forests, 2: Forest Steppe, 3: Bush Forest, 4: Cerrado, 5: Wet Tallgrass Savanna, 6: Dry Lowgrass, 7: True Steppe, 8: Wetland, 9: Desert.

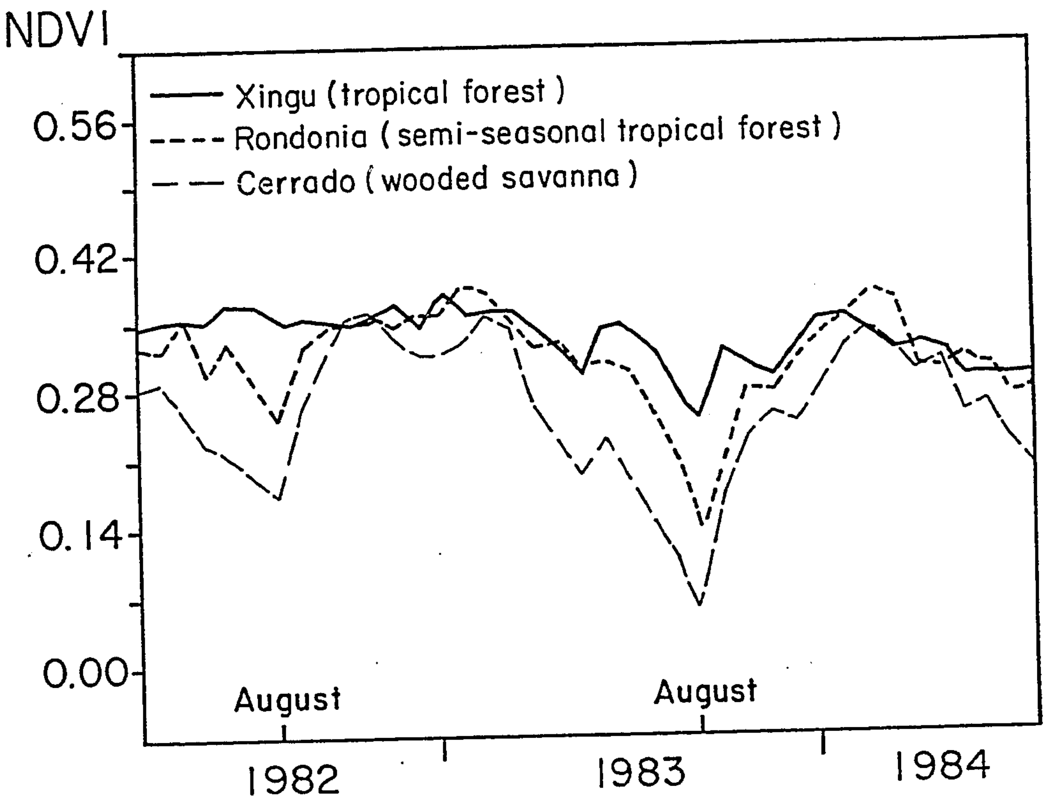

Figure 1.8. The use of multi-temporal AVHRR-derived NDVI data in the Amazon can distiguish two forest types and cerrado (from Malingreau and Tucker 1987).

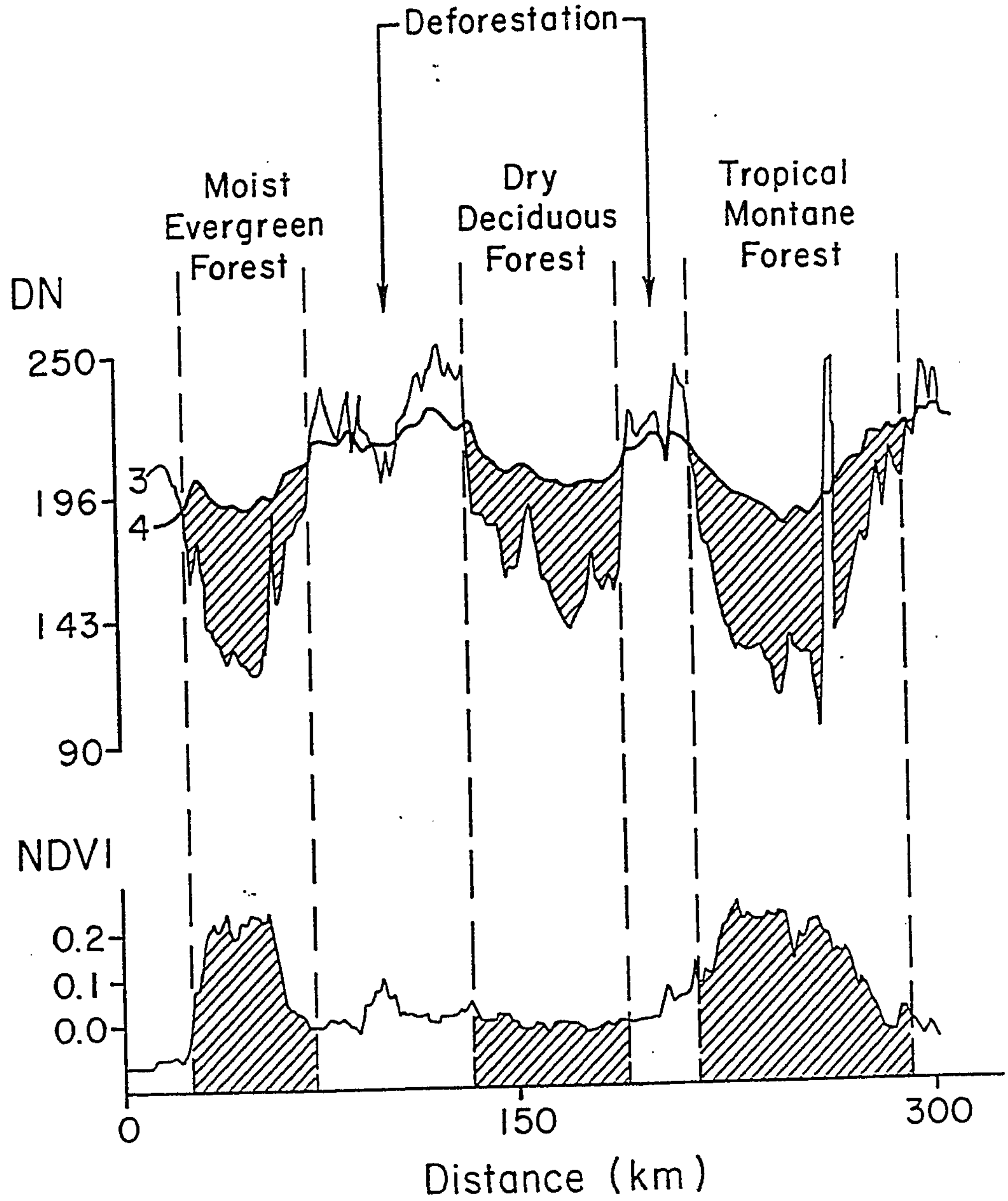

Figure 1.9. Thermal channels 3 and 4 on the AVHRR can be used togther to distiguish different forest types and deforestation in South Asia (from Malingreau 1986).

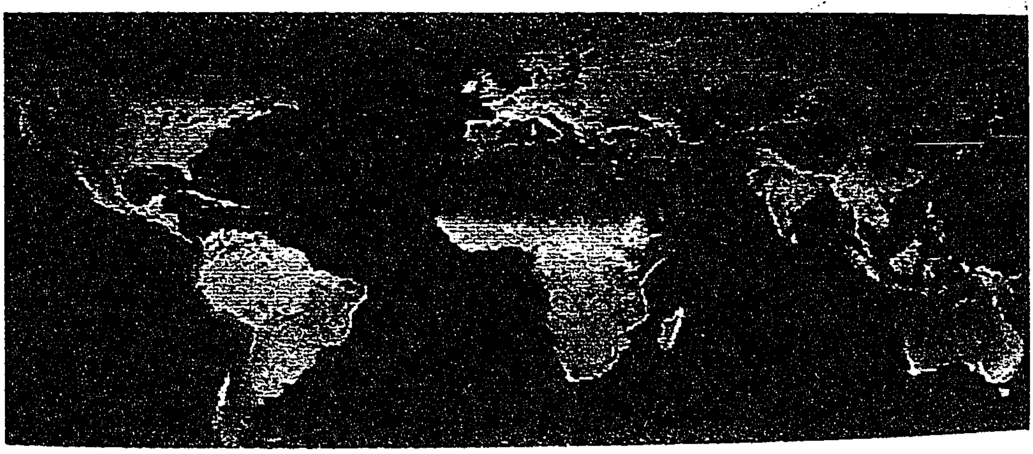

Figure 1.10. A global classification of vegetation based on phenology derived from multi-temporal changes in the NDVI.

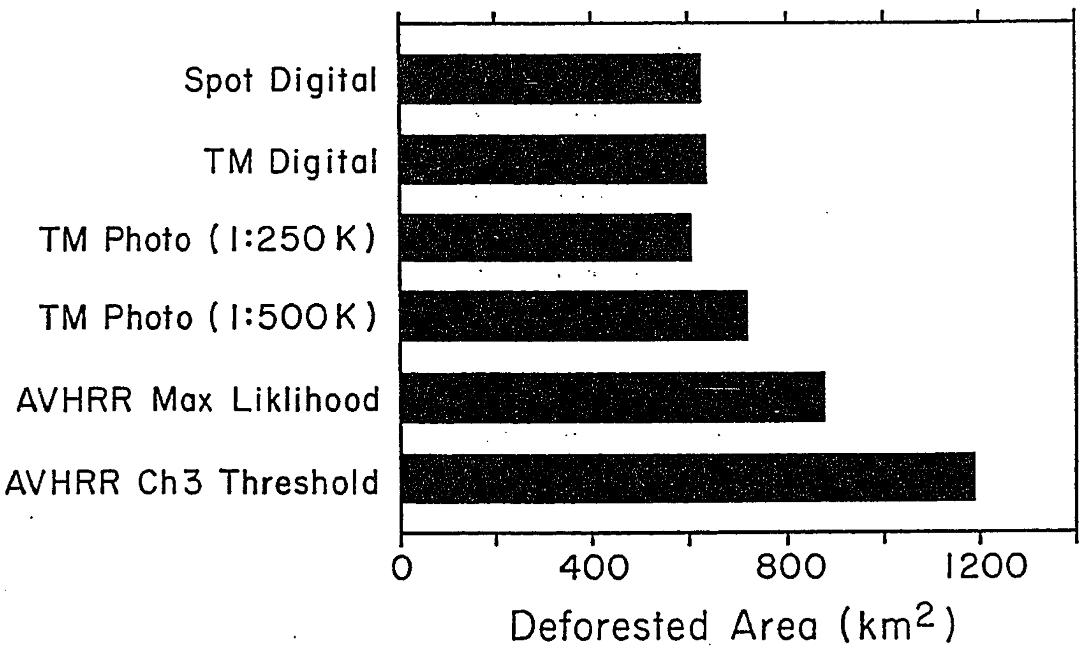

Figure 1.11. A comparison of different remote sensing methods for quantifying deforestation in the tropics. This figure shows results of a study in which TM, SPOT, and AVHRR data were acquired during the same period in 1988 in a study site in Rondonia, Brazil. SPOT data were processed at full resolution using supervised digital image processing techniques. TM data were processed at full resolution using supervised digital image processing techniques, and also analyzed at 1:250,000 and 1:500,000 scale using interpretation and GIS digitizing on top of single channel photoproducts. AVHRR-LAC data were processed using a multi-channel Maximum Liklihood classifier and channel 3 brightness temperature threshold.

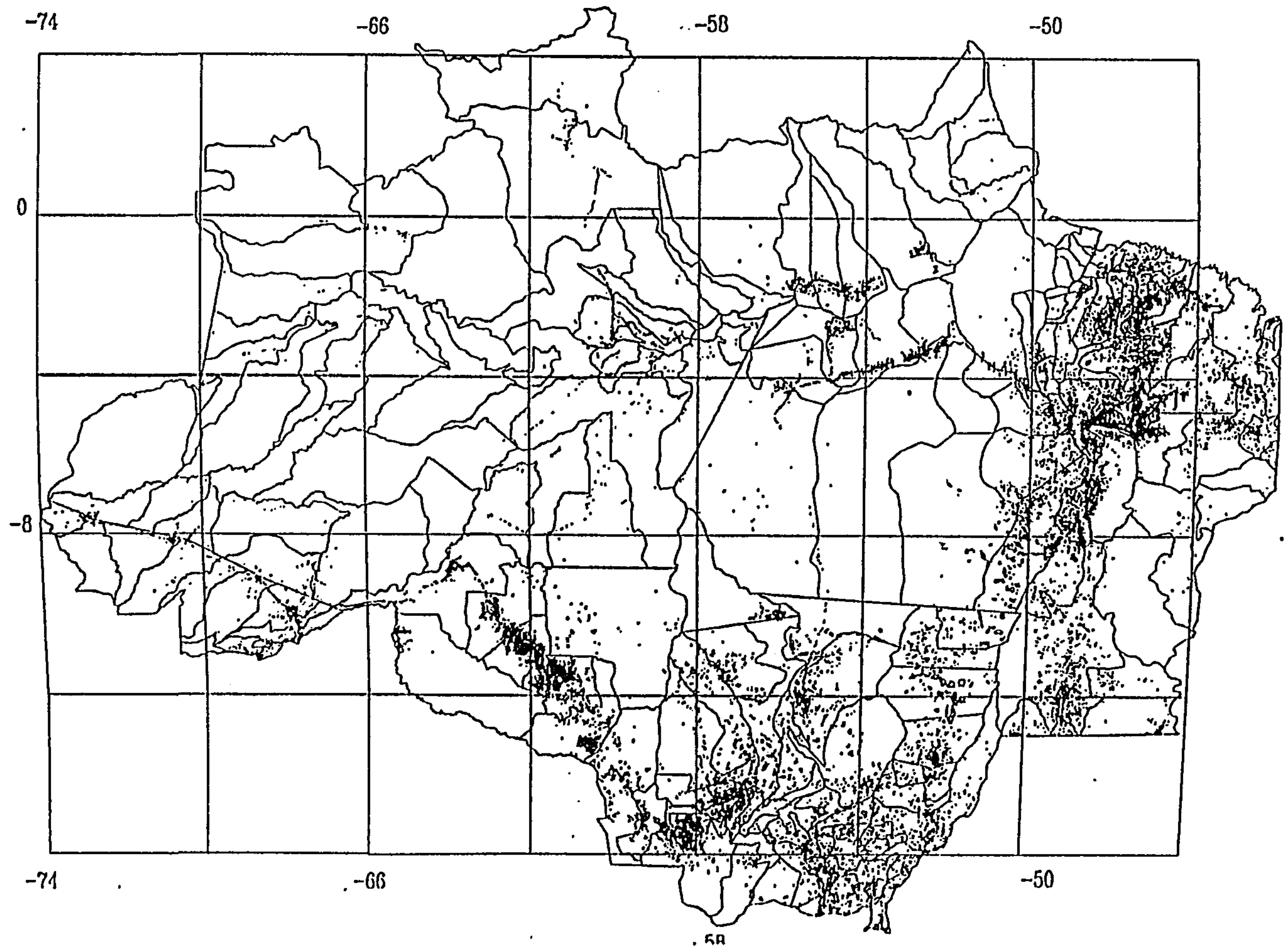

Figure 1.12. A geographically referenced dataset of deforestation in the Legal Amazon of Brazil for 1978. This dataset was compiled in a geographic information system from 1:500,000 scale maps but has been greatly reduced in size here. The dark areas show areas deforested between 1975 and 1978.

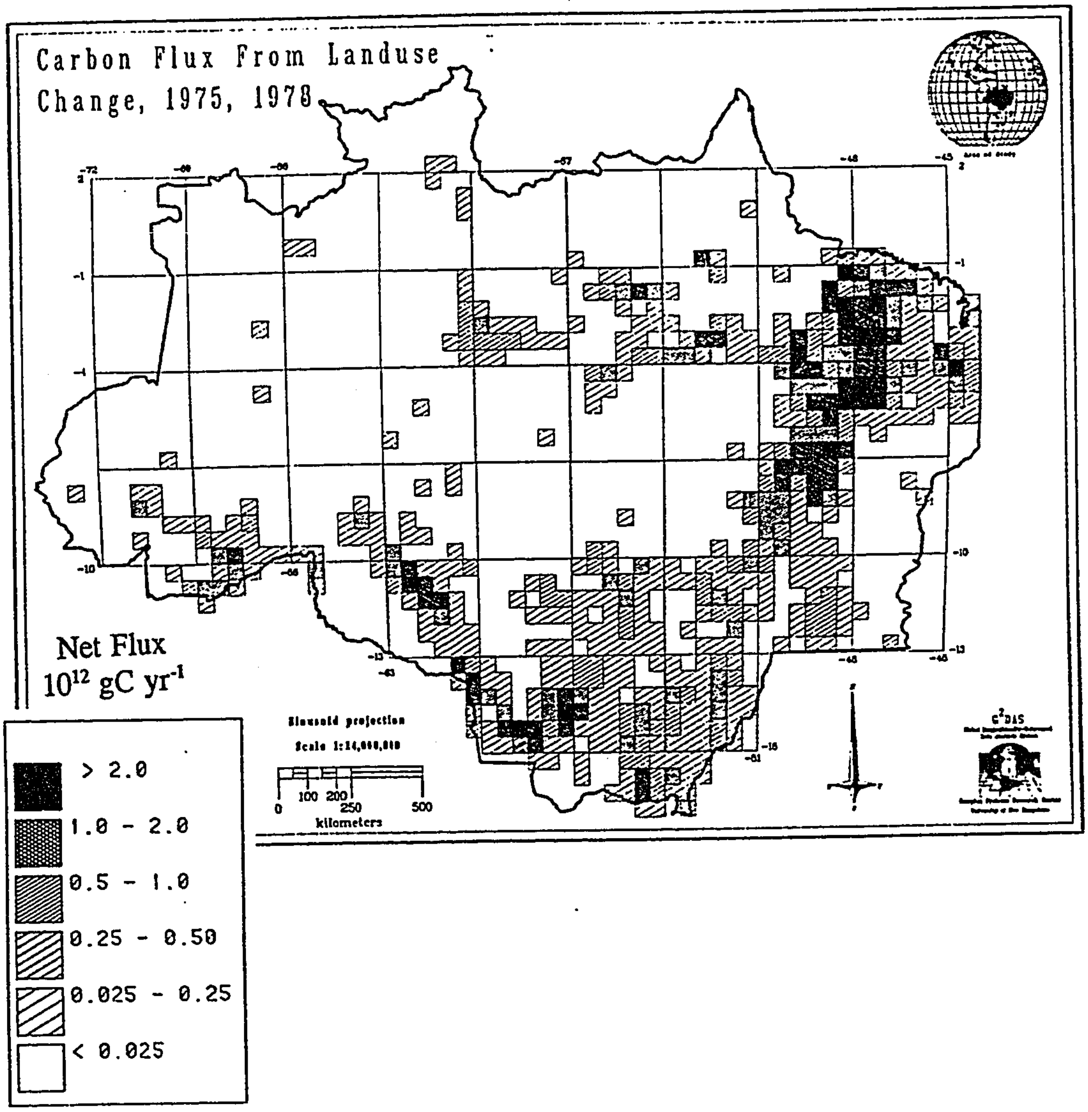

Figure 1.13. An estimate of the net annual flux of carbon from deforestation between 1975 and 1978 in the Legal Amazon of Brazil. The legend reports net flux in intervals of 10^{12} g C.

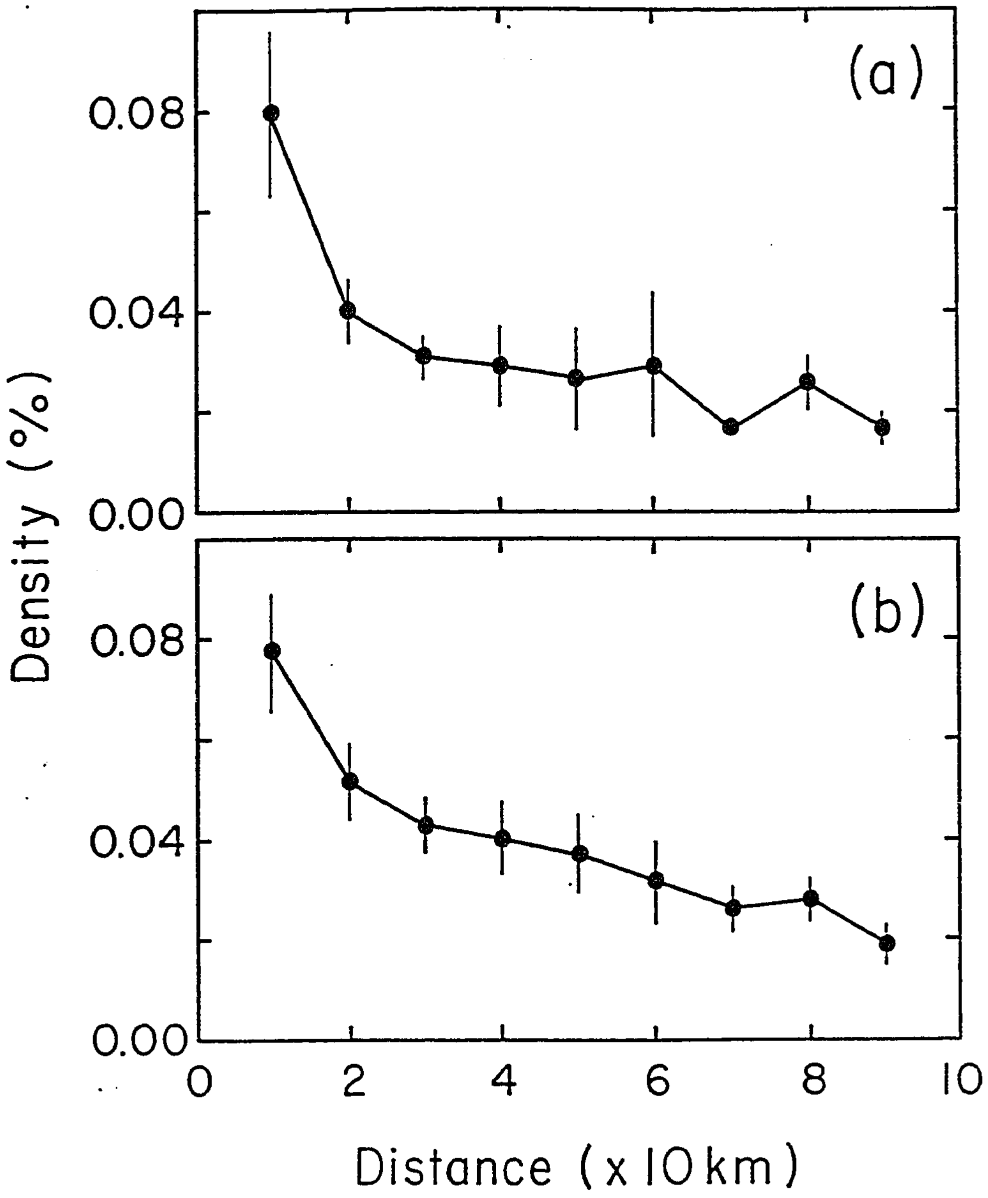

Figure 1.14. The spatial arrangement of deforestation shown as the density (percent of area) as a function of distance from dense settlements in 1975 (a) and 1978 (b).

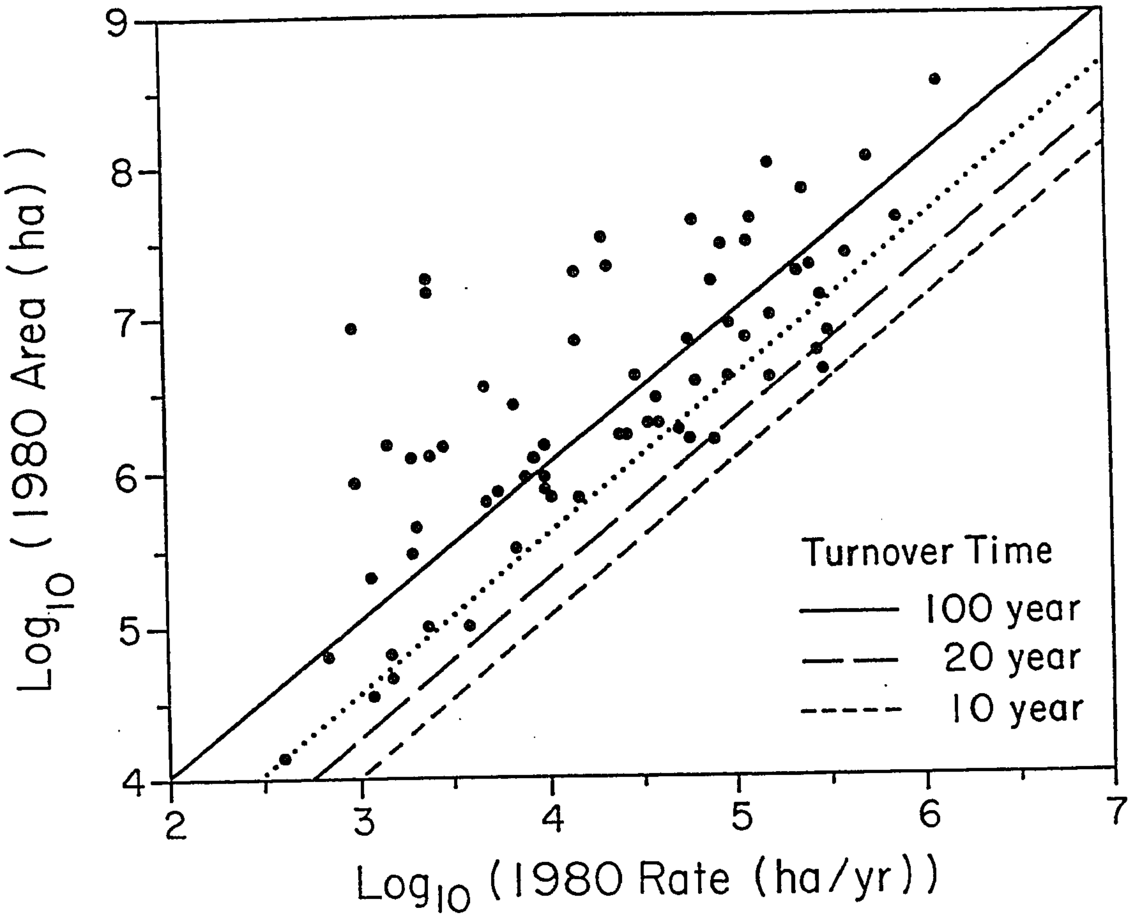

Figure 1.15. Tropical deforestation rates in 1980 plotted against area of closed forest in 1980 based on the FAO/UNEP data. Isolines show turnover times for various time periods. Turnover times were computed assuming constant rates of clearing andno regrowth. The dotted line shows a 20-year isoline assuming an exponential increase in the clearing rate which doubles in 20 years.

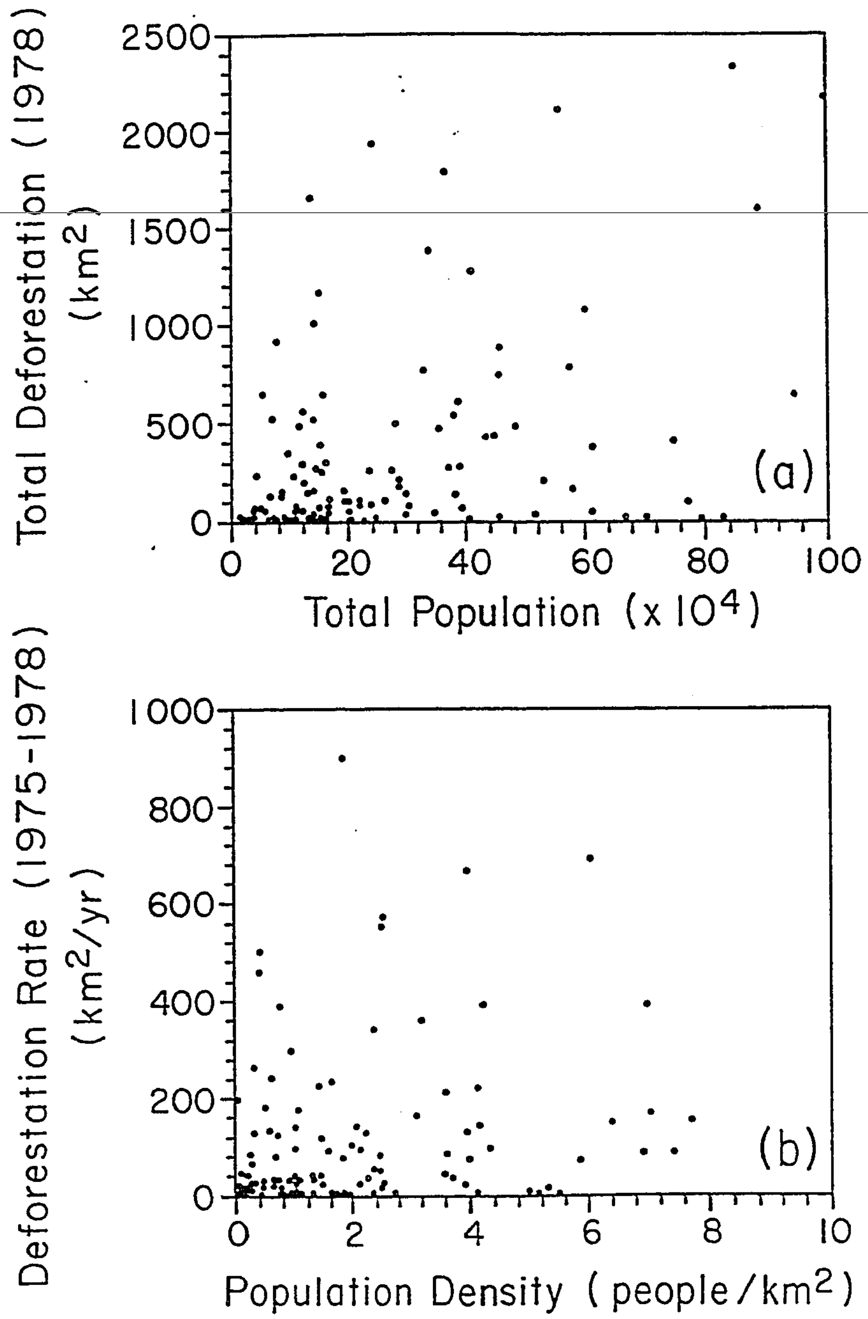

Figure 1.16. There appears to be no relationship between deforestation and population density. Scatter plots of population against total area deforested in 1978 (a) and population density against the deforestation rate in 1978 (b).

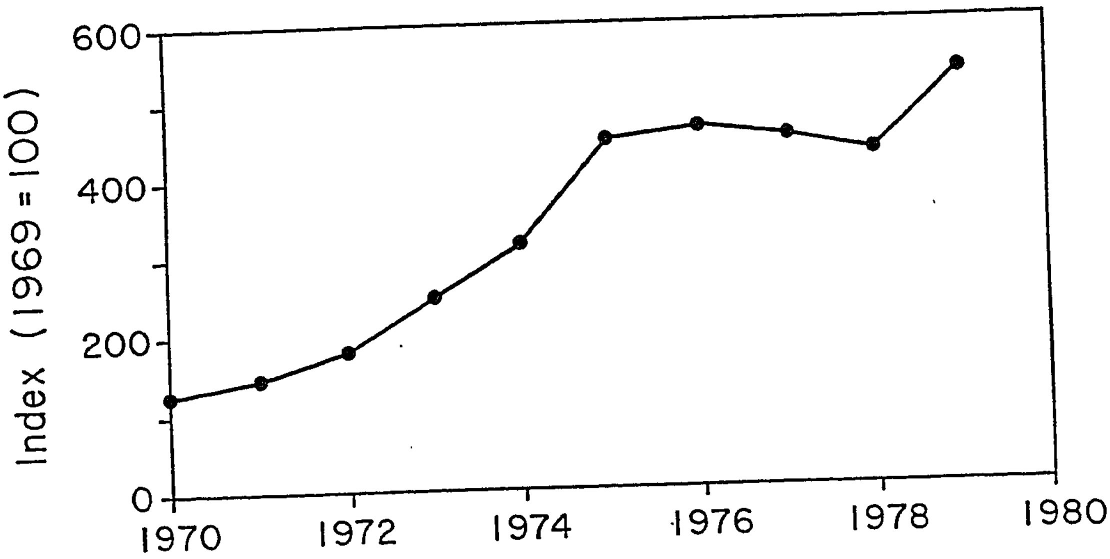

Figure 1.17. Change in the amount of crop credits provided to the agricultural sector in Brazil between 1970 and 1979.

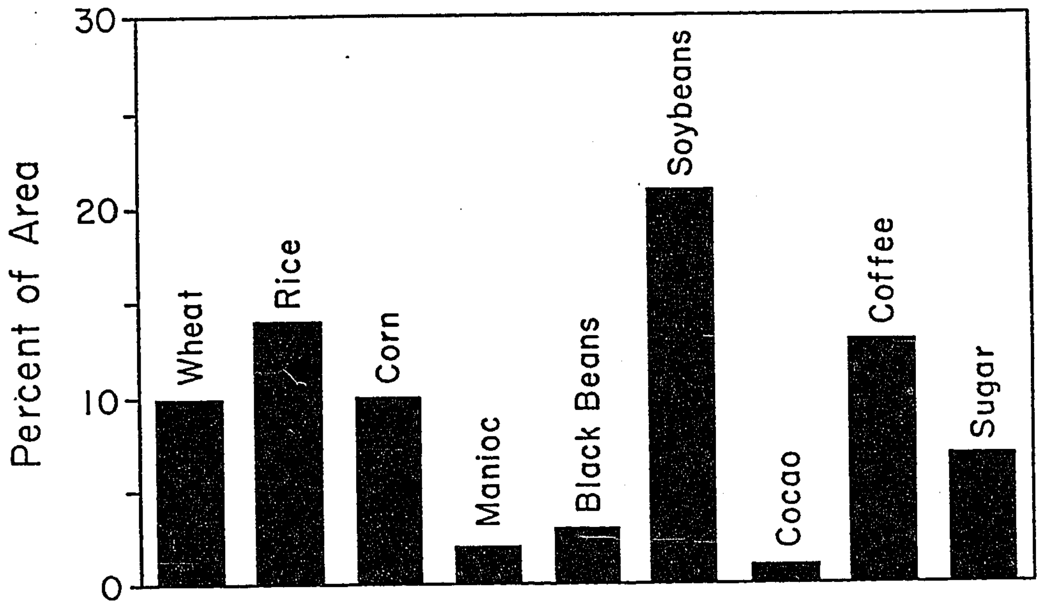

Figure 1.18. Allocation of crop credits in Brazil in 1978, as a percent of agricultural crop area.

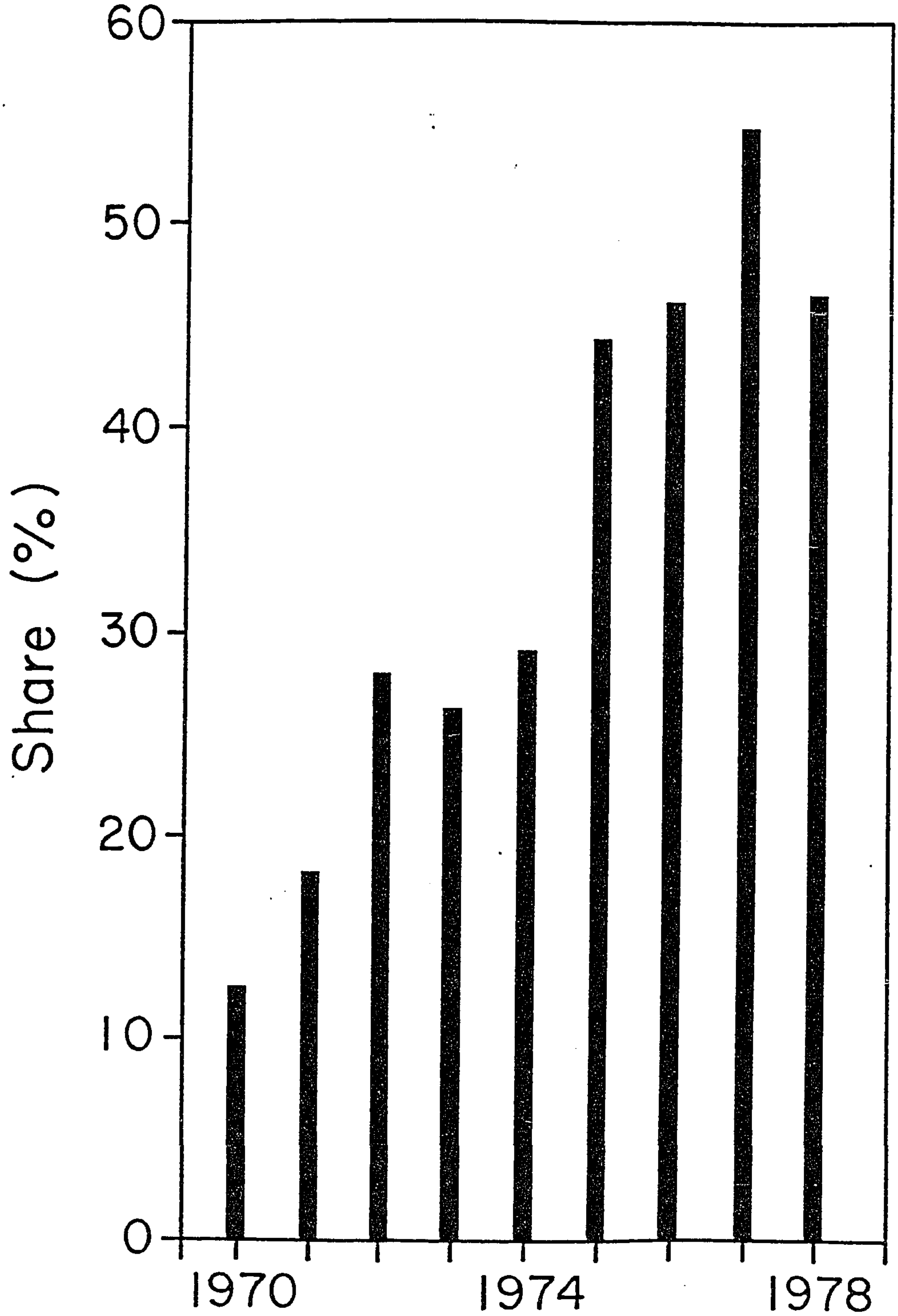

Figure 1.19. Brazil's share of the world soybean market from 1970 to 1978.

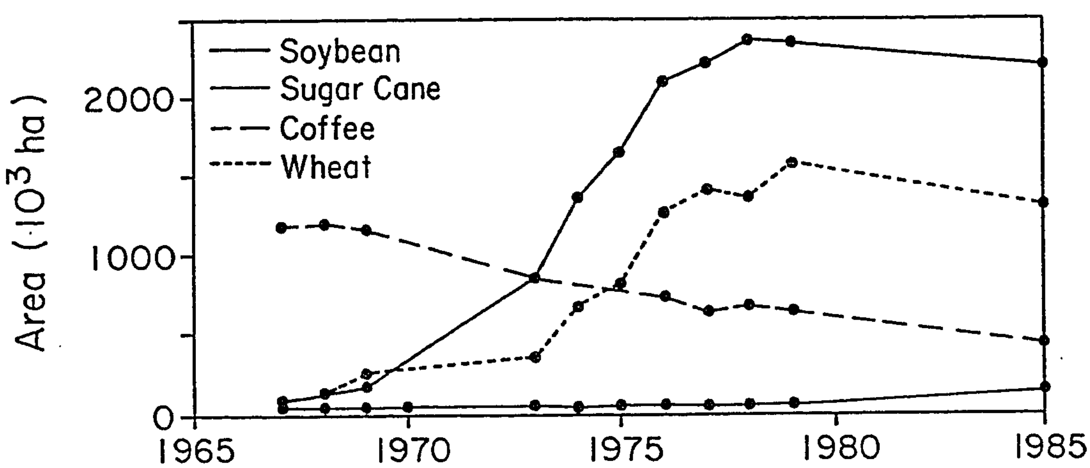

Figure 1.20. Change in area planted in major crops in Parana state between 1965 and 1985.

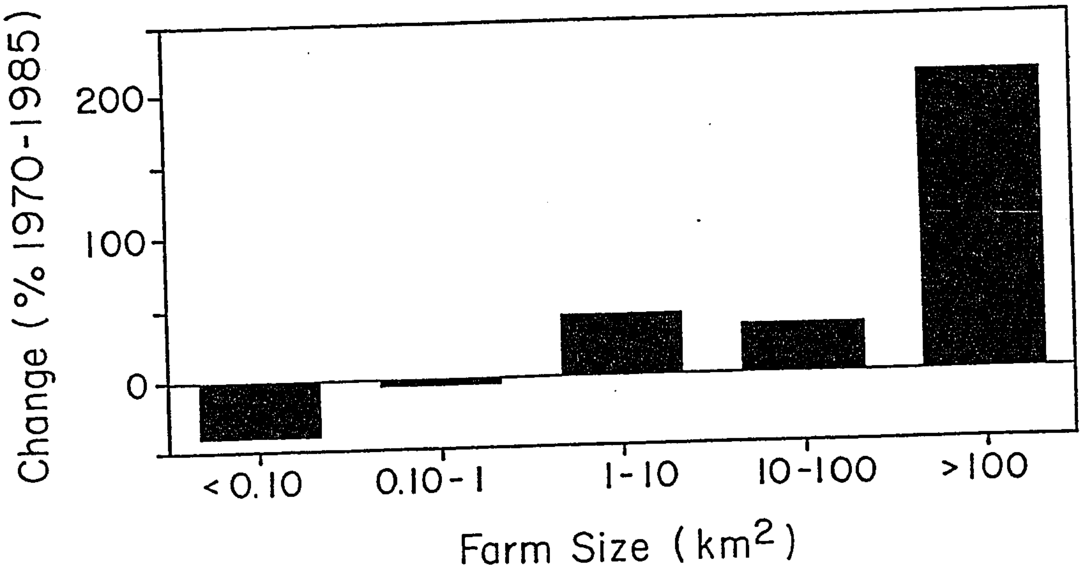

Figure 1.21. Change in the farm size distribution in Parana state between 1970 and 1985. Units are percent increase or decrease.

CHAPTER 2

SPATIAL ANALYSIS OF LAND COVER CHANGE AND CARBON FLUX ASSOCIATED WITH BIOMASS BURNING IN BRAZIL, 1970-1980

Imbalances in the Global Carbon Cycle

The atmospheric concentration of carbon dioxide has increased steadily since direct measurements have been taken in 1958. Carbon dioxide has risen from 315 ppmv to 351 ppmv in 1988 (Keeling et al. 1989, Boden et al. 1990). With the development of techniques to analyze the concentration of CO_2 in bubbles of air trapped in deep ice cores, it is also possible to estimate the historical atmospheric concentration of CO_2. Since 1750 there has been a steady increase, from 279 ppmv (Neftel et al. 1985). Human activities are largely responsible for the observed increases. Fossil fuel burning is currently the most important source of carbon dioxide. Evidence from ice core data suggests atmospheric concentrations of CO_2 began to rise before 1850, a time prior to significant inputs from fossil fuel combustion. Approximately 35 percent of the current net flux of carbon dioxide is biogenic. However, biogenic sources are also important. Moreover, the long-term historical release of carbon dioxide from human disturbances to the biota have been approximately equal to the release from fossil fuel burning (Houghton and Skole 1990).

Net additions to the atmosphere from fossil fuel and biomass burning and oxidation are partly removed by oceanic uptake. However, oceanic uptake is lower than the net additions, and the atmospheric concentration has risen as a result of this imbalance. Furthermore, measurements of the atmospheric increase when compared to estimates of the net flux of biogenic carbon, fossil fuel emissions, and ocean uptake cannot be accommodated in a balanced carbon budget. Houghton et al. (1983) and Houghton and Skole (1990) have used a simple equation of the form:

$$dA_t = B + F - O \qquad (1)$$

to describe this, where dA_t is the net increase in the atmospheric carbon at time, t, B is the net flux from land clearing and biomass burning, F is the net flux from fossil fuel burning, and O is the net oceanic flux. The units are 10^{15} g C yr^{-1}. When values for 1980 are substituted into the equation for each term, it is possible to describe the current situation:

$$3 = 1.8 + 5.2 - 2.5 \qquad (2)$$

The equation is not balanced. Explanations for this imbalance in the budget center on two possibilities. First, the individual terms of the equation may be in error, or improperly modeled. The emission from fossil fuels is well known and certain, as are the atmospheric measurements. However, the oceanic and biogenic terms are not.

Second, the individual terms of the equation may not be complete, and another term --the so-called missing sink--may be important.

Recent analyses by Tans et al. (1990) have suggested a large, unaccounted net sink in undisturbed, predominantly northern, forest ecosystems. The analysis of Tans et al. (1990) utilized a constrained approach, coupling observations of the atmospheric gradient of CO_2 from the GMCC flask network, measurements of oceanic pCO_2, estimates of land surface fluxes from fossil fuels and deforestation, and a general circulation model. The approach provides a geographically-specific assessment of sources and sinks, but is highly dependent on the magnitude of the tropical source term; the size of northern sink is related to the magnitude of the tropical deforestation source.

In another constrained analysis, Houghton and Skole (1990) have compared a model estimate of the historic net flux of carbon from land use change with estimates of the total biospheric net flux derived from a deconvolution of ice core data and ocean models (Siegenthaler and Oechgher 1987). This analysis, reproduced in Figure 2.1, shows general agreement between the estimates prior to about 1930, after which the net flux from land use change increases while the total biotic flux declines. This suggests either the land use or deconvolution analyses are wrong, or the difference reflects a net sink in undisturbed ecosystems. If a sink in undisturbed ecosystems exists, and is somewhat evenly distributed geographically, the amount per unit area would be too small to measure in the field. Thus, a combination of constrained analyses of this kind and ecosystem models would be required to further elucidate the nature of the sink.

An important consideration in analyses such as Tans et al. (1990) and Houghton and Skole (1990) is the importance of knowing the biogenic flux from land use change, particularly the tropical deforestation component. Improved definition of the imbalance in the global carbon budget will come with better definition of the individual terms of equation (1) above, with the biogenic term being particularly important. Moreover, the use of constrained analyses, in which additional terms to equation (1) are inferred as residuals from known terms, will require increased confidence in the estimate of biogenic fluxes.

Biogenic Fluxes of Carbon

Human activities have transformed the natural landscape over the past two hundred years in a variety of ways and to varying degrees. Quantitatively, the most important type of change has been the direct conversion of natural land cover to agriculture (Richards 1984). In recent years this form of land conversion has been especially common in the tropics. Large areas of South America, West Africa, and Asia are undergoing extensive land transformation as a result of population growth and economic development. Such changes in land cover influence the net exchange of carbon between the land and atmosphere (Detwiler and Hall 1988, Houghton et al. 1985b, Houghton et al. 1983, Woodwell et al. 1983, Moore et al. 1981, Bolin 1977).

The long term historical net flux of carbon due to land conversion has been documented by analyses based on direct estimates of land use data and ecosystem response characteristics (Houghton and Skole 1990). These studies suggest that while some land transformations increase the amount of carbon stored on land, the overall historical trend has been one of increasing forest conversion to agriculture. This has reduced the amount of carbon stored on land and resulted in a net flux of carbon to the atmosphere.

The net release of carbon from the world's biota has been increasing over the past 150 years. While large releases in recent history can be attributed to land cover conversion in the temperate zone systems, tropical deforestation appears to be the major source of the release today. The current global net flux of carbon from land cover conversion in the tropics is between 0.4 and 2.5 x 10^{15} g C, or approximately 90% of the net global flux (Houghton et al. 1985b). This represents between 18% and 49% of the release from fossil fuel combustion (Marland et al. 1985, Marland and Rotty 1984). On a long term basis, from 1700 to 1980, the total release from the biota was approximately equal to the long term total release from fossil fuels (Houghton and Skole 1990).

Most land conversion in the tropics is associated with burning.Recent observations using daily satellite remote sensing of the Brazilian Amazon have identified as many as 20,000 fires per month, accounting for an estimated area of 204,000 km^2 for the dry season of 1987 (Setzer and Pereira 1991, Kirchhoff et al. 1989). Most of these fires were on sites already deforested, but approximately 80,000 km^2 were estimated to be new clearings. Burning associated with deforestation in Latin America constitutes approximately 31% of the net flux of carbon (Houghton et al. 1990). Burning is an important step in the conversion of natural systems to agriculture; the process removes unwanted herbaceous cover and releases nutrients to improve soil fertility (Buschbacker 1986, Hecht 1983). In Brazil and elsewhere in the tropics there are two distinct types of anthropogenic biomass burning. The first occurs when natural ecosystems are initially cleared. This burning is often associated with deforestation, but also occurs in savanna and grassland systems opened up for the first time. The second is the repeated burning of existing pastures on a short rotation as a form of land management to maintain forage productivity.

The burning of biomass in the tropics results in the release of radiatively important carbon trace gases, such as CH_4 and CO. Based on measurements of elemental ratios in smoke plumes from fires in the Brazilian Amazon, 8-12% of the total carbon emission from forest and savanna fires is CO (Greenberg et al. 1984, Crutzen et al. 1985, Andreae et al. 1988). On a global basis some estimates put the source of CO from anthropogenic biomass burning in the tropics between 0.2 and 0.8×10^{15} g C, an amount approximately equivalent to industrial sources (Crutzen et al. 1979, Crutzen and Andreae 1990). The total global emission of CH_4 is lower at approximately 0.03-0.05 x 10^{15}g C, which is approximately 10% of all sources (Bolle et al. 1986, Crutzen 1983, Crutzen and Andreae 1990). Nevertheless, anthropogenic biomass burning might represent as much as 31 percent of the annual increase in global CH_4 emissions (Bolle et al. 1986, Seiler 1984).

Most global estimates of trace gas emissions from biomass burning utilize the few studies which have attempted to quantify the rate and geographic distribution of biomass burning (cf. Seiler and Crutzen 1980) in combination with emission ratios derived from in-situ measurements of the chemical composition of smoke plumes (Greenberg et al. 1984) and haze layers associated with plumes (cf. Andreae et al. 1988). There have been no studies which have attempted to define the relatively fine scale (50 km; 1:10 M scale) spatial distribution of carbon flux from biomass burning over time. There are a number of advantages to developing a geographically referenced analysis of terrestrial carbon fluxes in the tropics. For instance, the wide range in estimated current net flux of carbon results, in part, from uncertainties concerning the kind of vegetation converted to human uses and the rate of tropical deforestation. Since current analyses have not been able to geographically co-register maps of land cover with maps of land cover conversion activities, such uncertainty might be resolved, or precisely defined, by making geographically detailed analyses (Emanuel et al. 1985, Houghton et al. 1985a, Bolin 1984, Emanuel et al. 1984).

Among other things, this would permit the linking of flux estimates to tropospheric chemistry models, atmospheric circulation models, and direct observations.

The role of the tropics is important, but poorly understood. By coupling estimates of tropical biotic source terms, estimates of ocean uptake, a modeled atmosphere, and in-situ measurements of the latitudinal gradient of atmospheric carbon dioxide concentration, an analysis by Tans et al. (1990) suggests the possibility of sink for carbon in the mid to high latitudes. This conclusion depends in part on our knowledge of the tropical source term. The temperate zone sink is computed as a residual of several presumably known factors, one being geographical location and size of the net flux of carbon from tropical deforestation. The magnitude of the sink varies in their analysis by nearly a factor of 2 depending on the size of the tropical source term.

In this report, we present an analysis of the recent history of carbon flux from biomass burning in Brazil. Emphasis is placed on the derivation of a spatially detailed account of CO_2, CO, and CH_4 emission during the period, 1970-1980. We utilize global-scale geographic information system techniques (Skole et al. 1992) and a methodology for historical reconstruction based on direct estimates of land cover conversion in different ecosystems over time.

Method of Analysis

The overall goal of this study was to estimate and describe the spatial distribution of fluxes of CO_2, CO, and CH_4 as a result of anthropogenic biomass burning in Brazil during the period 1970 to 1980. We focus on biomass burning associated with the conversion of forests and variety of other natural land cover types to human use, but we also make an estimate of the flux associated with burnings for pasture maintenance. The latter flux is considered separately. This analysis does not consider natural fires.

Brazil was chosen as the location for this analysis for several basic reasons. It is continental in scale, encompassing the largest continuous tropical forest biome in the world, and thus provides an excellent place for a global-scale pilot study. It also encompasses a diversity of land cover types other than forests, including savanna systems, grasslands, and wetlands. It is a region which has undergone rapid and expansive land transformation in the recent past. It is an intensively studied region with relatively large amounts of ancillary data available. And finally, we have had access to a relatively rich and diverse set of data from tabular statistics, remote sensing analyses, and in-situ studies.

Brazil is also important in the context of global carbon cycle research. By current estimates, the flux of carbon in 1980 due to land cover conversion in Brazil is 0.336 x 10^{12} g C (Houghton et al. 1987). This represents approximately 20% of the total release of carbon from the tropics, making it the single largest source of biogenic carbon dioxide (Houghton et al. 1987). The rate of deforestation in Brazil, estimated by FAO/UNEP (1981) for 1980, is one-fifth of the global total. While these figures are impressive, there is very little detailed information on the geographical and temporal patterns of land cover conversion and carbon flux in Brazil.

The period of analysis (1970 - 1980) represents a time when Brazil was initiating intensive economic development programs, both inside and outside of the Amazon region, resulting in extensive land transformation. This period coincides with other studies of carbon flux dynamics (cf. Houghton et al. 1987, Houghton et al. 1990b), biomass burning field campaigns (cf. Greenberg et al. 1984), and remote sensing studies (cf. Tardin et al. 1980).

This period also offers the possibility to develop analytical methods for reconstruction of the recent past. Carbon cycle dynamics are sensitive to the long-term flux of carbon and it has been necessary for such investigations to estimate the historical net flux. The contemporary period (since the early 1980s) could best be assessed with satellite data, but prior to 1975 none exist.

This analysis employs an approach which links historical analyses to contemporary analyses from remote sensing to map the geographical pattern of land cover change using a geographic information system (GIS). This approach is shown in Figure 2.2. One advantage of a GIS approach is its ability to integrate a variety of highly detailed spatial datasets on land cover and land cover change. This permits an evaluation of land cover changes as they occur in different ecosystems of varying biomass. It also provides a potential capability for comparing results to direct observations through the coupling of the spatially detailed output to atmospheric circulation and tropospheric chemistry models.

To estimate the release of total carbon, we employed an approach similar to that described by Seiler and Crutzen (1980), but with an added spatial dimension:

$$FC_j = [(B_{ij} * 0.45) * A_{ij} * b_i] - U_{ij} \qquad (3)$$

where FC_j is the amount of C released at location j, B_{ij} is the aboveground biomass for cover type i at location j, A_{ij} is the area of cover type i burned at location j, and b_i is the combustion efficiency for cover type i. An uptake term, U, has been added to reflect the effect of abandoned and regrowing sites which will accumulate carbon in the process. The analysis here accounts for net changes in land cover, and therefor this term cannot be included in the calculation. Moreover, there is virtually no information on the amount of secondary growth on deforested sites. Such an analysis would have to use large amounts of high resolution satellite data, which are not available at this time. We assume a factor of 0.45 for the conversion of biomass to carbon.

The result is a two-dimensional representation of the release of carbon. Using published emission factors and the following equation, it is then possible to derive emission rates for the constituent gases:

$$FC_j = MCO_{2j} + (MCO_{2j} * ECO_{ij}) + (MCO_{2j} * ECH_{4ij}) \quad (4)$$

where MCO_{2j} is the CO_2-C released at location j, ECO_{ij} is the emission ratio of CO to CO_2 for cover type i at location j, and ECH_{4ij} is the emission ratio of CH_4 to CO_2 for cover type i at location j. The component terms for each gas can be iteratively solved from this equation. This analysis does not consider non methane hydrocarbons, but the approach would allow for such.

Data

Land Cover Conversion and Deforestation

To distribute land cover conversion and carbon flux on a geographical basis, data were tabulated for each of the 3973 town-level political districts in Brazil. Since there are no data on land cover conversion or deforestation directly, a method was developed to estimate conversion rates indirectly from land use statistics. Land use data was compiled from the Brazilian national agricultural census, Censo Agropecuaio, for the years 1970, 1975, 1980 (IGBE 1970, 1980). These sources provide data on the area in estabelecimentos, or total farmland, for each district.

Since the total farmland area includes undisturbed land, an adjustment to the data was made so that it represents only the disturbed portion. For instance, some of the farmland area remains in natural forest and is not directly converted. National summary statistical series (IBGE 1979, 1981) provide a detailed breakdown of the total farmland at the state level data into 9 subcategories of land use (temporary crops, permanent crops, planted pasture, natural pasture, fallow, natural forest, planted forest, unproductive land, and productive land not utilized). Ratios of converted land to total farmland for each state could be developed and applied to the district level data to scale the original figures to a more accurate estimate of area converted for each date.

Using a GIS, a digital map of the political borders of each geopolitical unit was constructed from maps ranging in scale from 1:100,000,000 to 1:3,000,000 (Figure 2.3). Each polygon in this data set represents the basic geographic data unit for which the land use data was tabulated in a relational database system. Each was assigned a numerical label corresponding to an identifier in the relational database of land use from IBGE data, thereby making it possible to assign the land use data to the map base.

To maintain some uniformity in the size of district polygons on the base map and to minimize a data management problems, some of the data for municipios in the eastern part of Brazil were aggregated up to the level of Micro-regions, the next smallest geopolitical unit in Brazil. This resulted in a manageable 515 individual districts. The resulting digital land use map could then be automatically combined with digital land cover maps and other pertinent datasets (Figure 2.2) to estimate the net flux of carbon. It is important to note here that the emphasis is placed on estimating the initial net release of carbon when natural ecosystems are converted to agriculture (crops and pasture). District boundaries as they existed in 1970 were used. The boundary of the Legal Amazon (IBGE 1982a) was also digitized so the analysis could differentiate activities inside the Legal Amazon region from activities in Brazil as a whole.

Remote sensing is probably the best source for land cover conversion data. However, such data can be obtained for recent years only. The first earth observation satellite was launched in 1972. Data for Brazil exist only since 1975, and most is after the mid 1980s (Tardin and Pereira da Cunha 1990, Maligreau and Tucker 1988, Nelson et al. 1987, Nelson and Holben 1986, Tucker et al. 1986, Tardin et al. 1980). Few or no data exist outside the Legal Amazon and of the data for the Legal Amazon region, most is concentrated only in a few key states.

Pasture Burning

The dataset discussed above provides information on conversion of land cover to crops and pastures. It also gives data on the areal extent of planted and natural pastures. Pastures in Brazil are regularly burned to maintain productivity. Thus, we are able to estimate the release of carbon and trace gases from pasture maintenance practices. The release of carbon from pasture maintenance is balanced by the uptake of carbon when the pasture regrows. This balance is maintained for CO_2 and the net flux is zero. For other trace gases, such as CO and CH_4, however this process might be an important net release.

Few data exist which give an indication of the average frequency of pasture burning. Some observers suggest an average period of 2-5 years in pastures of the Brazilian Cerrado (Eiten 1972). This is supported in principle by Buschbacher (1986) and Uhl and Buschbacher (1985), who report that after three or four years, new pastures lose vigor because of soil infertility and competition with unfavorable weed growth. This necessitates burning to revitalize the pasture. In this analysis we used a figure of 2.3 years for the average rotation period. This figure is applied to the total area given in the IBGE agricultural census documents (see above) in natural and planted pastures. This area is less than the total savanna area in Brazil. In the Legal Amazon, for instance, Fearnside (1990b) estimates approximately 20-30% of the area is savanna. This area, some 100-150 x 10^6 ha., is larger than the 31 x 10^6 ha. we use for the area in natural pasture. Some analysts have used the total savanna area as a basis for estimating this kind of gas flux (Hao et al. 1990). This analysis uses actual owned and occupied pastures, both in and out of the savanna region, as a basis. We believe this to be more accurate. It must also be noted that areas utilized for crops are also frequently abandoned to secondary growth, and then re-cleared and burned as a means to maintaining site fertility. The computation of pasture burning is done solely to estimate the additional associated flux of CO and CH_4, and is not considered in the estimate of the net flux of CO_2.

Dominant Natural Land Cover

This analysis considers land conversion and biomass burning in a variety of ecosystems. The distribution of these ecosystems is provided by a land cover dataset. A digital map database of the dominant natural land cover prior to disturbance was developed as the basis for later assigning biomass to ecosystems. We digitized a 1:15 M scale map of land cover developed by the Institute of Geography at Moscow State University (Figure 2.4). This map seemed to provide the most amenable set of land cover categories for assigning biomass. The land cover map thus produced represents natural, predisturbance cover. There are ten broad cover types in this dataset, which can be grouped into four general categories as shown in Figure 2.4 and Table 2.7.

The forest category represents closed canopy forest of the Amazon Basin, the Atlantic wet forest systems in the east of Brazil, and the southern forests. The woodlands classes contain three subgroups. Forest steppe is a sparse forest system with grass understory where grass predominates. It is comparable to Matthews' (1983) "grass with shrub cover." Bush forest is a dry open canopy woodland system, often referenced as Caatinga in Brazil. It is roughly comparable to Olson's (Olson et al. 1983) "tropical dry forest and woodland" or Matthews' "xeromorphic forest woodland." The sparse forest category is a savanna system often called Cerrado in

Brazil. It is roughly comparable to Olson's "tropical savanna and woodland" classification and Matthews' "grassland with 10-40% woody cover."

The Grassland Savanna/Steppe classification contains three generally non-forest classes. Wet tallgrass savanna includes land cover dominated by grasses, generally referenced as humid savanna but also including the Brazilian Pantanal, Campo de Varzea, and palm forest in the eastern Amazon. It is similar to Matthews' "grass with less than 10% woody cover." Dry lowgrass savanna includes what is often referenced as Campo and Campina in Brazil. It is generally similar to Olson's "warm shrub and grassland" classification. The true steppe category includes all other grassland formations. Wetlands, including coastal marshes and mangroves, comprise a small area in Brazil. These formations are grouped with arid systems as "other" in this analysis.

Other maps might have been adequate, but those already in digital form are more coarse than this one which we used (cf. Matthews 1983). The scale of this map corresponds roughly to the scale of a map which would have been derived from AVHRR satellite data. A Brazilian map of 1:5 M scale developed by the IBGE (IBGE 1982a) might have been more accurate. However, one goal of this analysis was to develop a global methodology using datasets with global coverage whenever possible.

Another approach might be the use of coarse-scale remote sensing data (cf. AVHRR). The use of satellite data would greatly enhance the classification of land cover by providing information on the exact location of boundaries, improved classification for the registration of biomass, and an objective method of delineating land cover types. Such datasets do not now exist. A simple land cover classification derived from AVHRR data has been made for south America (Townshend et al. 1987), but the major objective of this classification experiment was to test the robustness of different criteria rather than to define a real map. Moreover only very coarse resolution data (16 km) was used. The accuracy of this dataset is not optimal at this time and could be greatly improved (c.o. Justice, personal communication).

Stocks of Carbon in Natural Vegetation

Three general sources provided estimates of the aboveground stocks of carbon in vegetation which were used in this study. The first estimate was provided by the global summary of major ecosystems of Olson et al. (1983). The second source is provided by estimates based on the carbon stocks of life zones in Latin America (Brown and Lugo 1982) and forest inventories (Brown and Lugo 1984, Brown et al. 1989). The third source was from a varied list of authors reporting results from Brazil, including the summary by Fearnside (1987a). These data are presented in Table 2.1.

There is a paucity of biomass data for Brazil, and it was not possible to get enough data to truly capture the heterogeneity of biomass. Generally, the literature sources used three methods. Ecologists often report the results of direct measurements in experimental plots using destructive sampling or allometric regressions of tree height and dbh (diameter at breast height). These studies (cf. Whittaker and Likens 1973, Klinge et al. 1975, Brown et al. 1989) report total stand biomass in intact undisturbed communities. Another approach is based on forest stand inventories and/or volume data (cf. Brown and Lugo 1984, Brown et al. 1989). These values have been lower than those estimated on experimental plots. The lower results are likely due to two factors: a) the experimental plots often represent primary vegetation not geographically representative of typical sites, b) the stand inventories include sites which have been degraded over time by human use along with sites representing primary vegetation. The third approach uses the Life Zone concept (Holdridge 1947) to build a climate-based biomass distribution models (cf. Brown and Lugo 1984).

A distinction was made between the closed canopy equatorial forests of the Amazon region and the southern forests in the states of Parana, Rio Grande do Sul and Santa Catarina. These latter forests being sub tropical were given lower biomass than the Amazonian forests. The Atlantic forest, on the other hand, were assumed to have carbon contents similar to the Amazonian forests (see Table 2.1).

The Fate of Carbon Following Burning

The total flux of carbon is the net flux from several individual processes, including: soil respiration, the decay of slash and debris left on-site following disturbance, the decay of wood products taken off-site, biomass burned upon clearing, and the regrowth of vegetation and aggradation of soil organic matter during site succession. Each of these processes differ in timing. The flux from decaying vegetation is slow. The flux from biomass burning on the other hand is instantaneous. We only consider the release associated with burning, which may be 20-35 percent of the release from all processes (Houghton et al. 1991b). Belowground biomass of forests in Brazil averages 25 percent (Fearnside 1985, 1987a), but may vary considerably depending, in part, on soil fertility (Vitousek and Sanford 1986). When forests are cleared all of the belowground and some of the aboveground biomass (30-50 percent of total biomass) does not burn and instead decays on-site slowly over time (John 1973, Swift et al. 1979, Lang and Knight 1979). There is some evidence that in very hot savanna fires, some fraction of the belowground biomass is burned (Kauffmann et al. 1990). In this study, we assume that only the aboveground biomass burns.

Approximately 30% of the biomass is oxidized upon burning (Fearnside 1989, Houghton et al. 1991b). Based on qualitative observations Seiler and Crutzen (1980) estimated that 20-30% of the biomass is converted to elemental carbon (charcoal). More recent studies have found less elemental carbon formed, on the order of 2% (Comery 1981, Fearnside 1989). More carbon is oxidized when the drier savanna systems are burned. We assume 50 percent of the total biomass is oxidized. Nearly all the aboveground biomass of grassland and steppe ecosystems is oxidized when burned, approximately 50 percent of total biomass since much is belowground material.

Presumably, combustion efficiency is a function of site and vegetative moisture conditions. A useful approach would be one which considers the physical environment as well as the cover type to model combustion efficiencies. However the paucity of field measurements prevents such an approach. Table 2.2 presents the combustion efficiencies used to estimate the amount of carbon released from burning in each cover type.

Emission Factors

Emission factors derived from in-situ measurements of smoke plumes and ground sampling of fires in Brazil were used in Equation 4 above to estimate CO_2 and trace gas fluxes from total carbon. These are summarized as four estimates in Table 2.3. These data summarize average values from three research campaigns in Brazil. Emission factors within a single study or campaign often range considerably; Greenberg et al. (1984) report an order of magnitude range for CH_4 and a 5-fold range for CO. More recent studies report more narrow ranges. The variability between studies may reflect different meteorological conditions, or be related to the distance between the fire and where the sample was taken. Because of the variability between studies, we tested each one of these estimates individually in this study.

Greenberg et al. (1984) and Crutzen et al. (1985) report results from field programs during the dry season of 1979 and 1980. Aircraft sampling of smoke plumes and ground sampling were conducted in both savanna and forest fires. Greenberg et al. (1984) conclude there was little difference in the emission factors for savanna and forests. The factors given in Crutzen et al. (1985) represent both near (can samples) and somewhat distant (plume samples) measurements.

Andreae et al. (1988) report results from aircraft overflight sampling of haze layers associated with distant smoke plumes in forest fires during the Amazon Boundary Layer Experiment (ABLE 2A) campaigns in July/August 1985 (Harriss et al. 1988). These results report data for CO, but not CH_4. Methane emission factors were taken from plume measurements in Crutzen et al. (1985). These emission factors might be more typical of dilute haze some distance and time removed from the fires.

Aircraft sampling and ground measurements were made during the dry season of 1989 for the BASE-A experiments. These results are reported in Ward et al. (1990) individually for cerrado and forest fires. These estimates are considerably lower than previous estimates. Moreover, while Greenberg et al. (1984) found no significant difference between cerrado and forest emission factors during 1985, Ward et al. (1990)

report that forest emission factors for CO and CH_4 are noticeably higher than for cerrado.

This difference might be explained by environmental factors. The dry season of 1989 was unusually wet and it might be expected that cut fuel in the forest environment did not dry, thereby producing more reduced gases than usually occurs when it has a chance to dry out prior to burning. In this case, one would expect the inherently drier cerrado fuel to oxidize more efficiently than forest fuel. The dry season of 1979 and 1980 were more typical conditions when Greenberg et al. (1984) made their measurements. This argument suggests that environmental and site moisture conditions might determine differences in emission factors more than vegetation type.

It is difficult to provide a best estimate for this study. It is likely that each study provides merely different measurements, these differences reflecting different meteorological and site conditions, measurement techniques (i.e., distance from the burn), or different contributions of smoldering and flaming phases in the fires burning at the time of sampling.

Results

Land Cover Conversion and its Rate of Change

The maps presented in Figures 2.5-2.7 show our estimated distribution and changes in land cover. These maps show areas which had been converted to agriculture at three points in time, expressed as fractions of the total area. By 1970, most of the conversion had occurred in southern Brazil and along its coast. This pattern is not unusual since these are regions of long-term historical settlement. They are not, however, the only regions which experienced new conversion during the period of our analysis: 1970-1980. By comparing maps, one can see that most of the changes in land cover has occurred along two major fronts. One is a north-south corridor along the Belem to Brasilia highway. The other extends west from the state of Mato Grosso into the colonization areas of the state of Rondonia. Significant movement into Amazonia first begins between 1975 and 1980. By 1980 22.3% of all occupied areas in Brazil were in the Legal Amazon, compared to only 14.6% in 1970 (Table 2.4).

In terms of total area, most of the converted areas are in the states of Bahia, Minas Gerais, Parana, Sao Paulo, Rio Grande do Sul, Goias, Maranhao and Mato Grosso (Table 2.4). Other states are low in total area, but high in density relative to the size of the state (i.e., Alagoas and Sergipe) (Table 2.4).

The computed average annual land cover conversion in Brazil remained fairly constant between 1970 and 1980 at approximately 3×10^6 hectares per year (Table 2.5). Some regions, however, show large changes in the rate (Table 2.6). Most notable is the state of Rondonia which exhibits explosive increases in the rate of deforestation during the 1975-1980 period. Some states show negative rates, which imply net losses of agricultural land, or abandonment (Table 2.6).

Between 1970 and 1975, 45% of the new conversion occurred in the Legal Amazon, while 55% occurred elsewhere in Brazil (Table 2.5). Between 1975 and 1980, 56% of the new conversion occurred within the Legal Amazon, reflecting the early stages of a trend toward the expansion of agriculture and economic development in the region.

Rates of Conversion in Different Cover Types

For this analysis, we delineated nine different natural land cover types in Brazil. This classification is general, but seems to well characterize the major cover types. Table 2.7 shows our estimated original extent of these zones. Forests comprised the largest category at 461.8 x 10^6 hectares and 54.7% of the total land area. Also significant were sparse forests, or cerrado, systems with 160.6 x 10^6 hectares and 19.0% of the total area. All woodland and savanna systems totaled 31.5% at 265.9 x 10^6 hectares. Thus forests and woodland/savanna systems account for 86.2% of all land cover types in this analysis. Grassland systems account for 12.8%, or 108.3 x 10^6 hectares.

By combining the spatial land cover and land conversion databases, we estimated the distribution of conversion according to land cover type (this is an important consideration later when fluxes are calculated). Table 2.7 shows the total area converted in each cover type as of three dates. The distribution of converted areas (by cover type) is not the same as the distribution of natural cover. Conversion in forests comprised only 35% of the total conversion by 1980. Most conversion was in woodland/savanna systems (44%).

By 1980 10.8% of the original forest cover in Brazil had been converted, compared to 24.1% of woodland/savanna systems and 26.2% of grasslands (Table 2.7). Some cover types are estimated to have lost much higher fractions when considered individually; 40.4% in forest steppe and 31.0% in dry low grass savanna (Table 2.7). When computing average annual rates of new conversion between dates (1970-1975, 1975-1980), most of the activity occurred in the woodland savanna systems (Table 2.7). Actual deforestation in closed forests accounts for 38% of all new land conversion during the period of analysis, 1970-1980. The rest occurred in woodlands (47%) and grasslands (15%).

Release of Total Carbon

The estimated release of carbon from biomass burning is shown in Table 2.8 for each of the states of Brazil, for the Legal Amazon, and for Brazil as a whole. Between 1970 and 1980 1.233 x 10^{15} g C was released. During the period 1975-1980 0.626 x 10^{15} g C was released, and a slightly lower amount was released between 1970 and 1975 (0.607 x 10^{15} g C).

Approximately half the conversion which occurred between 1970 and 1980 was in the Legal Amazon, but this amounted to 55% of the total release of carbon (Table 2.8).

This results from the clearing of higher biomass systems in the Amazon basin, particularly forest ecosystems. The largest contribution to the total was from land cover conversion in the states of Mato Grosso and Para, constituting 39 % of the total release at 0.283 and 0.198 x 10^{15} g C, respectively.

The net release from the state of Rondonia was considerably lower (0.025 x 10^{15} g C between 1970 and 1980), but showed nearly a 6- fold increase in the latter half of the decade over the first half, more than any other state. Some places experienced significant declines. This occurred in the traditional cultivation regions of the south, including the states of Rio Grande do Sul, Sao Paulo, and Parana.

Figures 2.8 through 2.10 show the total net release of carbon from biomass burning associated with agriculture conversion of natural ecosystems mapped into grid cells measuring 0.5° X 0.5°. These maps show the geographical distribution of the net release of carbon due to biomass burning in Brazil at different intervals of time between 1970 and 1980. For comparison, Figure 2.11 shows the net flux when pastures burned for regular maintenance is also included. These figures also show the density of emissions when plotted as isolines of flux (0.5 Mt C / ha intervals for interdecadal periods, Figures 2.8 and 2.9, and 1 Mt C / ha intervals for the decade, Figure 2.10).

Figure 2.12 shows the net release from new conversions in different land cover classes. The largest fraction, as expected, is from the conversion of forests (70%). Another large release occurred in bush forest and cerrado systems (24%).

Release of Carbon Dioxide and Trace Gases

Table 2.9 presents the contribution the total carbon release from CO_2, CO, and CH_4 using three emission factor estimates. There is considerable variance between estimates, particularly for methane which varies by almost an order of magnitude. Table 2.9 also presents results when we separate forest and cerrado fires using factors reported by Ward et al. (1990). As expected this lowers the contribution of the reduced gases relative to CO_2 when compared to average values (estimate 2 in Table 2.9).

Discussion

Other than this study, there have been no attempts to map land cover conversion for all of Brazil. Isolated studies have been conducted in states or for large portions of Brazil (e.g., Fernside 1986). The Brazilian space agency, INPE, has in recent years mapped the distribution of deforestation in the Legal Amazon at scales ranging from 1:250,000 to 1:500,000 using satellite remote sensing (Tardin and Pereira da Cunha 1990, Tardin et al. 1980). Other remote sensing studies have been conducted in isolated regions or specific states (Malingreau and Tucker 1988, Tucker et al. 1986, Woodwell et al. 1986). There have been no remote sensing surveys for all of Brazil.

The FAO and UNEP have reported deforestation rates for 1975-1980 which reportedly cover the entire country, but as we discuss later are likely to have covered only the Legal Amazon region. This study's approach to coarse scale mapping in a geographic information system which is coupled to biogeochemistry models appears to be a feasible method for estimating geographically referenced fluxes of carbon and trace gases. The limiting factor appears to be the paucity of ground measurements of biomass, biomass allocation factors such as combustion efficiencies, and emission factors. In other parts of the world, where land use data is scarce or non-existent, the approach may not work quite so well.

This study suggests that by 1980, 6.5% of the Legal Amazon had been converted from its natural state to agriculture, and that almost half of this conversion occurred between 1970 and 1980, the period of this analysis. This estimate is higher than the estimate 5.1% made for 1988 by the Brazilian space agency (Tardin and Pereira da Cunha 1990, Periera da Cunha 1989), but this study limited itself to only closed canopy forests when much of the change occurred in Cerrado systems. This study also suggests that by 1980 17% of Brazil as a whole had been converted, but unlike timing in the Legal Amazon, most of this had occurred by 1970. Approximately half of all the conversion activities between 1970 and 1980 took place inside the Legal Amazon.

The use of net changes in land use inventories on decadal or semi-decadal intervals of time would result in an overestimate of carbon and trace gas emissions in regions where there is significant expansion and retraction of agriculture if the land clearing is taking place in areas of degraded or secondary systems. The best, and probably only feasible, approach is one based on annual or semi-annual satellite remote sensing surveys at a scale of 1:1 M or finer. This approach permits the tracking of land use change on a fine enough scale to delineate gross clearing and abandonment nearly on a parcel-by-parcel basis.

Our estimate of the average annual rate of land cover conversion in Brazil between 1970 and 1980 was 3.1×10^6 hectares. This estimate is higher than the 1.4×10^6 hectares per year reported for the period by FAO/UNEP (1981). The data from FAO/UNEP (1981) is for the conversion of forests only. When we consider only forest systems, including woodlands and savannas, we estimate a deforestation rate which is still nearly twice as high (see Table 2.7). On the other hand, when we consider only the deforestation in the Legal Amazon, we arrive at a number which is similar to the FAO/UNEP report (1.6×10^6 hectares). It is likely that the FAO/UNEP report only provides information on deforestation in the Legal Amazon. This is probably an underestimate of the total deforestation in Brazil. Moreover, since FAO/UNEP (1981) considers only forests, it also would underestimate all conversion and result in a low net release of carbon from biomass burning in all types of cover. This underestimate might be small since forests, including savannas and woodlands, comprise a large majority of the net carbon release according to our analysis (see Figure 2.8).

Using a highly aggregate model with less geographic detail than this study, Houghton et al. (1987) provide the only estimate of carbon release due to land clearing in Brazil. That analysis used the FAO/UNEP rates of deforestation. Thus, their estimate of 0.336 x 10^{15} g C must really represent the net release from deforestation only in Amazonia. The Houghton et al. (1987) estimate includes the release from all processes in the vegetation and soil. Carbon released from burning constitutes approximately 31% of the total net flux (Houghton et al. 1991b). Thus the Houghton et al. (1987) estimate of carbon released from burning in the Legal Amazon would be 0.104 x 10^{15} g when this adjustment is made to their total figure. Our estimate for the Legal Amazon only is 35% lower at 0.068 x 10^{15} g C yr^{-1}, but since, land clearing in the Legal Amazon represents only 55% of the release of carbon from all of Brazil (0.125 x 10^{15} g C), the Houghton et al. (1987) estimate probably under estimates the total net release for Brazil.

If we assume that biomass burning represents 31% of the total annual net flux of carbon, we can compare the results of this study with regional and global estimates. The global net flux is currently estimated at approximately 1.7 x 10^{15} g C per year in 1980, of which 0.680 x 10^{15} g C is from Latin America. This study suggests that Brazil's contribution is 24% of the global total and 60% of Latin America. This study also suggests that the tropical contribution to the global carbon budget is at least 0.400 x 10^{15} g C.

As much as 15% of the total carbon released is CO, but this might be as low as 4% depending on the emission factor used. Crutzen and Andreae (1990) suggest a global emission of CO from biomass burning in the tropics between 0.12 and 0.51 x 10^{15} g C yr^{-1}. If we use the medium estimate from 1975-1980 from Table 2.9 (ratios close to those used in Crutzen and Andreae (1990)) and include the burning for pasture maintenance as we have calculated it, the CO contribution from Brazil to the global budget would be 3-11%. However, our estimates might not be directly comparable to the global estimates of Crutzen and Andreae (1990), since our approach to pasture burning, which only includes pastures owned and occupied and not the total savanna extent, results in a much lower estimate from pasture maintenance.

The emission of CH_4 is small compared to total carbon (less than 3%). Khalil and Rasmussen (1983) estimate the global contribution from biomass burning is around 25 x 10^{12} g, with the southern tropics representing approximately 10 x 10^{12} g of this. Crutzen's (1983) global estimate of CH_4 from biomass burning is 30-110 x 10^{12} g C. Bolle et al. (1986) estimate the global contribution to be 55-100 x 10^{12} g C. Other estimates are similar; Seiler (1984) estimates 53-97 x 10^{12} g C and Blake (1984) estimates 25-100 x 10^{12} g C. If we assume a mean value of 58 x 10^{12} g C, our estimate for Brazil could be 4% of the global total (based on the Crutzen et al. 1985 emission factor).

This estimates seem low, suggesting the current global estimates are too high or that there are large areas of natural fires which this study does not account. The wide range in both emission factors and global budgets, however, prevents a precise estimate. Bolle et al. (1986) suggest that the net increase in the total flux of CH_4 globally between 1975 and 1980 is around 4 x 10^{12} g. Presumably this net increase is the result of anthropogenic biomass burning. Nearly all of the emission factors used in this study result in total emission greatly in excess of this number. In the context of the net increase in trace gas emissions, Brazil's contribution could be significant.

Published emission factors are a critical uncertainty when trying to extend an estimate of total carbon flux to individual gases. It is likely that new approaches to mapping as described here will greatly improve global carbon budgets, but will not improve our understanding of trace gas budgets without more field work.

A critical uncertainty in the estimates of total carbon given here arises from the paucity of biomass data for Brazil. A potentially fruitful approach would be to begin with a satellite-based classification of land cover at 10 km resolution (Justice et al. 1985). This would simultaneously help to define ecosystem/biomass distributions and elucidate the state of the ecosystem at the time of conversion. It is important, however, that this be coupled to field programs which provided the necessary in-situ measurements.

Improvements in quantifying the frequency, distribution, and possibly areal extent of burning could be made using satellite approaches. Setzer and Pereira (1991) have defined an approach using AVHRR thermal data to pinpoint fires in the Amazon. The coupling of multi-temporal, coarse resolution, satellite based analysis of fire locations with a database on land use data is a promising approach. These uncertainties notwithstanding, considerable progress has been in our understanding of land cover conversion and carbon flux dynamics.

The geographical patterns of land conversion documented in this study reflect what we know about the recent history of land development policy in Brazil. Another paper (Skole, in press) addresses these details, but it is an important observation that the fronts of deforestation identified in this study coincide in time and place with development activities of the period. The observed front extending along a corridor from Brasilia to Belem is the location of early road building and settlement projects around Altamira and Paragominas. The Atlamira colonization projects were important as catalysts for migration in the 1970s (Moran 1981). By some estimates the population in this region grew from approximately 100,000 in 1960 to over 2 million by 1970 (Resende 1973). Agricultural modernization and livestock development projects of the late 1960s and 1970s were important forces of land use change in eastern Para, which includes the towns of Paragominas and Braganca (Mahar 1989). In the latter half of the 1970s the initial trend in migration north and west into the state of Rondonia began as a part of a national integration and resettlement program and been well document by a number of observers (Fearnside 1983, Smith 1982, Smith 1981, Moran 1981). It seems almost too obvious to comment, but the geographical patterns and rates of land conversion show the tight correlation between road building programs and observed patterns of land conversion.

These results indicate that land cover change has been occurring in Brazil for some time. The causes are complex and relate to social, political and economic development factors, making future projections and policy options difficult to determine. It is clear that the momentum of recent history carries forward to land conversion processes today. It is likely too simplistic to consider population growth alone as a primary agent of change.

Table 2.1. Estimates of the carbon contained in the vegetation of different cover types in Brazil (10^6 g C ha^{-1}).

Cover Type	Carbon in Vegetation	Reference
Equatorial forest	180	This Study
	162	Fernside (1985, 1987)
	200	Olson et al. (1983)
	134-188	Brown and Lugo (1982)
	160	Cardenas et al. (1982)
	188	Brown et al. (1990)
Southern forest	55	Brown and Lugo (1984)
Bush forest	55	This Study
	50-90	Olson et al. (1983)
	55	Houghton et al. (1991b)
	42	Brown and Lugo (1982)
Sparse forest	33	This Study
	32	Fernside (1985, 1987)
	20-50	Olson et al. (1983)
	35	Brown and Lugo (1984)
Wet tallgrass savanna/steppe	20	This Study
	10	Houghton et al. (1991b)
	35	Fernside (1985, 1987)
	5-30	Olson et al. (1983)
Dry shortgrass savanna/steppe	10	This Study
	5-30	Olson et al. (1983)
	10	Houghton et al (1991b)
Forest steppe	15	This Study
	15	Olson et al. (1983)
Steppe	10	This Study
	10	Olson et al. (1983)
Desert/sand	5	This Study
	5	Houghton et al. (1991b)
Pasture	2.3	This Study
	1-5	Fernside (1985, 1987)
Cropland	5	This Study
	5	Houghton et al. (1991b)

Table 2.2. Estimates of combustion efficiency for various broad classes of vegetation and values used in this study. Units are percent of aboveground biomass burned.

Cover Type	Fraction Burned	Reference
Forest	0.40	This study
	0.25	Seiler and Crutzen (1980)
	0.30	Crutzen et al. (1989)
	0.40	Houghton et al. (1991b)
	0.48	Fernside (1990), (1989)
	0.60	Setzer et al. (1988)
Woodlands and Savannas	0.67	This study
	0.67	Houghton et al. (1991b)
	0.75	Seiler and Crutzen (1980)
	0.75	Setzer et al. (1988)
	0.83	Crutzen et al. (1989)
Grasslands and Steppe	0.90	This study
	0.80	Seiler and Crutzen (1980)
	1.00	Houghton et al. (1991b)

Table 2.3. Three estimates of emission ratios of CO and CH_4 to CO_2 used to estimated carbon trace gas emissions from biomass burning in the Brazil. The emission of all gases including CO_2 was determined from the amount of total C burned (see text for explanation). Units are $\Delta X / \Delta CO_2$ (V/V%).

Estimate	CO	CH_4	Remarks	Reference
A.	0.040	0.002	forest and savanna	Ward et al. (1990), Greenberg et al. (1984)
B.	0.085	0.017	forest and savanna	Andreae et al. (1989), Crutzen et al. (1985)
C.	0.150	0.012	forest and savanna	Crutzen at al. (1985), Kaufman et al. (1990)
D.	0.013 0.0435	0.00034 0.00225	savanna forest	Ward et al. (1990)

Table 2.4. Estimated area of land conversion for each state and the Legal Amazon region in Brazil for three dates of the analysis. The values represent the total area converted from natural land cover to agriculture as of the date specified. Also shown is the fraction of each state or region which had been converted to agriculture. Units are 10^6 ha.

STATE	1970	Fraction of state	1975	Fraction of state	1980	Fraction of state
Maranhao	6.153	0.1895	6.804	0.2096	8.322	0.2564
Piaui	3.671	0.1463	4.263	0.1699	4.814	0.1918
Ceara	4.905	0.3341	4.905	0.3341	5.315	0.3621
R.G. do Norte	1.722	0.3248	1.395	0.2631	1.437	0.2711
Paraiba	2.092	0.3711	2.139	0.3795	2.223	0.3943
Pernambuco	3.308	0.3366	3.284	0.3341	3.479	0.3539
Alagoas	1.376	0.4975	1.544	0.5585	1.629	0.5891
Sergipe	1.024	0.4716	1.049	0.4832	1.103	0.5082
Bahia	11.497	0.2053	12.062	0.2154	14.404	0.2572
Minas Gerais	12.337	0.2118	12.790	0.2195	13.314	0.2285
Espirito Santos	2.098	0.4602	1.826	0.4006	1.822	0.3997
Rio de Janiero	1.262	0.2915	1.377	0.3181	1.327	0.3064
Sao Paulo	13.035	0.5270	14.295	0.5780	14.168	0.5729
Parana	10.441	0.5263	11.991	0.6045	12.745	0.6425
Santa Catarina	3.313	0.3490	3.466	0.3651	3.714	0.3912
R.G. do Sul	8.003	0.2992	9.000	0.3364	9.205	0.3441
Goias	11.496	0.1778	15.045	0.2326	16.990	0.2627
Mato Grosso	10.235	0.0808	14.321	0.1131	18.715	0.1478
Para	3.784	0.0317	4.576	0.0383	5.993	0.0502
Rondonia	.479	0.0197	.524	0.0216	.968	0.0398
Roraima	.143	0.0062	.219	0.0095	.296	0.0129
Amazonas	.844	0.0054	1.564	0.0101	1.738	0.0112
Amapa	.094	0.0067	.194	0.0140	.193	0.0139
Acre	.167	0.0110	.185	0.0121	.192	0.0126
Legal Amazon	16.626	0.0337	23.582	0.0477	32.148	0.0651
fraction of Brazil	--	0.1465	--	0.1831	--	0.2231
Brazil	113.481	0.134	128.822	0.153	144.108	0.171

Table 2.5. Estimates of net conversion rates between 1970 and 1980. Net conversion represents the difference in the total area of conversion for 1970-1975 and 1975-1980. Units are 10^6 hectares or percentages.

Region	1975-1970	%¹	%²	%³	1980-1975	%¹	%²	%³
Legal Amazon	6.956	1.42	1.46	45.34	8.566	1.73	1.82	56.04
Brazil	15.342	1.82	2.10		15.286		1.81	2.14

Notes:

1 Calculated as the net conversion divided by estimated area of the Legal Amazon (493,918,700 ha.) or Brazil (844,245,599 ha.):

[D(n+1) - D(n) / A] * 100

where D(n+1) and D(n) are the total conversion areas as successive dates from Table4 and A is the total area in the Legal Amazon or Brazil.

2 Calculated as the net conversion during the period as a percent of the previously undisturbed area:

[D(n+1) - D(n) / A - D(n)] * 100

where D(n+1) and D(n) are the total conversion areas from Table 4, and A is the area of the Legal Amazon or Brazil.

3 The fraction as a percent of total net conversion between dates which occurred inside the Legal Amazon.

Table 2.6. Estimated net conversion rates for each state in Brazil. Units are hectares.

STATE	1975-1970	%	%	1980-1975	%	%
Maranhao	651356	0.0201	0.0248	1518196	0.0468	0.0592
Piaui	591821	0.0236	0.0276	551182	0.0220	0.0265
Ceara	-213	-0.0000	-0.0000	410303	0.0279	0.0420
R.G. do Norte	-326776	-0.0616	-0.0913	42306	0.0080	0.0108
Paraiba	47214	0.0084	0.0133	83798	0.0149	0.0240
Pernambuco	-24128	-0.0025	-0.0037	194742	0.0198	0.0298
Alagoas	168631	0.0610	0.1214	84575	0.0306	0.0693
Sergipe	25200	0.0116	0.0220	54215	0.0250	0.0483
Bahia	564716	0.0101	0.0127	2342161	0.0418	0.0533
Minas Gerais	453659	0.0078	0.0099	523610	0.0090	0.0115
Espirito Santo	-272118	-0.0597	-0.1106	-4121	-0.0009	-0.0015
Rio de Janeiro	115007	0.0266	0.0375	-50374	-0.0116	-0.0171
Sao Paulo	1260251	0.0510	0.1077	-126718	-0.0051	-0.0121
Parana	1551146	0.0782	0.1651	753657	0.0380	0.0961
Santa Catarina	152756	0.0161	0.0247	248095	0.0261	0.0412
R.G. do Sul	996538	0.0372	0.0532	204739	0.0077	0.0115
Goias	3548733	0.0549	0.0667	1945457	0.0301	0.0392
Mato Grosso	4086351	0.0323	0.0351	4393325	0.0347	0.0391
Para	791756	0.0066	0.0068	1417074	0.0119	0.0123
Rondonia	45437	0.0019	0.0019	443354	0.0182	0.0186
Roraima	76186	0.0033	0.0033	76806	0.0033	0.0034
Amazonas	719855	0.0046	0.0047	174127	0.0011	0.0011
Amapa	100626	0.0072	0.0073	-1707	-0.0001	-0.0001
Acre	17891	0.0012	0.0012	7211	0.0005	0.0005

Notes:

1 Calculated as the net conversion divided by estimated area of each state:

[D(n+1) - D(n) / A] * 100

where D(n+1) and D(n) are the total conversion areas as successive dates from Table4 and A is the total area in the state.

2 Calculated as the net conversion during the period as a percent of the previously undisturbed area:

[D(n+1) - D(n) / A - D(n)] * 100

where D(n+1) and D(n) are the total conversion areas from Table 4, and A is the area of the state.

Table 2.7. Estimated land cover conversion associated with each cover type in Brazil. The data shows the total conversion in each cover type as of the dates specified along with the fraction of each type converted as of the date and the fraction of total conversion which it represents. Units are 10^6 hectares.

Cover Type	Area	%	by 1970	of cover	of total	by 1975	of cover	of total	by 1980	of cover	of total
1.Forests	461.8	0.57	38.006	0.08	0.33	44.071	0.09	0.34	49.663	0.11	0.35
2.Woodlands and Savanna	265.9	0.31	49.787	0.19	0.44	56.746	0.21	0.44	64.052	0.24	0.44
2.1 Forest Steppe	26.1	0.03	9.387	0.36	0.08	10.332	0.40	0.08	10.549	0.40	0.07
2.2 Bush Forest	79.2	0.09	20.143	0.25	0.18	20.840	0.26	0.16	22.915	0.29	0.16
2.3 Sparse Forest (Cerrado)	160.6	0.19	20.255	0.13	0.18	25.574	0.16	0.20	30.588	0.19	0.21
3.Grassland savannas/ steppe	108.3	0.13	23.885	0.22	0.21	26.135	0.24	0.21	28.429	0.26	0.20
3.1 Wet tallgrass savanna	47.9	0.06	7.899	0.16	0.07	8.688	0.18	0.07	9.580	0.20	0.07
3.2 Dry lowgrass savanna	37.8	0.04	11.377	0.30	0.10	12.583	0.33	0.10	13.338	0.35	0.09
3.3 true steppe	22.6	0.03	4.609	0.20	0.04	4.864	0.21	0.04	5.511	0.24	0.04
4.Other	8.3	0.01	1.804	0.22	0.02	1.871	0.22	0.01	1.965	0.24	0.01
4.1 Wetlands and Mangrove	8.2	0.01	1.778	0.22	0.02	1.846	0.22	0.01	1.939	0.24	0.01
4.2 Desert and arid	0.1	0.00	0.026	0.26	0.00	0.025	0.25	0.00	0.026	0.26	0.00
Total	844.3	1.00	113.482		1.00	128.823		1.00	144.109		1.00

Table 2.8. Estimated net release of total carbon from biomass burning in Brazil, 1970-1980. This table presents the total release integrated over each time period from new conversions, from pasture maintenance, and from the total of new conversions and pasture maintenance. Units are 10^{12} g C.

State	Total 1970-1980	New Conversions 1975-1980	New Conversions 1970-1975	Pasture Maintenance 1975-1980	Conversions and Pastures 1975-1980
Roraima	5.57	2.94	2.63	1.75	4.68
Amapa	5.77	2.07	3.71	0.34	2.41
Para	198.04	121.99	76.05	6.21	128.20
Amazonas	28.35	13.88	14.47	0.06	13.94
Maranhao	146.31	74.01	72.30	6.11	80.12
Piaui	25.16	13.92	11.24	4.00	17.92
Ceara	36.33	26.478	9.85	6.44	32.91
R.G. do Norte	4.57	4.57	0.00	2.52	7.10
Goias	133.68	43.39	90.28	31.52	74.91
Paraiba	4.50	3.34	1.16	2.69	6.04
Acre	4.89	1.92	2.97	0.12	2.04
Pernambuco	11.95	7.54	4.41	5.01	12.55
Mato Grosso	283.14	157.073	126.07	27.41	184.48
Rondonia	25.09	21.321	3.76	0.30	21.62
Bahia	88.52	67.89	20.62	20.85	88.75
Alagoas	26.38	7.88	18.49	2.36	10.25
Sergipe	5.14	2.82	2.32	1.89	4.71
Minas Gerais	28.87	14.43	14.44	46.26	60.69
Espirito Santos	2.88	2.88	0.00	4.61	7.49
Sao Paulo	79.93	9.62	70.31	22.86	32.48
Rio de Janiero	8.98	0.97	8.00	3.38	4.35
Parana	50.14	15.85	34.29	7.32	23.17
Santa Catarina	11.51	7.00	4.51	2.97	9.97
R.G. do Sul	17.93	3.11	14.82	18.89	21.99
Legal Amazon	678.11	393.06	285.06	37.62	430.68
fraction of total	0.55	0.63	0.47	0.17	0.51
Brazil Total	1,233.62	626.91	606.72	225.91	852.82

Table 2.9. Estimates of the net release of constituent gases from biomass burning in Brazil and the Legal Amazon. See Table 2.3 for emission factors used. Units are 10^{12} g C.

	1975-1980			1970-1975			1975-1980 New Conversion Plus Pasture		
	CO_2	CO	CH_4	CO_2	CO	CH_4	CO_2	CO	CH_4
A. Low Estimate									
Legal Amazon	377	15	1	274	11	1	413	16	1
Brazil	601	24	1	582	23	1	818	33	2
B. Mid Estimate									
Legal Amazon	357	30	6	259	22	4	391	33	7
Brazil	569	48	10	551	47	9	774	66	13
C. High Estimate									
Legal Amazon	338	51	4	245	37	3	370	56	4
Brazil	539	81	6	522	78	6	734	110	9

D. Savanna burning and Forest burning separated, 1975-1980 (from Ward et al. 1990).

	Total-C	CO_2	CO	CH_4
Forest	433	422	18	1
Non-forest	195	193	2	---
Sub Total	627	614	20	1
Pastures	226	223	3	---
Total	853	837	24	1

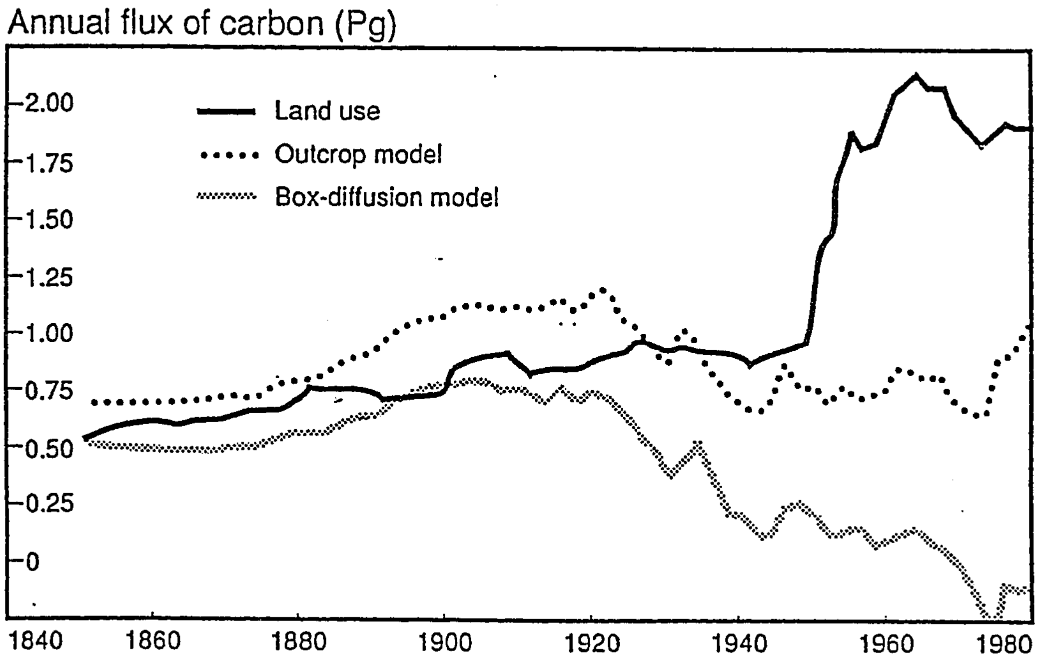

Figure 2.1. Comparison between global estimates of net flux of carbon from land cover conversion (solid line) and net biotic flux from a deconvolution of ice core data using two ocean models.

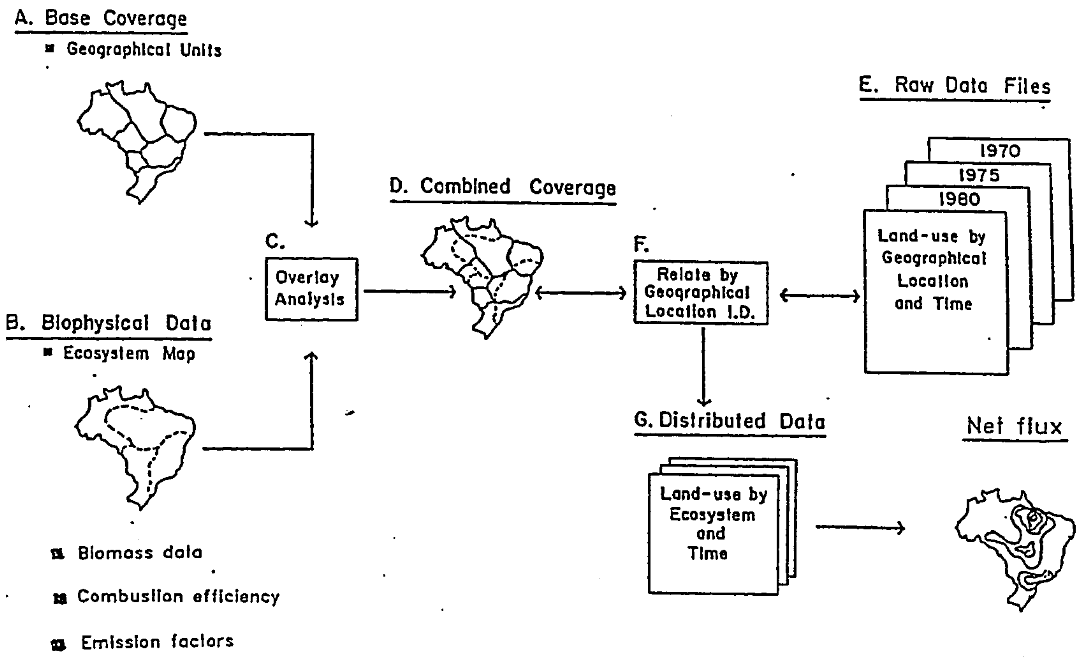

Figure 2.2. The general scheme used in this study. The approach makes use of the relational database capabilities of a geographic information system to utilize various spatial databases in a variety of formats. The approach combines spatial databases on land cover and land cover conversion rates, with tabular and in-situ data on biomass and land use.

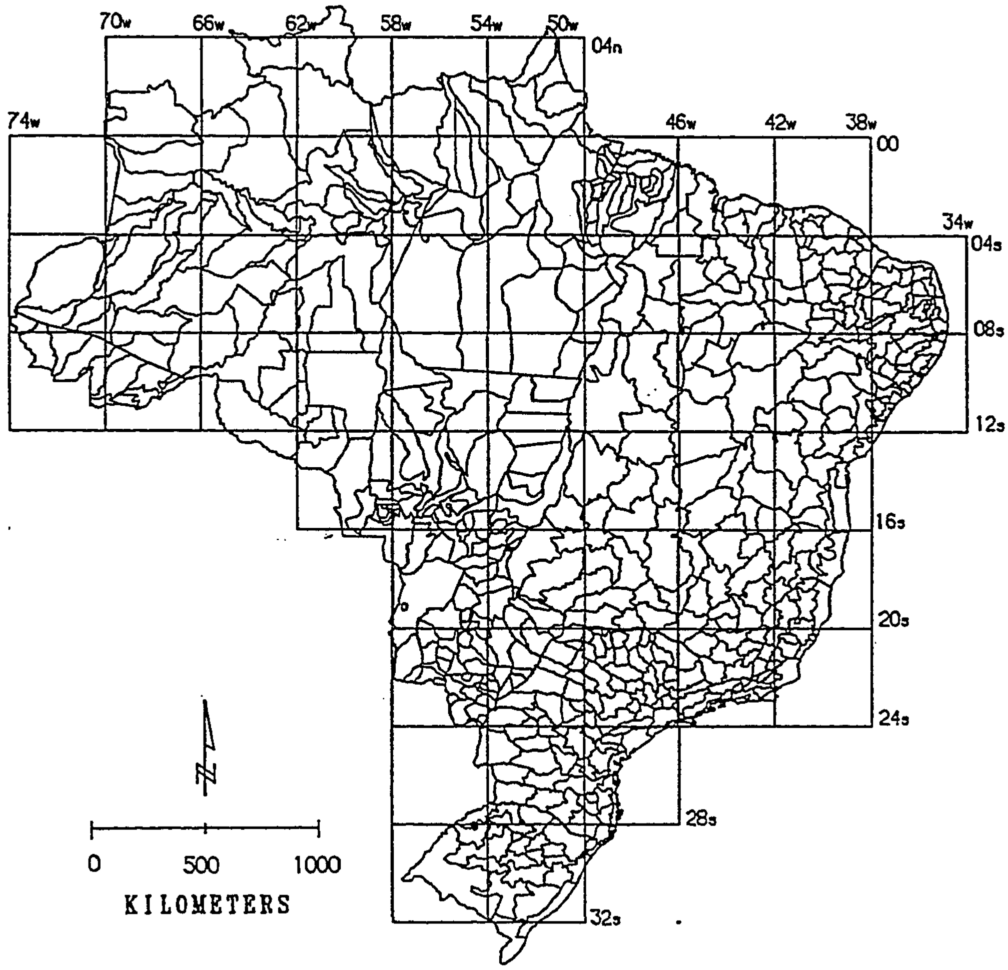

Figure 2.3. The base map of geopolitical units used to georeference land use data from the Brazilian agricultural census. The base map shown is comprised of 513 districts built up from 3973 towns.

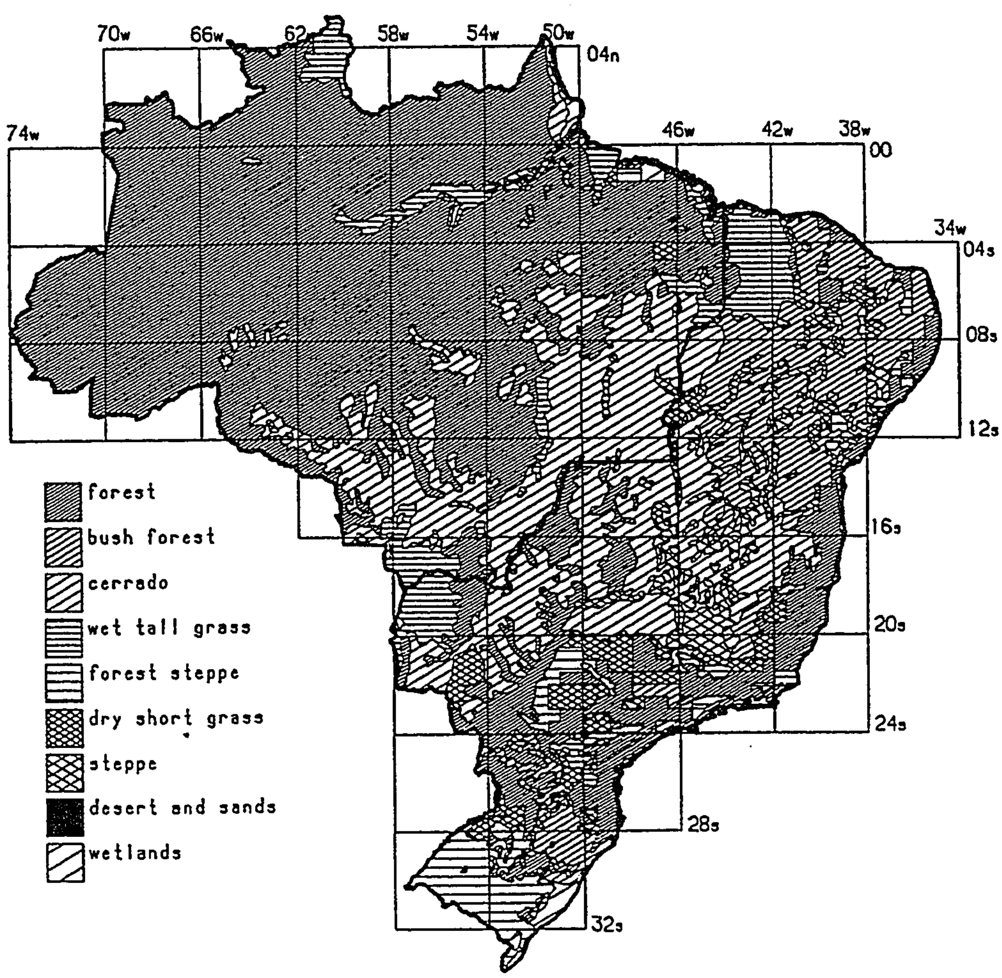

Figure 2.4. The pre-disturbance natural land cover map used in this analysis. This is a digital database derived from a 1:15M scale cartographic product described in the text.

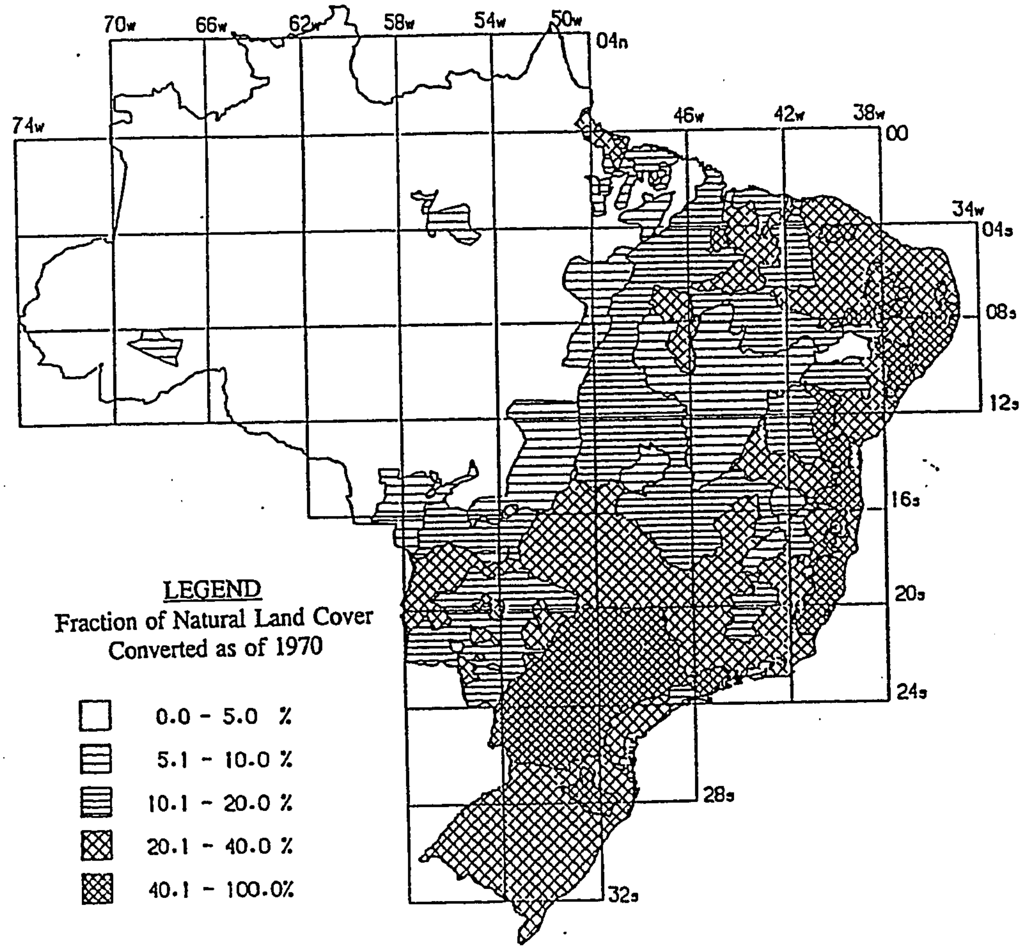

Figure 2.5. Total areas of land conversion as of 1970. The map shows the raw data mapped and shaded according to 5 broad density classes. It represents the geographical distribution of natural systems which had been converted to agriculture as of 1970. The net conversion and associated biomass buring is computed by change detection algorithm between maps of successive dates.

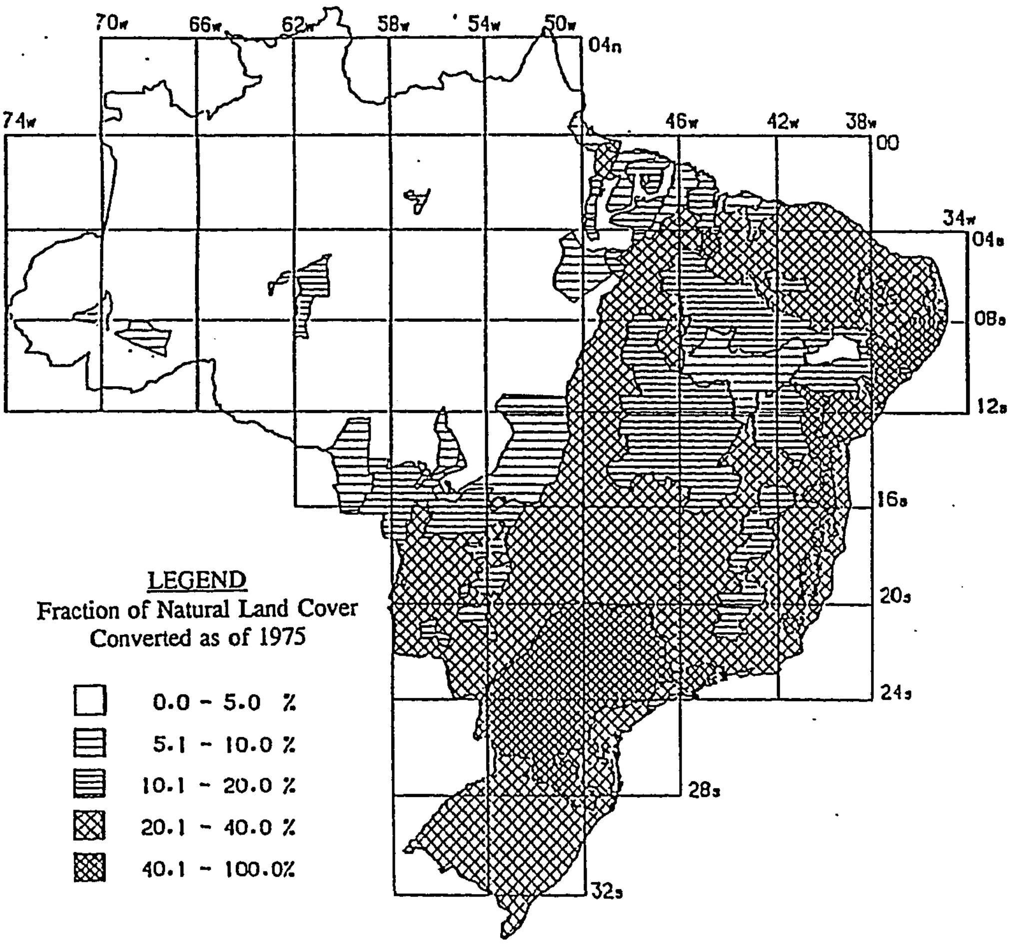

Figure 2.6. The geographical distribution of land conversion as of 1975.

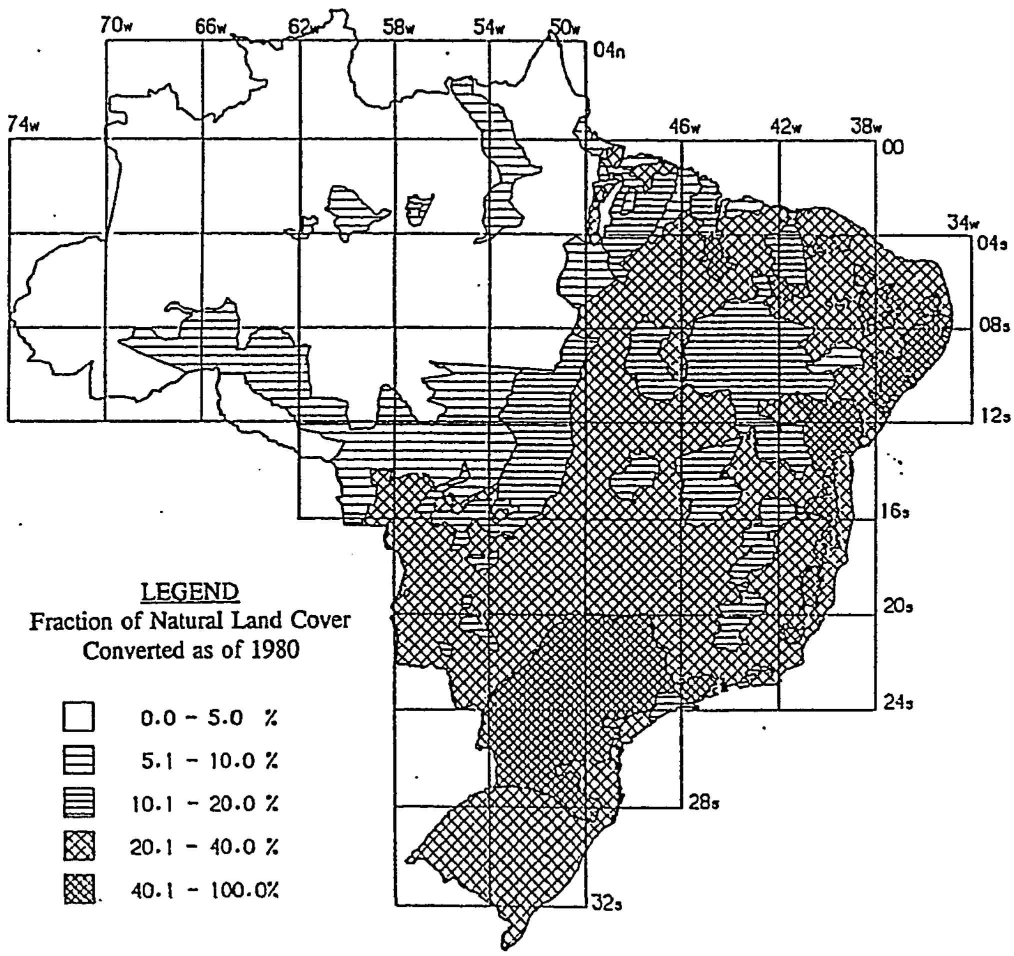

Figure 2.7. The geographical distribution of land conversion as of 1980.

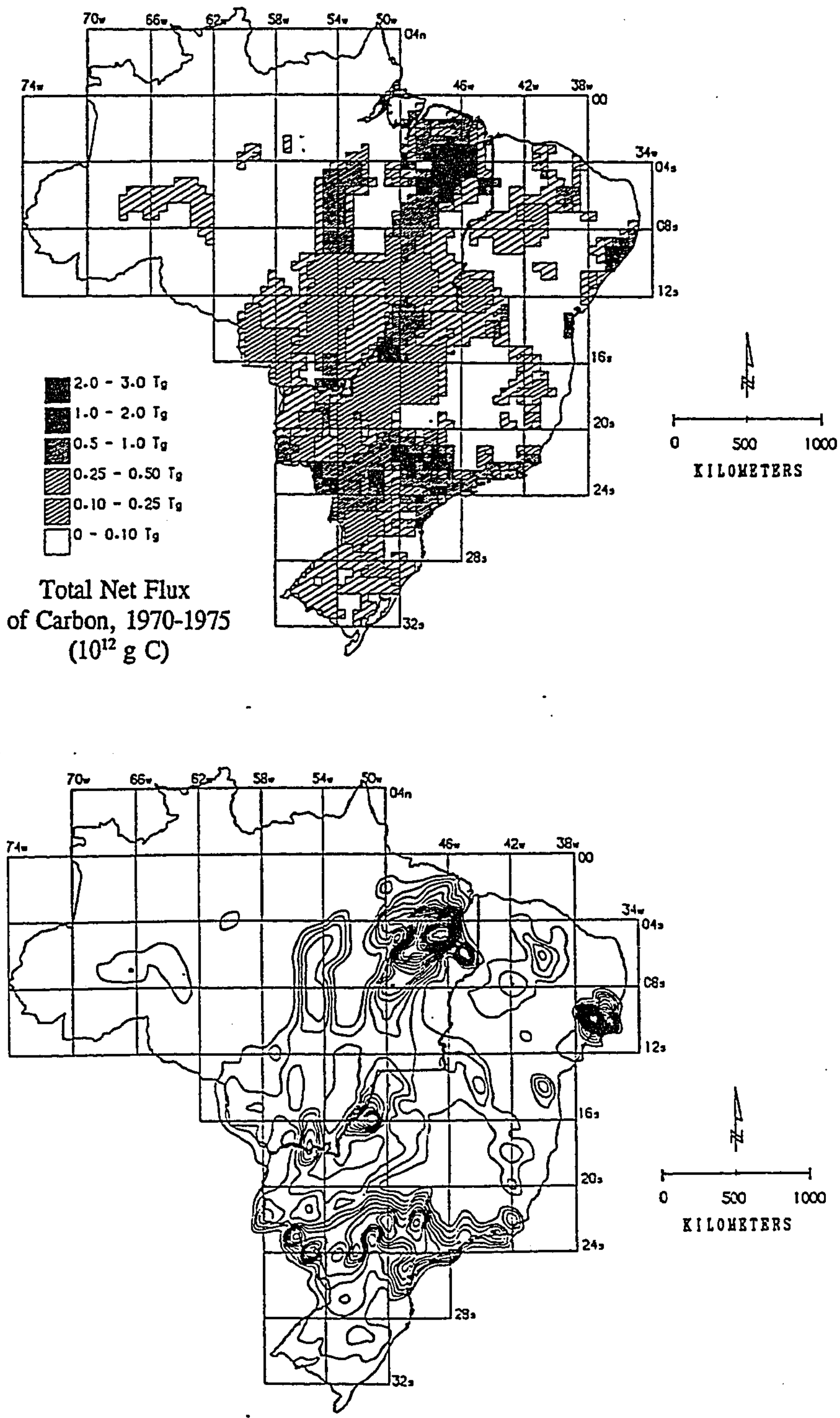

Figure 2.8. A map of the net release of total carbon and the associated isolines of average emission density on the surface for the period 1970 - 1975.

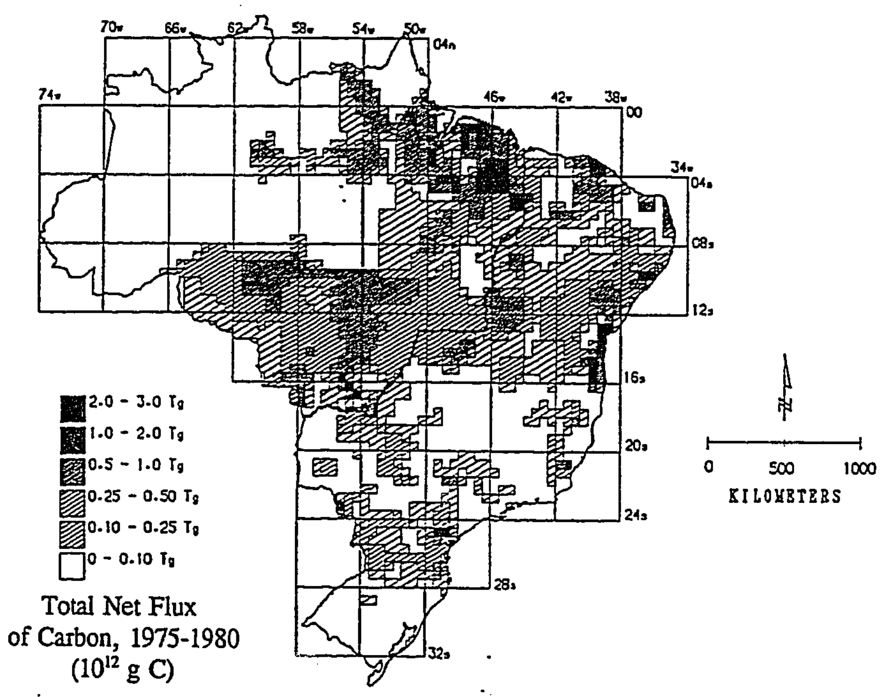

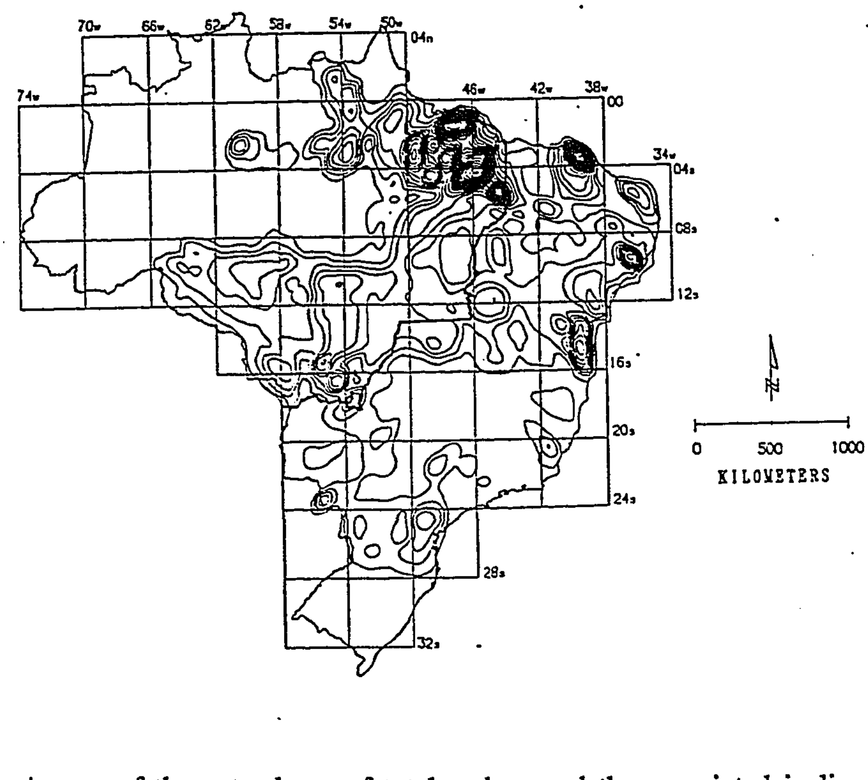

Figure 2.9. A map of the net release of total carbon and the associated isolines of average emission density on the surface for the period 1975 - 1980.

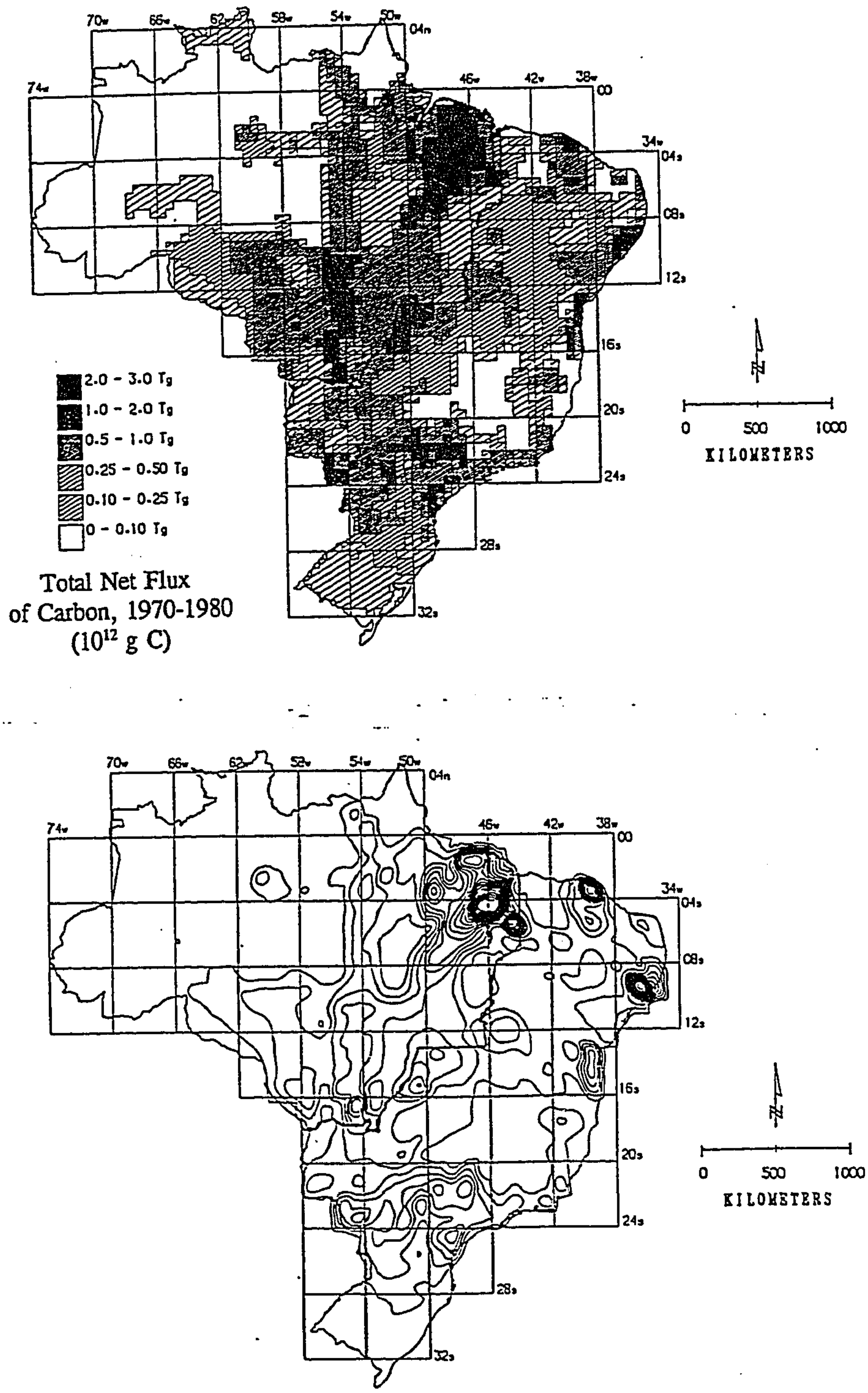

Figure 2.10. A map of the net release of total carbon and the associated isolines of average emission density on the surface for the period 1970 - 1980.

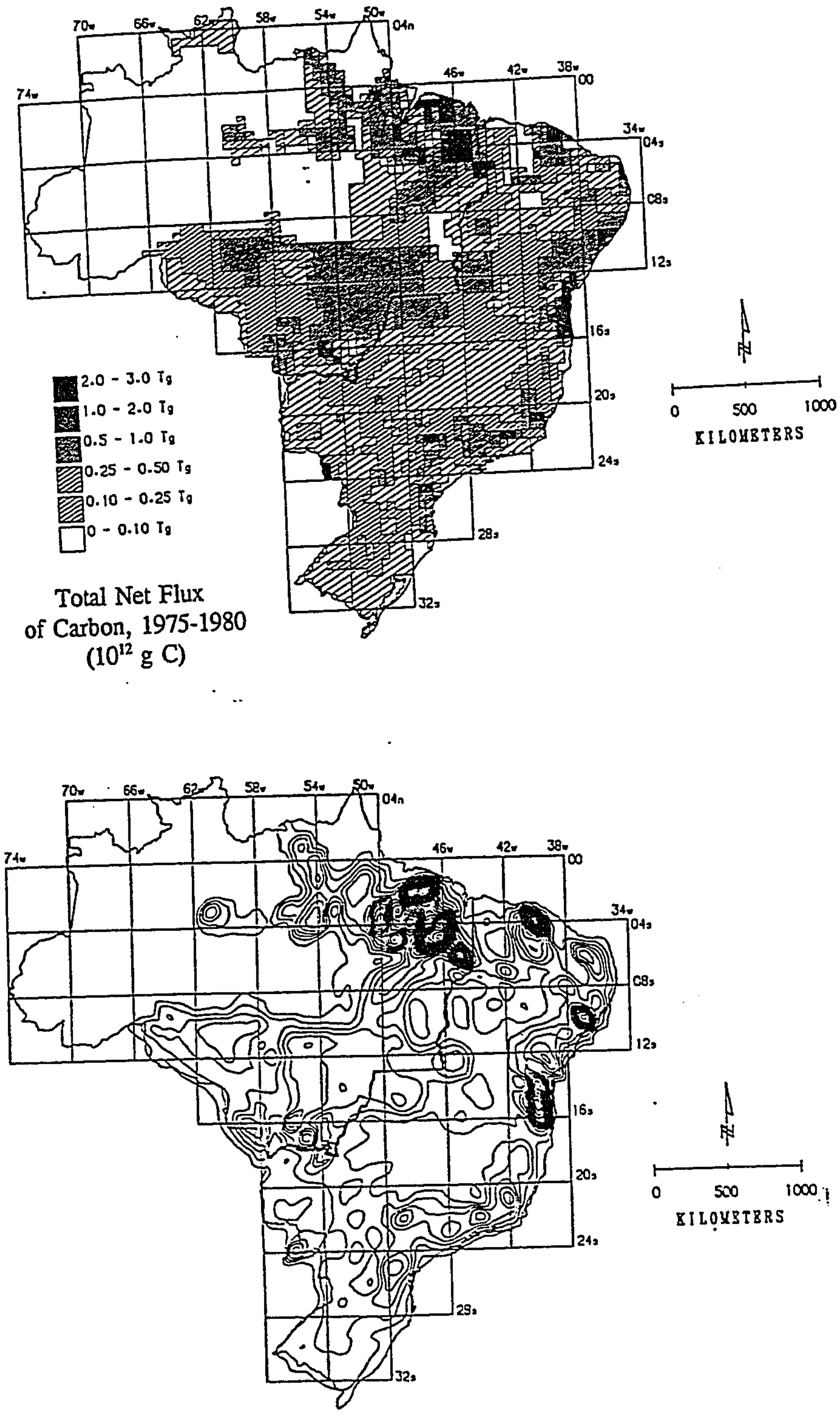

Figure 2.11. A map of the net release of total carbon, including pasture maintenance, and the associated isolines of average emission density on the surface for the period 1975-1980.

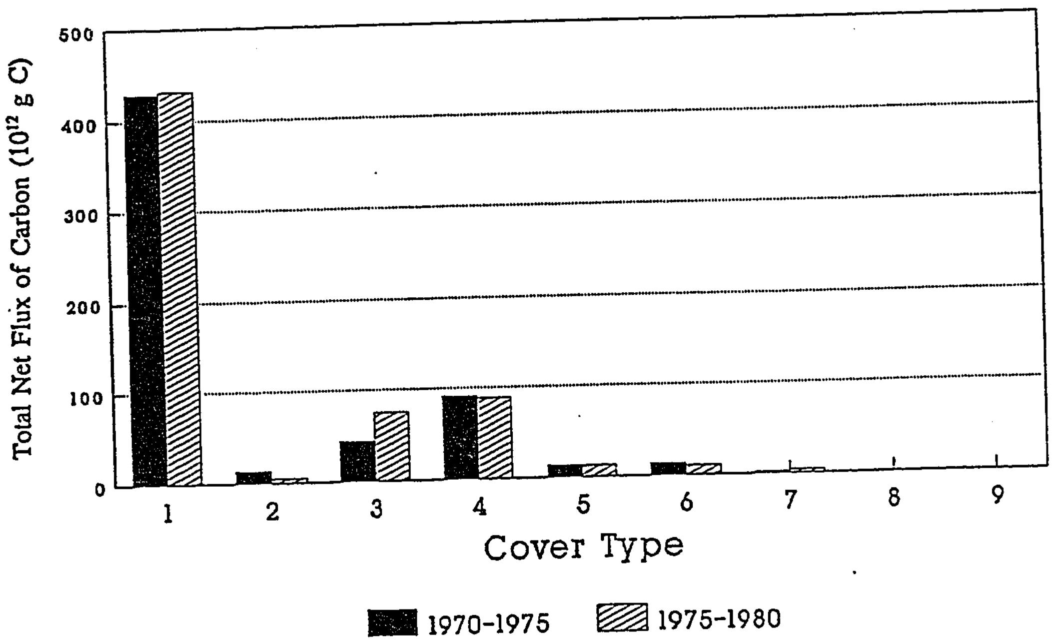

Figure 2.12. The net release of total carbon between 1970 and 1975 and between 1975 and 1980 distributed by cover type. The cover types are 1: Forests, 2: Forest Steppe, 3: Bush Forest, 4: Sparse Forest (Cerrado), 5: Wet Tallgrass, 6: Dry Lowgrass, 7: True Steppe, 8: Wetlands, 9: Deserts.

CHAPTER 3

MAPPING DEFORESTATION IN THE BRAZILIAN AMAZON USING A GEOGRAPHIC INFORMATION SYSTEM

Introduction

Deforestation has occurred throughout history and has been an important agent of environmental change in all parts of the world at one time or another. In the past it has been important in the temperate zone. In the last twenty years, deforestation has become an important tropical phenomenon, and has been accelerating as a result of population pressure and economic development. Yet, the precise rate and geographic distribution of tropical deforestation is unknown and poorly documented, in spite of the growing need for this kind of data to support both international policy and basic research.

The concern over tropical deforestation arises because of its potential impact on the global environment. The anthropogenic conversion of forests and woodlands contributes to the increase in atmospheric carbon dioxide (Moore et al. 1981, Houghton et al. 1983, 1987, Houghton and Skole 1990). Best estimates suggest that 20-30% of the total annual input of carbon dioxide to the atmosphere is from land cover conversion in the tropics (Houghton et al. 1985b, 1991a, 1991b, Palm et al.

1986, Detwiler and Hall 1988, Houghton and Skole 1990, Houghton 1991b). Also, the clearing of forests and woodlands is frequently accompanied by biomass burning, a process which is a potentially important factor in atmospheric chemistry and the release of radiatively important trace gases other than CO_2 (Crutzen and Andreae 1990, Setzer and Pereira 1990). Deforestation may have an important further influence on regional hydrology and climatology (Shukla et al. 1990). A clear understanding of how significant these large-scale impacts are to global change is now limited by the absence of well documented and quantitative data sets on deforestation.

One problem has been the paucity of spatial data sets. The spatial arrangement of forest disturbance is an important factor in estimating its influence on biogeochemistry and climate. For instance, one component of the uncertainty in modeling the net flux of carbon between terrestrial ecosystems and the atmosphere is the paucity of data on the type of ecosystems which have been cleared. This is important since terrestrial ecosystems vary considerably in the amount of aboveground biomass and moisture content. Deforestation in low biomass woodlands may result in lower emissions of carbon dioxide than in closed canopy forests. Burning in moist forests would release more reduced forms of carbon, such as CO and CH_4, than in dry systems. The spatial arrangement of deforestation will also influence the results of model simulations of continental scale climate and energy balance (Pielke et al. in press). Deforestation distributed as a few large blocks may have a greater influence on sensible and latent heat flux than the same area distributed as many, widely scattered small patches.

Finally, there is increasing concern that deforestation in the humid tropics will result in the loss of a significant number of species. The impact of deforestation on biodiversity is related to the total area of forest conversion and the amount of forest fragmentation (Wilson and Peter 1988, Ehrlich and Wilson 1991, Soule 1991). Quantifying fragmentation requires an understanding of the spatial arrangement of cleared areas. These examples demonstrate the importance of knowing more than just the magnitude of deforestation; we must also know where deforestation occurs and its spatial characteristics.

At this time we know very little about the coincident distribution of land cover, land cover attributes, and its conversion. We know even less about the geometry and spatial organization of deforestation. One way to address this uncertainty is to develop geographically-referenced data sets (Emanuel et al. 1985, Houghton et al. 1985a, Skole in press). We have been developing geographically referenced data sets of deforestation in tropical regions using geographic information systems (GIS) to support carbon cycle and climate models. This paper presents the results of an effort to create a digital database of deforestation in the Amazon Basin of Brazil for the period 1975-1978 using detailed maps made by the Brazilian forestry and space agencies (Tardin et al. 1980). This data set will form the baseline for a larger effort to document a time series from 1975 to 1988 in the Amazon using high-resolution satellite imagery. As a demonstration how such databases would be used to support global change research, we also estimate the net flux of carbon using a GIS-based numerical model.

Background

The Brazilian Amazon encompasses approximately 5×10^6 km^2, an area larger than half of the United States. It comprises the largest extant coverage of tropical forest in the world; approximately 31% of the world's closed tropical forests are here. Most of the region is in closed forest, but there are also extensive areas of woodland and savanna vegetation. Discussions of deforestation in the Amazon have frequently been obscured by problems defining which ecosystems constitute forests (Fearnside 1990b). This confusion has also made it difficult to compare various estimates, since rates are usually reported as totals or percentages of administrative districts, not according to vegetation zones. Moreover, many studies of deforestation have only reported conversion rates for closed forests and thereby omit a large fraction of the overall conversion activities in the region which occur in open forests (Fearnside 1990b). From the perspective of carbon cycle and climate models, disturbances to a variety of vegetation types are of interest.

The Legal Amazon has historically been a frontier with very low population densities and little in the way of agricultural activity. Beginning in the early 1970s the region was rapidly settled and colonized in response to government programs, spontaneous migration due to population pressure and displacement in the south and northeast of Brazil, and economic development projects (Moran 1981, 1984, Bunker 1984a,b, Sawyer 1984, Wood and Wilson 1984, Fearnside 1987b). Agricultural expansion was, and remains, the most important cause of deforestation. This movement of people into the region stimulated large scale deforestation in both forests and woodlands, but the precise rate and location has been poorly known. It is believed that forest conversion rates in the Legal Amazon are the highest in the world. The FAO/UNEP 1980 Forest Assessment (Lanly 1982) estimated the global tropical deforestation rate between 1975 and 1980 to be 11.3 x 10^6 ha yr^{-1}, of which 20% occurred in the Brazilian Amazon. Recent estimates suggest the current clearing rate might be as high as 80 x 10^3 km^2, and further suggesting that 85% of the net increase world-wide since 1980 has been in the Amazon (Setzer and Pereira 1990, WRI 1990).

In the late 1970s the Brazilian Institute for Forest Development (IBDF) and the Institute for Space Research (INPE) conducted a series of joint analyses of pasture formation and deforestation in the Amazon using satellite remote sensing data as the primary data source (Santos et al. 1977, 1979, Tardin et al. 1980). Maps were produced at a scale of 1:500,000, on which deforested areas were delineated by interpreting Landsat MSS single-channel photoproducts. These were some of the first and most comprehensive analyses of deforestation, and remain today a benchmark for future studies. However, the maps produced have never been used in any subsequent analyses.

In the study reported here we have built upon these early studies. The paper maps have been encoded in digital form and have been incorporated into a geographic information system for the Amazon basin. The estimate of areas has been improved over the early estimates by the use of precise line encoding using a vector-based GIS. And, the dataset has been merged with new digital data on the location of the forest-cerrado boundary derived from cartographic and remote sensing sources, something which was not done by IBDF and INPE.

Methods

Geographic Information Systems

Geographic information systems (GIS) make it possible to utilize spatial data for a variety of global change research applications. In this study we have utilized GIS technology to make precise estimates of areas from existing maps and remote sensing imagery. In addition, the GIS approach has made it possible to integrate multiple layers of data on political districts, vegetation type, and other geographical features. These data may be obtained from a variety of sources and at different scales since the GIS permits projection and georeferencing many data sets to a common coordinate system. The encoding of deforestation data in a GIS facilitates direct comparison with other analyses, and provides a medium to openly exchange data.

Generally, there are four sources of geographical data: (1) maps, (2) tabular summaries and documents, (3) remote sensing data, and (4) in-situ studies or point measurements. These data provide information which is both thematic and numerical. Thematic data represent attributes which describe a land surface characteristics according to some naming convention. Vegetation and soil maps are typical thematic datasets. These may provide geographic distributions of features, but in of themselves do not provide quantitative information. In this study we make use of vegetation data sets to which we assign numerical measures such as biomass. Similarly, the thematic delineation of landscape features into areas deforested in 1975 and areas deforested in 1978 can then be directly converted to numerical estimates of deforestation areas and rates.

Whatever the source, data must be encoded into a computer in some kind of formal structure, or data model. Geographic information systems employ two broad classes of data models (Peuquet 1984). The first class is the tessellated model. The grid and raster structures are the most common form of tessellation. Other tessellations include the quad tree, triangulated irregular networks, or TIN, generalized balanced ternary hexagons, and the quaternary triangulated mesh. Vector-based systems comprise the second class of data models. Vector models are often called polygon systems, but it is important to note that in a vector system points and lines are also considered. Vector systems store line-segment information in which coordinates are defined as a series of nodes and vertices. They provide the most accurate representation of map features and their areas. This study employed the use of a vector-based GIS to encode the detailed network of polygons of deforestation. Vegetation maps derived from an analysis of satellite imagery were encoded in grid form.

A data management system in the GIS organizes these data into discrete geographical entities (grid-cells or polygons) with their associated attributes. Most relational geographic information systems partition the functions of data management into two components: (a) a cartographic component, and (b) a thematic component. The cartographic component stores all coordinate information for each geographical unit or feature, while the thematic component stores the basic related information, such as deforested area, vegetation type, biomass, or administrative district name.

One key characteristic of a GIS approach is that numerous datasets from a variety of different sources can be integrated through a coordinate and projection system. There is no a-priori co-registration of these data, yet very fine scale data in both grid and vector formats may be precisely merged, even if from independent sources. This approach differs from, and is more efficient than, those which pre-define an array of cells by a longitude/latitude grid. The GIS commonly uses the data layering approach to organize various general classes of data which may have been derived from separate sources. Deforested areas might constitute one layer, vegetation type another, and political districts yet another. These layers can readily be merged or cross referenced spatially or thematically. Another utility is the automated ability to determine spatial relations within large databases. That is, questions can be asked concerning such relationships as between amount of deforestation and distance from a road or urban center.

Data Encoding

Original map sheets from the INPE/IBDF study were digitized into the GIS at their original scale and projection. Maps were digitized at 1:500,000 scale in a UTM (Universal Transverse Mercator) projection. Gradicules in latitude/longitude and UTM coordinates were available on the maps, providing sufficient ground control points to register the maps with an RMS error less than 0.002. Continuous line digitizing was done by hand with tolerances of 1 vertex per 25 meters of ground position.

Each map comprised a single data module, of which there were 28 (Figure 3.1). Each of these modules spans a single UTM zone. Several feature classes were defined: 1) areas deforested as of 1975, 2) the increment of new deforested areas occurring between 1975 and 1979, 3) rivers and 4) urban and developed areas, including roads. Each feature class was digitized as a separate data layer. Digitizing, editing and the initial compilation of the data were done individually in each module. Digitized modules were edited and cleaned in the computer, and checked against the original maps for accuracy and coherence using velum overlays. We utilized the ARC/INFO system, and all procedures follow methods defined in (ESRI 1990).

After editing and error-checking, each finished module was projected into UTM coordinates and stored in the computer. To compile a master database for the entire region, each map module was projected into geographic coordinates (latitude/longitude), edge-matched, and combined into a seamless data layer. The use of geographic coordinates was necessary to facilitate the merging of modules spanning several UTM zones. This full dataset could then be projected into any number of equal area projections.

The deforestation dataset was merged with ancillary features. We encoded administrative districts from individual state maps prepared by the Brazilian statistics and census agency (IBGE 1982b) which ranged in scale from 1:1M to 1:3M. These maps show the borders of 200 municipios, or towns, in the Legal Amazon as of 1980. The encoding of these maps made it possible to delineate deforestation by municipality and as well as state for 1975 and 1978. In association with the polygon coverage of municipalities we also digitized points for the urban center within each municipio. Roads were encoded as line data directly from the IBDF/INPE maps of deforestation.

Accuracy Assessment

The encoding of vectors always has some inaccuracy or imprecision associated with it, and such errors will translate into uncertainty in the measurement of polygon areas. Therefore, a detailed assessment was made of digitizing errors related to positional accuracy following the methods described by Dunn et al. (1990). Two test areas were chosen based on the pattern of deforestation (Table 3.1). Each area is characteristically different in shape; taken together they represent a cross section of the variation in pattern and geometry of deforestation in the Amazon. Test area 1 is a highly convoluted pattern with high perimeter/area ratios, while test area 2 is a rectilinear pattern with low perimeter/area ratios. Digitizing error occurs when attempting to encode boundaries. The position of the line encoded in the GIS presumably is accurate only to some level; although only one line is encoded in the database, it can be assumed that there exists some variance in position and location about this line which can be empirically determined.

The error-estimation technique employed here provides a measure of the variance in distance perpendicular to any line being digitized. The variance can be defined as an epsilon band around the line being encoded into the database. The width of this band can be multiplied by the total perimeter of all polygons in the digital dataset to determine the margin of error in measuring area due to positional error. In each test area, 3 polygons of deforestation were digitized 5 times by 5 different digitizing technicians. Thus, each polygon was measured 25 times (75 per test area). At regularly spaced intervals around each polygon in each test area, 50 measurements were made of the width of the epsilon band. The average epsilon error was estimated to be $\pm$ 7.8 meters, which would result in an error in area estimation of $\pm$ 3 percent for the database[1] (Table 3.1).

---

[1]The epsilon band defines the uncertainty in positioning a line in space, and hence the ability to define a boundary between two attributes. Since the location of the boundary itself has some variance associated with it, defined as the width of the epsilon band, the area encompassed also has some variance. The magnitude of the variance is a function of scale and the geometry of the polygons being digitized. Thus, one would expect polygons with high perimeter:area ratios to have higher uncertainty than polygons with low ratios. Our analysis chose two types of polygons, which generally bracket the range in perimeter:area ratios in our dataset, as shown in Table 4.1.

Delineation of Deforestation in Forest and Cerrado

The analysis delineates separately areas of deforestation occurring in closed and open forests. Open forests generally refer to those of the cerrado type, while closed forests generally include the closed canopy equatorial humid forests which dominate the basin. A forest/cerrado dataset was obtained by processing satellite remote sensing data. We obtained 288 weeks of the NOAA Global Vegetation Index (GVI) from 1985 to 1989. The GVI is a 16 km resolution product of weekly composites of the normalized difference vegetation index (NDVI) derived from channels 1 and 2 (Tarpley et al. 1984, Justice et al. 1985, Kidwell 1990). Weekly compositing is done in an attempt to remove clouds. We reprocessed the data into single monthly composites representing the average NDVI for all years, thus compressing the 288 individual data files into 12. To remove certain anomalies in the GVI, the mean and standard deviation were computed from weekly composites for each month, and pixel values outside $\pm$ 2 S.D. were removed before the final average was computed (other anomalies relating to co-registration between weekly composites were also corrected). Although there are a number of recognized problems with the GVI product (Goward et al. 1990), only some of which were corrected using these techniques, this data set is probably adequate for making a coarse, and rather obvious, delineation between forest and cerrado in the Amazon Basin.

The resulting GVI dataset provides phenology for an average 12 month period. Recent work by Malingreau and Tucker (1987) and Townshend et al. (1987) have shown that multi-temporal variations in the NDVI can be used to discriminate forest and cerrado vegetation during the dry season. From the 12-month average dataset, we extracted the data for the dry season months (August, September and October), and used these data in an unsupervised classification (statistical clustering) which resulted in ten broad classes of vegetation. These ten classes were recoded into forest and cerrado using existing maps and selected Landsat TM photoproducts for ground verification. The resulting forest/cerrado map is shown in Figure 3.2.

A Geographically-Referenced Terrestrial Carbon Model

To estimate the net flux of carbon, we couple the dataset to a numerical model which estimates the net flux of carbon between the land surface and the atmosphere as a result of land cover conversion. The model used in this study is based on a Terrestrial Carbon Model (TCM) which we haven used in the past to estimate the net flux of carbon from land use change in the tropics, and is fully described in Houghton et al. (1985b), Palm et al. (1986), and Houghton et al. (1991b). It has been modified here to incorporate spatial datasets. This Geographically-referenced Terrestrial Carbon Model (GTCM) links directly to the GIS and its associated datasets on land cover types and deforestation to produce a two-dimensional estimate of the net flux of carbon from the burning and decay of biomass and soil organic matter. The model uses the rate of deforestation in different land cover types (forest and cerrado here) as its forcing function. A series of response curves describe for each land cover type initial biomass and soil carbon, and the response of carbon stocks following disturbance. The response of carbon following disturbance is related to the rate of decay and fraction of burned and unburned material (Houghton et al. 1991b). The model estimates the net flux from the three major components: biomass which is burned, decay of slash, debris, wood removals, and charcoal which are not burned, and decay of organic matter in soil. For this assessment the model was parameterized using the data described in Table 3.2 of Houghton et al. (1991b). Data for closed and open forests from Table 3.2 were assigned to the forest and cerrado classes of the remote sensing classification of vegetation described above. These data parameterize the model for biomass, soil organic matter, and response characteristics.

Results

Area, Rate and Spatial Pattern of Deforestation

The digital map of deforestation in the Brazilian Amazon is presented in Figures 3.3 and 3.4. This figure shows the GIS database as a contiguous, seamless regional map of deforested areas. For presentation, the dataset has had to be greatly reduced in scale. Details of two sample areas are shown in Figures 3.5 and 3.6. In these detailed enlargements it is possible to identify areas of deforestation in 1975 as well as the increment of new deforestation between 1975 and 1978. The total area deforested in 1978 is the sum of the 1975 area and the 1975-1979 increment. Most of the deforestation in the Legal Amazon occurs in a crescent along the eastern and southern fringe of the Legal Amazon, with intrusions into Rondonia and the central Amazon basin along roadway corridors. This is not too surprising considering what has been reported in some of the recent literature (Fearnside 1986, Malingreau and Tucker 1988, Setzer and Pereira 1990). However, we know of no reports which explicitly portray the spatial organization of deforestation in a seamless digital database as shown here.

From our GIS-based measurements of the original maps, we estimate the total area deforested by 1975 to be 33,884 km^2. By 1978 the total deforested area increased approximately 200% to 100,016 km^2 (Table 3.2). In terms of total deforested area, most was in eastern Amazonia; approximately 68% of the total deforested area was in the two states of Para and Mato Grosso. Deforestation in Para has occurred at least since the 1960s, most of it in a 6-degree by 6-degree area centered on Latitude 4-S and Longitude 48-W (Figure 3.4), which also includes part of the state of Maranhao. Other states, such as Maranhao, Goias, and Rondonia were also important regions. Between 1975 and 1978 the average annual rate of deforestation was approximately 22,000 km^2 (Table 3.2). Although the largest total area of deforestation was measured in the eastern Amazon, the greatest rate of change occurred in the newly colonized state of Rondonia, which experienced explosive deforestation rates in the late 1970s; the deforested area increased over 300% between 1975 and 1978.

By overlaying a digitized map of administrative district (municipios) borders on the deforestation delineation, this new database provides estimates of deforestation at the municipality level. These data are reported in Annex 1, which shows the total deforested area in 1975 and 1978, as well as the average annual rate of deforestation between 1975 and 1978, for each municipality in the Legal Amazon. Also reported is the fraction of area of each municipality deforested for each date. We know of no other study which has reported deforestation at this level of detail. There is considerable variation between municipalities in terms of total area deforested in 1978. This suggests deforestation in the Amazon does not occur as a continuous advancing front, but as a highly concentrated phenomenon which makes advances along a network of roads and rivers or in proximity to settlement "poles." This characteristic has been noted qualitatively by others as well (cf. Fearnside 1986). This observation is further borne out when deforestation is measured as a function of distance from municipio centers (Figure 3.7). Localized concentration of deforestation in some municipalities was significant: Imperatriz in Maranhao state, Paragominas in Para, and Extremo Norte Goiano in Goias. Some municipalities with lower total deforested area were still significant in terms of the fraction of the municipality converted and the rate of deforestation (see Annex 1).

Deforestation in Forests and Cerrado

The use of GIS permitted a spatial analysis of deforestation by ecosystem type. Table 3.3 shows results of spatially merging the deforestation data layer with the vegetation classification data layer in the GIS. In 1978, 68 percent of the total deforested area was in closed forests and 32 percent in cerrado, indicating only a slight change from 1975. Most states had very little (less than 5%) deforestation in cerrado. However, the two states of Mato Grosso and Goias had large amounts of the total area deforested coming out of cerrado systems (68% and 62% respectively in 1978). Moreover, the relative proportion of clearing in cerrado vegetation increased between 1975 and 1978 in these two states, while remaining constant in the others. The average annual clearing rate in closed forests during the period was 14,575 km^2, and the average annual rate in cerrado was 7,469 km^2.

Biogenic Emissions of Carbon Dioxide

Spatially detailed, geographically-referenced data on deforestation were used to improve estimates of the net flux of carbon. The geographically-referenced annual net flux of carbon between 1975 and 1979 as estimated from the numerical model and spatial databases on deforestation and land cover is shown in Figure 3.8. Fluxes shown in this figure have been summed into 0.5° x 0.5° grid cells, and then contoured (Figure 3.8). The net flux of carbon from deforestation during this period is 0.36×10^{15} g C yr^{-1} (Table 3.4). The burning and decay of aboveground biomass following clearing constitutes 86% of the total net flux. As one would expect the largest fluxes are associated with regions with the highest deforestation rate; the largest releases seem to have occurred in a crescent-shaped region of high deforestation along the eastern and southern perimeter of the basin. Largest fluxes occurred in central Rondonia, western Mato Grosso, Maranhao, and eastern Para. These are forested regions with high rates of deforestation and high biomass. Table 3.5 shows the annual net flux estimated for each state. Almost 90% is from the four states of Para, Mato Grosso, Maranhao, and Rondonia.

Table 3.5 also presents results after the GIS sorts the flux estimates according to state and vegetation type. The largest fluxes are estimated in forest regions. Of the total net flux 86% was derived from closed forest regions, while 14% came from clearing of cerrado. Cerrado clearing constituted a large fraction of the net flux estimates in Mato Grosso and Goias. Fluxes from forest clearing predominated in the other states.

Discussion and Conclusion

The analysis reported here represents an comprehensive approach to the use of geographically-referenced data from satellites and other sources for global change research. Obtaining geographically referenced data on deforestation is the first step toward improving our understanding of the role of human-induced ecosystem modifications in the global carbon cycle and climate system (Houghton et al. 1985a, Skole in press). The current range in the estimate of the global net flux of carbon from tropical deforestation is between 0.4 and 2.5 x 10^{15} g C yr^{-1} (Houghton et al. 1985b, Detwiler and Hall 1988); most of the uncertainty due to a paucity of good data on deforestation and biomass. One way geographically-referenced data and models could improve current terrestrial carbon cycle models is by providing coincident data on deforestation rates and ecosystem distributions so that it is possible to know what systems are disturbed at each time interval. Previous estimates of the net flux of carbon from land use change need to rely on separate sources of land use and ecosystem data, making it difficult to know how to distribute clearing rates among different ecosystem classes (Houghton 1986). Using GIS methodologies applied at continental to global scales, it is possible to develop geographically-referenced data on deforestation and solve some of these problems. The results from our compilation of a dataset on deforestation in the Legal Amazon during the late 1970s provide great improvements over existing data. The approach taken here has made it possible to overlay areas of conversion with maps defining the distribution of major ecosystems.

The conversion of closed forests of the Brazilian Amazon was more important than cerrado clearing, both in terms of area and carbon emissions. The amount of cerrado cleared was, nonetheless, important when compared to other regions worldwide. Of the 38,000 km^2 of open forest converted worldwide in 1980 reported by Lanly (1982), cerrado clearing in the Brazil Amazon comprised 20 percent. This fraction is actually slightly larger than the fraction of closed forests cleared (19 percent). Analyses of cerrado clearing should be included in studies of land cover conversion in the Amazon, but has frequently been omitted in favor of concentrating attention on the closed forest region.

Our delineation of the area of cerrado clearing might be high if there is considerable confusion in the satellite classification of areas of large-scale clearing along the forest-cerrado boundary or with areas of old secondary growth which have long been deforested but appear spectrally similar to cerrado. Our GIS analysis of a Radambrasil map of vegetation in the Amazon Basin derived from data obtained in the 1970s (Ministerio das Minas e Energia, no date[2]) suggests 14% less area in cerrado than we obtained using multitemporal AVHRR data from the 1980s. However, our classification of total cerrado area (839,874 km^2) is within 6% of the area of cerrado and savanna estimated by Fearnside (1990b) (793,279 km^2). And our estimate of the total area in closed forest of 4,204,387 km^2 almost exactly agrees with the estimate of 4,195,660 km^2 made by Fearnside (1990b). Indeed, improvements in the classification of continental vegetation could be made; our assessment provides a first-order remotely sensed stratification of broad vegetation classes which generally conforms to other analyses (Lanly 1982, Fearnside 1990b, Houghton et al. 1991a). An improved classification, with more vegetation classes, could be developed in the future using a combination of finer resolution, multi-temporal AVHRR data, high resolution Landsat data, and cartographic information.

Our measurement by GIS techniques of the annual deforestation rate from the original maps reported in Tardin et al. (1980) was 22,044 km^2 yr^{-1} between 1975 and 1978. These numbers generally agree with, but are slightly higher than, those reported by Tardin et al. (1980) and others (Fearnside et al. 1990) using the same map base. It

---

[2]This vegetation map of the Legal Amazon produced at 1:2,500,000 scale was digitized and merged with the deforestation dataset. The deforested area falling within the boundaries of the cerrado class were then tabulated and compared to the satellite-based analysis.

is likely that our current figures using vector-based GIS techniques represent more accurate area-estimations than were obtained by Tardin et al. (1980) using a dot-grid estimation. The possible error in our estimate due to measurement or positional inaccuracies is no more than 3%, as calculated from our accuracy assessment. We cannot attest to the accuracy, both positional and interpretive, of the original maps.

Although this rate represents approximately one fifth of the global total tropical deforestation during that period, the total area deforested as of 1978 was only 2% of the Legal Amazon. Only 1% of cerrado had been cleared as of 1978. These fractions are small, but even small fractions in a large place such as the Amazon Basin mean potentially large emissions of carbon dioxide. The dataset developed in this analysis was coupled to a numerical model to estimate the net flux of carbon from deforestation between 1975 and 1978, and thus demonstrate the utility of spatial data of this kind. This net flux, as reported above, is estimated to be 0.36×10^{15} g C yr^{-1}. This estimate generally agrees with other published estimates for Brazil (Houghton et al. 1987). The estimate could, however, would be high if a large fraction of the deforested area was in some stage of abandonment or secondary growth. The mapping of net conversions as described in this analysis cannot separately delineate new clearings from secondary growth. Deforested land which is recovering following abandonment represents areas of carbon uptake from the atmosphere. There is no direct estimate of the amount of second growth or abandonment in the Amazon Basin, but based on our own cursory examination of recent Landsat and SPOT satellite data and field work in Rondonia this could be an important question. An analysis of secondary growth would need to be developed using sampling with high resolution satellite data.

The estimate of carbon flux might also be high if the historic time-series trend in deforestation rates before 1975 were lower than the rates in 1975-1978. Since satellite observations are not available in the Amazon Basin much before 1975, this could not be assessed directly. However, it might be possible to develop an analysis of land cover conversion for the historical period using published tabular data on land use from the agricultural census (Censo Agropecuario) of the Instituto Brasileiro de Geografia e Estatistica (IBGE 1960, 1970a, 1980a). These tabular data, reported by municipio, provide information on changes in the area of crops and pastures back to the 1960 census and before. These data could be mapped into the municipio data layer described above, and coupled to remote sensing analyses for the period when satellite observations are available. Figure 3.9 demonstrates this approach for the state of Rondonia, where we have compared the IGBE data with other published satellite remote sensing estimates[3]. There appears to be continuity between the tabular and remotely sensed approaches.

[3]Data for 1960, 1970, 1975, 1980, and 1985 were taken from the Censo Agropecuario and compared to Landsat data published from different sources. Landsat data for 1975 and 1978 were taken from this study and Tardin et al. (1980). Landsat data for 1980, 1983, and 1986 were derived from Instituto de Pesquisas Espaciais (1989).

The approach described here could be extended to more recent time periods to improve estimates of deforestation and more accurately estimate the net flux of carbon. In fact, the net flux of carbon from land use change is highly dependent on the time series of clearing rates. It is possible that the rate of deforestation in the 1980s has increased since the 1970s. Fearnside (1990b) gives an estimate of the current (1988) deforestation of 38,000 km^2 yr^{-1}, of which 20,298 km^2 is in closed forest and 18,245 km^2 is in cerrado. This estimate for forest conversion is slightly lower than one reported by the Brazilian Agency for Space Research (INPE) for a 1988 rate of 26,700 km^2 yr^{-1} (Fearnside et al. 1990). These estimates compared to those reported here for the late 1970s also suggest that the rate of deforestation in cerrado has increased faster than in closed forests.

These estimates when compared to our database suggest the rate of deforestation today is some 75% higher than in the 1970s, but at this time there is a wide difference in the current estimates for the Amazon (Skole in press). An estimate by the World Resources Institute (1990) suggest a rate of closed forest clearing in the late 1980s at 80,000 km^2 yr^{-1}. Myers (1989) provides an estimate of 50,000 km^2 yr^{-1} in closed forests in 1989. Data from Setzer and Pereira (1990) indicate a closed forest conversion rate of 32,000 km^2 yr^{-1} for 1987. To estimate the effect on carbon fluxes, the estimates of WRI (1990), Myers (1989), and Fearnside (1990b) were used in conjunction with the GIS-based numerical model discussed above. The geographically-referenced rates from dataset for 1975-1978 reported here, were uniformly increased linearly over the decade, 1978-1988. The results suggest a considerable difference in the estimate of net carbon flux, from 1428 x 10_{12} g C yr^{-1} for the WRI (1990) estimate, to 937 x 10^{12} g C yr^{-1} for Myers (1989), to 586 x 10^{12} g C yr^{-1} for Fearnside (1990b).

Fluxes of these magnitudes would certainly be important and would suggest earlier estimates of the net flux of carbon from human induced change in terrestrial ecosystems has been underestimated (Houghton et al. 1985b, Houghton 1991). However, the data for current deforestation rates in the Amazon and elsewhere in the tropics are sparse and imprecise. New efforts must be initiated to reliably quantify deforestation and its geographic distribution. Efforts to utilize high resolution remote sensing in conjunction with geographic information systems are the most promising. These efforts must be simultaneously coupled to efforts to classify the natural land cover types. These efforts too could best be done utilizing remote sensing, but might be achieved at a coarser resolution, using AVHRR-GAC (4 km) data (Townshend et al. 1990). However, any retrospective work would also need to use maps and tabular information.

The use of remote sensing data forms the first level of an approach to improving the estimates of carbon emissions and our understanding of climate impacts by providing consistent, geographically-referenced data on deforestation rates. Such an approach would provide the basis for spatial analysis of water/energy dynamics or forest fragmentation assessments. Efforts such as these would go a long way toward improving the database for decision-making as well. For instance, unlike the generally point-source pollution problem presented by the introduction of CFCs into the global environment, the emission of carbon dioxide and trace gases from deforestation is widespread and spatially diffuse. At the present time there are no data on deforestation sufficient to form a foundation of fact for any reasonable set of international negotiations. The results of this study suggest that a methodology now exists, from which digital datasets of this kind could be developed in an objective, reproducible, and verifiable manner.

Table 3.1. Geometric characteristics of each of the three test polygons in the test area and the average width of the epsilon band for each test area. Units given are in digitizer board inches. The epsilon band width is reported in meters.

	AREA	PERIMETER	P / A	EPSILON BAND (meters)
Test Area 1				17.6
Polygon A	0.139	5.009	36.035	
Polygon B	0.653	13.281	20.338	
Polygon C	0.314	9.035	28.774	
Test Area 2				13.6
Polygon A	2.123	7.844	3.695	
Polygon B	0.474	5.627	11.871	
Polygon C	0.678	5.548	8.183	

Table 3.2. Total deforested area and the average annual deforestation rate in 1975 and 1978 estimated and derived from the vector-based GIS dataset.

State	1975 (km^2)	1978 (km^2)	Increase (%)	Annual Rate (km^2 yr^{-1})
Rondonia	1,537	6,352	313	1,605
Acre	1,180	2,250	91	457
Amazonas	917	2,344	156	476
Roraima	74	209	182	45
Para	11,366	30,768	171	6,467
Amapa	185	233	26	16
Maranhao	2,951	11,196	279	2,748
Mato Grosso	11,739	37,130	216	8,464
Goias	3,935	9,234	135	1,766
Legal Amazon Total	33,884	100,016	195	22,044

Table 3.3. Total area deforested in closed forest and cerrado land cover types for the Legal Amazon in 1975 and 1978. Units are km^2.

State	1975		1978	
	Forest	Cerrado	Forest	Cerrado
Rondonia	1,516	21	6,266	86
Acre	1,180	0	2,550	0
Amazonas	917	0	2,344	0
Roraima	74	0	208	1
Para	10,766	600	29,573	1,195
Amapa	185	0	233	0
Maranhao	2,868	83	10,811	385
Mato Grosso	4,483	7,256	11,895	25,235
Goias	1,818	2,117	3,652	5,582
Legal Amazon	23,807	10,077	67,532	32,484

Table 3.4. An estimate of the annual net flux of carbon between 1975 and 1978 using the GIS-based deforestation dataset and a geographically-referenced terrestrial carbon model. Units are 10^{15} g C yr^{-1}.

From biomass burned	0.10
From decay of on-site slash, debris, charcoal	0.21
From decay of soil organic matter	0.05
Total net flux	0.36

Table 3.5. Net flux of carbon from clearing closed forests and cerrado between 1975 and 1978 in the states of the Legal Amazon. Units are 10^{12} g C yr^{-1}.

State	Closed Forest	Cerrado	Total
Rondonia	33.54	0.14	33.68
Acre	9.67	0.0	9.67
Amazonas	10.1	0.0	10.1
Roraima	0.95	0.01	0.96
Para	132.78	1.29	134.07
Amapa	0.34	0.0	0.34
Maranhao	56.09	0.66	56.75
Mato Grosso	52.34	39.09	91.43
Goias	12.95	7.53	20.48
Total	308.76	48.72	357.48

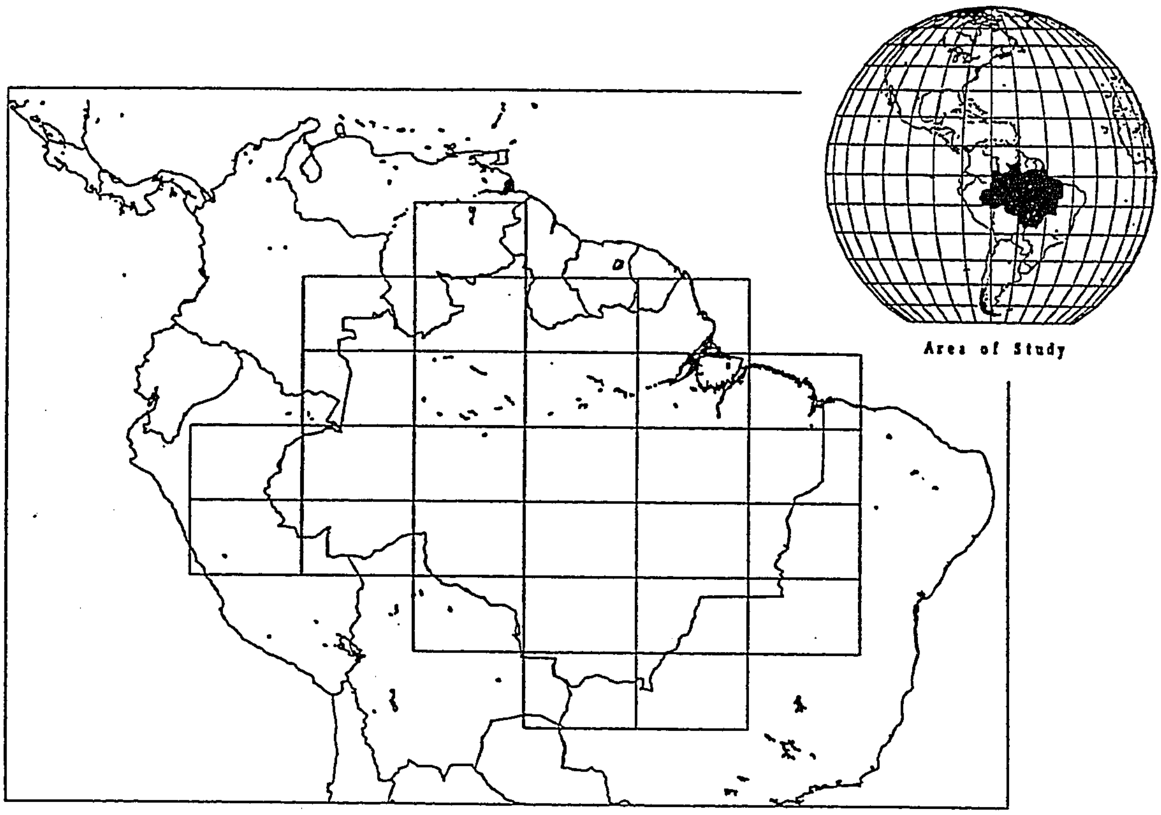

Figure 3.1. Orientation of each of the map digitizing modules which comprised the full dataset.

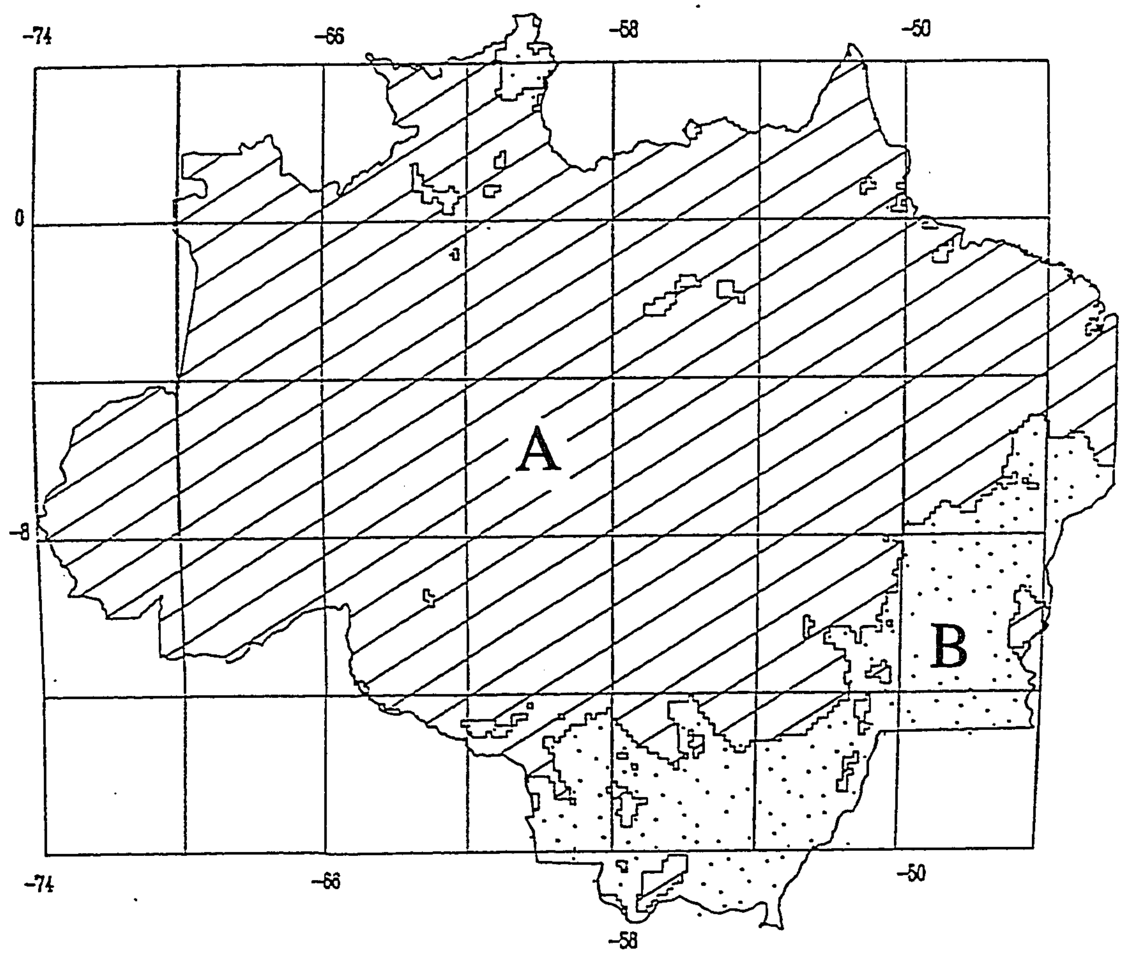

Figure 3.2. Digital map of forest (A) and cerrado (B) vegetation derived from multispectral and multitemporal classification of the Global Vegetation Index satellite data.

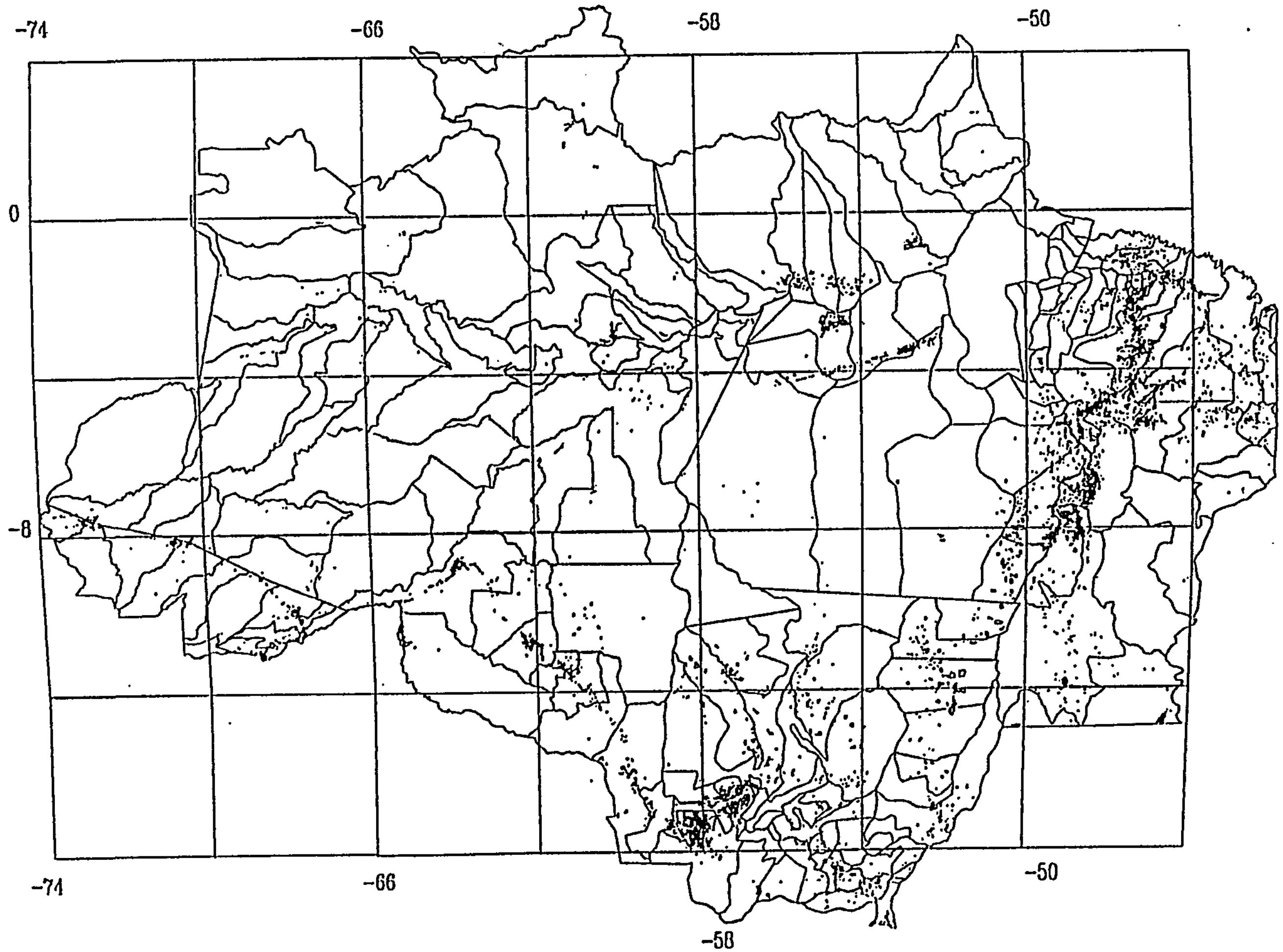

Figure 3.3. The GIS-based deforestation dataset showing areas which had been deforested as of 1975 in the Legal Amazon, including boundaries of each municipio. Dark areas show the location of polygons of deforestation but considerably reduced in scale.

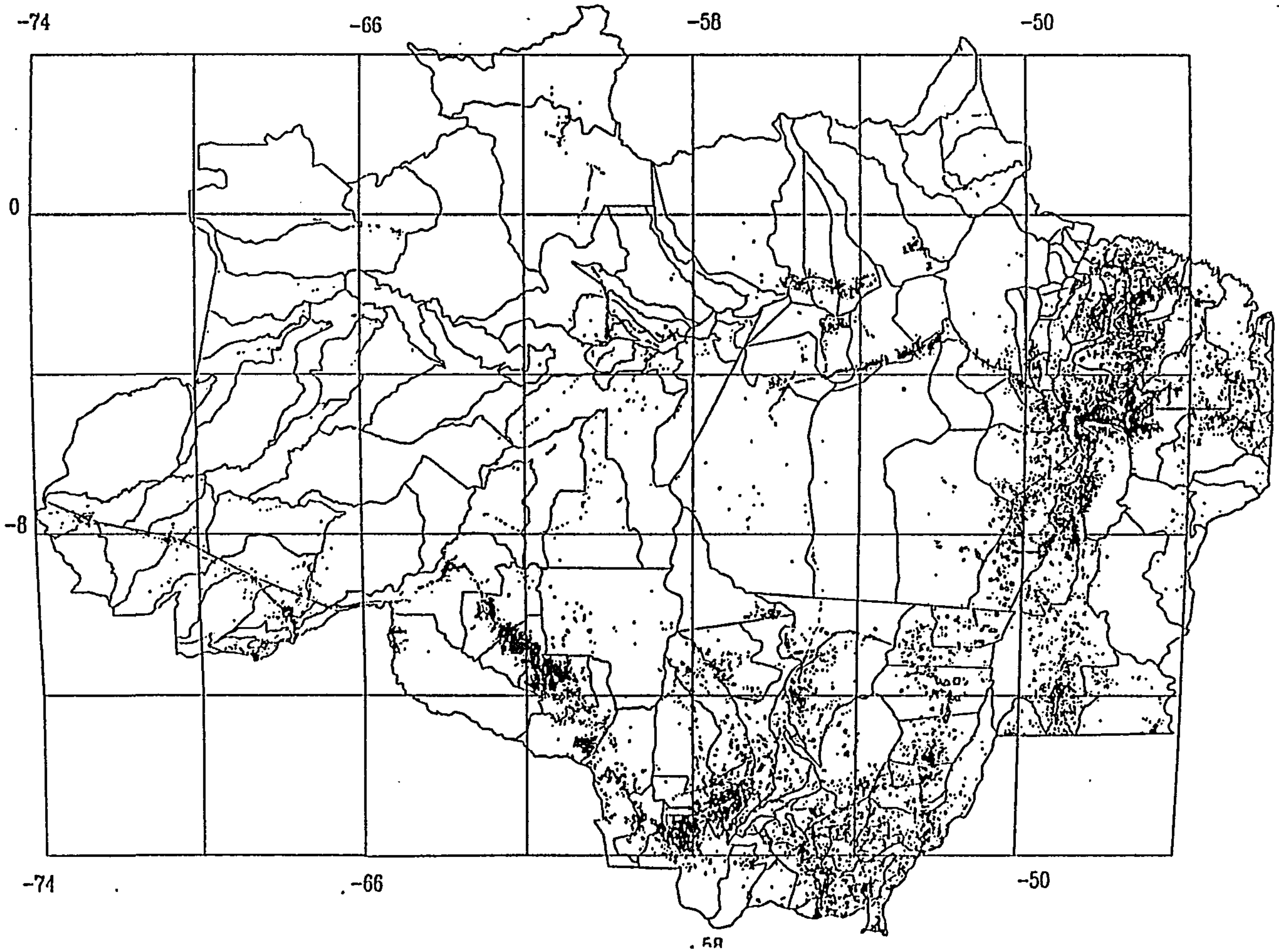

Figure 3.4. The GIS-based deforestation dataset showing areas of new deforestation which occurred between 1975 and 1978 in the Legal Amazon.

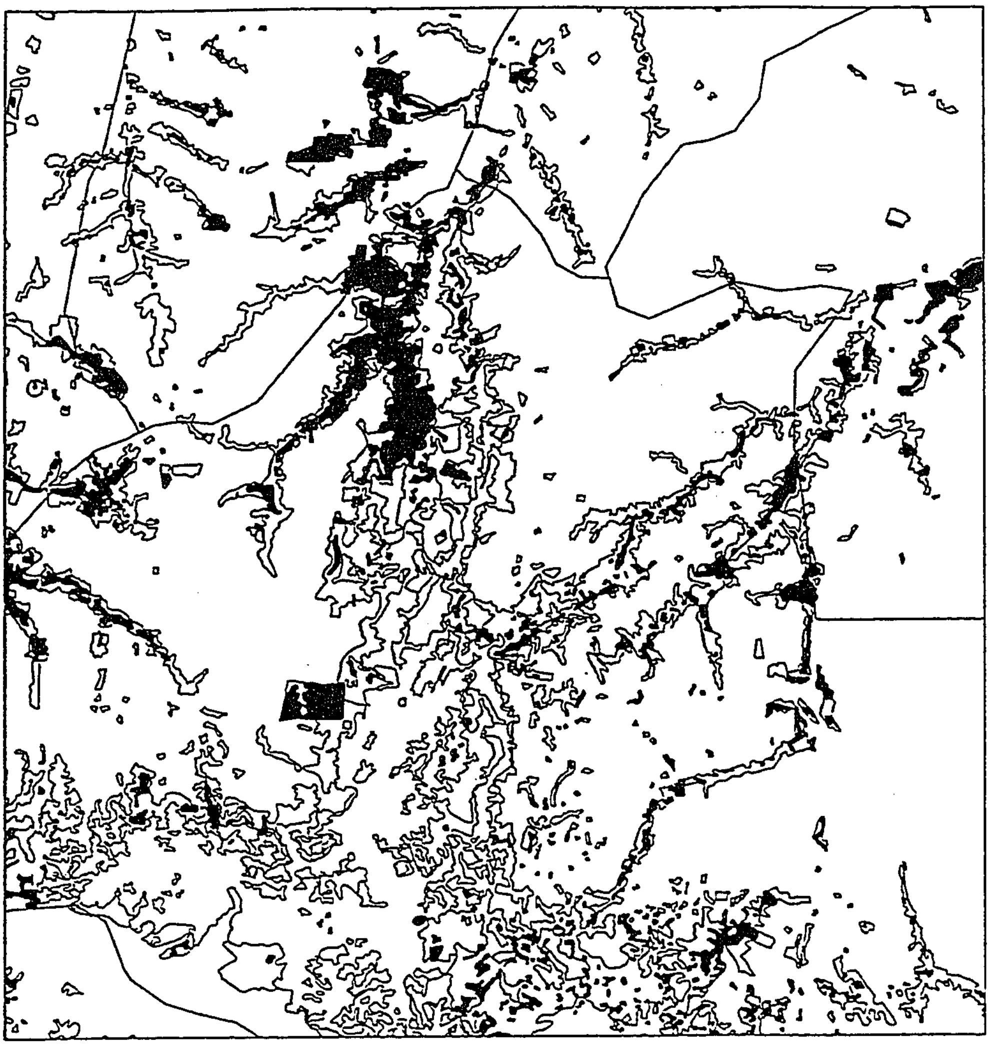

Figure 3.5. Enlargement of an area from Figure 3.4. Dark shaded polygons represent areas deforested as of 1975. Light shaded polygons represent new deforestation which occurred between 1975 and 1978.

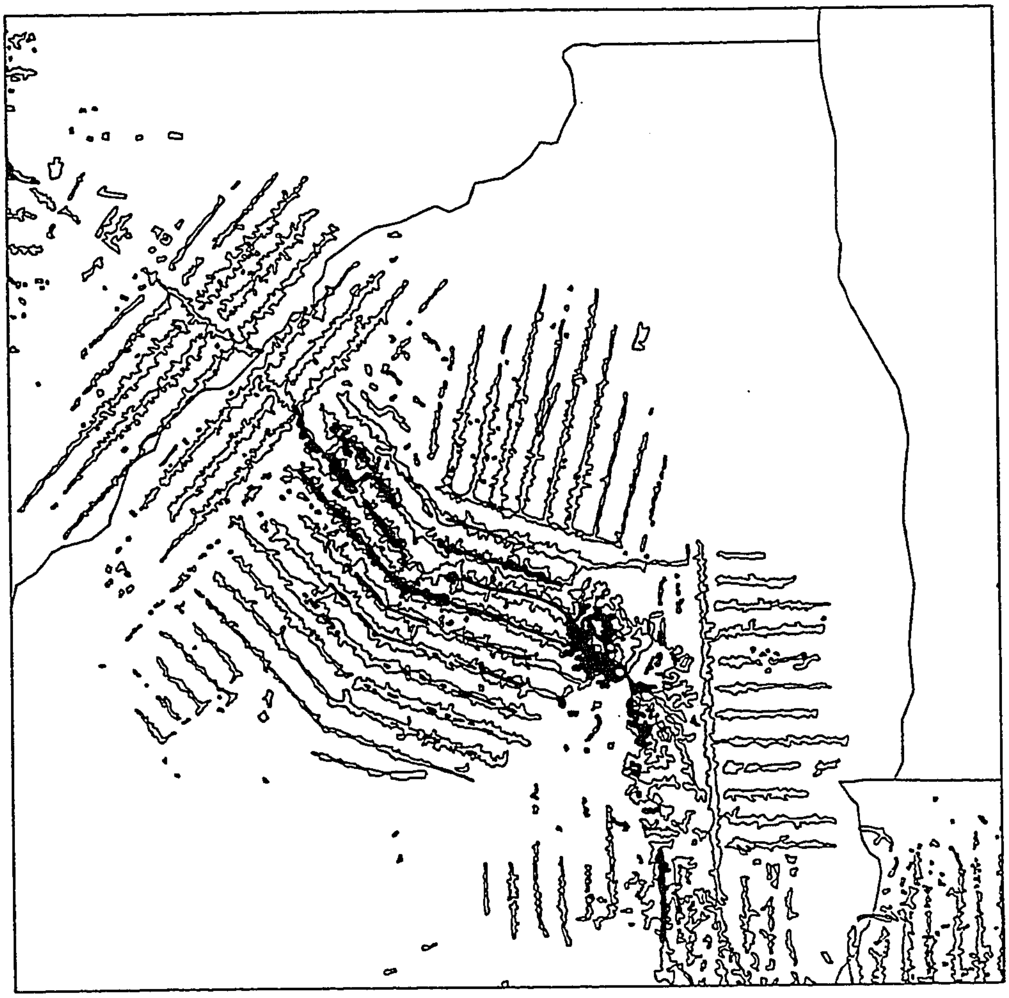

Figure 3.6. Second enlargement of an area from Figure 3.4. Shading pattern is the same as Figure 3.5.

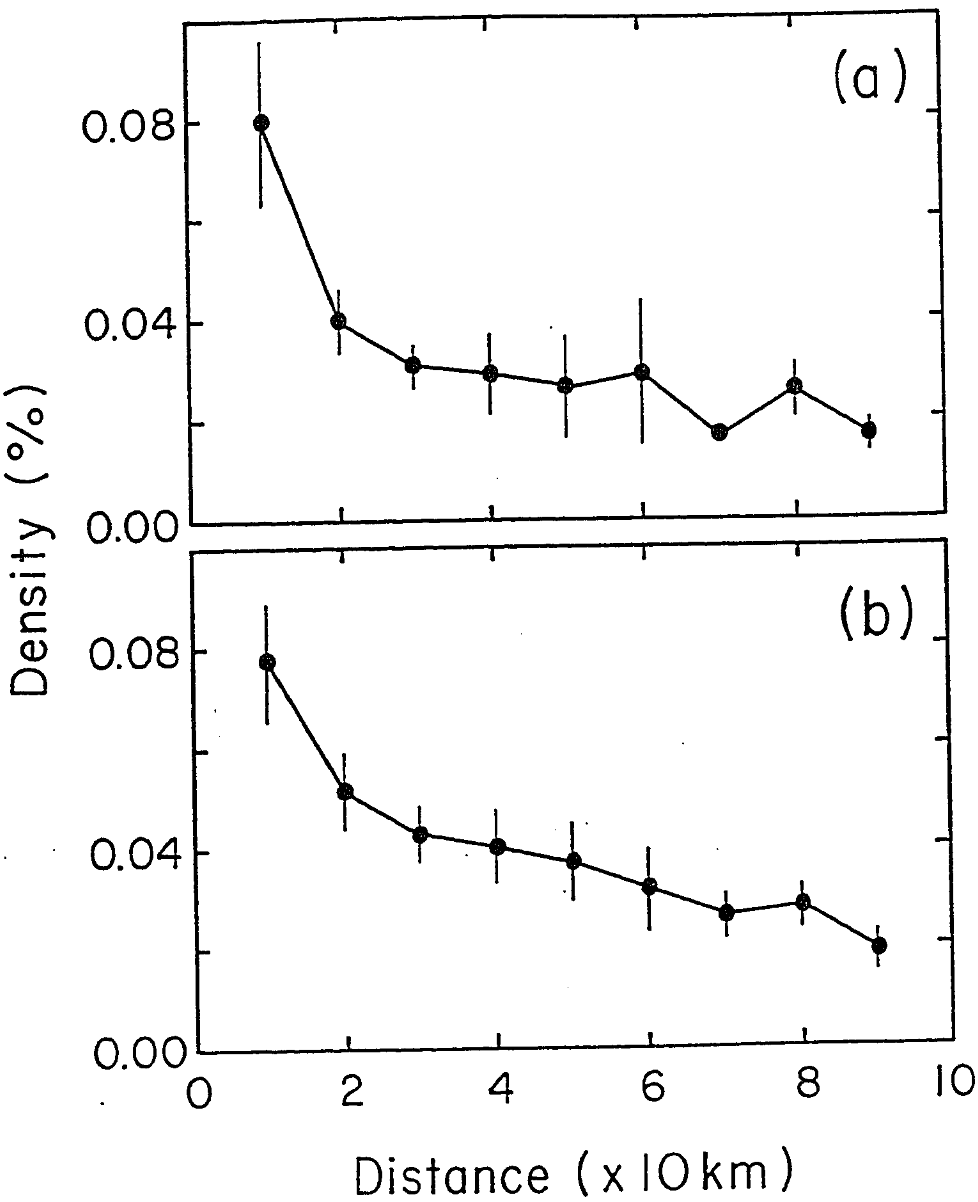

Figure 3.7. Deforestation as a function of distance from municipio centers in 1975 (A) and 1978 (B). The curve represents the average density computed for all municipios at regular intervals from the municipio center. Error bars show ± 1 standard deviation.

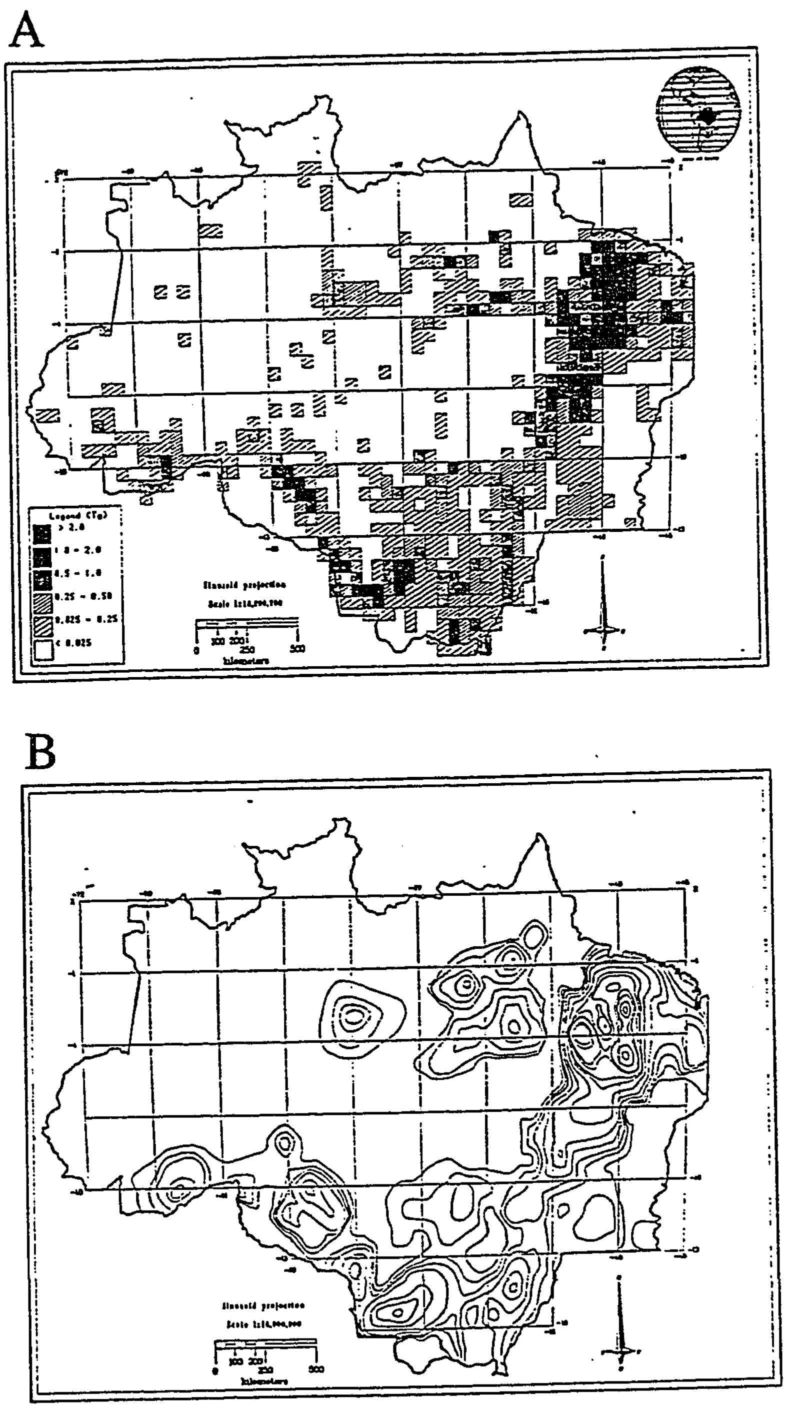

Figure 3.8. Geographically referenced total net flux of carbon from deforestation between 1975 and 1978 computed for 0.5° x 0.5° grid cells (A) and contoured (B). Grid cells have been shaded according to ammount as shown in Figure legend, unit are 10^{12} g.

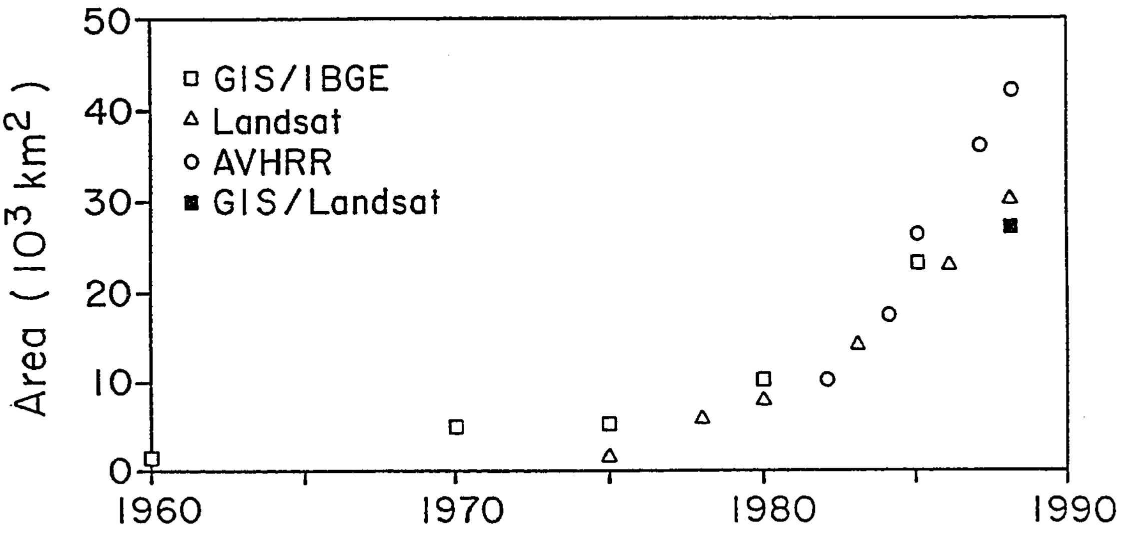

Figure 3.9. Comparison of estimates of deforestation in the state of Rondonia derived from tabular data from IBGE agricultural census with recent estimates from Landsat and AVHRR remote sensing analyses. Open squares were derived from tabular agricultural census data (Chapter 2), open triangles were derived from published Landsat surveys by INPE, closed triangles represent this study, open circles are from previous AVHRR analyses, and the closed square is from analysis in Chapter 6.

CHAPTER 4

A COMPARISON OF METHODS FOR REMOTE SENSING OF DEFORESTATION

Introduction

Recent estimates suggest tropical deforestation rates have increased 100 to 140 percent since the late 1970s (Myers 1991, WRI 1990). However, there is considerable uncertainty in these estimates. One problem is the absence of a uniform and consistent source of data or method for measuring deforestation. Because data on rates of deforestation are directly used to estimate fluxes of carbon dioxide between the land and atmosphere, such uncertainties are important and will result in uncertainty in the estimate of carbon dioxide emissions (Houghton 1991b, Houghton and Skole 1990).

Estimates of the current net flux of carbon between the biota and the atmosphere due to deforestation in the tropics range from 0.4 to 2.5 x 10^{15} g C yr^{-1} (Detwiler and Hall 1988, Houghton 1991b, Houghton et al. 1987, Houghton and Skole 1990). Three uncertainties contribute to this wide range: (1) estimates of tropical deforestation rates, (2) a poor quantitative understanding of the fate of deforested land (i.e., the amount of secondary forest regrowth and re-clearing), and (3) sparse and isolated sampling of biomass and soil organic matter and their response to disturbance. The most tractable uncertainties to resolve are probably the first two, particularly if a remote sensing method could be employed to provide maps of deforestation and regrowth. Such improved geographic and temporal data on deforestation rates would contribute significantly to increasing the precision of estimates of the next flux of carbon and our understanding of the global cycle.

Satellite remote sensing provides perhaps the best way to quantify temporal and spatial variations in deforestation rates. Several methods have been developed in recent years in small-scale pilot studies. Research by Tucker et al. (1984), Nelson and Holben (1986), Nelson et al. (1987), Malingreau and Tucker (1987, 1988), Malingreau et al. (1989), Malingreau (1990), and many others have demonstrated potential methods from which an objective measure of tropical deforestation can be made. If remote sensing data are used as the basis for a systematic tropical forest monitoring program to support terrestrial carbon cycle models (Dale 1990, Dale et al. 1991), the approach would need to be simple, low in cost, and accurate. It should capable of making measurements accurately over large areas.

In this paper several techniques for measuring deforestation with remote sensing data were explicitly compared in terms of their ability to quantify the total extent of deforestation in closed tropical forests of the Brazilian Amazon. Simultaneous acquisitions of SPOT, TM, and AVHRR data were made in 1988 and then classified using common techniques found in the current literature.

Background

Remote sensing studies in the Brazilian Amazon have appeared in the literature for several years. The first studies used Landsat data, while more recent studies have focused on large scale surveys using AVHRR data (Fearnside et al. 1990, Malingreau 1990, Malingreau and Tucker 1987, 1988, Malingreau et al. 1989, Nelson and Holben 1986, Nelson et al. 1987, Santos 1977, Setzer and Pereira 1991, Stone et al. 1991, Stone and Woodwell 1987, Tardin et al. 1980, Tardin and Pereira da Cunha 1990, Tucker et al. 1984, 1986, Woodwell et al. 1987, 1986). The AVHRR has practical appeal since it can be acquired daily to make cloud-free composites, and each scene covers a large area and is low in cost. Using AVHRR thermal emission data, Nelson et al. (1987) concluded that the AVHRR should only be used as a stratification tool, due to the poor relationship between fire activity observed with the AVHRR and deforestation rates derived from coincident MSS and TM visible and near infrared spectral data. However, later studies of Amazon deforestation suggested AVHRR analysis was a promising approach for large-area mapping of tropical deforestation. Malingreau and Tucker (1988) used a brightness temperature threshold on the AVHRR channel 3 data to enhance contrast between the forest and cleared areas. A series of papers by Woodwell and colleagues reported similar success with the channel 3 (Woodwell et al. 1984, 1986, 1987), and also with other channels in unsupervised classification (Stone et al. 1991). Similarly, Cross (1990) reported success using

AVHRR data in the Amazon, but suggested that a Maximum Likelihood classification would be better than the channel 3 threshold approach. Based on the results of these studies, a number of reports have hence advocated the use of AVHRR as the basis for global monitoring programs.

Most of these studies have been for single test sites, and have never been applied to the entire Brazilian Amazon. Recently, Setzer and Periera (1991) have estimated the deforestation rate in 1987 for the entire Amazon using the distribution of fires determined from the AVHRR-LAC thermal information and assumptions on the duration of fires and the burned area within each 1.1 km pixel. Another Amazon-wide assessment was made by the Brazilian space agency, INPE, (Fearnside et al. 1990, Tardin and Pereira da Cunha 1990) for 1988 using 3-channel Landsat-TM color photo products, but reported much lower estimates. These recent estimates by INPE were developed using a method employed for large-area deforestation mapping which has its antecedents in studies dating back to the late 1970s (Santos et al. 1979, Tardin et al. 1979, 1980).

Recently, some work by Batista and Tucker (in prep.) and Cross et al. (1991) suggest that the AVHRR might be overestimating the area of deforestation in the Amazon. Indeed, the analyses of Cross (1990) and Stone et al. (1991) appear to result in higher estimates than those being reported by the Brazilian space agency. For instance in the state of Rondonia where deforestation has been measured by coarse and high resolution satellite data, estimates for the total area deforested as of 1988 range from 29,000 to 40,000 km^2. These differences are unsettling, since they suggest there is as yet no clear definition of an approach for systematic, large-area mapping of deforestation using satellite data.

Methods

The General Study Area

The state of Rondonia, Brazil, (Figure 4.1) has experienced some of the most rapid and extensive deforestation anywhere in the tropics. Recent studies suggest the total deforested area increased over 300% between 1975 and 1980 (Skole et al., submitted), and by 1500% between 1975 and 1988 INPE (1992). As much as 15% of the forest cover has been removed (Fearnside 1990b).

Since the early 1970s government programs aimed at establishing new human settlements in the Amazon Basin have moved settlers to the once-forested region. Government incentive programs for pasture development and the creation of infrastructure have been coupled with free land entitlement programs to create a strong magnet for migration into this part of the Amazon Basin. Between 1970 and 1980 the state's population grew from 111,000 to 491,000 (IBGE 1989); it was the fastest growing state in Brazil during the 1980s, with a population in 1988 of over 1 million. Approximately 60% of the population is classified as rural, mostly migrants from the south and northeast of Brazil. The largest cities are Porto Velho and Ariquemes, the former is the state capitol and the latter is the site of one of the largest colonization centers (Figure 4.1).

Most of the land clearing has been for agriculture. Approximately half the agricultural clearing is for pasture and half for temporary and permanent crops (IBGE 1980a, IBGE 1989). Principal crops are rice, milho, coffee, beans, cacao, and manioc. Eighty percent of the farms are less than 100 ha in size (IBGE 1989). The regional climate is tropical. Temperature varies only slightly throughout the year, averaging 25° C, with relative humidity frequently above 85%. Total annual precipitation is approximately 2000 mm, with an extended rainy season from October to April. The primary dry season is from June to September, when most clearing and burning takes place. This period provides a window of opportunity to obtain cloud-free satellite data, as long as the imagery is not obscured by smoke in the visible bands.

The Test Site

A test site was established in the northern part of the state, between the towns of Ariquemes and Porto Velho (Figure 4.1). The test site was established to directly compare different satellite instruments and provided a location for ground-level field verification of classifications. The entire site is 120 km by 60 km (7,200 km^2), encompassing the area of two SPOT scenes (Figure 4.1). Deforestation is active in this area. Large colonization projects occur in the southern portion of the site, with the characteristic extensive fishbone-like pattern of roads, while the northern portion is characterized by many variously-sized and scattered clearings. The Cuiaba-Porto Velho highway, BR364, runs diagonally through the area, with its associated roadside clearings and towns. The massive Samuel hydroelectric project is in the northern portion of the test site. The geometry and pattern of deforestation is varied, an important criterion for the selection of this test site.

Data Acquisition

Table 4.1 presents an overview of the sensor characteristics of the data acquired for this study. These data vary in the spatial resolution, frequency of coverage, placement of spectral bands, and orbit inclination with respect to the equator. SPOT multispectral data can be obtained at 20m spatial resolution (IFOV) at nadir in three spectral bands, two visible and one infrared. Landsat Thematic Mapper (TM) data are acquired at 30m spatial resolution (IFOV) in 3 visible bands and 3 infrared bands.

The AVHRR on board the NOAA polar orbiting satellites acquires data with 1.1 km resolution at the satellite subpoint in five channels: one visible, one near infrared, and three thermal infrared. The first two channels (0.58-0.68 um and 0.73-1 um) can be used to monitor vegetation distribution and vegetation phenology (Justice et al. 1985, Malingreau 1990, Townshend and Tucker 1984, Tucker et al. 1985, 1986) since the normalized difference vegetation index (channel 2 - channel 2 / channel 2 + channel) is closely correlated with green leaf biomass and leaf area over time. Channel 3 of the AVHRR (3.55-3.93 um) is a mixed band; sensing in both reflected and emission infrared wavelengths (Kidwell 1991). It is possible to acquire both day and night data since the satellite has both ascending (daytime) and descending (nighttime) equatorial crossings within a 24-hour period. Daytime acquisition of channel 3 AVHRR data can be used to detect deforestation since it seems to enhance the contrast between forest and deforestation. Nighttime acquisitions, in the absence of daytime albedo, can be used to detect thermal anomalies representing forest fires (Kaufman et al. 1990a, Malingreau 1990, Setzer and Pereira 1991). This study only focuses on the use of daytime channel 3 data.

Separate acquisitions of SPOT, Landsat-TM, and AVHRR-LAC data were acquired in the test site within a common time period of $\pm$ 1 week, during 1988. A 1988 acquisition date was chosen because most previous studies of deforestation using remote sensing methods of various sorts have been conducted for this time period. Two SPOT multispectral scenes were acquired on 10 July 1988 (k,j = 675,369; k,j = 675,368) with less than 10% cloud cover. Two Landsat TM data were acquired on 21 July 1988 (wrs = 232,67; wrs = 232,66) also with less than 10% cloud cover. AVHRR local area coverage (LAC) data were acquired 14 July 1988. All data were clear of smoke or haze. This is not always possible in this region, but this particular time the area was cloud-free at the end of the rainy season and burning had yet to begin.

SPOT and TM digital data were co-registered in UTM coordinates using cubic convolution resampling. The AVHRR data were first processed to radiances and brightness temperature and then registered to UTM coordinates. Black and white photo products of the TM data were made from channel 5, one at 1:250,000 scale and another at 1:500,000 scale. Scaled enlargements were made using negatives produced from the full resolution of the image; no image degradation was done to create photo products. All data were clipped to match the area covered by the two adjoining SPOT scenes. This area represented the largest area in common between all three data sources (Figure 4.1).

Image Processing and Interpretation

We compared six different techniques for the delineation of deforestation:

(1) digital image processing of full-resolution SPOT data using supervised classification,

(2) digital image processing of full-resolution Landsat TM data using supervised classification,

(3) visual interpretation of 1:250,000 scale single channel TM photo products using a vector-based geographic information system to digitally encode the boundary between forest and deforested areas,

(4) visual interpretation of 1:500,000 scale single channel TM photo products using a geographic information system,

(5) a brightness temperature threshold on channel 3 of the AVHRR digital data,

(6) a supervised classification of the AVHRR LAC data using channels 1 and 2.

These approaches include or closely approximate the predominant techniques which have been used, or are being proposed, for tropical deforestation monitoring. Each has its own advantages and limitations. Our objective was to make a simple land cover classification from the data, recording three features: intact forest, deforested areas, and water.

Image processing and analysis was done at the remote sensing laboratory of Institute for the Study of Earth, Oceans, and Space at the University of New Hampshire using an ERDAS system on Prime mainframe and Sun workstation computers. The GIS digitizing analysis of TM photo products was done using the ARC/INFO vector-based system on a Prime mainframe computer.

Digital Image Processing of SPOT and TM data

Bands 3,4,5 of the TM data were used for digital image classification. This combination of bands has been noted to be the optimal set for deforestation detection

(Nelson et al. 1987). All three bands of the SPOT data were used. Both forest and deforested classes contain several spectral sub-classes. For instance the deforested class also contains secondary growth, bare soil, and pavement. The forest class includes all extant natural cover other than water, and might also have cases of shadow or sun glint in areas of relief or in highly textured canopies. Although the test site was of uniform relief, the high spatial resolution of the SPOT data presented a heterogeneous, textured forest canopy signature.

Spectral sub-classes within the deforested category were delineated for SPOT and TM data with individual training sites and then combined for the final analysis. Training areas for supervised classification were established by visual inspection of the SPOT and TM digital imagery. Extensive field work in the test site in 1989 and 1990 further defined training areas. Because this study focuses on the simple, binary delineation of natural forest and deforested land, training sites could readily be defined from direct inspection of the imagery on a display device or from field observations. The selection of training sites was made first using the SPOT data and field observations, and the coordinates of polygons thus defined were also used with the TM data. This was possible since both datasets were co-registered to UTM coordinates. Deforestation training areas were established in a range of site conditions, reflecting the pattern of deforestation and spectral sub-classes. A supervised Maximum Likelihood classification was used for the SPOT and TM data; the separate sub-classes were then clustered into forest and deforested classes.

Digital Image Processing of AVHRR LAC Data: Channel 3 Threshold

Digital numbers from the AVHRR LAC subscene were converted to radiances and then to brightness temperature using the inverse of Plank's radiation equations and central wave coefficients for temperatures 275 - 320° K from Kidwell (1991). Brightness temperatures were recorded to the nearest tenth of a degree K. The data were then clipped to form two datasets covering: (a) the entire state of Rondonia, and (b) the test area. Geographic registration was to UTM coordinates, using a cubic convolution rectification of the image.

The precise threshold used by other authors was not available. So, to compare this analysis to what has been described by other analyses in the literature, a threshold was chosen such that the resulting deforested area for the entire state of Rondonia was equal to that which has been reported elsewhere (Malingreau and Tucker 1988, Malingreau et al. 1989, Stone et al. 1991, Woodwell et al. 1986). The location of natural savanna vegetation in the state is well documented and such areas were not included in this tabulation. A brightness temperature threshold between 298.3 and 298.6 provided a total deforestation area for the state close to that reported by Malingreau and Tucker (pers. comm.) and Stone et al. (1991). These threshold values were then used to classify the test area.

Digital Image Processing of AVHRR LAC Data: Maximum Likelihood

The AVHRR dataset was classified with a Maximum Likelihood classifier using channels 1, 2, and 4. The method follows the technique described by Cross (1990) and is similar to Stone et al. (1991). The entire state of Rondonia was classified, choosing training sites from the areas identified on the SPOT scene, and by direct visual inspection of the imagery on the display device. A subset from the entire state representing the area of the test site was then made of the classified scene. In previous work reported in the literature supervised classification of AVHRR by Cross (1990) compared very well with the unsupervised classification of Stone et al. (1991) in the state of Rondonia. We too compared supervised and unsupervised approaches, and found very little difference. Our estimate using this technique agreed with that of previous authors for the entire state.

Visual Interpretation from Photo Products

Channel 5 from the TM data was used to prepare 1:250,000 and 1:500,000 scale photo products. Channel 5 optimizes contrast between forest and cleared areas, and reduces the effect of smoke and haze. The photos were placed on a digitizing board and the boundary between forest and deforested areas was digitized directly into a geographic information system. We used the ARC/INFO system and all techniques for digitizing, editing, and processing followed methods described in ESRI (1991).

The vector digitizing of areas of deforestation from TM photo products, as with any GIS digitizing work, entails some degree of positional variance. Positional variance limits the ability to overlay digitized linework in a GIS on digital imagery or classified imagery in the image processing system, and is a factor in the comparison between results derived separately using GIS-based photo interpretation and digital image processing. An analysis of positional accuracy in digitizing was made using the approach described in Skole et al. (submitted) and Dunn et al. (1990). This analysis showed that positional accuracy on 1:250,000 scale photo products in the test site results in a variance of $\pm$ 8 meters orthogonal to the line digitized, or less than 3% in terms of polygon area. Thus, any variation between results obtained this way and digital image processing can be attributed to interpretation and classification alone.

Results

Overall Comparison Between Methods

Results of the digital classification of SPOT, TM, and AVHRR data and photo interpretation at 1:250,000 scale are shown in Figure 4.2a-e. Figure 4.3 shows the photo-interpretation classification overlaid on a subsection of the SPOT multispectral imagery. In all cases except possibly the AVHRR classification, results look similar when visually compared; AVHRR results are considerably more coarse than the results from TM or SPOT. Nonetheless, the general location and spatial distribution is similar. This general tendency of the AVHRR data to register location and spatial distribution of deforestation has been shown by others (Cross 1990, Malingreau and Tucker 1988, Malingreau et al. 1989, Stone et al. 1991, Woodwell et al. 1986).

The total area of deforestation measured by each technique is shown in Table 4.2. The table also reports the relative difference between each method and the SPOT digital method. The selection of the SPOT digital analysis as the reference is somewhat arbitrary. It was chosen simply because SPOT data have high spatial resolution, and are thus the most precise method. The area estimated by digital image processing of SPOT and TM are within 6% of each other. The analysis using visual interpretation at 1:250,000 scale was also close to both the SPOT and TM digital analyses, approximately 8% less than the digital SPOT analysis. Visual interpretation at 1:500,000 scale overestimated deforestation compared to the SPOT digital analysis by approximately 6%. Both analyses using AVHRR LAC data greatly overestimated deforestation compared to digital analysis of SPOT.

Sub-site Spatial Analysis

To investigate the variance within the test site across different patterns and sizes of clearings, and to check the aggregate results, a spatial analysis was made by subsampling within a 16.5 x 16.5 km grid overlay. Each grid cell represents a sample unit. This analysis also investigates the consistency of results listed in Table 4.2 above at sub-aggregate levels of analysis. We use the results of the SPOT digital analysis again as a reference for these comparisons, and the relationship between the SPOT analysis and other methods was made using regression analysis.

With the regression, the slope of the line indicates the degree of offset between methods. A direct relationship would have a slope of 1.0, while slopes greater than this suggest over estimation relative to SPOT, while slopes less than this suggest under estimation relative to SPOT. The coefficient of determination, r^2, will indicate the degree of variability between the two methods relative to each other. In one sense the slope represents a measure of accuracy (relative to SPOT as a reference), while r^2 represents precision and consistency of one method relative to SPOT.

The coefficient of determination for the regression of SPOT and TM digital analyses is high (r2 = 0.98) with a slope close to 1 (1.09) suggesting close correspondence between methods with a slight offset in Y with respect to X (Figure 4.4). Similarly, the correlation with visual interpretation at 1:250,000 is high, with $r^2 = 0.98$, and a slope of 1.11 (Figure 4.5). The correlation between the SPOT analysis and the AVHRR Maximum Likelihood classification is high ($r^2 = 0.94$) but the slope of the line (1.73) is also high (Figure 4.6). This suggests the AVHRR generally and consistently over estimates deforestation compared to the SPOT analysis. The channel 3 threshold at 298.6 °K however has lower correlations ($r^2 = 0.91$) and a higher value for the slope (Figure 4.7). Interestingly, a lowering of the threshold only 0.3 °K appears to have noticeable influence on these parameters; it increases the variability and the offset (Figure 4.8). This extreme sensitivity of the AVHRR temperature threshold approach was also noticed when we compared estimates of deforested area for different thresholds for the test site. A range in the threshold from 298.3 °K to 298.7 °K results in area estimates from 1729 km^2 down to 1012 km^2.

Large-Area Measurements of Deforestation

The estimate of the deforested area using 1:250,000 scale photo products was consistently close to the area estimated using SPOT and TM digital methods in the sample units of the test site, suggesting large-area evaluations could be made over a range of site and conditions and clearing patterns with visual interpretation and GIS methods. To evaluate the deforested area in the entire state of Rondonia, 15 photo products from TM channel 5 were acquired and processed using the visual interpretation methods described above and the GIS methodology described in Skole et al. (submitted). Figure 4.9 shows the results of this complete survey of deforestation in 1988 for the state of Rondonia mapped into a GIS. From this analysis we estimate that 24,416 km^2 had been deforested by 1988.

This value is much lower than the ~34,000 - 39,000 which has been given by others using AVHRR (Cross 1990, Stone et al. 1991, Woodwell et al. 1986). This estimate of the total area deforested in the state is lower than the ~45,000 km^2 of burned areas reported for a single year, 1987, by Setzer and Pereira (1991). Our estimate is within 20% of the 30,000 km^2 reported by INPE (1992).

Discussion and Conclusions

Satellite remote sensing provides an objective and reproducible approach to mapping forest conversion directly at global or regional scales. It is a substantial improvement over existing, non-remote sensing methods which rely on agricultural land use statistics, forest inventories, and other tabular sources of information (Dale et al. 1991, Flint and Richards 1991, Houghton 1986, Houghton et al. 1991a). In our examination of specific remote sensing methods for measuring deforestation in the closed forests of the Amazon Basin, the use of single-channel photo products appears to be a straightforward and cost-effective remote sensing approach, which when implemented using geographic information system methods could provide a detailed mapped database of the area deforested and its rate of change. Such an approach, which does not require expensive digital data or special hardware and software could be an appropriate way to implement forest monitoring programs in many developing countries. Improvements could be made using color photographic products, particularly when also considering secondary growth. Moreover, color could provide better separation of natural cover classes and deforestation in areas of savanna, old second growth, degraded forests, and other spectrally confusing areas.

The 1:250,000 scale photo product analysis closely approximated the results of digital image processing. The analysis using 1:500,000 scale products, which required several-fold less time and effort remained within 10% of the digital approach, suggesting some gain in efficiency with marginal loss in accuracy. This is an important consideration in light of the fact that the current estimates of deforestation rates in the Amazon vary considerably more than 10%, and real improvements in our estimates of deforestation could be made using simple, straightforward methods.

The close agreement between the photo-interpretation results and the digital image processing results was maintained when the test site was subdivided into 16 x 16 km subscene sample units, as shown in Figure 4.1. Although the patterns and sizes of deforestation within each sample unit varied, the high correlation coefficient suggests that variance was consistently low throughout the test site. Moreover, the slope of the linear regressions between the photo interpretation method and TM and SPOT digital analyses was close to 1.0, which implies the estimates were very similar in magnitude. The overall indication is that photo-interpretation, even with single channel data, results in consistently good estimates over a variety of deforestation geometries.

The estimate of the area deforested in the state of Rondonia in 1988 based on complete coverage for the state of TM photo products was close to the estimate provided by INPE using color photo products. However, it is much lower than what has been reported by Stone et al. (1991), Cross (1990), or Tucker et al. (1986) using various methods with AVHRR data. Figure 4.10 graphs various estimates of deforestation for the state of Rondonia from 1960 to 1988, including the estimate from this study. The suggestion from this study is that previous estimates using the AVHRR have been too high, and it could be argued that the estimates using TM data are more accurate and probably more precise as well.

The overestimation bias and high variance we observe with the AVHRR data appears to be related to the pattern and size of deforestation. In regions where the geometry of clearing is highly complex and variegated, as in the case in the lower half of the test site, the bias is the greatest. We hypothesize that this overestimation tendency would increase when the perimeter of a cleared area is high relative to the cleared area itself. Thus in places such as the state of Rondonia where the deforestation geometry is a convoluted fishbone-like pattern, AVHRR would strongly over estimate deforestation. In areas, such as the state of Mato Grosso, where the deforestation pattern is dominated by large rectangular ranches, the AVHRR tendency to overestimate would be expected to be less. Cross et al. (1991) also note that the AVHRR tends to overestimate deforestation compared to TM data in such situations.

While generally the case that AVHRR overestimates, close inspection of Figure 4.7 suggests that for deforestation areas in the sample units less than 750 km^2 the AVHRR erratically estimates deforestation; that some detection limit exists below which the coarse resolution sensor underestimates or randomly estimates deforestation.

A strong, if not obvious, relationship exists between the high estimate bias of the AVHRR (defined as AVHRR estimate divided by the Visual Interpretation area) and the density of deforestation (defined as the present of each sample unit deforested). Figure 4.11 shows this relationship for all sample units where the deforestation estimate from AVHRR was higher than the visual interpretation. Thus, we suggest that the AVHRR might be a better estimator when the deforestation is dense and the clearings have distinct, rectilinear boundaries with low perimeter to area ratios.

A deforestation map of the Legal Amazon was prepared using visual interpretation techniques discussed above. The analysis is found in Skole and Tucker (in prep.). These results mapped in a geographic information system provide a comprehensive spatial database of deforestation. In Figure 4.12 we have subdivided this map of deforestation into 16.5 x 16.5 km grid cells as we did for the test site. The density of deforestation (% of sample unit) was then tabulated and color coded as shown in Figure 4.11. This map provides an estimate of the overestimation error which would be introduced by an AVHRR analysis, and thus indicates where we would expect AVHRR to be most useful and where TM would be most useful. The areas colored red are areas where the overestimation would be slight, and where it might be possible to apply AVHRR with some success. In other areas (shaded blue) AVHRR would be expected to give inaccurate and variable results. This also suggests why some earlier analysis (Stone et al. 1991) reported close agreement between AVHRR and TM methods in validation sites, while nonetheless giving results much higher than those reported here for the entire state of Rondonia.

Our results agree with the image degradation experiments by Townshend and Justice (1988). Their results show that land cover conversion and land cover change would best be monitored using spatial resolutions of 250 m or less. The spatial resolution of the 1:500,000 scale photo products is approximately 250 m. The inaccuracies of coarse resolution sensors such as AVHRR are as much a function of the scale of deforestation itself as the sensor characteristics, even though the brightness temperature threshold seems to be a hair trigger.

Thus, coarse resolution data would be useful for identifying the location of deforestation, and might be useful for quantifying deforestation in areas of high deforestation densities. High resolution data would be the most useful approach for measuring deforestation, and would be necessary for mapping. Moreover, mapping secondary growth and the deforestation rate will require high resolution data.

The rate and geographic distribution of deforestation is an important parameter for global change research. A research program to measure and map deforestation in tropical forests would best be implemented using high resolution data such as TM. The costs could be contained using photo products. In fact, the simple binary delineation between intact forest and deforestation could be easier accomplished using photo-interpretation methods. This approach would also be easier to implement by in-country programs since they could readily utilize the interpretation skills of local forestry experts without expensive or sophisticated image processing and computer technology.

Table 4.1. A comparison of different satellite data acquired for this study.

	SPOT	Landsat TM	AVHRR-LAC
Date	10 July 1988	21 July 1988	14 July 1992
Number of Spectral bands	3	7	5
Spectral Range (um)	0.50 - 0.59 0.61 - 0.68 0.79 - 0.89	0.45 - 0.53 0.52 - 0.60 0.63 - 0.69 0.76 - 0.90 1.55 - 1.75 2.08 - 2.35 10.4 - 12.5	0.58 - 0.68 0.73 - 1.1 3.55 - 3.93 10.5 - 11.3 11.5 - 12.5
Swath Width	60 km	185 km	~2600 km
Resolution	20 m	30 m	1.1 km
Processed for this study	digital image processing using statistical classifier: Maximum Likelihood	1. digital image processing using a statistical classifier: Maximum Likelihood 2. visual interpretation with continuous-line digitizing of channel 5	1. digital image processing using a statistical classifier: Maximum Likelihood 2. digital image processing using a threshold: channel 3.

Table 4.2. Comparison between different methods for measuring deforestation in closed tropical forests, from co-incident analyses in the test site (km^2).

Method	Deforested Area	Relative to SPOT
SPOT digital analysis	668	---
Landsat TM digital analysis	629	0.94
Landsat TM visual interpretation, 1:250,000 scale	615	0.92
Landsat TM visual interpretation, 1:500,000 scale	710	1.06
AVHRR-LAC statistical classifier: Maximum Likelihood	875	1.31
AVHRR-LAC channel 3 brightness temperature threshold at 298.6 °K	1140	1.71

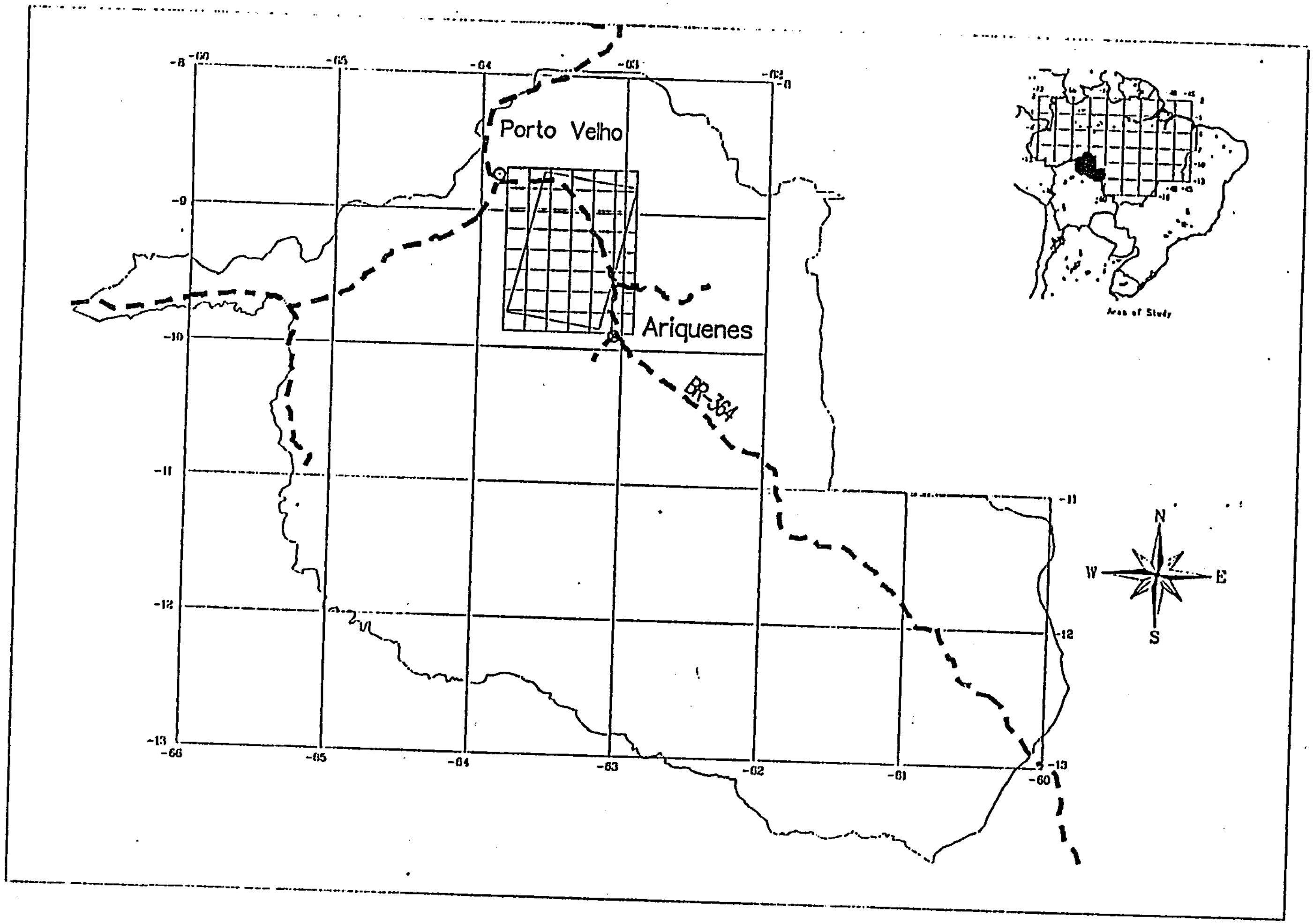

Figure 4.1. Location map showing the state of Rondonia, Brazil and the study site. The study site is an area equivalent in size to two SPOT scenes. The figure shows the 16km by 16km grid mesh was used to define the primary sampling units.

(a)

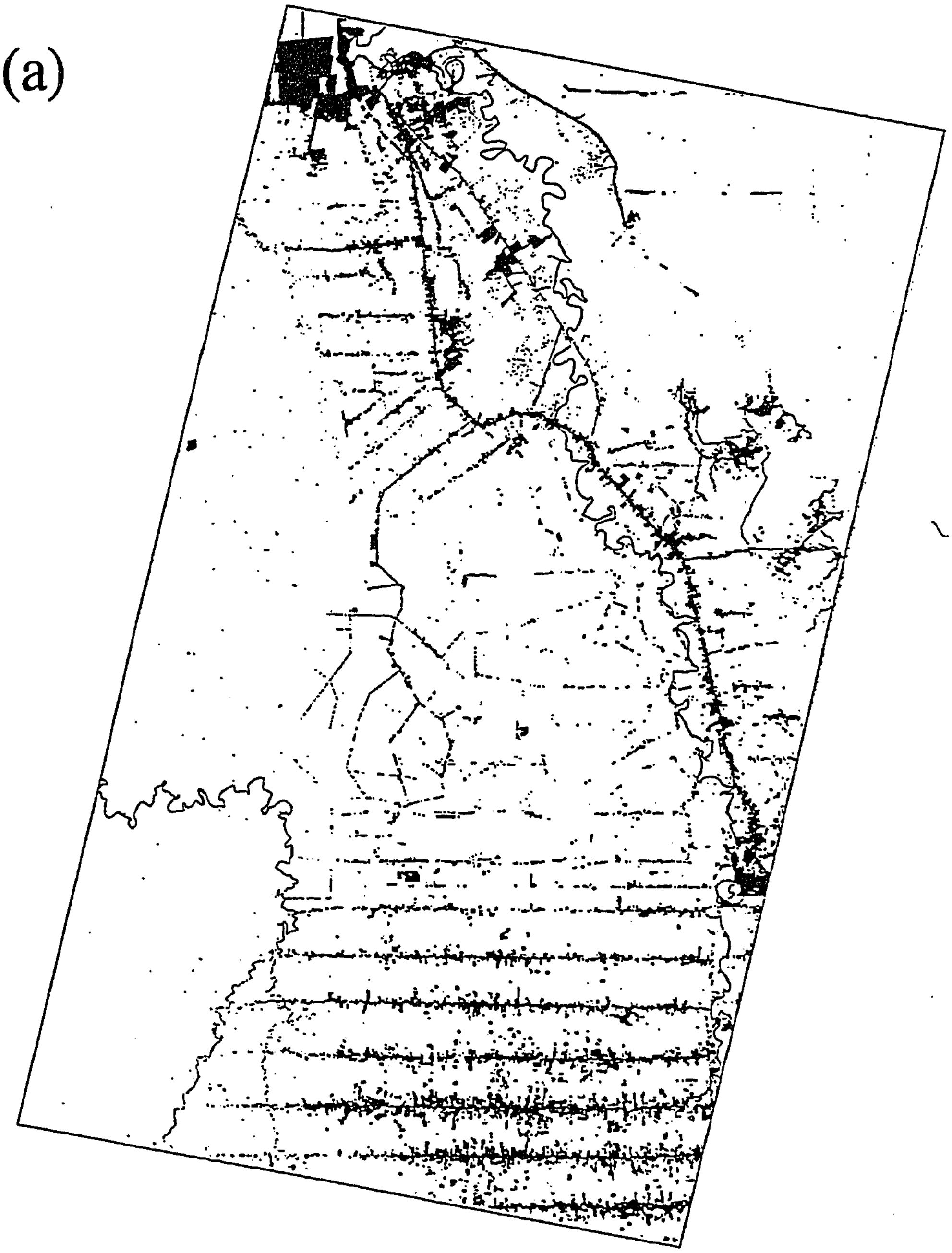

Figure 4.2. Results from a simple forest-deforested classification for each remote sensing method analyzed in this study: (a) SPOT 20m multispectral data classified using digital image processing and a maximum likelihood statistical classifier, (b) Landsat Thematic Mapper 30m resolution multispectral data classified using digital image processing and a maximum likelihood classifier, (c) Landsat Thematic Mapper data from channel 5 produced as a 1:250,000 scale photographic product interpreted visually and encoded with vector GIS techniques, (d) AVHRR-LAC data classified using a maximum likelihood statistical classifier, and (e) AVHRR-LAC data classified using a channel 3 brightness temperature threshold.

(b)

Figure 4.2b. Results from a simple forest-deforested classification for Landsat Thematic Mapper 30m resolution multispectral data classified using digital image processing and a maximum likelihood classifier.

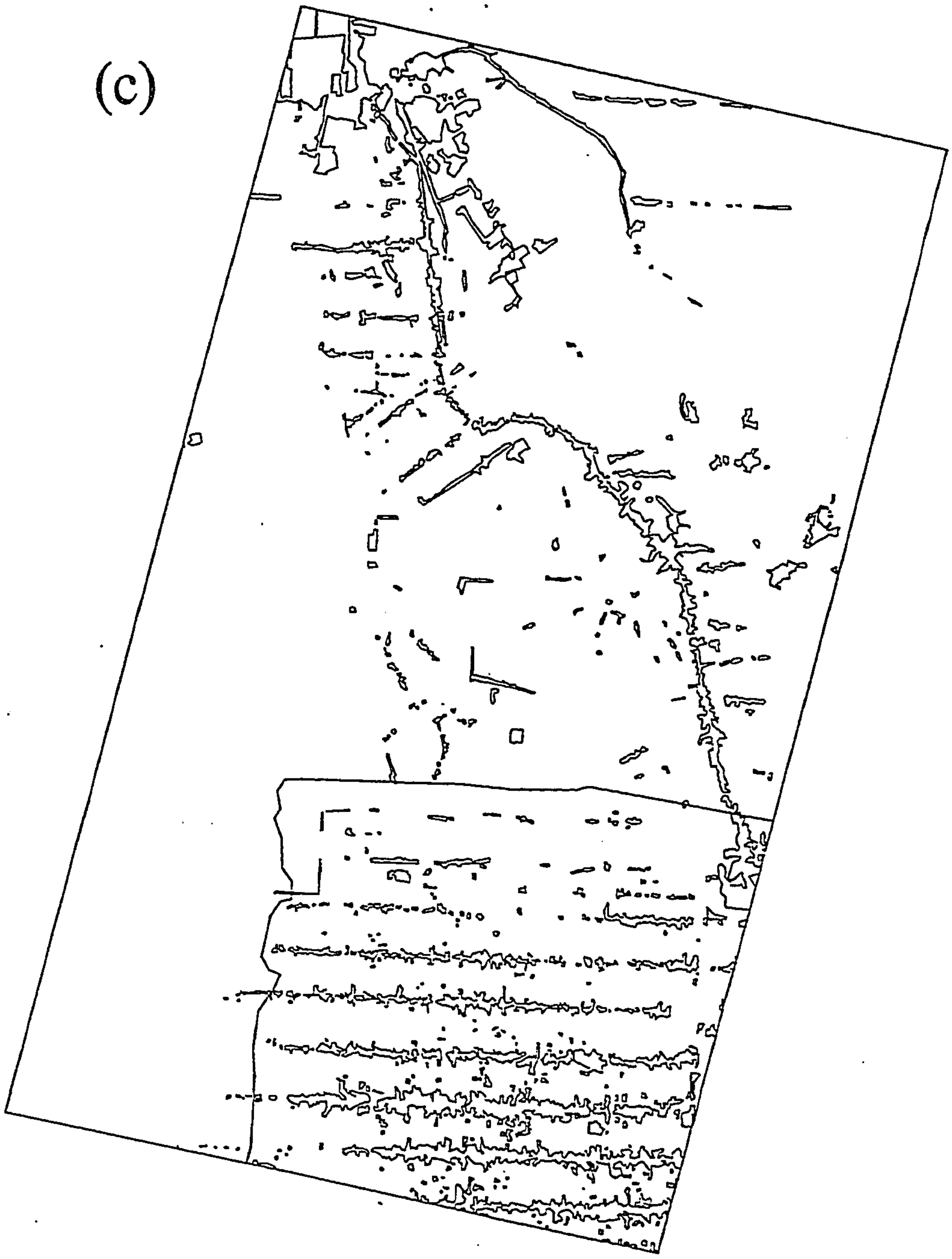

Figure 4.2c. Results from a simple forest-deforested classification for Landsat Thematic Mapper data from channel 5 produced as a 1:250,000 scale photographic product interpreted visually and encoded with vector GIS techniques.

(d)

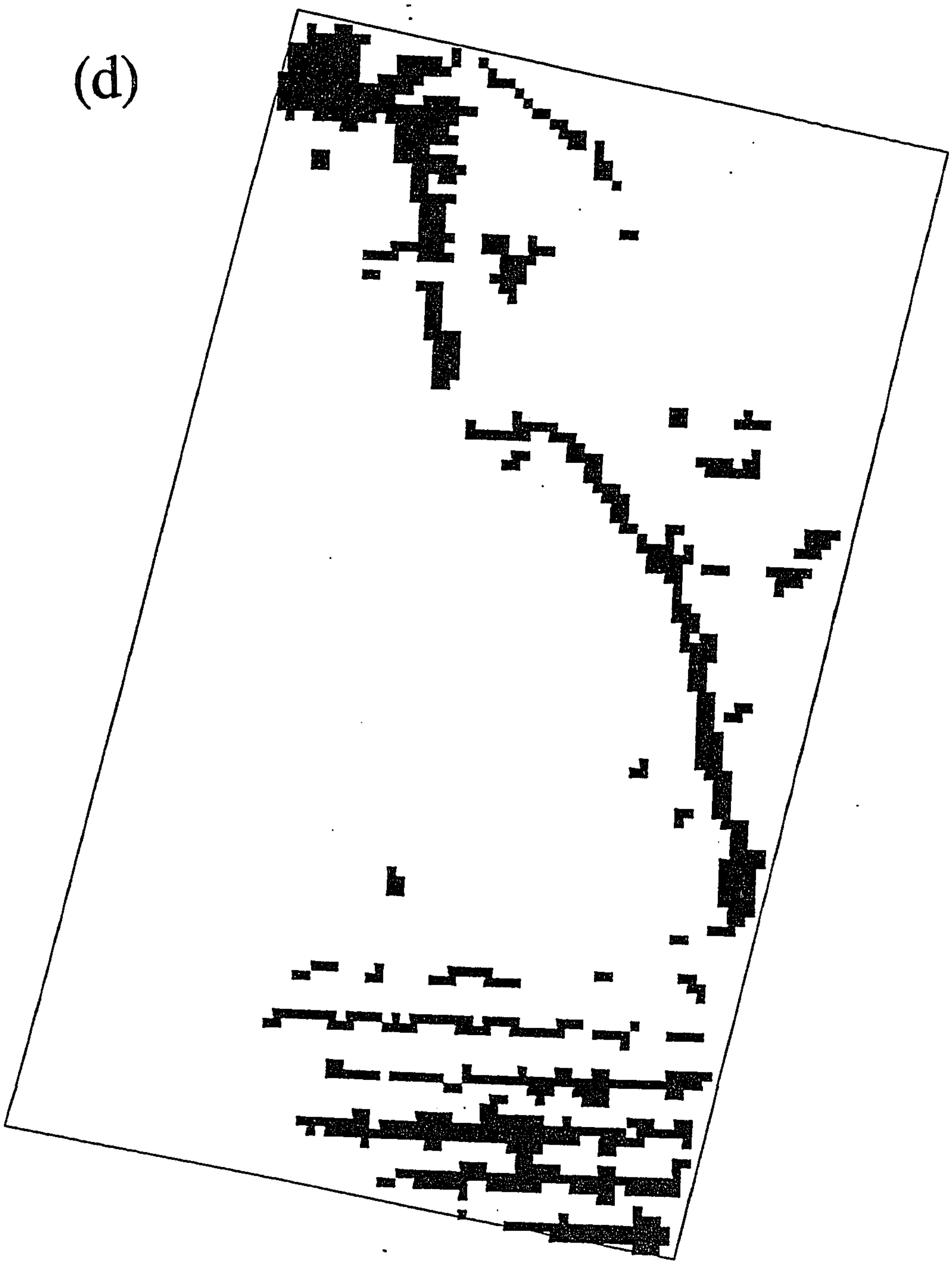

Figure 4.2d. Results from a simple forest-deforested classification for AVHRR-LAC data classified using a maximum likelihood statistical classifier.

Figure 4.2e. Results from a simple forest-deforested classification for AVHRR-LAC data classified using a channel 3 brightness temperature threshold.

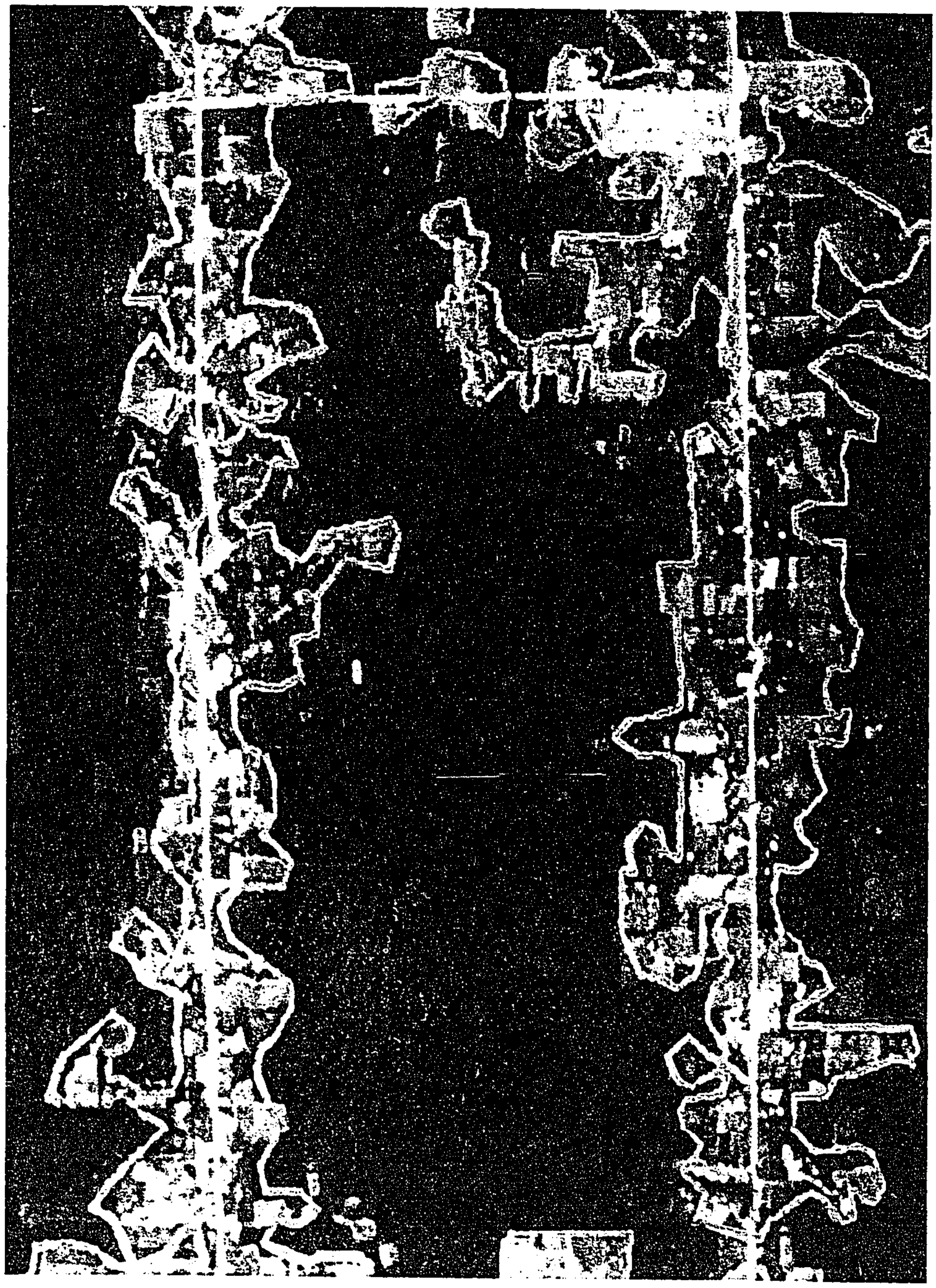

Figure 4.3. Results from the visual interpretation of Landsat TM data at 1:250,000 scale overlaid on a SPOT image from the same area.

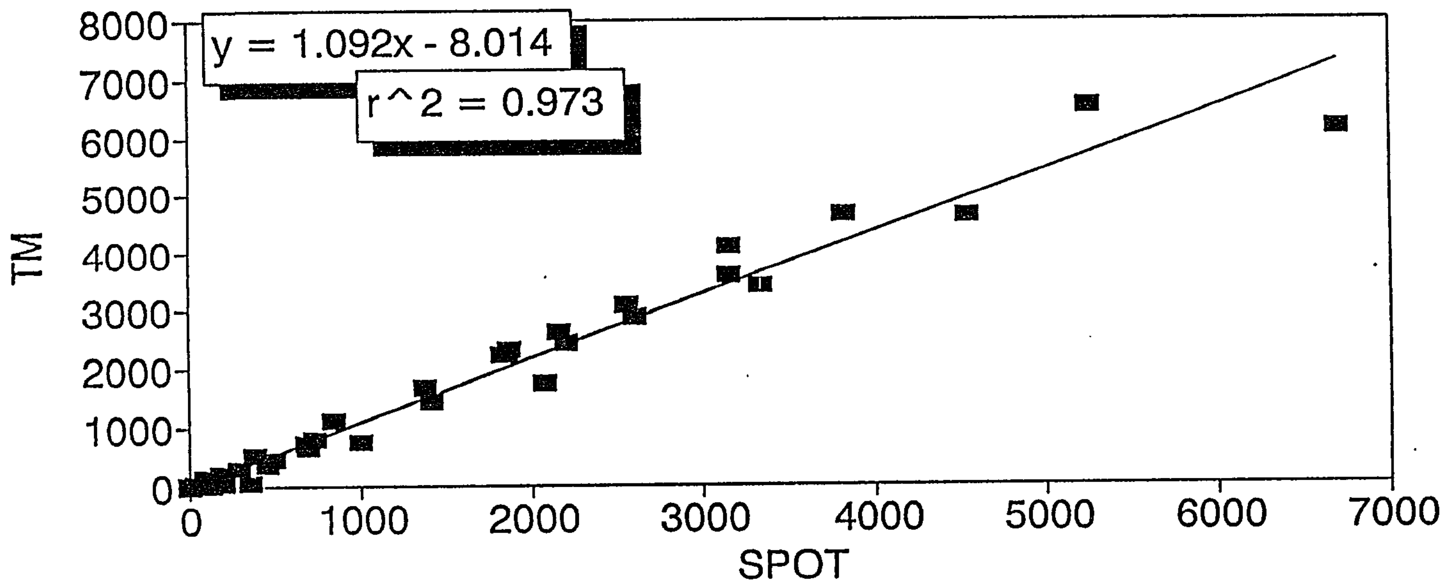

Figure 4.4. Linear regression of SPOT digital image processing results from each of the primary sample units against Landsat Thematic Mapper results using digital image processing. (Units are total hectares deforested.)

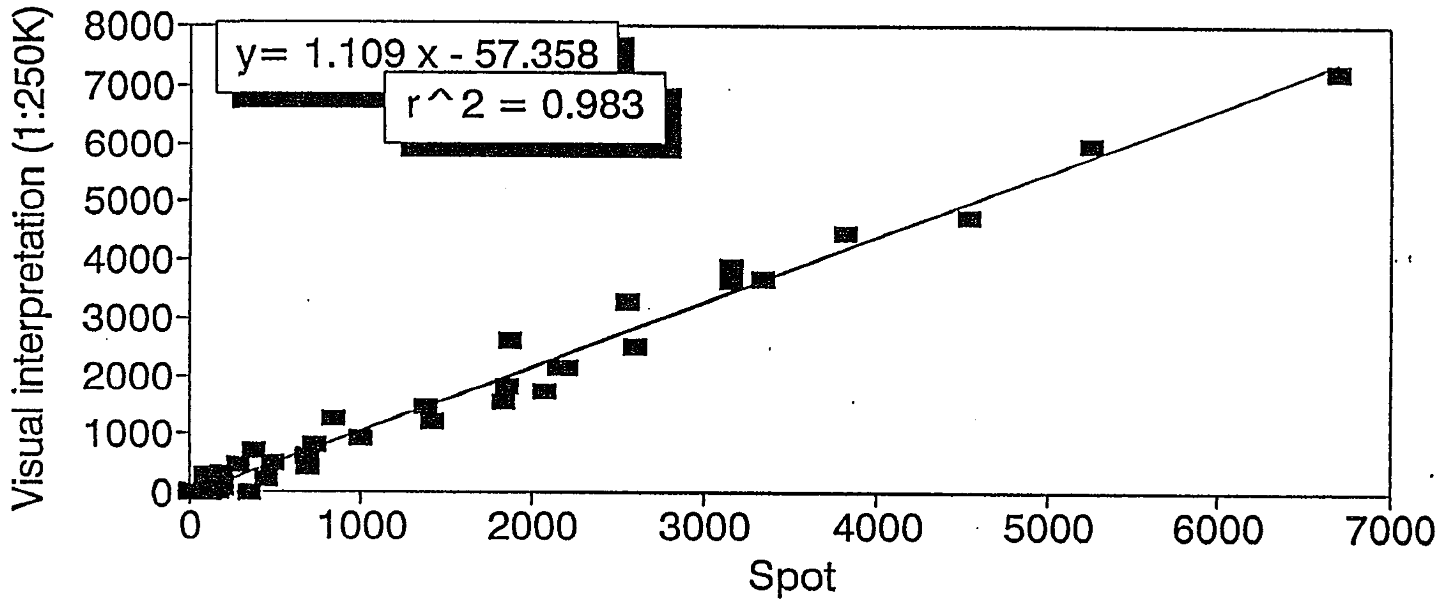

Figure 4.5. Linear regression of SPOT digital image processing results from each of the primary sample units against Landsat Thematic Mapper results using visual interpretation at 1:250,000 scale. (Units are total hectares deforested.)

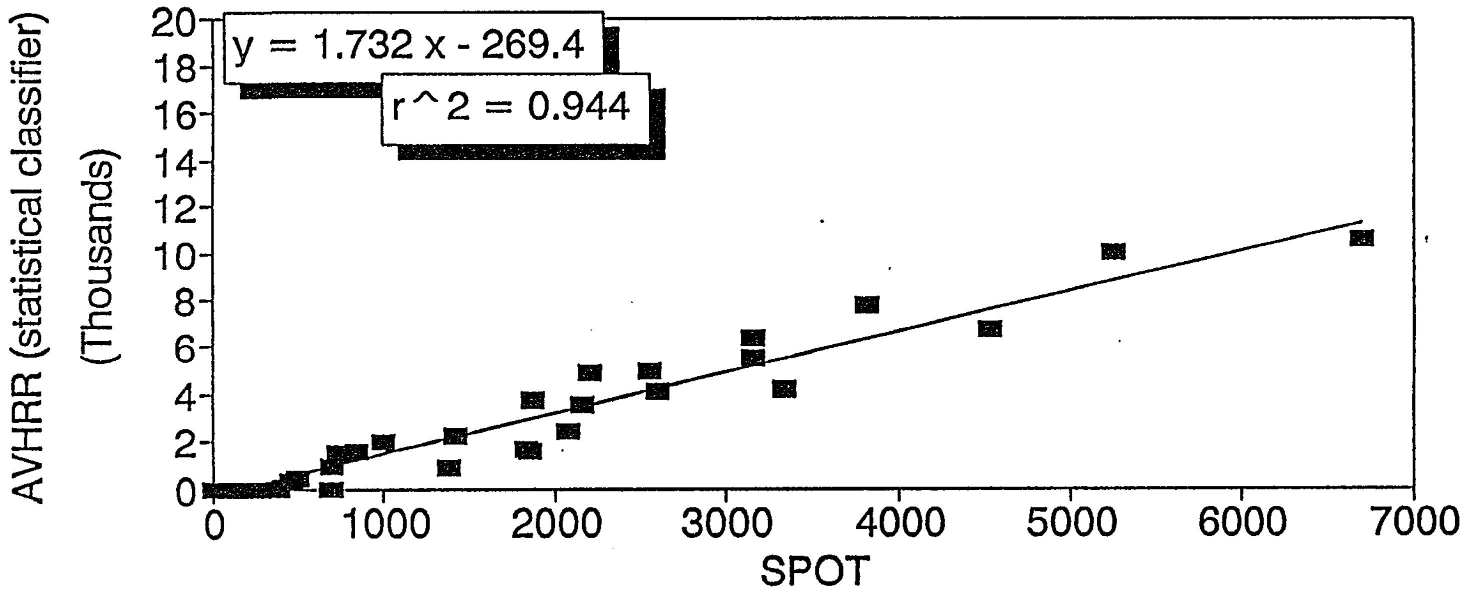

Figure 4.6. Linear regression of SPOT digital image processing results from each of the primary sample units against AVHRR-LAC results using statistical classifier. (Units are total hectares deforested.)

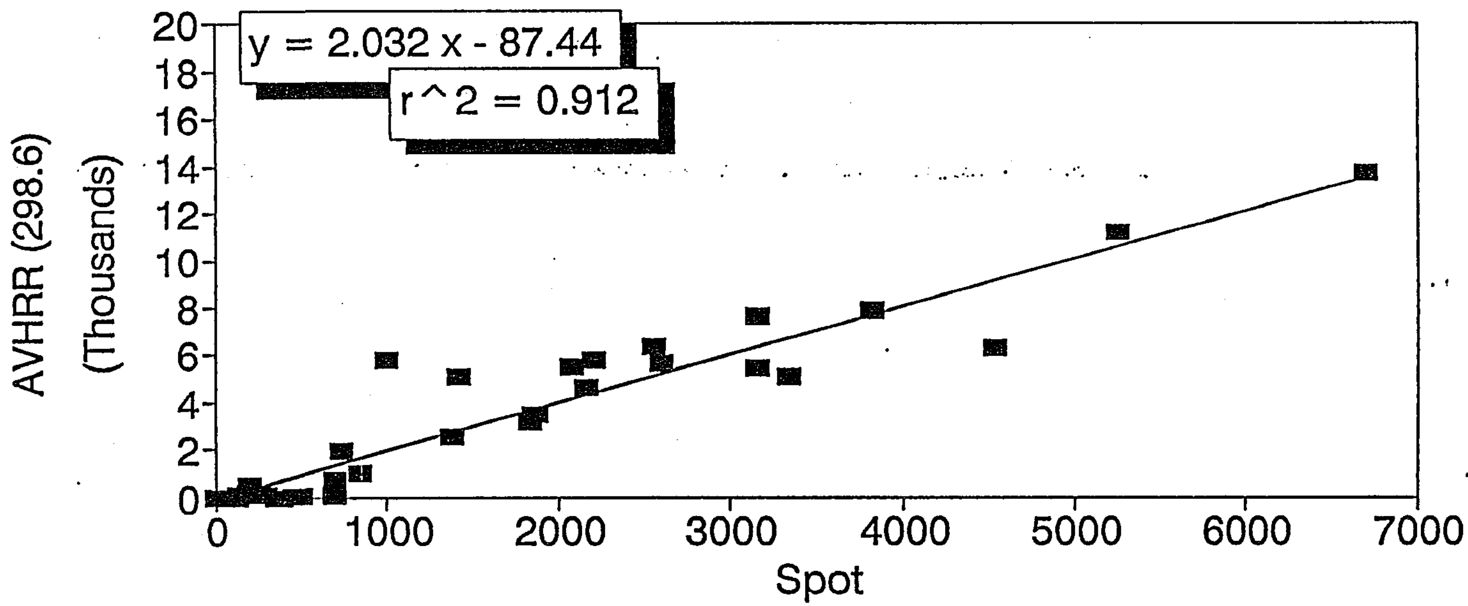

Figure 4.7. Linear regression of SPOT digital image processing results from each of the primary sample units against AVHRR-LAC results using a brightness temperature threshold of 298.6 degrees Kelvin on channel 3. (Units are total hectares deforested.)

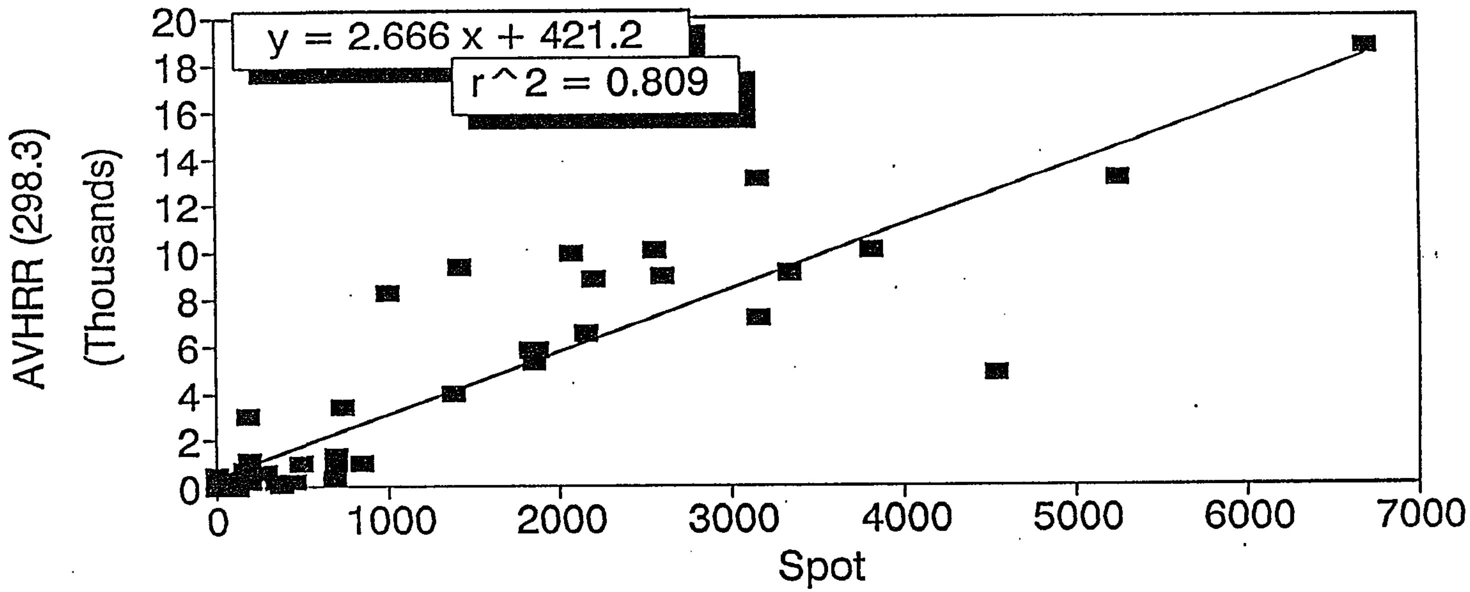

Figure 4.8. Linear regression of SPOT digital image processing results from each of the primary sample units against AVHRR-LAC results using a brightness temperature threshold of 298.3 degrees Kelvin on channel 3. (Units are total hectares deforested.)

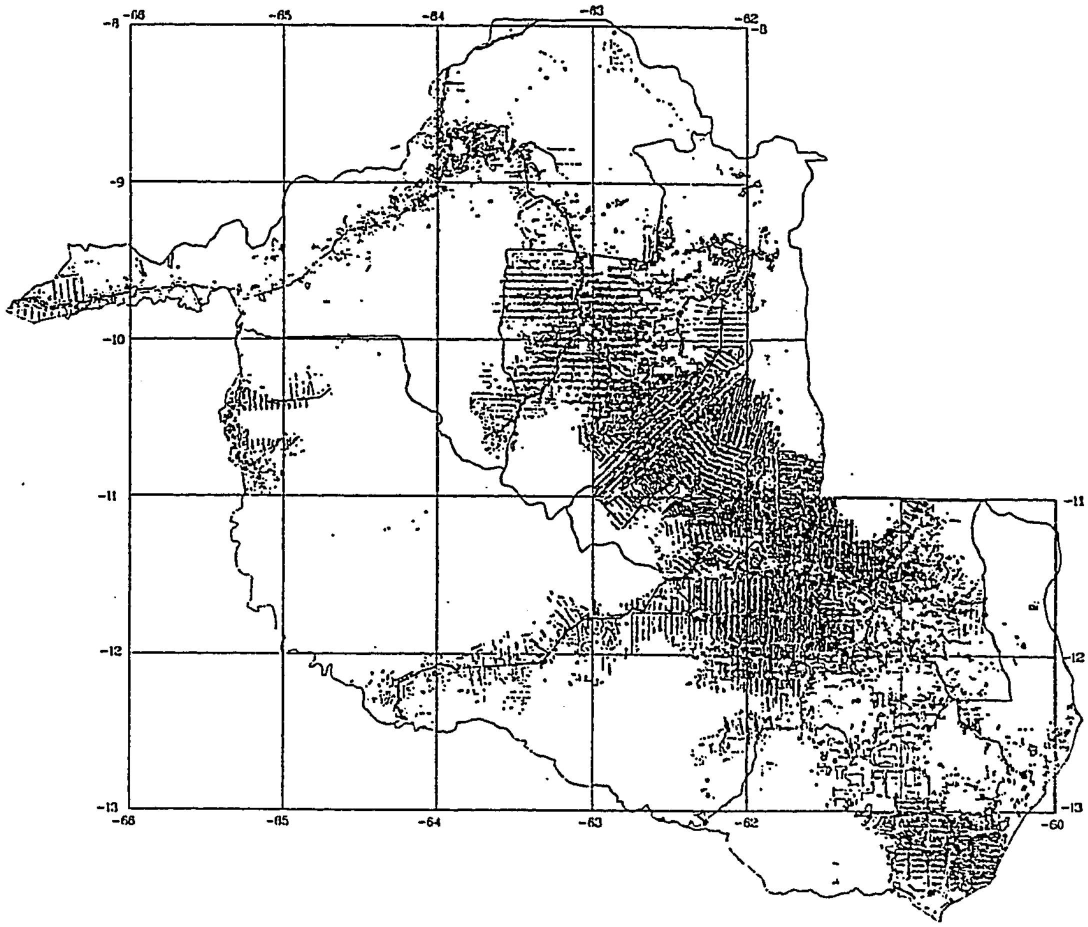

Figure 4.9. Deforested area mapped from Landsat TM photo interpretation for the entire state of Rondonia.

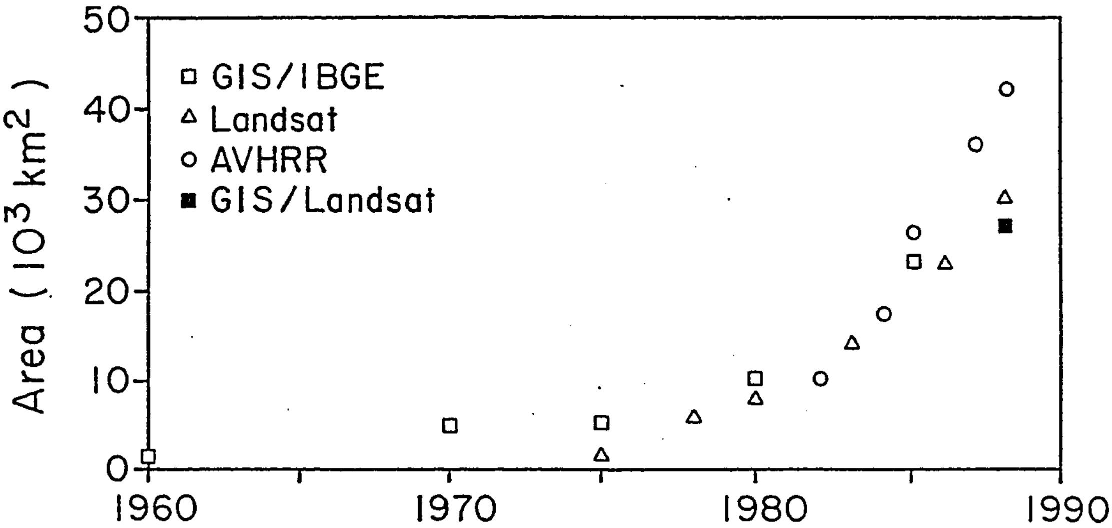

Figure 4.10. Recent estimates of deforestation in the state of Rondonia using various methods.

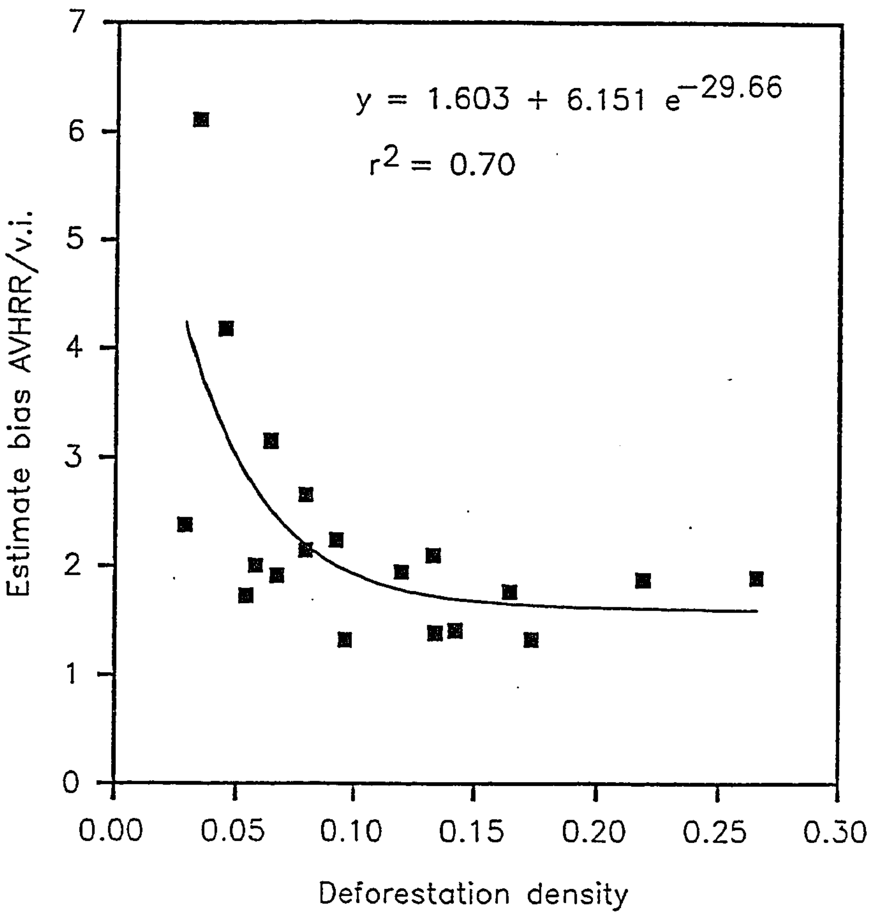

Figure 4.11. The estimate bias of the AVHRR-LAC as a function of deforestation density in each of the primary sample units. The estimate bias is calculated as the ration of the AVHRR result divided by the visual interpretation result for each primary sample unit.

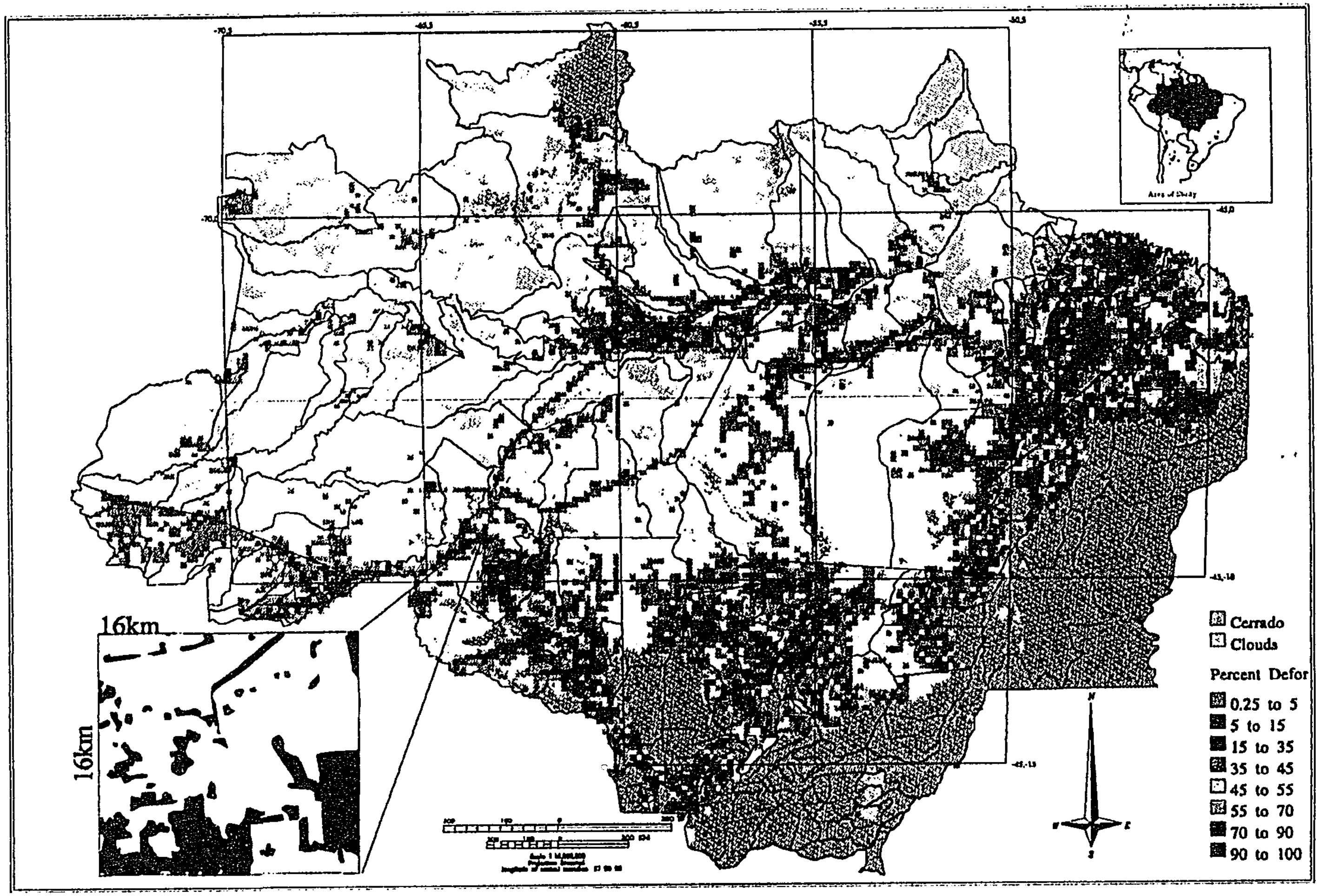

Figure 4.12. Deforestation densities in 16 km by 16 km grid cells mapped for the entire Amazon in 1988. The legend indicates the color code for the different densities, expressed as a fraction of the grid cell.

CHAPTER 5

DYNAMICS OF DEFORESTATION AND SECONDARY SUCCESSION IN TROPICAL FORESTS OF THE AMAZON BASIN

Introduction

The highest rates of tropical deforestation are in the Brazilian Amazon. Each year, approximately 21 x 10^3 km^2 are cleared (Fearnside 1990b), accounting for an estimated 30% of all tropical deforestation worldwide (FAO 1990, FAO/UNEP 1981, Lanly 1982). Deforestation estimates for the Brazilian Amazon, and throughout the tropics, often report only natural forest conversion. There are no estimates of the amount of deforested land which is abandoned and returned to secondary succession, or the total extant area of second growth vegetation. Also, it is not known what fraction of this secondary vegetation is subsequently cleared and re-cycled into active agriculture each year, or the length of time land remains in each of these transition states. Without such measurements, we know very little about the overall pattern and character of land cover change in tropical forests, in spite of the fact that this information is important to basic research in biogeochemistry, trace gas dynamics, and water and energy balance (Crutzen and Andreae 1990, Houghton 1991b, Keller et al. 1991, Matson et al. 1989, Shukla et al. 1990).

There are reports of large areas of abandoned pasture in the Amazon, where "mature tropical forests are islands in a sea of successional vegetation" (Uhl 1987). The situation in the Brazilian Amazon appears to be one characterized by large areas of secondary vegetation on former pastures which are abandoned when soil fertility declines following 4-8 years of continuous use (Buschbacher 1986, Uhl 1987, Uhl et al. 1988). Some have suggested that secondary forests are widespread throughout the tropics (Brown and Lugo 1990). Observations such as these have opened a discussion concerning the current net flux of carbon from tropical deforestation, suggesting these successional systems are potentially large sinks for atmospheric carbon (Wisniewski and Lugo 1992). If biomass accumulation associated with secondary vegetation growth is high and persistent for several years, this phenomenon could be an important sink for carbon (Houghton 1991b). However, any resolution of such questions will require precise measurements of the amount of secondary vegetation and its long term fate, and improved documentation of its role in the overall dynamics of land cover change in the tropics.

Using remote sensing imagery it is possible to separately distinguish areas of intact forests, deforested land, and secondary vegetation. Sequential acquisitions of such data for a particular site over time makes it possible to measure transitions between these cover states (Hall et al. 1991). In this paper we report results from an analysis of high resolution, multispectral data acquired from the French SPOT satellite for a test area in the Brazilian Amazon from 1986 to 1989. This analysis documents the amount of secondary growth and the transition rates between forest, agriculture, and successional cover types. The results suggest that large areas of secondary vegetation exist, and are increasing. Further, land cover change in this region appears to be a highly dynamic processes of clearing and abandonment to secondary succession, with rapid re-clearing once the land is abandoned.

Materials and Method

We acquired SPOT HRV scenes in August 1986, July 1988, and August 1989 in a test area in the state of Rondonia, Brazil (Figure 5.1). The spatial resolution of the SPOT data is 20 m, making it ideal for mapping land use transitions. The imagery were completely clear of clouds and smoke. Two adjacent scenes along the same orbital path were acquired for each date. Table 5.1 describes these data. We refer to the northern scene as Scene A, while the southern scene is referred to as Scene B. After the data were co-registered using pixel matching techniques, they were geometrically rectified and geographically referenced using cubic convolution. The data were geographically referenced to UTM coordinates. Ground control points were determined from 1:250,000 scale maps from the Brazilian Diretoria de Servico Geografico (DSG). The area covered by these data was 642 x 10^3 ha. A portion of the test area (~53 x 10^3 ha, 7.3%) was flooded by the Samuel hydroelectric project in 1989 and the inundated area was not considered in the analysis.

Deforestation is active in this area, and clearing patterns are spatially heterogeneous. The test site selected for this study represents a broad cross section of the types and patterns of deforestation which exist in the Amazon at large. Settlement projects occur in the Scene B. This area has a characteristic fish bone network of roads, where most clearings are associated with this road network. The deforestation geometry here is typical of settlement areas, having a high ratio of perimeter to area. Scene A in the northern part of the test site has many variously-sized and scattered clearings. The Cuiaba-to-Porto Velho highway, BR364, runs diagonally through the entire area, with its associated roadside clearings and towns. Most of the land clearing has been for agriculture. Approximately half the agricultural clearing is for pasture and half for temporary and permanent crops (IBGE 1980a, IBGE 1989). Eighty percent of the farms are less than 100 ha in size (IBGE 1980a). Very little clearing has been the result of commercial timber harvest.

Each satellite scene was classified independently using supervised classification methods. Training sites were selected in the field in 1989 and 1990 and from visual inspection of the imagery. Spectral separability was possible for three basic classes: (1) intact forest and water, (2) deforested areas, and (3) secondary growth (Figure 5.2). The deforested areas were occupied by active agriculture, including pasture and various types of cropland. Within the secondary growth class we separate areas of forest which were degraded by incomplete clearing or thinning from abandoned land. We considered these degraded areas to be in secondary growth since they are quickly occupied pioneer species. The classified imagery were then compared between dates, and the following transition states were determined: (a) forest to agriculture, (b) agriculture to second growth, (c) second growth to agriculture, and (d) forest to secondary growth through degradation. In this multitemporal analysis, where each parcel of land is tracked over time, we also determined transition histories from 1986 to 1989. An example of a transition history is: forest in 1986, agriculture in 1988, and secondary growth in 1989. We tabulated 14 possible transition histories (see Table 5.3).

In addition to the detailed temporal analysis for the test site, a complete inventory of second growth vegetation in the state of Rondonia was determined using complete coverage of the state with 12 Landsat MSS scenes from 1986. MSS data have a spatial resolution of 80 m, but were suitable for a large-area inventory to which we compared the specific analysis from the test site. Classification was made using supervised classification. Training sites were selected visually on each image. These 12 Landsat MSS scenes covered an area of $\sim 41 \times 10^6$ ha, which represents about 10% of the entire Brazilian Amazon.

An assessment of accuracy of the classification was performed in the test site. Classification maps were checked in the field in 1989 and 1990. Approximately 12 sites were selected a priori. In all cases the classification was correct. However, the most important aspect of this accuracy assessment was not the classification itself, since the simple classification scheme consisting of only four simple categories of land cover was somewhat straightforward. The more difficult problem is the delineation and measurement of area, particularly related to the delineation of the boundary between classes. The geometry of clearings in the test site results in a large amount of high convoluted clearings with a large amount of edges. Moreover, the data acquired in 1988 was of a somehwat oblique look angle (see Table 5.1), resulting in uncertainty in the placement of edges. By estimating that this resulted in an uncertainity of $\pm$ 20 meters on either side of the true edge, this would result in an uncertainty in the measurement of area of 10%. It was also possible to compute the uncertainty through the determination of the number of "misclassified" pixels--those transition histories that did not make sense, such as pasture to forest. On this basis, the error or uncertainity in the estimate was calculated to be 7.8%.

Results

Pool Sizes and Their Change

The total area deforested in the test site, which includes the secondary growth areas, was 35 x 10^3 ha in 1986, increasing to 46 x 10^3 ha in 1988 and to 60 x 10^3 ha in 1989 (Table 5.2). Most of the deforested area was in the southern section, or Scene B, of the test site. Approximately one-third of the total deforested area was in secondary growth. However, the pool of secondary vegetation increased throughout the period of analysis for both sections of the test area, and increased faster than active agricultural areas. The area in secondary growth increased steadily throughout the period of analysis, from 89 x 10^3 ha in 1986 to 20 x 10^3 ha by 1989, a 2.3-fold increase. By contrast, the area in agriculture increased from 26 x 10^3 ha in 1986 to 40 x 10^3 ha in 1989, only a 1.5-fold increase. Thus, the fraction of total deforested land in secondary vegetation increased in both sections of the test area, from 30% to 37% in Scene A and 23% to 32% in Scene B.

Table 5.2 also shows the average annual change in area of secondary vegetation and agricultural land for the two periods, 1986-1988 and 1988-1989. Annual increases in total deforested area, agricultural area, and second growth are higher between 1988 and 1989 than during the previous interval, 1986-1988, suggesting the annual rate of forest conversion is not constant but is increasing, and increasing more rapidly in Scene B which starts with more deforested area. On the other had, the annual increase in second growth appears to be increasing faster in Scene A. In Scene A, the annual rate of creating new areas of secondary growth more than tripled but the rate of creating new agricultural land remained nearly constant.

Transitions and Transition Histories

Changes in the size of the pool of agricultural land discussed above are the net sum of several land cover changes: increases from primary forest conversion and secondary vegetation clearing, and losses due to abandonment of agricultural land to second growth. These gross transitions were measured. Figures 5.3 and 5.4 show land cover transitions which occurred in the test area during two intervals, 1986-1988 and

1988-1989. Table 5.3 shows specific transition histories. The values are annual transition rates for each period. Between 1986 and 1988, new agricultural land came from clearing 4.1 x 10^3 ha yr^{-1} of primary forest and 2.0 x 10^3 ha yr^{-1} of secondary vegetation. Between 1988 and 1989, 8.6 x 10^3 ha yr^{-1} of primary forest and 6.2 x 10^3 ha yr^{-1} of secondary vegetation was cleared for agriculture. The amount of agricultural land annually retained in the pool from 1986 to 1988 was 10.1 x 10^3 ha yr^{-1}, and 25 x 10^3 ha yr^{-1} between 1988 and 1989.

A large amount of natural forest was partially cleared or degraded, 1.54 x 10^3 ha yr^{-1} between 1986 and 1988 and 5.29 x 10^3 ha yr^{-1} between 1988 and 1989. This degradation, or thinning, of a site is distinguished from complete clearing for agriculture. It can be seen in the satellite imagery and was verified in the field. In this analysis we consider this a transformation to second growth, since the site will eventually begin regrowing following disturbance. Degradation of primary forest represented 27% of all primary forest conversions each year between 1986 and 1988, increasing to 38% between 1988 and 1989. A large fraction of areas thus degraded and left in secondary growth is retained as secondary growth from one time period to the next. Of the 3.1 x 10^3 ha degraded between 1986 and 1988 (total for 2 years), only half was subsequently cleared to agriculture during the next time interval (Table 5.3).

The history of agricultural land in this area is dynamic. About 11% of the agricultural pool was abandoned each year between 1986 and 1988, while 89% was retained to the next time period (Figure 5.3, Table 5.2). But between 1988 and 1989, a period which had more than two-fold more forest clearing, 22% of the agricultural land was abandoned annually (Figure 5.4, Table 5.3). Interestingly, of the 5.8×10^3 total ha which were abandoned to secondary growth between 1986 and 1988, 2.6×10^3 ha or 45% was quickly re-cleared during the next period (Tables 5.2 and 5.3). The clearing of secondary vegetation is an important source of new agricultural land; for instance, between 1988 and 1989 42% of the new agricultural land created was from clearing of secondary growth.

Large-area Inventory of Secondary Growth

In the test site secondary vegetation is important in magnitude and a highly dynamic transition. For the 12 scenes covering the state of Rondonia we estimated a total deforested area of 2.5×10^6 ha in 1986. This estimate is close to other published and reported values (Fearnside 1990b). Of this amount 28%, or 0.71×10^6 ha, were in some stage of secondary growth. This relative proportion for the entire state is close to the value we obtained in our test area.

Discussion and Conclusions

There have been two approaches to estimating tropical deforestation. The first involves the use of tabular statistics from land use censuses (Flint and Richards 1991, Houghton 1986, Skole in press). For instance, the Censo Agropecuario (IBGE 1980a), a routine government inventory of agricultural land in Brazil can be used to document land cover conversion, but it reports only areas of cropland and pasture. There is no direct estimate of the area in secondary vegetation. Similarly, forest inventories, such as the FAO Forest Assessment (FAO/UNEP 1981) consider forests which have been removed from productive or commercial use, and thus do not explicitly consider secondary vegetation. A second approach has been to use satellite remote sensing (Justice et al. 1985, Malingreau 1990, Malingreau et al. 1989, Townshend et al. 1990, Townshend and Justice 1988, Tucker et al. 1986). Even these studies have typically clustered all deforested land together into one category without indication of the fraction in regrowth.

The results of this study suggest that the amount of secondary growth in the Brazilian Amazon represents a potentially large fraction of the total deforested area. In the study site, the area of secondary vegetation was increasing, although follow-on studies will be required to determine how persistent this trend is. Previous measurements of deforestation rates have underestimated the importance of secondary growth. The extent to which the magnitude observed in this study is typical of the Amazon or the entire tropics depends on results from more analyses over larger areas.

Abandonment of agricultural land is an important land cover transition. In this study area abandonment rates were 70% of clearing rates from primary forests in 1986-1988, and 83% in 1988-1989 (Figures 5.3 and 5.4). As mentioned above, one fifth of the agricultural land pool is abandoned each year, suggesting an average steady state turnover time of about 5 years. This is generally consistent with what other observers have seen (Buschbacher 1986, Buschbacher et al. 1988, Uhl et al. 1988) where land fertility and productivity decline to the point that the farmer abandons the land after about 5 years.

Our findings are important to carbon cycle research. They suggest the estimates of carbon emissions from the Amazon have been too high since the occurrence of secondary succession is large in magnitude and, based on our analysis for the entire state of Rondonia, appears widespread. However, its exact magnitude of the effect on carbon accumulation depends on the complex interaction of a number of factors. The first is the amount of regrowth over time relative to the clearing rate. If clearing rates are declining, for instance, and abandonment rates continue, the pool of areas accumulating carbon will grow relative to the areas releasing carbon. The second is the time-dependent rate of carbon accumulation in secondary vegetation. We know very little about such patterns, and field work would be required. Studies of patterns and rates of secondary succession in the Amazon (Uhl 1987) suggest that it takes more than 5-10 years before a successional site is a net sink for carbon. In this study area much of the second growth persists for only a short period of time before being re-cleared. Finally, the area-weighted distribution of various stages of regrowth, which is a function of past deforestation and abandonment rates, as well as the average duration of second growth before re-clearing influence the net flux at any given time. It is possible that these factors could interact in complex ways and greatly influence the net flux at any given time.

If, however, the carbon accummulation rates are high as a result of the widespread occurrence of secondary vegetation in the equatorial regions, there could be an explanation for the imbalances in the carbon cycle. This point has been suggested by Joos et al. (in press). Keeling et al. (1989) suggest the occurrence of a large sink for carbon in the tropical regions, thus corroborating the results we have presented and their implications for the global carbon cycle.

Any method for estimating and monitoring carbon emissions in the tropics based on emission inventories, such as that proposed for the IPCC (IPCC 1992), needs to incorporate an inventory the secondary growth area as well as the deforested area. To do this, high resolution satellite-based monitoring program will be required, or revisions in the data acquired for national census records.

Table 5.1. Description of satellite imagery acquired for this study.

Sensor and Product level	Time of scene center	Location: path/row	Scene center (degree, minute, second)	Angle of Incidence[1]	Orien-tation
SPOT 1, HRV1, 1A (Scene A)	14:36:42 08/23/86	K = 675 J = 368	Lat: S 009 01 02 Lon: W 063 16 27	Right 2.3°	8.9°
SPOT 1, HRV1, 1A (Scene B)	14:36:50 08/23/86	K = 675 J = 369	Lat: S 009 31 05 Lon: W 063 23 18	Right 2.3°	8.9°
SPOT 1, HRV1, 1B (Scene A)	14:24:03 07/10/88	K = 675 J = 368	Lat: S 009 01 01 Lon: W 063 18 19	Right 25.4°	9.6°
SPOT 1, HRV1, 1B (Scene B)	14:24:11 07/10/88	K = 675 J = 369	Lat: S 009 31 03 Lon: W 063 25 28	Right 25.4°	9.6°
SPOT 1, HRV1, 1B (Scene A)	14:40:04 08/24/89	K = 675 J = 368	Lat: S 009 01 01 Lon: W 063 16 20	Left 6.0°	8.7°
SPOT 1, HRV1, 1B (Scene B)	14:40:13 08/24/89	K = 675 J = 369	Lat: S 009 31 03 Lon: W 063 23 07	Left 6.0°	8.7°

[1] An indication of Right means the satellite passed to the east of the scene center; an indication of Left means the satellite passed to the west of the scene center.

Table 5.2. Area of land cover pools, 1986-1989 in the test site (units are ha).

Year	Regrowth	Agricult.	Total	Regrowth as a % of Total	Average Annual Increase Regrowth	Average Annual Increase Agric.	Average Annual Increase Total
FULL TEST SITE							
1986	8,859	25,855	34,714	25.5			
1988	13,803	32,239	46,042	30.0	2,472	3,192	5,664
1989	20,090	39,880	59,970	33.5	6,287	7,641	13,928
SCENE A: NORTH PART							
1986	3,309	7,709	11,018	30.0			
1988	5,049	11,623	16,672	30.3	870	1,957	2,827
1989	8,080	13,818	21,767	37.1	3,031	2,195	5,226
SCENE B: SOUTH PART							
1986	5,550	18,146	23,696	23.4			
1988	8,754	20,616	29,370	29.8	1,602	1,235	2,837
1989	12,010	26,062	38,072	31.6	3,256	5,446	8,702

Table 5.3. Land cover transitions in the test site, 1986-1989. (Units are ha.)

Code	Scene A North	Scene B South	Total	Comments
FFA	3,236	5,397	8,633	Primary forest clearing 1988-89
FFS	1,960	3,334	5,294	Degradation/thinning 1988-89
FAA	2,400	2,845	5,245	Primary forest clearing 1986-88
FAS	1,566	1,431	2,997	Clearing 1986-88, abandonment 1988-89
FSA	877	664	1,541	Degradation, followed by clearing
FSS	822	724	1,546	Degradation/thinning and left fallow
AAA	5,075	12,194	17,269	Always in agriculture
AAS	1,130	1,727	2,857	Abandonment 1988-89
ASS	890	2,317	3,207	Abandonment 1986-88
ASA	678	1,918	2,596	Abandonment then re-clearing of 2nd growth
SSS	1,094	1,746	2,840	Always secondary vegetation
SSA	689	1,385	2,074	Secondary growth, then re-clearing 1988-89
SAA	859	1,663	2,522	Re-clearing of 2nd growth 1986-88
SAS	667	756	1,423	Rapid re-clearing and abandonment

Key to codes: F = forest, S = secondary growth, A = cleared agricultural land. Combinations show transition series, e.g., FAS = Forest converted to agriculture then abandoned to secondary vegetation.

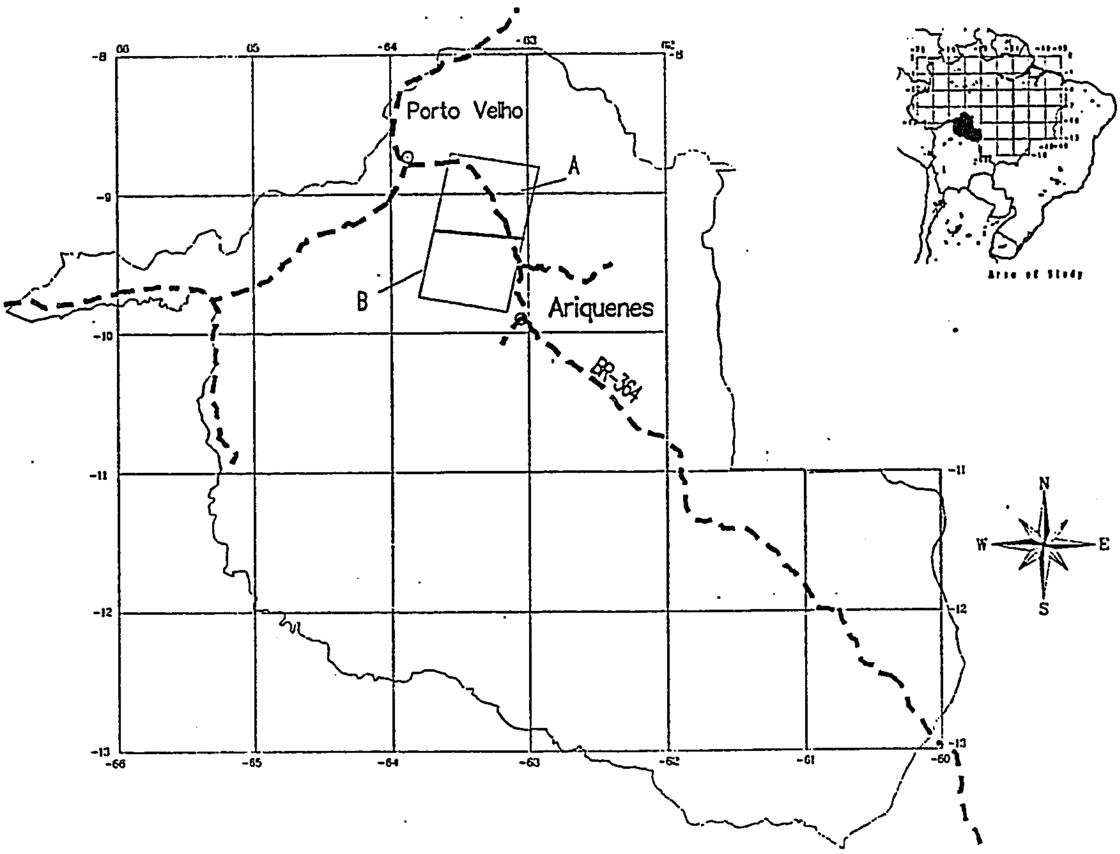

Figure 5.1. The study site, located in the state of Rondonia in the western Amazon. We acquired two scenes, labeled Scene A and B, for each of 3 sample years, 1986, 1988, 1989.

Figure 5.2. An example of the land cover classes considered in the study shown on a SPOT multispectral image. (a) active agriculture, (b) secondary growth, (c) intact forest.

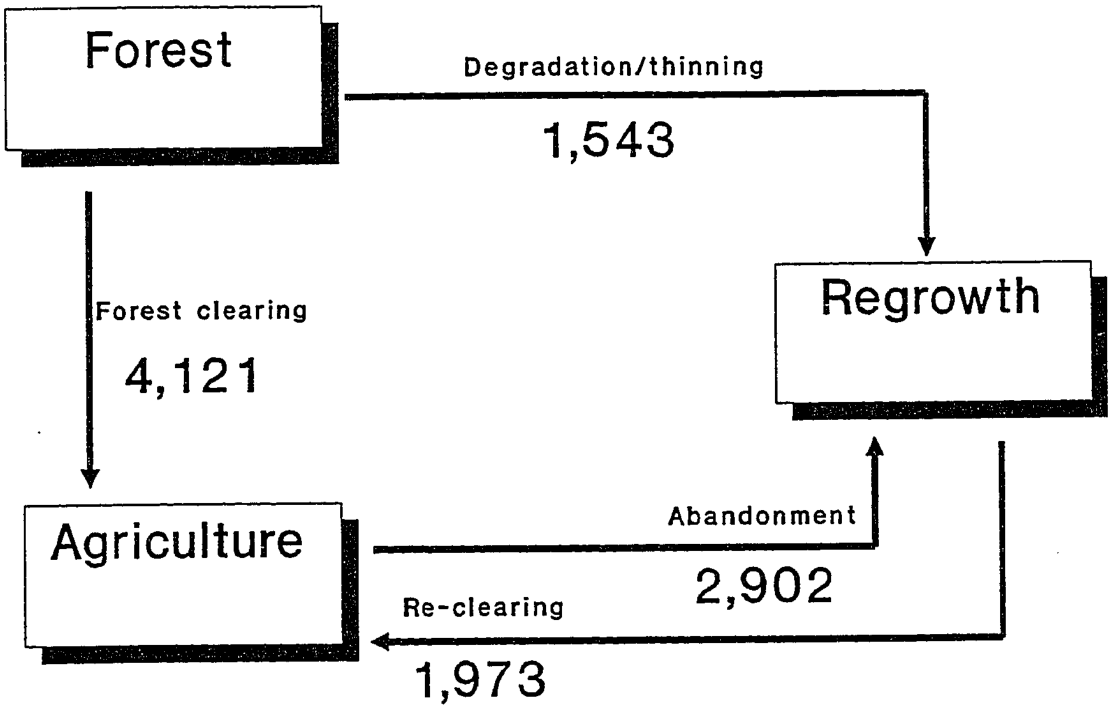

Figure 5.3. Average annual transition rates for the period 1986-1988. Values are hectares per year.

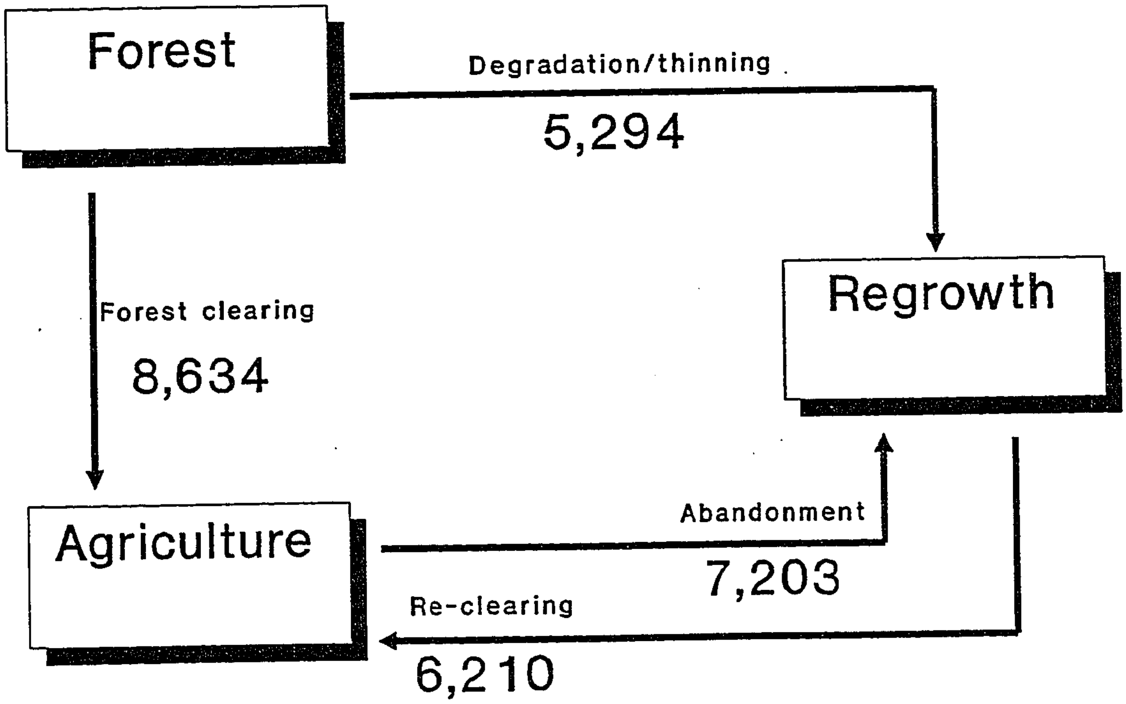

Figure 5.4. Average annual transition rates for the period 1988-1989. Values are hectares per year.

CHAPTER 6

AREA DEFORESTED AND RATE OF DEFORESTATION IN THE BRAZILIAN AMAZON, 1978-1988

Introduction

Deforestation has been occurring in both temperate and tropical regions throughout history (Richards 1984, Tucker and Richards 1983, Williams 1989, 1990a,b). Today, most deforestation occurs in tropical forests and it seems likely that the rate of conversion is higher than it has ever been in recorded history. As much as 40% of the original tropical forests may have been lost to deforestation (Myers 1991). In the 1980s the rate of tropical deforestation in Latin America was greater than in any other region. In the Brazilian Amazon, which alone contains a third of the world's remaining tropical forests and over half of Latin America's agricultural expansion, economic development, and population growth have placed increased pressure on the remaining forests, particularly in the last two decades. Recent estimates have suggested that Brazilian deforestation contributes 40-50% of all tropical deforestation worldwide (Myers 1991, WRI 1990). Because of the immense size of the Brazilian Amazon forest biome, deforestation activities there receive a great deal of attention. But there have been very few quantitative data on the extent and rate of deforestation in the Amazon to underpin either science or policy discussions.

Because of its potential effect on the global environment, tropical deforestation is an important scientific and policy issue. Tropical deforestation is a key aspect of several global change questions. It has been shown to influence large scale patterns of water balance, biogeochemistry, atmospheric chemistry, and climate (Dickinson 1981, Gash and Shuttleworth 1991, Houghton 1991, Houghton et al. 1985b, Keller et al. 1991, Salati 1987, Salati and Nobre 1991, Shukla et al. 1990). Recent research using numerical models suggests that tropical deforestation contributes to the observed increase in atmospheric concentration of carbon dioxide and other trace gases (Houghton 1991, Houghton and Skole 1990, Houghton et al. 1991b). Yet uncertainty in the precise rate and geographical distribution of deforestation in the tropics now constrains research. A recent report from the Intergovernmental Panel on Climate Change (IPCC 1992) states that the paucity of data on tropical deforestation is a key factor limiting our understanding of the carbon cycle and climate change. Since any uncertainty in rates translates directly into uncertainty in the net biotic flux, improved estimates of the biotic source term for CO_2 will require quantitative measurements of deforestation.

Deforestation in the tropics has a potentially important influence on ecosystem structure and function. While occupying less than 7% of the terrestrial surface, tropical forests are the home for a vast majority of our planet's plant and animal species. Destruction of tropical forests causes the loss of habitat and biodiversity, either through the direct loss of habitat or as a result of habitat fragmentation. Some estimates suggest the rate of species loss through habitat destruction and fragmentation is 4000 species annually (Ehrlich and Wilson 1991), but estimates such as these are very uncertain since they rely heavily on current estimates of deforestation and fragmentation.

Improved evaluation of the consequences of tropical forest conversion requires improved estimates of the rate, scale, geographic distribution, and spatial pattern of deforestation. In this study, we employed geographic information system and remote sensing methods to measure and map deforestation in the ~4,000,000 km^2 forested region of the Brazilian Amazon. We used 210 individual Landsat Thematic Mapper scenes as the primary data source. Our results contradict some earlier held views, and suggest that the rate of forest conversion is much lower than previously estimated.

Recent Estimates of Tropical Deforestation

Global Estimates

The first direct survey of tropical deforestation worldwide was conducted by the UNEP and FAO for 76 tropical countries (FAO/UNEP 1981, Lanly 1982). The study relied heavily on national forest inventories, with only a few remote sensing surveys where they had been done. The study estimated an annual deforestation rate for 1976-80 of 6.9×10^6 ha in closed forests. The interim report of FAO's current tropical forest assessment (FAO 1990) now raises the 1980s deforestation rate approximately 40% higher than the first assessment for the late 1970s. Myers (1991) has compiled a recent estimate of tropical deforestation rates for the late 1980s. Myers estimates a global rate of 13.9 x 10^6 ha yr^{-1} in closed forests. When this estimate is compared to the first FAO/UNEP estimate for the late 1970s, the current annual rate of deforestation appears to have increased by 100 percent since the late 1970s. The World Resources Institute (WRI 1990) has also published global estimates of deforestation rates in closed forests for the late 1980s. Their estimate is higher than Myers at 16.5 x 10^6 ha yr^{-1}. Here, deforestation rates appear to have increased 140 percent. It is significant to note that approximately 80 percent of the increase in global deforestation rates since the late 1970s is attributed in these reports to a single location, the Brazilian Amazon Basin.

Estimates for the Brazilian Amazon

The Amazon Basin of Brazil has been defined by law to include all of the states of Acre, Amapa, Amazonas, Para, Rondonia, Roraima, plus part of Mato Grosso, Maranhao and Tocantins and is referred to as the Legal Amazon. It comprises an area of ~5,000,000 km^2, of which ~4,000,000 km^2 is forested, ~900,000 km^2 is cerrado, and 100,000 km^2 is water. Before 1972, with the launch and operation of the Landsat satellites, it was impossible to obtain data required for a study of deforestation in such a large area. Since 1975 satellite data have been available from a ground receiving station in Brazil, and used for estimating deforestation. Brazilian scientists at the Instituto Nacional de Pesquisas Espaciais (INPE) have made deforestation estimates for Brazil from 1975 through 1991 using data from the ground station (Fearnside et al. 1990, INPE 1992, Tardin et al. 1980, Tardin and Pereira da Cunha 1990). These studies constitute the official government estimate of deforestation rates in the Legal Amazon. The total area deforested in 1988 was estimated at 280×10^3 km^2. The average annual rate between 1978 and 1988 reported in these studies is 21×10^3 km^2 yr^{-1}. Estimates from 1988 to 1991 suggest this rate declined each year after 1988 to a current rate of 11×10^3 km^2 yr^{-1}. These government estimates have never been published in the open literature, but remain a significant component of recent discussions and controversy over the actual rate in this important tropical region. A review of the Brazilian estimates is provided in Fearnside (1990b). Other scientists from INPE have used daily NOAA advanced very high resolution radiometer (AVHRR) data to locate fires in the Legal Amazon, and have then used this information to derive deforestation estimates (Setzer and Pereira 1991). These results are considerably higher, at 80×10^3 km^2 yr^{-1} for 1987.

Mahar (1989) published a World Bank Report on deforestation in the Legal Amazon of Brazil by extrapolation of data presented by Fearnside (1986) who had summarized the Landsat studies by Tardin et al. (1980). Mahar's (1989) exponential extrapolations resulted in extremely high estimates of deforestation, especially for the states of Amazonas, Acre, and Rondonia. Mahar (1989) quoted a total of 598.9×10^3 km^2 deforested within the Legal Amazon of Brazil as of 1988. The average annual rate for the period, 1978-1988, by Mahar (1989) is 59×10^3 km^2 yr^{-1}. Myers' (1991) estimate for Brazil in 1989 is 50×10^3 km^2 yr^{-1}, while the World Resources Institute (WRI 1990) estimate is 80×10^3 km^2 yr^{-1}. It is not readily obvious from the analyses, but the estimates by Myers and World Resources Institute use secondary sources; the authors did not directly measure deforestation themselves. All of these studies have much higher estimates than the official estimates from the Brazilian government. This wide range of estimates is perplexing in a region which has been the focus of so much study. Yet there has been no concerted effort to systematically and independently evaluate the discrepancies.

Remote Sensing of Deforestation in the Legal Amazon

Remote sensing studies of deforestation in isolated study areas in the Legal Amazon have appeared in the literature for several years. Some of the first studies employed the use of Landsat data (Nelson and Holben 1986, Nelson et al. 1987, Woodwell et al. 1984), while more recent studies have focused on the use of large scale surveys with AVHRR data (Malingreau 1990, Malingreau and Tucker 1988, Malingreau et al. 1989, Stone et al. 1991, Tucker et al. 1984, Woodwell et al. 1986). The AVHRR has practical appeal since it can be acquired daily to make cloud-free composites, can cover large areas in a single pass of the satellite, and is low in cost.

Using AVHRR thermal information, Nelson et al. (1987) concluded that the AVHRR might only be useful as a stratification tool, due to the poor relationship between fire activity and the deforestation rate derived from MSS and TM spectral data. However, several later studies of Amazon deforestation suggested it could be a promising technique for large-area mapping of tropical deforestation. Malingreau and Tucker

(1988) used a brightness temperature threshold in channel 3 to enhance the contrast between the forest and cleared areas, making it possible to extract areas of deforestation rather easily. A series of papers by Woodwell and colleagues reported similar success with the channel 3 (Woodwell et al. 1986), and also with other channels in unsupervised classification (Stone et al. 1991). Similarly, Cross (1990) reported success using AVHRR data in the Amazon, but suggested that a Maximum Likelihood classification would be better than the channel 3 threshold approach. These studies covered large areas, but never the entire Legal Amazon. Recently, Setzer and Periera (1991) have made an estimate of the deforestation rate in 1987 for the entire Amazon by looking at the distribution of fires determined from the AVHRR-LAC thermal information and some assumptions on the duration of fires and the area affected in each 1.1 km pixel.

Recently, AVHRR has been suspected of over estimating deforestation (Cross et al. 1991, Rock et al. 1992, Skole et al. in prep, Tucker and Batista pers. comm.). This has lead to a new view favoring high resolution remote sensing, such as that provided by Landsat. However, the limited spatial coverage provided in each scene of Landsat data has raised concern regarding difficulties analyzing large number of scenes, and its associated cost.

Measurement of Deforestation in the Brazilian Legal Amazon

A Simple Method for Large-Area Mapping

The large area which would need to be covered in an assessment of deforestation for the entire Legal Amazon necessitates using a method which is low in cost and simple, yet accurate. In experiments in a test area in the state of Rondonia, we have compared various potential remote sensing methods. Landsat, SPOT and AVHRR-LAC data were simultaneously acquired in a large (7.2×10^3 km^2) test area during a two week period in July 1988. These data were then analyzed for deforestation using the methods discussed above, which have been reported in the literature in recent years. Details of this analysis are provided in Skole et al. (in prep.). SPOT and Landsat TM imagery (20 and 30 meter spatial resolution, respectively) were classified using multispectral digital image processing techniques. The AVHRR-LAC data (1.1 km spatial resolution) were classified using two techniques. The first employed a channel 3 brightness temperature threshold. The second employed a supervised classification. Single-channel photo products were also produced at 1:250,000 and 1:500,000 scale from channel 5 of the TM imagery. The photo products were visually interpreted by continuous-line digitizing of the boundary between intact forest and deforested areas. Digitizing was done directly from the photos into a vector-based geographic information system. The results of this analysis show that low-cost visual interpretation of Landsat TM photo products give results very similar to digital processing of full-resolution, multispectral TM and SPOT data (Table 6.1). Moreover, the analysis suggests that approaches based on 1.1 km resolution AVHRR may over estimate the area of deforestation (Batista and Tucker 1992, Cross et al. 1991, Stone and Schlesinger 1990).

The AVHRR 1.1km data are excellent as a stratification tool for initially identifying areas where deforestation is occurring. AVHRR data are not appropriate for detailed Amazon Basin deforestation studies because they over-estimate deforestation, particularly in areas of complex terrain. SPOT data are also not appropriate because they are too expensive, cover only 60 km x 60 km (10% of 1 Landsat scene), and lack the middle infrared bands of the thematic mapper. The extrapolation of AVHRR-based fire estimates into deforestation estimates (Setzer and Pereira 1991) is conditional upon several multiplicative conversion factors. To date there has been no substitute for direct measurement of deforestation with Landsat data, and visual interpretation techniques supported by geographic information systems provide a way to quickly analyze large areas at low cost.

Geographic Information Systems

Geographic information systems (GIS) make it possible to encode and analyze spatial data. In this study we have utilized GIS technology for three purposes. First, we use GIS to precisely delineate and measure areas of deforestation observed on Landsat imagery. This is an analytical problem of encoding the boundary between intact forest and deforested land over very large areas at a fine spatial scale. Moreover, GIS provides a way to handle coordinate and projection information with precision.

Accurate area estimates, and large-scale data management are thus made possible using GIS technology. Second, GIS facilitates the integration of multiple layers of data on political districts, vegetation type, and other geographical features for stratification of the analysis. These layers can readily be merged or cross-referenced spatially or thematically. Delineation of Landsat images into areas of forest, cerrado, and water is necessary before any systematic study of tropical deforestation can begin. Finally, with a GIS it is possible to develop analyses of spatial relationships. That is, questions can be posed concerning the relationship between the mapped areas of deforestation and its geometry, distance from other features, or location.

Data Acquisition

Two hundred and ten Landsat thematic mapper channel 5 (1.55-1.75 um) black and white photographic images at 1:500,000 scale were acquired for the entire Legal Amazon of Brazil: 175 images were from 1988; 8 images were from 1987; 7 images were from 1989, and 20 were from 1986. The acquisition of complete coverage with satellite data for a single year was possible because the Brazilian ground receiving station routinely acquires all data in the line-of-sight between the satellite and the station antenna. Although most of the data collected throughout the year is heavily contaminated with clouds, it is possible to choose single scenes with little or no cloud cover by having access to the entire catalog of scenes in the ground station archive. It must be pointed out that such capabilities do not exist everywhere in the tropics.

Data Encoding

Individual scenes were digitized using visual interpretation and standard vector GIS techniques. The exact boundary between intact forest and deforested land was digitized in the Universal Transverse Mercator (UTM) projection, and then edited and error-checked using clear velum plots of the line-work overlaid on each photographic image. Each Landsat scene contained coordinate control points in decimal degree units, such that each scene could be geographically registered within precise tolerances and mosaicked together. When digitizing, vertices were placed approximately every 50 meters of ground position. Tests of positional accuracy in digitizing followed those of Dunn et al. (1990) and indicated that polygon area-estimation uncertainty due to errors in position were less that 3% (Skole et al. submitted). When finished, individual digitized scenes were projected into geographic coordinates (latitude, longitude), edge-matched and merged in the computer to form a single, seamless dataset for the entire Legal Amazon. This dataset was then projected into a Sinusoid equal area projection to create the final digital map from which all calculations of area were made.

All areas of closed canopy forest which had been deforested by 1988 were delineated, including areas of secondary growth on abandoned fields and pastures when identifiable. Areas of long-term forest degradation along river margins by farmers in central Amazonia were also included, as were scattered small clearings associated with rubber tappers and other small features. All visible roads, power line right-of-ways, pipelines, and similar human-made features were also digitized into the GIS. Interpretation of deforestation was done by the authors, who have field experience in the Amazon. To aid in interpretation, 50 digital Landsat MSS scenes from 1986 were available for detailed examination at ~1:100,000 scale in the states of Acre, Rondonia, and Para. Only areas of deforestation in the closed forests of the Legal Amazon were measured in this study. A digital data layer of the forest-cerrado boundary was also created from the photo products.

To determine the extent of deforestation in 1978 we used the GIS to digitize areas of deforestation shown on 1:500,000 scale paper maps produced from single-channel Landsat MSS data by the Brazilian forest (IBDF) and space (INPE) agencies (Skole et al. submitted, Tardin et al. 1979, 1980). These maps did not differentiate between forest and cerrado clearing, so we used the forest-cerrado dataset digitized from the Landsat images described above to define the forest boundary and separate areas of forest clearing from cerrado clearing. The deforestation dataset for 1978 and 1988 could be digitally merged in the GIS. A digital map of deforestation rates between 1978 and 1988 could then be prepared by subtracting one from the other.

Results

Figure 6.1 shows the geographical distribution of deforestation in the Legal Amazon as of 1988 mapped from our high resolution satellite data. For simplicity of display, the data have been aggregated into 20 km x 20 km grid cells. Figure 6.2 shows the dataset for the state of Rondonia as it appears in the GIS. Figure 6.3 presents a detailed enlargement of the data, and this shows more clearly the level of detail and spatial resolution obtained throughout the dataset. Most of the deforestation is concentrated in a crescent along the southern and eastern fringe of the Amazon, a spatial pattern similar to the distribution of fires observed from thermal anomalies in AVHRR data (Kaufman et al. 1990, Setzer and Pereira 1991). We estimate the total area deforested in 1988 to be 251,082 km^2 (Table 6.2). This estimate suggests 6.1% of the closed forests have been cleared to-date over the entire Legal Amazon. This fraction is somewhat higher in certain states. In Maranhao, for instance, as much as 27% of the forest cover has been converted. Forest clearing in this part of eastern Amazonia has been occurring since the earliest settlements in the last century. However, 11.5% of the forests of Rondonia have been cleared, where most deforestation began only in the mid 1970s.

Figure 6.4 shows the net change between 1978 and 1988, or average annual deforestation rate in the 1980s in map form. The total area deforested since 1978 increased almost 4-fold overall, and by at least a factor of two in every state except Amapa (Table 6.2). It is likely that the deforested area in Amapa is higher than that which is reported here, since excessive cloud cover in this region prevented complete coverage. The average annual deforestation rate in the closed forests of the Brazilian Legal Amazon during the period 1978-1988 was 18.4 x 10^3 km^2 yr^{-1} (Table 6.2). The rate between 1978 and 1988 is approximately 26% higher than it was between 1975 and 1978 (Fearnside 1986, Skole et al. submitted, Tardin et al. 1980), suggesting deforestation rates have indeed increased in the 1980s. Nonetheless, our estimates are considerably lower than recent estimates in the 1980s by Myers (1991) (50 x 10^3 km^2 yr^{-1}), Mahar (1989) (59 x 10^3 km^2 yr^{-1}), World Resources Institute (WRI 1990) (80 x 10^3 km^2 yr^{-1}), and Setzer and Pereira (1991) (80 x 10^3 km^2 yr^{-1}). Our estimates of the total area deforested in 1988 are within 10% of the Brazilian estimates made by the Brazilian space agency (INPE 1992). The average rate is within 15%.

There were marked differences between states in the Amazon. The large state of Para contained most of the deforested area (38%) and had the highest rate. Mato Grosso (22%), Maranhao (15%), and Rondonia (10%) were also important. Generally, the interior states contain the lowest density of deforestation; the vast central forests of the Amazon remain largely intact as of 1988. The average rate of forest conversion is approximately 0.5% per year, based on our analysis of the extent and area of the closed forest zone.

Discussion and Conclusions

Relation to Previous Estimates of Deforestation in the Amazon

Previous estimates of the total area deforested in the Amazon have probably been too high. For instance, our estimate is less than half the estimate of 598 x 10^3 km^2 by Mahar (1989). The estimate by Mahar was made by exponential extrapolation from earlier estimates. Fearnside (1982) also used exponential extrapolation to derive similarly high figures. These estimates of total area deforested and exponential growth in the deforested area over time are not borne out in this analysis. The exponential growth argument is largely derived from analyses of isolated areas in the state of Rondonia. One observation clearly drawn from our analysis is the geographical and spatially heterogeneous nature of deforestation and its rate throughout the Amazon.

Previous estimates of the rate of deforestation also appear to be high. Clearly the estimate by the World Resources Institute is unrealistic, and probably that of Myers as well. Table 6.3 places our results in a global context. If one uses the deforestation rate for the late 1970s from FAO/UNEP (FAO/UNEP 1981, Lanly 1982) and Myers and World Resources Institute estimates for the late 1980s, the rate of tropical deforestation appears to have increased 140% worldwide and 187% in Latin America. Based on our analysis of the Brazilian Amazon only, and substituting our new estimates in place of those from Myers and World Resources Institute, it appears the rate of deforestation has increased by only 50% worldwide, and 25% in Latin America. These differences raise doubt about the other country estimates heretofore given. As methods such as those presented in this study are applied in other regions, we will have a better sense of the actual rate of deforestation worldwide.

Implications for Recent Estimates of the Net Flux of CO_2

These results raise questions concerning the net flux of carbon from land clearing and biomass burning. Current estimates of the net flux of carbon associated with land clearing in the Brazilian Amazon are approximately 0.6 x 10^{15} g C yr^{-1} (Houghton 1991), based on model calculations using values reported by Myers (1991). Our analysis of deforestation using high resolution satellite imagery suggests that these estimates are too high. Based just on our estimate of rates which were only 26% higher than they were in the late 1980s, the net flux from deforestation in the Amazon for the late 1980s should be closer to what it was in the late 1970s, or about 0.4 x 10^{15} g C yr^{-1} (Skole et al. submitted).

An accurate estimate of the tropical source term is critical to improving our understanding of global carbon cycle generally. Measurements of the atmospheric increase when compared to estimates of the net flux of biogenic carbon, fossil fuel emissions, and ocean uptake cannot now be accommodated in a balanced carbon budget (Houghton and Skole 1990, Post et al. 1990). Explanations for this imbalance in the budget center on two possibilities. First, the individual terms of the budget may be in error, or improperly modeled. The emission from fossil fuels is well known and certain, as are the atmospheric measurements. However, the oceanic and biogenic terms are not. Second, the budget may not be complete, and another term--the so-called missing sink--may be additionally important.

Recent analyses by Tans et al. (1990) have suggested a large, unaccounted net sink in undisturbed, predominantly northern, forest ecosystems. The analysis of Tans et al. (1990) utilized a constrained approach, coupling observations of the atmospheric gradient of CO_2 from the GMCC flask network, measurements of oceanic pCO_2, estimates of land surface fluxes from fossil fuels and deforestation, and a general circulation model. The approach provides a geographically-specific assessment of sources and sinks, but is highly dependent on the magnitude of the tropical source term; the size of northern sink is related to the magnitude of the tropical deforestation source. In another analysis, Houghton and Skole (1990) have compared a model-derived estimate of the historic net flux of carbon from deforestation with estimates of the total biospheric net flux derived from the deconvolution of ice core data and ocean models (Seigenthaler and Oeschger 1987). This comparison shows general agreement prior to about 1930, after which the net flux from deforestation increases while the total biotic flux declines. This suggests either the deforestation or deconvolution analyses are wrong, or possibly the difference reflects a net sink in undisturbed ecosystems.

An important consideration for analyses such as Tans et al. (1990) and Houghton and Skole (1990) is the biogenic flux from deforestation, particularly the tropical component. Improved definition of the global carbon budget will come with better definition of its individual terms. The use of constrained analyses, in which some unknown terms of the budget are inferred as residuals from other known terms, will require increased confidence in the estimate of biogenic fluxes.

Three factors now contribute to the current uncertainty in estimates of biogenic fluxes: (1) rates of deforestation, (2) the fate of deforested land (i.e., the amount of secondary forest regrowth and re-clearing), and (3) the stock of biomass and soil organic matter and their response to disturbance. The first two uncertainties are the most tractable to resolve in the near term, since this study demonstrates that high resolution remote sensing can be used to measure deforestation over large areas of tropical forests.

The Question of Forest Regrowth

An aspect of the problem which has not been addressed by any study, including this one, is the amount of secondary growth which exists on once-deforested land. The use of single-channel data made it extremely difficult to detect all secondary growth, and it is possible that this area could be large (Buschbacher 1986, Uhl 1987, Uhl et al. 1988). If this area is indeed large, estimates of the net flux of carbon could be further reduced, since these areas accumulate carbon in regrowing biomass. Currently there are no large-area measurements of the fate of deforested areas. Satellite-based analyses offer the opportunity to specifically distinguish intact canopies, deforested areas, and secondary vegetation. Moreover, multi-temporal analyses can be used to track the land use history of an area as forests are cleared, used, and abandoned (Hall et al. 1991).

Skole et al. (in prep.) report an analysis of high resolution multi-spectral SPOT data which were acquired in a test site in the Brazilian Amazon in 1986, 1988, and 1989 to measure patterns of secondary growth. This analysis suggested that the amount of secondary growth in the Amazon is probably quite large relative to the areas which are deforested. The analysis also showed that the area of secondary vegetation was increasing. This study suggested that at any one point in time, approximately 30% of the deforested area is in some stage of abandonment, and quite likely that nearly all deforested land becomes abandoned after approximately 5 years.

The next step in the analysis of deforestation is to document secondary growth as a separate category within the GIS. This would require the use of color photographic products or digital data.

Mapping versus Sampling

This study provides a complete inventory of deforestation. Another way to measure deforestation would be by sampling. Some proposals have called for a global sampling scheme with a 10% sample stratified by forest type (FAO 1992). It is beyond the scope of this paper to fully address the question of sampling. However, a cursory examination of the problem is made possible by the fact that we now have a dataset upon which sub-sampling experiments could be conducted from the entire population. To this end, the location of each Landsat scene (corner points) was encoded in the geographic information. A random, 10% sample of scenes was made, and the average fraction of the scenes deforested was computed. This average deforestation density in the sample was then applied to all scenes covering the Legal Amazon and an estimate of the total area deforested was determined. This procedure was repeated in 30 individual trials, and the range of estimates was tabulated. An actual, sample-based deforestation assessment would only have one selection rather than the 30 which we simulated. Thus, the range in estimates provided in the 30 trials indicates the domain of possible estimates one would expect from sampling in this way. In our analysis the range extended from 115.34 x 10^3 km^2 to 602.86 x 10^3 km^2 for 1988, or between 48% and 252% of the actual value. Clearly, more samples or some method for stratification of would improve the estimate. Nonetheless, it would appear that even a sampling scheme would be improved by first delineating a base map from which future stratifications could be made.

Spatial Analysis

Deforestation is not dispersed uniformly throughout the Amazon, but is concentrated around local foci, such as large human settlements and the roads which connect them. Large settlements are here defined as the municipality centers which are officially recorded in census documents (IBGE 1980a, IBGE 1980b). An analysis made of the spatial characteristics of the dataset using distance buffering in the GIS show that 80% of the deforestation occurs within 50-80 km of town centers or road. Moreover, the density gradient becomes less steep with time (Figure 6.5). This suggests that deforestation in the Amazon proceeds as diffusion from several dispersed nodal locations, rather than as a continuous advancing front. It also suggests that over short time intervals of a decade or less the rate and geographic distribution might be predicted or modeled from a base map without having to introduce overly complex analyses of social dynamics or their parameters.

Implications for Forest Fragmentation Analysis

The use of GIS also made it possible to count and measure forest fragments. Fragmentation is an important factor in analyses of the impact of deforestation on biodiversity. The total number of isolated fragments of forest polygons, which were surrounded by deforestation on all sides is shown in Table 6.4. This table also shows the size class distribution of isolated fragments. Only 18.3 x 10^3 km^2 of forest "islands" were found by our analysis. This represents a small fraction of the total area deforested outright (7%), suggesting that the outright loss of habitat is far more significant than the fragmentation and isolation of habitat. This finding suggests that fragmentation in the Amazon might not be as important, in terms of magnitude, as previously suspected. We must note that the scale of this analysis might have been too coarse to observe much of the fragmentation.

A New Approach for Forest Monitoring

These new estimates of Amazonian deforestation suggest studies using coarse resolution satellite data, such as AVHRR, in limited study areas probably overestimated deforestation. Stone et al. (1991), for instance estimated the area of forest cleared by July 1988 in the state of Rondonia was between 37,200 and 37,900 km^2. Cross (1990) found the total area deforested in Rondonia to be 33,730 km2 as of 1988. Trends to 1988 from analyses of deforestation made through 1986 by Malingreau and Tucker (1988, pers. comm.) and Woodwell et al. (1986) suggest estimates similar to these. Our estimate for Rondonia (Table 6.2) is considerably lower than these at 24.4 x 10^3 km^2. Early proposals which called for the use of AVHRR to monitor deforestation for global carbon cycle modeling (Dale 1990, Woodwell et al. 1986, 1987) would likely result in overestimates of deforestation and carbon flux.

The use of low-cost photographic products is a feasible way to improve measurements of deforestation and habitat fragmentation. The method could be improved with the use of three-channel color composites, since secondary growth and natural savannas would be easier to identify. The approach developed here could be extended to an operational global tropical forest monitoring program. The low cost, "low-tech" approach is amenable to in-country participation, and photo products could routinely be used by national forest agencies and their expert personnel in the field. This approach makes complete surveys on a regular basis possible, and might provide one approach which could be implemented to satisfy the requirements of the IPCC (1992). The encoding of data in a GIS, which could be developed on personal computers or workstations, enables precise estimates of area and provides the framework for complex spatial analyses. It has potential as a data management system for the next generation of global change models.

Table 6.1. Comparison between different methods for measuring deforestation in closed tropical forests, from co-incident analyses in the test site (km^2).

Method	Deforested Area	Relative to SPOT
SPOT digital analysis	668	---
Landsat TM digital analysis	629	0.94
Landsat TM visual interpretation, 1:250,000 scale	615	0.92
Landsat TM visual interpretation, 1:500,000 scale	710	1.06
AVHRR-LAC statistical classifier: Maximum Likelihood	875	1.31
AVHRR-LAC channel 3 brightness temperature threshold at 298.6 °K	1140	1.71

Table 6.2. Area of deforestation in closed forests in 1978 and 1988, and the average annual deforestation rate for individual states in the Legal Amazon.

State	1978 (km^2)	1988(km^2)	Rate per year	Change
Rondonia	6,266	24,416	1,819	3.81
Acre	2,550	6,149	360	2.41
Amazonas	2,344	11,730	939	5.00
Roraima	208	1,953	174	9.39
Para	29,573	96,236	6,666	3.25
Amapa	233	260	27	1.12
Maranhao	10,811	38,653	2,784	3.58
Mato Grosso	11,895	55,717	4,382	4.68
Tocantins	3,652	15,968	1,232	4.37
Legal Amazon	**67,532**	**251,082**	**18,383**	**3.72**

Table 6.3. Recent estimates of the rate of tropical deforestation in the late 1970s and 1980s. This table shows results from three global studies and how their estimates would change if results from the analysis of the Brazilian Amazon reported in this study were used instead. (Units are 10^3 km^2.)

Study: Time Period	Africa	Asia	Central and South America	Total
FAO/UNEP: late 1970s	13.19	17.67	38.07	68.93
Myers: late 1980s (% increase since 1970s)	15.80 (20)	46.00 (160)	76.80 (102)	138.60 (101)
WRI: late 1980s (% increase since 1970s)	13.59 (3)	42.76 (142)	109.09 (187)	165.44 (140)
This Study: late 1980s (% increase since 1970s)			**47.47 (25)**	**103.82 (51)**

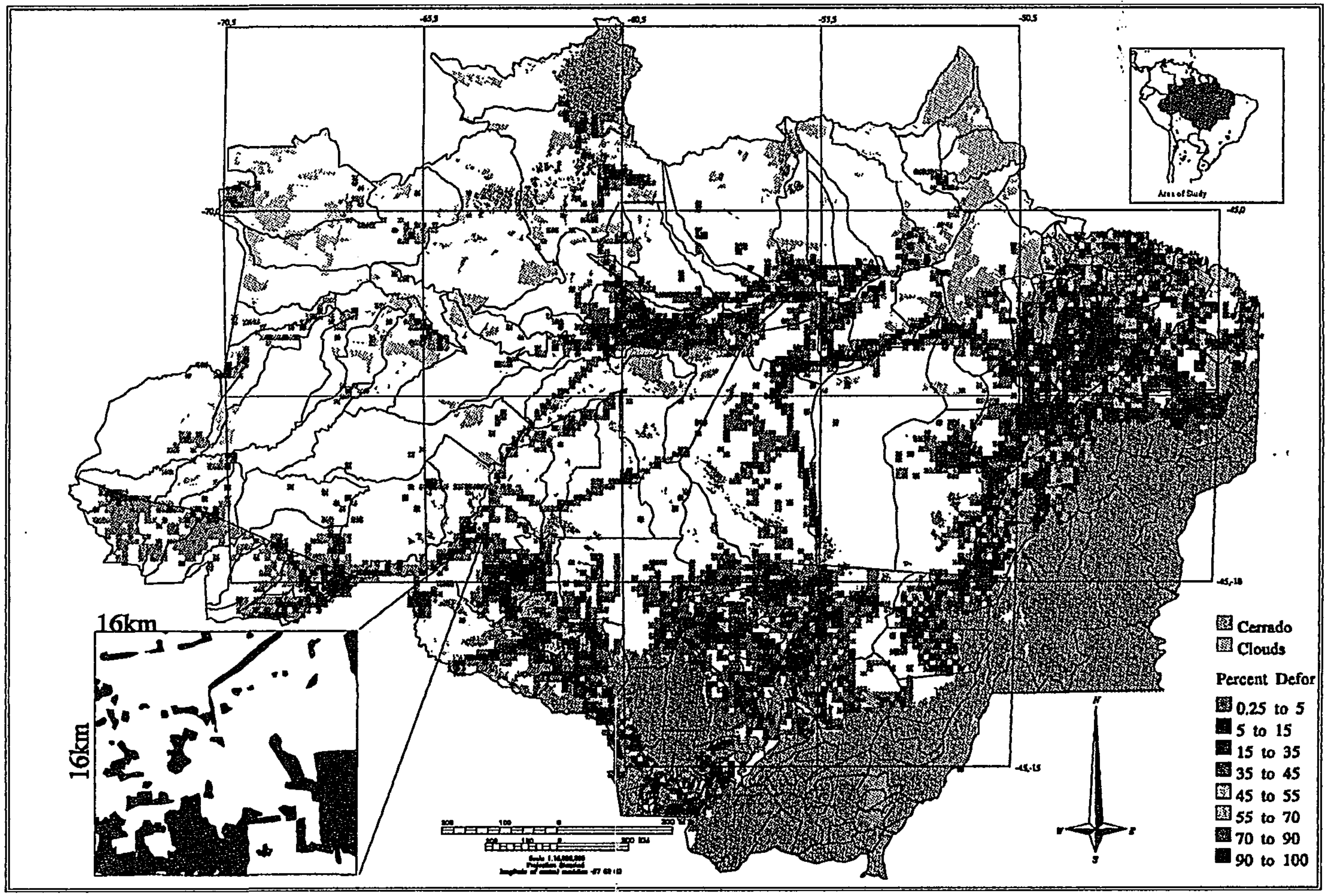

Figure 6.1. Deforestation in the Brazilian Amazon in 1988 mapped from Landsat TM data. The vector dataset has been gridded for simplicity of display. As shown on the legend, each color represents a deforestation density, expressed as a percentage of the grid cell. The inset shows detail from the vector dataset.

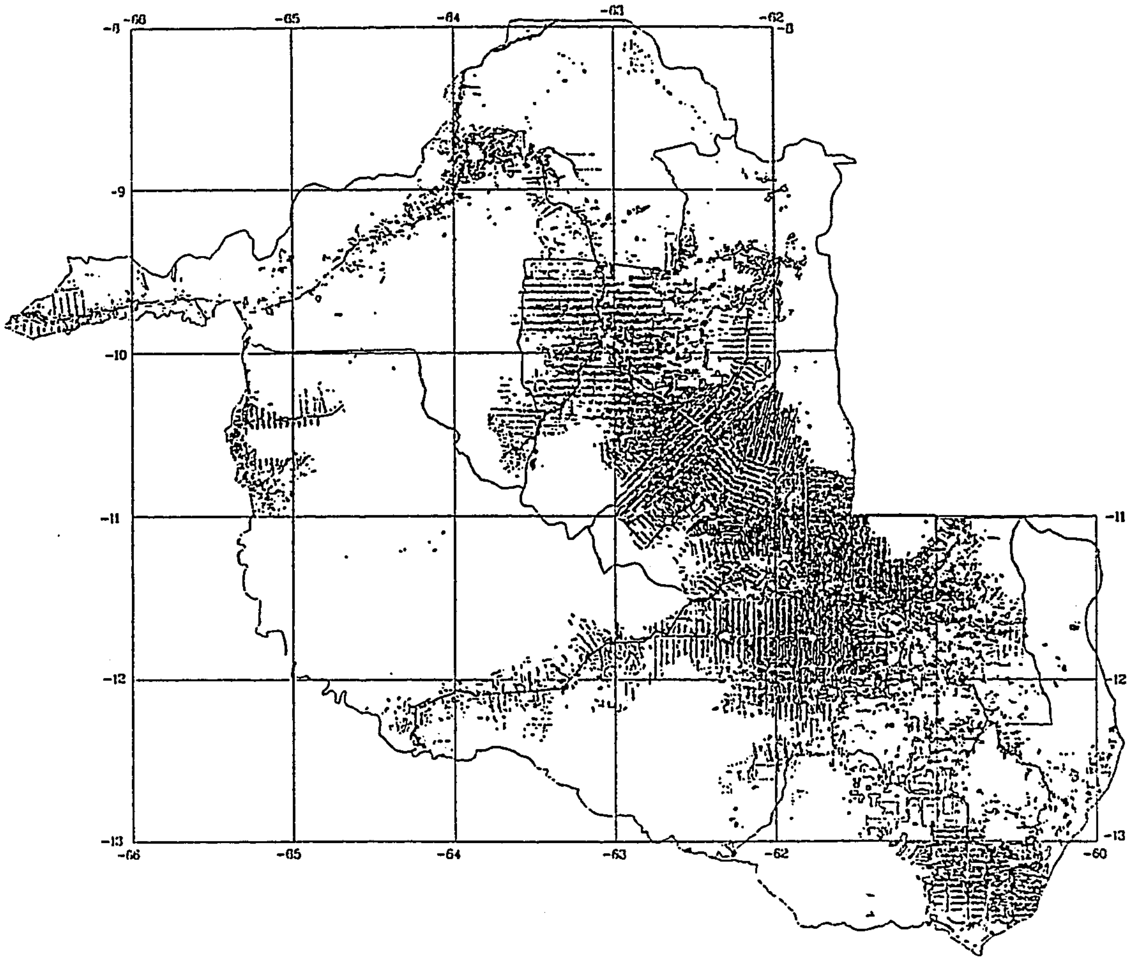

Figure 6.2. The state of Rondonia shown as it appears in the dataset in vector format.

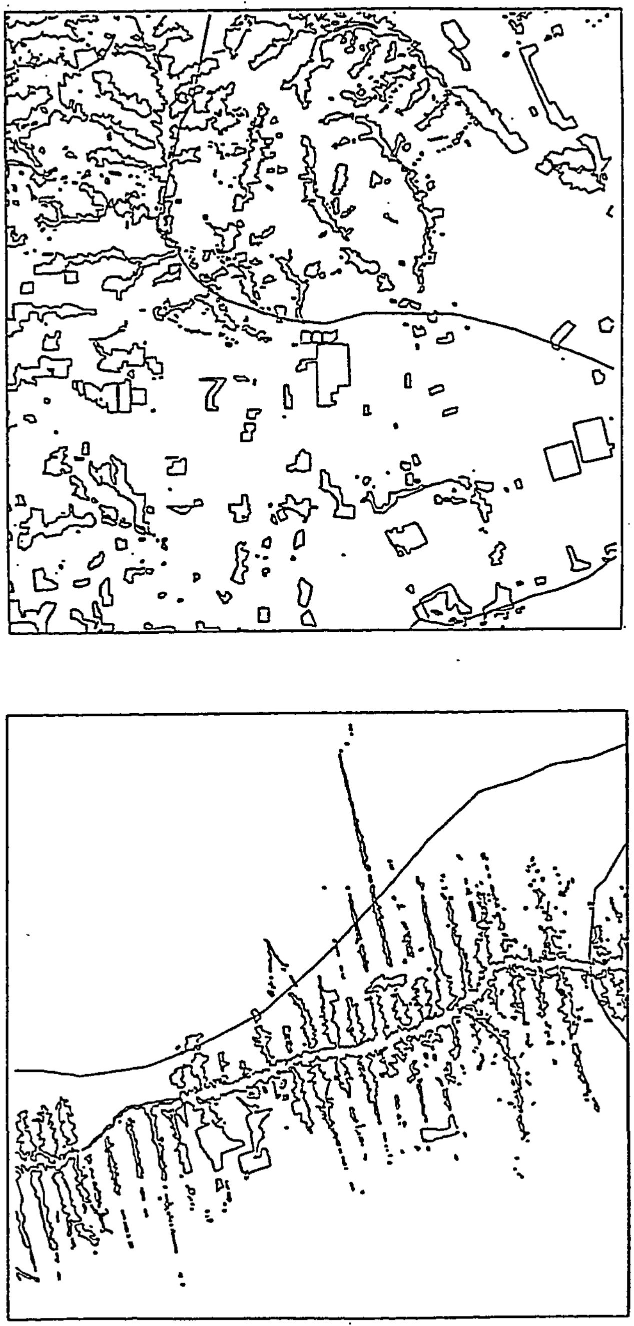

Figure 6.3. Enlargements from two sections of the dataset showing the level of detail recored in the dataset.

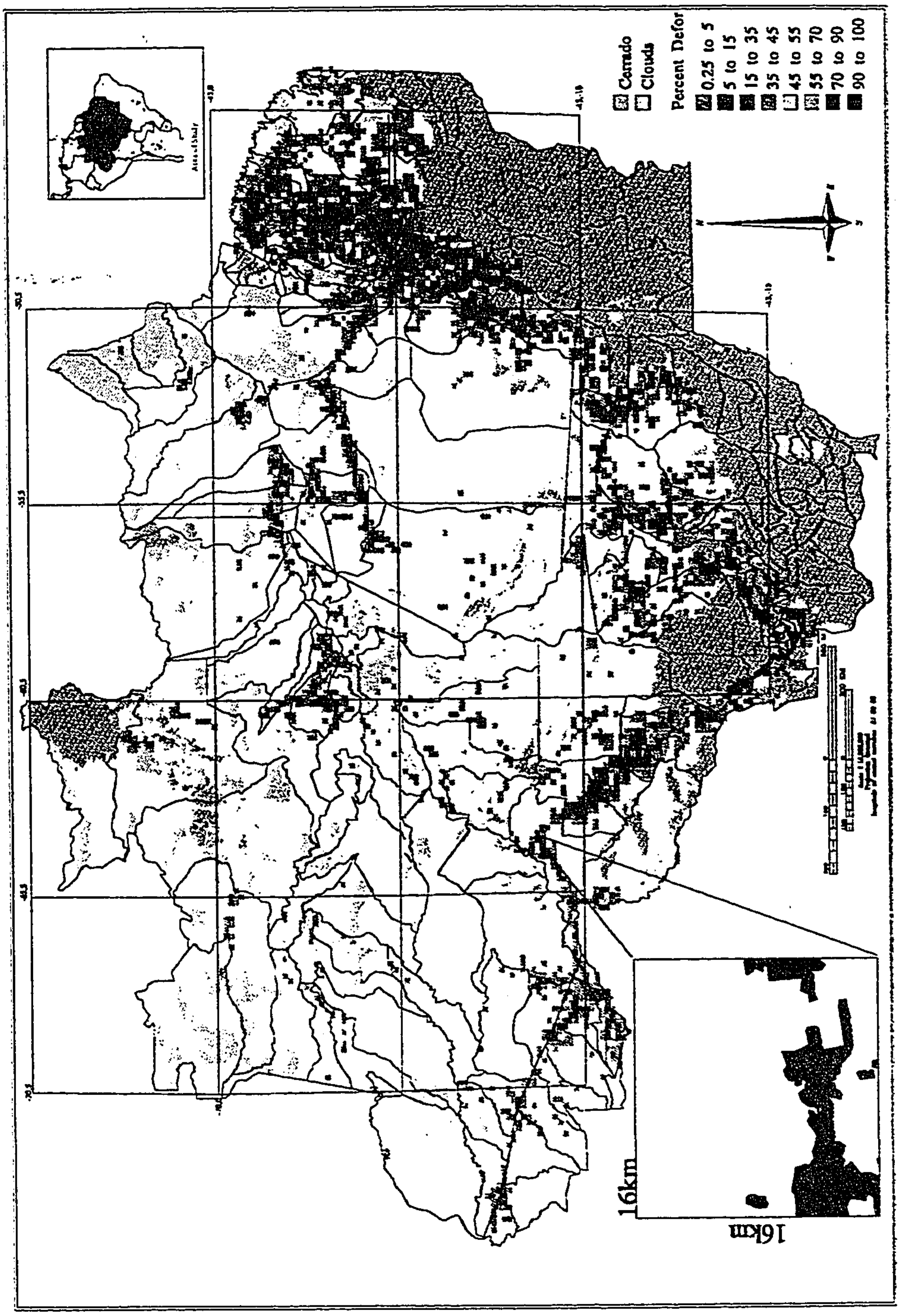

Figure 6.4. Deforestation in the Brazilian Amazon in 1978. The difference between this map and Figure 6.1 represents the average annual deforestation rate over the decade, 1978–1988.

CHAPTER 7

WHAT IS DRIVING DEFORESTATION IN THE BRAZILIAN AMAZON?

Introduction

Theories which relate population growth directly to environmental change have been popular in both academic and public policy circles in recent years (Keyfits 1991, Turner and Meyer 1991). Such interest in the role of population growth stems, in part, from a general awareness of the current exponential growth in the human population and its apparent pressure on natural resources around the world. This view has often been focused on developing countries, where environmental and food resource problems are acute (Repetto 1985). An emphasis has been placed on the specific problem of population and land use change (Allen and Barnes 1985, Browder 1988, Cline-Cole et al. 1990, Myers 1991 , Rudel 1989).

However, little progress has been made toward understanding the complex interactions between demographic change, economic development, and environment. The tendency by a few vocal scholars has been to view population as the paramount external driver of environmental degradation (Ehrlich and Ehrlich 1990, Ehrlich and Holdren 1971). The problem is most obvious in the context of global environmental change. Although there have been many models for explaining why humans deforest the landscape, there are few detailed country case studies--which is the scale where social and economic factors can be accounted for.

In this paper we explore the human dimensions of global environmental change as they relate to deforestation in the Amazon Basin of Brazil. We focus the analysis on the role of demographic and economic factors. Brazil presents an interesting case study because it is a rapidly developing country where deforestation is the highest of any single country, contributing 30% or more of the net global biotic emission of carbon dioxide today (Houghton 1991b, Houghton et al. 1987). The link between explosive rates of deforestation and economic development over the last twenty or thirty years provides insights as to how land cover change, an emerging theme in global change research, is couple to land-use change and its human factors.

Recent Social and Economic Trends

Economic statistics for Brazil (1950-1987) suggest considerable recent growth in the country's industrial economy, agricultural output, and population. The GDP grew at an average annual rate of 9% between 1965-1980 and 3.3% between 1980 and 1987 (World Bank 1989). This growth in the economy was similar to the growth rate in energy consumption (9% in 1965-1980, 4% in 1980-1987). Per capita energy consumption grew from 802 kg (petroleum equivalent) in 1970 to 1,277 kg in 1987 (IBGE 1989). Exports grew throughout this period, and in 1985 they generated a net trade surplus of $13B (Pool and Stamos 1987). This period of growth has often been called the "Brazilian Miracle."

However, economic growth has also been accompanied by mounting inflation, which went from 31% per year in the period 1965-1980 to 166% per year in the period 1980-1987 (World Bank 1989). In 1985, it was as high as 225% (Pool and Stamos 1987). These years witnessed rising external debt (from $5.1B in 1965-180 to $106B in 1980-1987), as long term debt service has consumed a third of total exports. In spite of recent improvements in the economy and increased earnings from exports, economic development in Brazil has been characterized as being uneven and unequal; economic growth is not filtering down to the majority of the population. Half of total income is earned by ten percent of households (IBGE 1989, World Bank 1989).

It is important to note that agricultural modernization has been an important national goal (Bunker 1984b, Hecht 1989, Mahar 1989, Moran 1981, World Bank 1982). In the last 20 years, total farmland area has increased more than 60% and the land actually in crops increased 176% (IBGE 1970a,b, 1975, 1981, 1989, World Bank 1982). Availability of crop credits increased, and the use of machinery and other commercial inputs grew as Brazil has become a leading agricultural exporter of soybeans, oranges and several other commodities. The agricultural modernization programs also brought important changes in land allocation and land tenure, particularly in programs of the late 1970s. While modernization has been focused in the south of Brazil, settlement programs in the Amazon have stimulated the opening of the rain forest frontier, as migrants moved there from the south and northeast.

Recent Demographic Changes in Brazil, 1950-1987[1]

In 1950 Brazil was a rural country. The rural population was almost twice as large as the urban population. Approximately 36% of the population were in urban areas as of 1950 (Table 7.1). By 1990 urban dwellers comprised 75% of the population (Table 7.2). From recent estimates of the national census and the work of Merrick (1984), it appears that total fertility rates in both rural and urban groups has been declining, but somewhat faster in the urban group. The 1970 total fertility rate was 4.6 and 7.7 for urban and rural populations, respectively. The 1980 total fertility rate was 3.6 and 6.4 for urban and rural populations, respectively (see Table 7.2).

Actually, rural-to-urban migration has influenced the numbers and distribution of rural and urban populations more than fertility itself. In 1970, for instance, the rate of urban population growth was 7 times the rural population growth (Table 7.3). The state with the highest growth rate between 1970 and 1980 was Rondonia. The state with the smallest growth rate was Parana. There appears to be an important relationship between this fact and trends in large-scale deforestation in Rondonia in the

[1] Unless cited otherwise, all demographic, economic, and agricultural statistics in this section were obtained from the various primary census sources for Brazil: IBGE 1960; IBGE 1970; IBGE 1970; IBGE 1970; IBGE 1975; IBGE 1980; IBGE 1980; IBGE 1981; IBGE 1989.

1970s, which we discuss more below. As a general rule, urban population growth rates are higher than rural growth rates. But this is not always true. In frontier states, such as Rondonia and Para, where active colonization is occurring, rural and urban growth rates look quite similar.

In 1950 there were two major cities with populations over 1 million. By 1987 there were twelve. While nearly all were located in the coastal regions, but one--Manaus--sprang up in the middle of the Amazon frontier. The largest cities were not necessarily the fastest growing. The trend in urbanization in Brazil can be divided into two components:

1) Fast growing cities in the rural frontier or in close proximity to large metropolises. Some cities grew up as boom towns in Amazonia, such as Porto Velho, the capital of Rondonia, which grew almost 3-fold between 1970 and 1985 (8-fold between 1950 and 1985) as government sponsored colonization programs drew large numbers of migrants to the region. Other cities grew in response to growth in large magnet cities, such as Campinas on the outskirts of Sao Paulo, which grew almost 2-fold between 1970 and 1985 as an industrial and manufacturing center.

2) Very large magnet cities. These cities often grew at slower rates, but were large in absolute population. As financial and industrial centers, they stimulate growth in their region. Sao Paulo, for instance grew 70% between 1970 and 1985, but at 10

million people is the one of the largest cities in the world. Approximately 21 % of the Brazilian population lives in the 12 largest of these cities.

With economic growth and increased urbanization, interstate migration has also increased. Figure 7.1 shows rates of out-migration in states of Brazil in 1950 and 1980. This figure only reports the fraction of people (%) who migrated out the state between 1940 and 1950. It does not reveal anything about net growth since it does not account net in-migration. However, it does provide an indication of the overall mobility of the society. Note that in the majority of cases out-migration, and hence mobility, increased. This is re-enforced in Figure 7.2, which plots the difference as a percent change between out-migration rates in 1970 and 1980. The states with negative values (Amazonas, Sao Paulo, Rio de Janeiro) are those in which the outflow of people declined. These regions are essentially magnets which tend to hold people once they are resident there, and are also states with growing urban-industrial centers. What stands out on this figure, however, is the large increase in out-migration rates in the state of Parana. As we will discuss in a later section, agricultural modernization programs in the 1970s resulted in changes in land tenure and farm size distribution. This, in turn, may have lead to large transnational migration flows into new settlement fronts in the states of Para and Rondonia. Thus, while the overall trend in Brazil (and other Latin American countries) has been one of *depeasantization* (Bunker 1984a) occurring concurrently with urbanization, the Amazon frontier presented a special case of rural population growth.

Deforestation

Large-Scale Patterns

Deforestation, primarily in the Amazon region (Legal Amazon as it is often referenced) is a large source of carbon dioxide to the atmosphere (Houghton 1991b, Houghton et al. 1987, 1991b, Skole et al. in press). The best estimates suggest between 0.3 and 0.6 x 10^{15} g C per year are currently released as forests are cut and burned for agriculture, by far the largest amount of any country in the world (Houghton 1991b). In Brazil, as in the rest of the tropical world today, clearing for agriculture is the primary cause of deforestation. This includes permanent and temporary cultivation, as well as pasture formation.

The current rate (ca. 1987-1989) of deforestation in the Legal Amazon region is uncertain, but best estimates suggest between 2 and 3 x 10^6 ha per year (Fearnside 1990b, INPE 1992, Tardin and Pereira da Cunha 1990). Estimates by the World Resources Institute (WRI 1990) are 8 x 10^6 ha. Estimates made by Myers (1991) are 5 x 10^6 ha per year. These latter estimates are probably too high, since they were based on published estimates from studies of fires, which are burdened by a number of assumptions necessary to convert thermal anomalies on a satellite sensor to areas deforested (Kaufman et al. 1990, Setzer and Pereira 1991).

Large scale deforestation in the Amazon had its beginning in the mid-1970s. It is worthwhile examining the nature and pattern of deforestation during this initial period of Amazonian frontier development.

The most important agent of deforestation in the Amazon was agriculture, both small farmer settlements and commercial activities, including conversion for pasture formation. If one examines the geographical pattern of agricultural expansion in Brazil during the 1970s some interesting patterns emerge. Figure 7.3a-c shows the distribution of agriculture at three dates: 1970, 1975, and 1980 taken from Skole et al. (in press). The highest density of agriculture is in the south of Brazil. In 1970 most of the agriculture was in the south and east.

Through the late 1970s, however, agriculture quickly expanded along two geographical fronts: (a) along a north-south corridor adjacent to the Belem to Brasilia highway, and (b) a northwesterly corridor into the state of Rondonia (see Figure 7.3c). Thus although the south continued to have the highest density of agriculture during the period, the Amazon was the locus for the most dramatic increases, as agriculture rapidly replaced forests in states such as Rondonia.

Figure 7.4 shows areas of new deforestation which occurred between 1975 and 1978. The major front of deforestation existed as a crescent along the southern fringe of the Legal Amazon. This trend continues today. Table 7.4 shows data on the rate and extent of deforestation in the Brazilian Amazon in between 1978 and 1988. The average annual rate of deforestation during this period was 18.38 x 10^3 km^2. Most of the deforestation during the late 1970s and through the 1980s occurred in the states of Para, Maranhao, and Mato Grosso (Table 7.4). The fastest growth, particularly in the late 1970s, occurred in the state of Rondonia.

Local-Scale Patterns

Large scale patterns of deforestation are the cumulative result of small scale activities. In this section we describe typical small-scale patterns of deforestation in the state of Rondonia, where many of the new Amazon settlements have developed.

Since the early 1970s government programs aimed at establishing new human settlements in the Amazon Basin have moved settlers to this once-forested region. Government incentive programs for pasture development and the creation of infrastructure have been coupled with free land entitlement programs to create a strong magnet for migration into this part of the Amazon Basin. Between 1970 and 1980 the state's population grew from 111,000 to 491,000 (IBGE 1989); it was the fastest growing state in Brazil during the 1980s, with a population in 1988 of over 1 million. Approximately 60% of the population is classified as rural, mostly migrants from the south and northeast of Brazil. The largest cities are Porto Velho and Ariquemes, the former is the state capitol and the latter is the site of one of the largest colonization centers.

Most of the land clearing has been for agriculture. Approximately half the agricultural clearing is for pasture and half for temporary and permanent crops (IBGE 1980a, 1989). Principle crops are rice, milho, coffee, beans, cacao, and manioc. Eighty percent of the farms are less than 100 ha in size (IBGE 1989). The regional climate is tropical. Temperature varies only slightly throughout the year, averaging 25° C, with relative humidity frequently above 85%. Total annual precipitation is approximately 2000 mm, with an extended rainy season from October to April. The primary dry season is from June to September, when most clearing and burning takes place.

The change in the amount of agricultural land represents the net sum of several land cover changes: increases from primary forest conversion and secondary vegetation clearing, and losses due to abandonment of agricultural land to second growth. These transitions were measured using satellite data in an 7.2×10^5 ha settlement area. Figures 7.5 and 7.6 show land cover transitions which occurred in this area during two intervals, 1986-1988 and 1988-1989. The values are annual transition rates for each period. Between 1986 and 1988, new agricultural land came from clearing 4.12×10^3 ha yr^{-1} of primary forest and 1.97×10^3 ha yr^{-1} of secondary vegetation. Between 1988 and 1989, 8.63×10^3 ha yr^{-1} of primary forest and 6.21×10^3 ha yr^{-1} of secondary vegetation was cleared for agriculture. The amount of agricultural land annually retained in the pool from 1986 to 1988 was 10.06×10^3 ha yr^{-1}, and 25.04×10^3 ha yr^{-1} between 1988 and 1989.

A large amount of natural forest was impartially cleared or degraded, 1.54×10^3 ha yr^{-1} between 1986 and 1988 and 5.29×10^3 ha yr^{-1} between 1988 and 1989. This degradation, or thinning, of a site is distinguished from complete clearing for agriculture. It can be seen in the satellite imagery and was verified in the field. In this analysis it is considered a transformation to second growth, since the site will eventually begin regrowing following disturbance. Degradation of primary forest represented 27% of all primary forest conversions each year between 1986 and 1988, increasing to 38% between 1988 and 1989. A large fraction of areas thus degraded and left in secondary growth is retained as secondary growth from one time period to the next. Of the 3.087×10^3 ha degraded between 1986 and 1988 (total for 2 years), only half was subsequently cleared to agriculture during the next time interval.

The history of agricultural land in this area is dynamic. About 11% of the agricultural pool was abandoned each year between 1986 and 1988, while 89% was retained to the next time period (Figure 7.5). But between 1988 and 1989, a period which had more than two-fold more forest clearing, 22% of the agricultural land was abandoned annually (Figure 7.6). Interestingly, of the 5.804×10^3 total ha which were abandoned to secondary growth between 1986 and 1988, 2.596×10^3 ha or 45% was quickly re-cleared during the next period. The clearing of secondary vegetation is an important source of new agricultural land; for instance, between 1988 and 1989 42% of the new agricultural land created was from clearing of secondary growth.

Abandonment of agricultural land is an important land cover transition. In this study area, abandonment rates were 70% of clearing rates from primary forests in 1986-1988, and 83% in 1988-1989 (Figures 7.5 and 7.6). As mentioned above, one fifth of the agricultural land pool is abandoned each year, suggesting an average steady state turnover time of about 5 years. This is generally consistent with what other observers have seen (Buschbacher 1986, Buschbacher et al. 1988, Uhl et al. 1988) where land fertility and productivity decline to the point that the farmer abandons the land after about 5 years.

If abandonment increases in this region, a large scale migration, or "second wave of migration," might be expected. Farmers that settled the region in the late 1970s farm for a period, abandon the land and move to new areas within the region. Eventually, however, the pull of large magnet cities, such as Porto Velho, the state capitol, or Manaus which is now a growing free trade zone will draw farmers away from the region. Thus changes in small-scale activities reflect response to local conditions such as poor soils, lack of commercial credit, and emerging employment options (or the perception of new employment options). And these local responses eventually manifest themselves at the aggregate level. It might also be suggested here that the local conditions today are the legacy of past macro-level trends, such as the large-scale government sponsored programs to create new settlements in the Amazon and the subsequent migration of people from the south of Brazil.

This analysis also suggests the important and apparently inseparable coupling between land in active agriculture and secondary growth. The mode of production in this region is predicated upon maintaining both classes of land use. Thus, local ecological conditions, methods agro-ecosystem resource management, and local-scale decision-making are as much a driving factor in deforestation as is demographic factors. It is conceivable to suggest in fact that demographic trends, such as the tendency toward higher fertility rates in these rural areas as mentioned in a previous section, is itself an artifact of these factors, rather than its principle driving factor.

In the next section we look at population growth and its empirical relationship to deforestation rates in the Amazon. We then approach the problem from the larger perspective of changing social and economic organization and structures in Brazil, focusing on the early period of initial migration to the Amazon frontier.

Population and Deforestation: Correlation or Causality

Regression Models

Allen and Barnes (1985) surveyed population and deforestation data for 76 tropical countries using statistical correlation. They also examined multiple regressions of deforestation against other variables such as arable land, roundwood production, and GDP. Their analysis suggested a low, but significant, correlation between population growth rates in 1970-1978 and deforestation reported for the period 1975-1980 in the FAO Forest Assessment (Lanly 1982). They also showed low, but significant, correlation between arable land change and deforestation. GDP was not a significant variable. Their conclusion was that the cause of deforestation is population growth.

Reis and Margulis (1990) have made a cursory examination of economic explanations for large and increasing deforestation rates in the Legal Amazon during the mid-1980s. Their analysis is interesting in that they relate demographic and economic factors to deforestation. One conclusion they draw is that population growth appears related to deforestation when one plots population density against deforestation density (defined as the fraction of an administrative district deforested). Yet, they also develop a multiple regression model ($r^2 = 0.8$) which relates deforestation to the spatial density of population and a set of other measurable economic factors:

$$D = 0.3p + 0.4a + 0.11c + 0.04w + 0.28r - 0.02d + 2.42$$

where D is the deforestation rate, p is population density, a is the area in arable land, c is the density of cattle, w is the wood harvest per square km, r is the number of roads, and d is the distance from the state capital.

Using data which we have compiled on deforestation from both statistical land use surveys and satellite data (see earlier chapters), it is possible to look at deforestation trends in Brazil in relation to population growth. The remote sensing data were for the period 1975 and 1978/9. By simple change detection, an average annual rate can be computed. This rate was regressed against the 1980 rural population for each municipio in the Legal Amazon (IBGE 1980b). The results are shown in Figure 7.7. The coefficient of determination, r^2, is low. The apparent relationship to population density found by Allen and Barnes (1985) at the global level and Reis and Margulis for the Legal Amazon several years later is not apparent. It must be noted that although the correlation was weak, it was significantly different from zero (p less than 0.001). A better predictor might be the change in population. However, regressions computed using this independent variable was also poorly correlated with deforestation rates.

Simple regressions of this kind are difficult since various regions could be behaving independently, but still be well correlated within the region. That is, different regions could have different, but internally consistent linear relationships and this would not show up when viewed collectively. Therefore, we performed a simple Rank (Spearman's) correlation. The results are shown in Table 7.5. Again there appears no strong correlation.

Explanation and Causality

The regression approaches are straightforward, and present a promising approach for prediction over short time periods (cf. to design a remote sensing sampling scheme), but do not provide a causal explanation for the explosive rates of deforestation in the Amazon. Hecht (1983, 1989) studied cattle ranching in the Amazon and concluded that government policies, fiscal incentives, and the nature of individual farmer decision-making in an inflationary economy (i.e., cattle are a good hedge against uncertain economic conditions) control deforestation rate more than demographic considerations. She argues that "it is ludicrous to describe environmental degradation in this situation as only a function of demographics." This view is shared by others who have studied the situation in the Amazon (Browder 1988). A similar view has come out of recent studies of declining wood stocks in sub Saharan Africa (Anderson 1986, Anderson and Fishwick 1984). In these case studies population growth is seen as part of a multiple feedback system, where it is as much a consequence of poverty and land degradation as it is a cause.

Nonetheless, we believe it is useful to develop explanatory conceptual framework which links to demographic and "modernization" factors, some of which we have already discussed (i.e., rural to urban migration, increasing substitution of machinery for labor in a rapidly developing industrial economy). In this next section we present a conceptual model which relates deforestation, and its concomitant release of carbon dioxide, with demography and spatial organization. We focus on Rondonia as a case study.

Deforestation in Rondonia, 1970-1980

The highest deforestation density is in the state of Rondonia, where 13% of the forests have been cleared as of 1988 (Fearnside 1990b, INPE 1992). The state of Rondonia has experienced nearly exponential deforestation rates over the last 30 years as new colonization and settlement and programs opened large tracts of forest. These settlement programs, as well as specific fiscal incentives were established in the 1970s as a way to encourage migration to the region from overpopulated, poverty-stricken, and drought-ridden regions in the south and northeast of the country. It was once suggested that Rondonia and other colonization "poles" in the state of Para were oriented for "people without land in a land without people" (Moran 1981). The vast Amazonia was seen by many as an empty frontier, which at once could be consolidated under Brazilian national sovereignty and provide opportunity for millions of poor and landless (Bunker 1984b).

In my view of this, deforestation in Rondonia is the result of changing demographic and economic conditions in the south of Brazil, particularly the state of Parana, during the period. We will focus my discussion on changes in the state of Parana in the early 1970s and explore how changes in land tenure and land use there directly influenced land use in Rondonia. But first it is important to consider certain international activities which were taking place at the time, particularly related to world oil production, distribution, and price.

The Flood of Petro-dollars

After the OPEC-stimulated increase in the price of oil in the mid 1970s, large amounts of what have been called petro-dollars flooded international money markets. This is discussed by Pool and Stamos (1987). The price of oil went from $1.30 a barrel in 1970 to $10.72 per barrel in 1975 and to $28.67 by 1980. Most energy-dependent countries paid OPEC prices, resulting in a large net transfer of wealth from industrial economies to OPEC. OPEC, in turn, deposited these revenues in U.S. and European banks. Since banks must pay dividends or interest to depositors, U.S. commercial institutions were eager to find borrowers.

Developing countries such as Brazil were eager for foreign capital to fund economic development, modernization, and industrialization programs. Moreover, they also needed dollars to pay for oil (since oil is bought and traded in dollars). Brazil's strategy appears to be twofold: (a) reduce the amount of imported oil and develop their own sources from sugar cane alcohol, hydroelectricity, and domestic oil off-shore or in the Amazon (discussed above), (b) borrow heavily to finance domestic economic development programs, much of them oriented toward exports. One important development program in the 1970s was agricultural modernization, since it was viewed that agricultural products could provide a profitable export industry, which in turn would help pay for loans to modernize agriculture and the rest of the country (Mahar 1989).

Agricultural Modernization in Brazil in the 1970s[2]

Between 1970 and 1980 there was large-scale investment in agriculture. Figure 7.8 shows an index of crop credits in Brazil since 1970. It increases almost five-fold (World Bank 1982). We have no direct data which shows the amount of these credits derived from foreign loans. It is probably safe to suggest that the deployment of credits was an effort to build an active agricultural export system, this being done to balance foreign debt and offset the rising cost of petroleum (World Bank 1982). Such investment did however require large amounts of capital from abroad. Such investment programs resulted in some degree of success; rising crop credits produced increasing crop output; the net value of agricultural output increased 2.7-fold between 1970 and 1980. By 1977 more than 50% of the total value of principal crops were accounted for by export crops.

Figure 7.9 shows the distribution of crop credits by crop type. Three general patterns emerge. First, the export crops of wheat, soybeans, and coffee consumed almost half of all crop credits. Second, the largest fraction was invested in soybean production. And third, very little of the credits were allocated to local food crops such as black beans and manioc.

[2] Unless otherwise cited, agricultural and economic statistics in this section came from primary census sources: IBGE 1989; IBGE 1981; IBGE 1975; IBGE 1970.

Soybean production was a major success story. The area harvested increased 6-fold in the 1970s, ten times more than any other crop except oranges and wheat; yields increased five-fold. The combination of land, fertilizers, improved seeds, and government-sponsored fiscal credits and incentives resulted in producing an internationally competitive export program. Soybeans became one of Brazil's major export crop. Figure 7.10 shows Brazil's changing share of world trade in soybean meal. From a small producer at 10% of the international markets, Brazil was able to compete with the United States by 1980.

One reason for Brazil's competitiveness in the soybean market might be related to comparative costs of production. Table 7.6 shows production costs for soybean production in Brazil compared to the United States, the world's leading exporter in the early 1970s. As might be expected the cost of fertilizers and pesticides in Brazil is higher than in the U.S., reflecting poorer growing conditions. In fact, total variable costs are higher for soybeans grown in Brazil. Contrary to popular belief, the comparative advantage does not lie in labor costs, since they are nearly the same. The key difference lies in fixed costs, particularly land. Land costs in the Brazilian soybean production system are half the land costs in the U.S. Thus, actual production costs are lower for Brazilian soybeans than U.S. beans. But because commercialization costs (the "middle man") are much higher in Brazil, total port costs are slightly higher. The conclusion is that Brazilian soybeans could be produced at highly competitive prices, primarily because of Brazil's competitive advantage in having relatively low land values.

Most of the soybean production was concentrated in two states: Rio Grande do Sul and Parana. The history of soybean cultivation during this period is interesting. Figure 7.11 shows the trend in area planted in some important crops in Parana during this period. Soybean production (and wheat) replaced coffee as the major crop in the region. Unlike soybeans, the international market for coffee was highly variable and undependable. Government programs concentrated on replacing coffee fields with soybeans (World Bank 1982).

Agricultural Modernization and Demographic Change

Just as the industrial sector was modernizing, so was agriculture as discussed above. A labor-intensive agricultural system was being transformed into an important energy- and machinery-intensive component of the national economy, particularly in Parana. Land prices rose significantly (World Bank 1982), as it was consolidated into larger holdings. Coffee, a labor intensive crop, was replaced by soybeans and wheat which utilize machinery. This transformation of land use changed land tenure. Figure 7.12 shows the change in farm size distribution in Parana. It shows a loss of small farms and an increase in very large farms.

It has already been noted that the period 1970-1980 saw increased migration from rural to urban areas. Part of this migration was in response to "pull" factors as industrial development created increased opportunities for wages in urban areas. As well, commercialization of agriculture in Parana shifted the mode of production from labor to machinery, creating a "push" factor. Looking at Figure 7.2 presented earlier we see that large numbers of people left the state of Parana during this period, the out-migration rate was higher than any other state.

Undoubtedly, many, if not most, of the migrants left for urban areas, which would be in keeping with what we found earlier. But a large number also went to new opportunities in the Rondonia frontier (Hecht 1989).

Effect on Deforestation in Rondonia State

Much has been made of the large-scale government programs to facilitate the opening of the frontier (e.g., Mahar 1989, Moran 1981, Bunker 1984b, Fearnside 1990a), and the various reasons for doing so, which range from the military-oriented view of the need to consolidate the hollow frontier to the need to provide a population safety valve. Indeed there were a number of reasons for opening the Rondonia frontier. The long-term drought in the northeast certainly played prominently. Moreover, much has been made of the massive road building projects, suggesting it to be the key determinant of change in the region. All of these factors must be considered, but must be view largely as mechanisms which facilitated a transformation which had more fundamental underpinnings.

Clearly, migration to the region was largely a response to events and conditions far removed from Rondonia. They involve changes in land tenure in the south of Brazil, and changes in the structure of rapidly developing national economy which was fueled to a large degree by excess petro-dollars. The demographic trends discussed in the earlier sections, and which influence the nature of fossil fuel energy use are related to the processes which have also stimulated deforestation and biomass burning in the Amazon.

Conclusions

The deforestation of Amazonia is exemplary of the challenges encountered in trying to link human driving forces through land use change to land cover change. It demonstrates that:

1) The land use change which drives land cover change is closely tied to a variety of interrelated human factors, some of which may be spatially distant from the area affected.

2) In the Amazon, the processes involved in land cover and land use change operate across many spatial scales.

3) An understanding of land cover change would be incomplete (e.g., leading to inadequate projections) if its causes were sought only in the proximate sources of change or in forces operating within the region in question (e.g., land clearance or population growth). In this case, events in the international economy influenced the course of deforestation in the Brazilian Amazon.

4) Simple correlations between human causes and land cover consequences found at the global aggregate scale cannot be expected to appear at sub-global scales.

Table 7.1. Total population and its rural and urban components in Brazil from 1950 to the present, with a projection to the year 2000. All values are millions of individuals. Values in parantheses represent the average annual growth rate.

Year	Total Population	Urban Population	Fraction Urban	Rural Population	Fraction Rural
1950	51.94	18.78	36%	33.16	64%
1960	70.19 (3.5%)	31.30 (6.7%)	45%	38.77 (1.7%)	55%
1970	93.14 (3.3%)	52.08 (6.6%)	56%	41.05 (0.6%)	44%
1980	120.14 (2.8%)	80.43 (5.4%)	67%	38.57 (-0.6%)	33%
1990	150.37 (2.5%)	112.74 (4.0%)	75%	37.62 (-0.3%)	25%
2000	179.49 (1.9%)	143.11 (2.7%)	80%	36.38 (-0.3%)	20%

Table 7.2. Urban and rural total fertility rate, 1950 to 1980 in Brazil, by state.

STATE	1950	1960	1970			1980		
			Total	Urban	Rural	Total	Urban	Rural
BRAZIL	6.21	6.28	5.76	4.55	7.74	4.35	3.63	6.40
1. Rondonia	-	-	9.72	8.90	10.77	6.18	5.59	6.82
2. Acre	-	-	9.90	7.56	10.97	6.88	5.03	8.81
3. Amazonas	8.44	9.07	8.55	6.67	10.18	6.75	5.47	9.38
4. Roraima	-	-	8.57	7.44	9.65	6.05	5.87	6.45
5. Pará	7.48	7.99	7.72	6.34	9.12	6.31	5.04	7.78
6. Amapá	-	-	8.24	7.88	8.58	6.97	5.70	9.03
7. Maranhão	6.86	7.11	7.26	7.07	7.36	6.93	5.88	7.40
8. Piaui	8.10	7.78	7.84	7.06	8.23	6.54	5.09	7.80
9. Ceará	7.88	7.53	7.74	6.46	8.80	6.05	4.91	7.75
10. R.G. do Norte	8.31	8.21	8.44	7.19	9.81	5.67	4.73	7.45
11. Paraiba	8.07	7.58	7.74	6.53	8.78	6.19	5.13	7.65
12. Pernambuco	7.17	7.18	7.03	6.04	8.45	5.40	4.35	7.59
13. Alagoas	7.25	7.33	7.58	6.42	8.46	6.67	5.23	8.39
14. Sergipe	7.44	7.24	7.87	6.43	9.29	6.03	4.72	8.05
15. Bahia	7.39	7.32	7.48	6.37	8.41	6.23	5.13	7.57
16. Minas Gerais	7.56	7.69	6.17	4.97	7.79	4.31	3.70	5.95
17. Espirito Santo	7.19	7.63	6.44	5.01	7.89	4.28	3.77	5.50
18. Rio de Janeiro	4.38	4.53	3.80	3.50	6.94	2.94	2.82	4.79
19. São Paulo	4.65	4.87	3.94	3.56	6.06	3.24	3.11	4.59
20. Paraná	6.27	6.51	6.40	4.72	7.64	4.12	3.53	5.23
21. Santa Catarina	7.23	7.30	6.10	4.75	7.32	3.82	3.39	4.60
22. R.G. do Sul	5.22	5.11	4.29	3.40	5.62	3.11	2.86	3.78
23. Mato Grosso	6.99	6.57	6.75	5.35	8.06	4.70	4.23	5.69
24. Goiás	6.72	6.77	6.46	5.21	7.54	4.73	4.02	6.14
25. Distrito Federal	-	6.85	5.56	5.47	8.77	3.62	3.54	7.34

Table 7.4. Rural and urban population growth rate (per 100 inhabitants) from 1950 to 1980 in Brazil, by state.

STATE	1950-1960			1960-1970			1970-1980		
	Total	Urban	Rural	Total	Urban	Rural	Total	Urban	Rural
BRASIL	2.99	5.15	1.55	2.89	5.22	0.57	2.48	4.44	0.62
1. Rondonia	6.39	7.99	5.44	4.76	7.03	2.66	16.03	14.39	17.69
2. Acre	3.20	4.32	2.94	3.13	6.13	2.20	3.42	8.34	0.81
3. Amazonas	3.33	5.30	2.33	3.03	5.71	1.45	4.12	7.76	0.43
4. Roraima	4.65	8.84	2.17	3.75	3.71	3.78	6.83	10.80	2.66
5. Pará	3.11	4.61	2.18	3.55	5.21	2.28	4.62	5.02	4.25
6. Amapá	6.14	9.44	3.35	5.37	6.02	4.65	4.36	5.21	3.26
7. Maranhão	4.50	4.68	4.42	1.94	5.59	0.98	2.93	5.26	2.04
8. Piaui	1.69	5.20	0.88	3.07	6.51	1.81	2.44	5.28	0.82
9. Ceará	2.96	4.84	0.85	2.84	4.94	1.62	1.95	4.67	0.41
10. R.G. do Norte	1.65	5.28	0.04	3.07	5.59	1.26	2.05	4.22	0.37
11. Paraiba	1.52	4.25	0.36	1.76	3.69	0.58	1.52	3.76	0.44
12. Pernambuco	1.86	4.49	0.19	2.34	4.41	0.35	1.76	3.02	0.04
13. Alagoas	1.38	3.85	0.37	2.36	4.16	1.33	2.24	4.45	0.51
14. Sergipe	1.54	3.47	0.50	1.82	3.66	0.49	2.38	4.05	0.74
15. Bahia	2.01	4.90	0.80	2.38	4.26	1.26	2.35	4.21	0.84
16. Minas Gerais	2.33	5.09	1.04	1.49	4.65	1.10	1.54	4.01	2.08
17. Espirito Santo	3.51	6.52	1.92	2.11	6.66	0.47	2.38	6.00	1.82
18. Rio de Janeiro	3.46	4.31	0.85	3.13	4.25	2.46	2.30	2.75	1.63
19. São Paulo	3.39	5.17	1.00	3.33	5.94	3.10	3.49	4.51	2.04
20. Paraná	7.16	9.31	6.33	4.97	6.73	4.10	0.97	5.97	3.32
21. Santa Catarina	3.04	6.28	1.86	3.20	6.34	1.38	2.26	5.63	1.16
22. R.G. do Sul	2.54	5.20	0.84	2.19	4.08	0.41	1.55	3.99	2.08
23. Mato Grosso	4.29	6.69	4.64	6.12	7.13	5.26	6.64	13.97	2.80
24. Goiás	4.62	8.73	3.22	4.38	7.96	2.43	2.76	6.86	1.53
25. Distrito Federal	-	-	-	14.39	19.31	8.46	8.15	8.24	5.88

Table 7.4. Area of deforestation in closed forests in 1978 and 1988, and the average annual deforestation rate for individual states in the Legal Amazon.

State	1978 (km^2)	1988 (km^2)	Rate per Year	Change
Rondonia	6,266	24,416	1,819	3.81
Acre	2,550	6,149	360	2.41
Amazonas	2,344	11,730	939	5.00
Roraima	208	1,953	174	9.39
Para	29,573	96,236	6,666	3.25
Amapa	233	260	27	1.12
Maranhao	10,811	38,653	2,784	3.58
Mato Grosso	11,895	55,717	4,382	4.68
Tocantins	3,652	15,968	1,232	4.37
Legal Amazon	**67,532**	**251,082**	**18,383**	**3.72**

Table 7.5. Correlation matrixes for population and deforestation variables.

(a) Simple Correlation

	POP	POPDEN	DEFOR	DELTA	DELDEN	DEDEN
POP	1.0000					
POPDEN	0.6695	1.0000				
DEFOR	0.2928	-0.0290	1.0000			
DELTA	0.2873	-0.0513	0.9679	1.0000		
DELDEN	0.0379	0.0965	0.3058	0.3241	1.0000	1.0000
DEDEN	0.1908	0.3011	0.3551	0.3208	0.8955	

(b) Spearman's Rank Correlation

	POP	POPDEN	DEFOR	DELTA	DELDEN	DEDEN
POP	1.0000					
POPDEN	0.6077	1.0000				
DEFOR	0.4463	0.2656	1.0000			
DELTA	0.3875	0.2497	0.9654	1.0000		
DELDEN	0.2151	0.5904	0.7170	0.7591	1.0000	
DEDEN	0.2817	0.6088	0.7805	0.7689	0.9646	1.0000

Legend:

POP = Total population in 1980
POPDEN = Population density in 1980
DEFOR = Total deforested area in 1980
DELTA = Deforestation rate 1975-1978
DELDEN = Deforestation rate expressed as a fraction of total area
DEDEN = Fraction of area forested (deforestation density)

Table 7.6. A comparison of the costs of crop production in Brazil and the United States: Soybeans. (Units are arbitrary but have been corrected for exchange rates.)

	U.S.	Brazil
1. Variable Costs		
Machinery	737	672
Labor	457	241
Inputs	964	2,299
Other	62	404
Subtotal	2,220	3,617
2. Fixed Costs		
Depreciation	781	427
Interest on capital	293	141
Labor	449	170
Land	2,029	937
Other	365	51
Subtotal	3,315	1,727
3. Total Costs per ha	6,136	5,343
4. Yield (kg/ha)	1,900	1,920
5. Unit Costs (per ton)	3,229	2,783
6. Port Costs	3,368	3,882

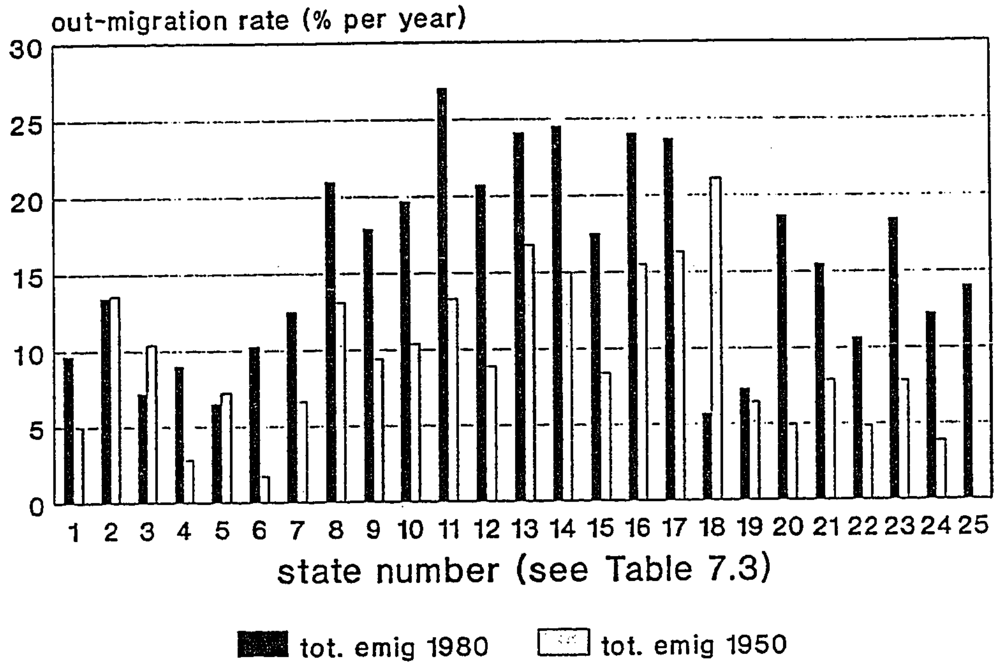

Figure 7.1. Out-migration rates in 1980 and 1950 for the states of Brazil. See Table 7.3 for for state names corresponding to the numbers on the figure. (Units are %.)

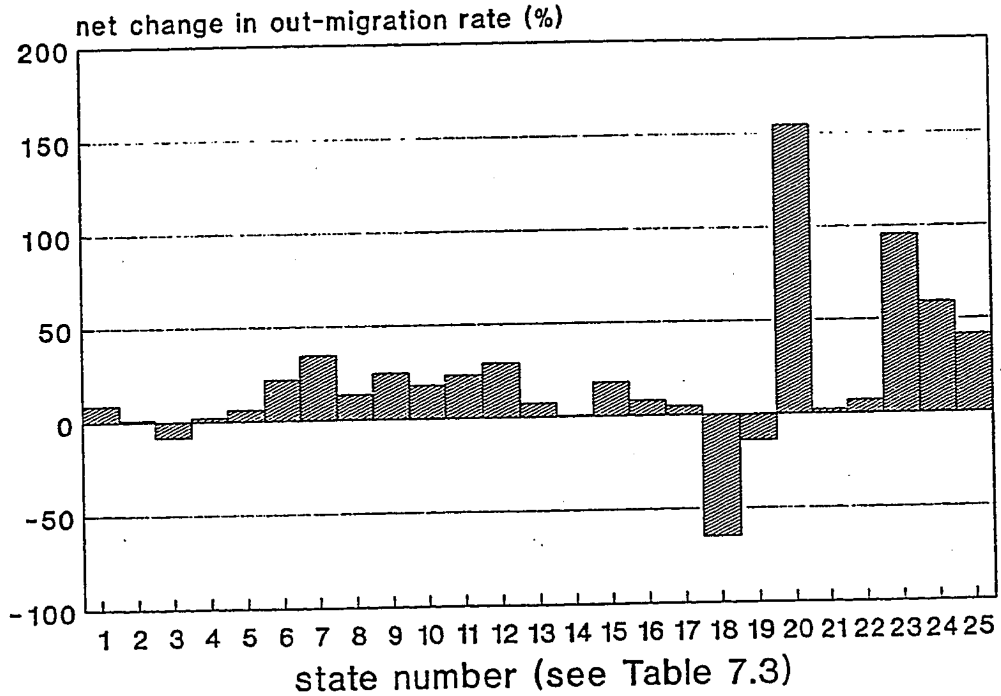

Figure 7.2. Net change in the out-migration rates for each state in Brazil between 1970 and 1980. (Units are % change.)

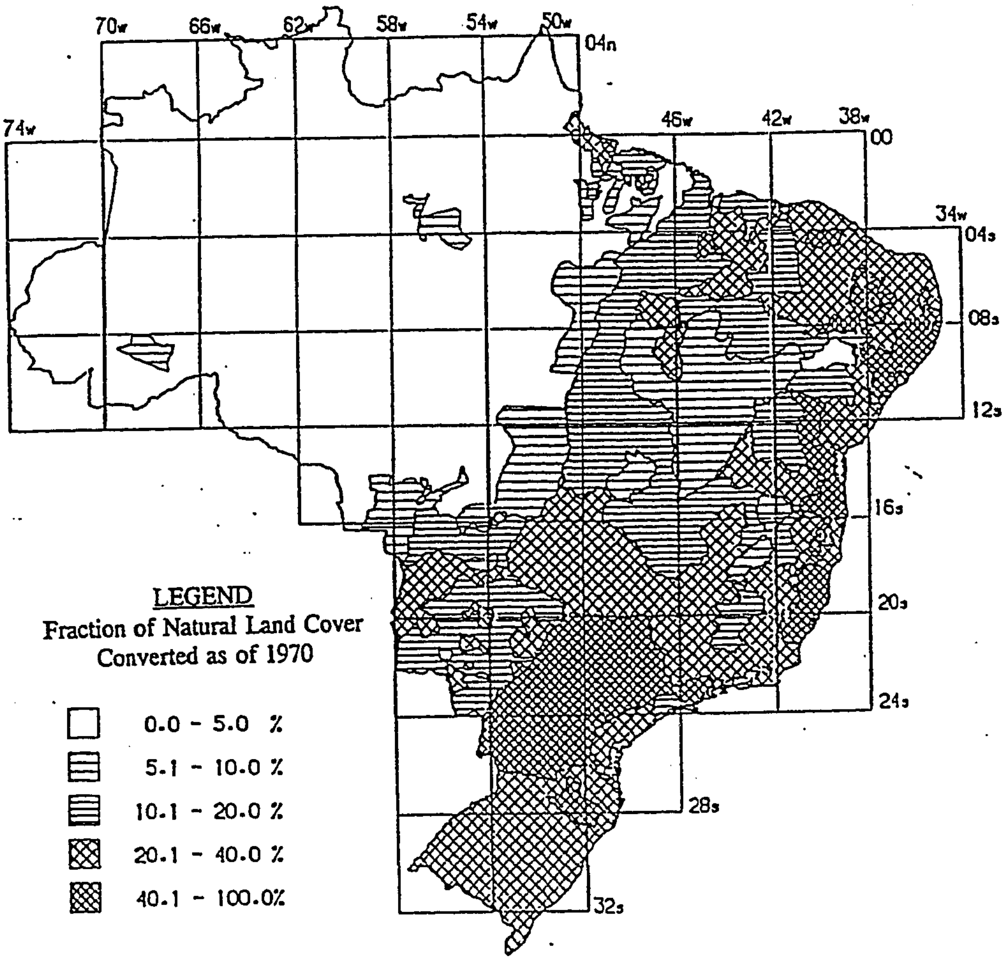

Figure 7.3. The results of mapping tabular data in a geographic information system to estimate the geographic extent of land cover conversion in Brazil in (a) 1970, (b) 1975, and (c) 1980. Legend shows the fraction (%) of natural land cover converted to human use for each date.

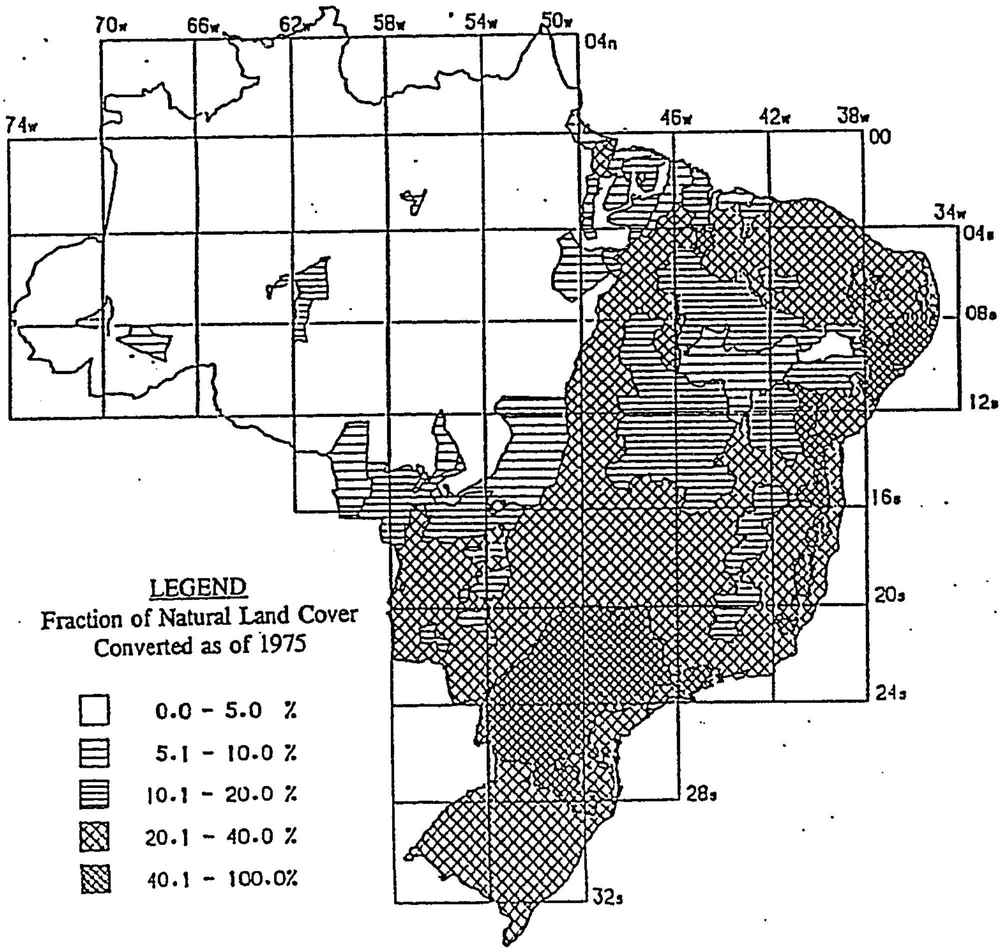

Figure 7.3b. The results of mapping tabular data in a geographic information system to estimate the geographic extent of land cover conversion in Brazil in 1975. Legend shows the fraction (%) of natural land cover converted to human use for each date.

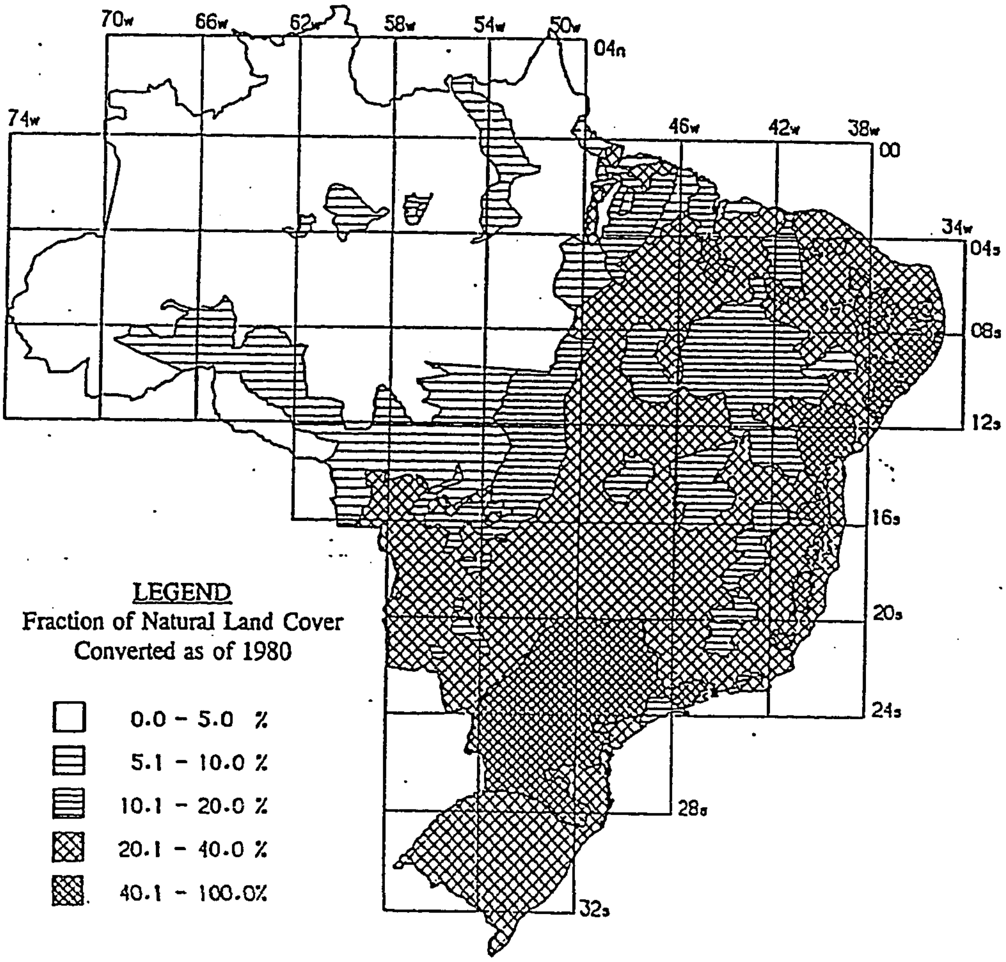

Figure 7.3c. The results of mapping tabular data in a geographic information system to estimate the geographic extent of land cover conversion in Brazil in 1980. Legend shows the fraction (%) of natural land cover converted to human use for each date.

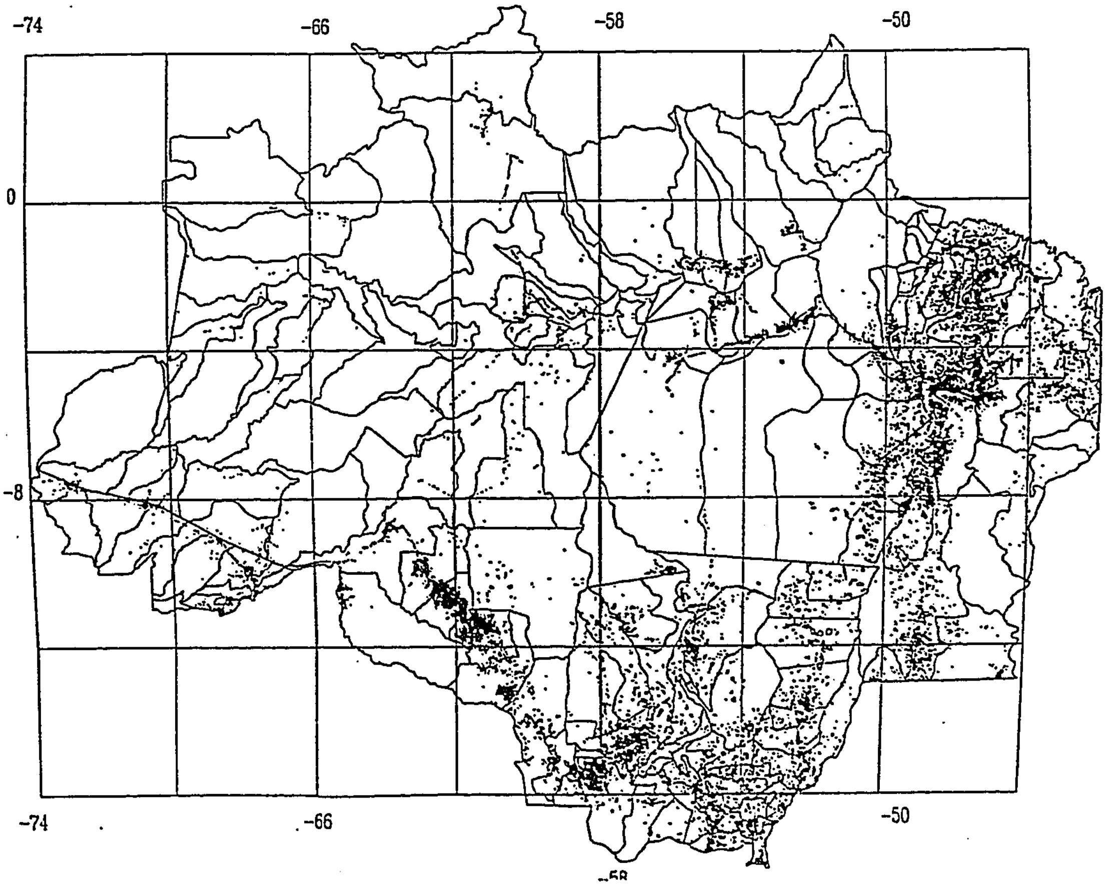

Figure 7.4. A geographically-referenced dataset of deforestation in the Legal Amazon of Brazil for 1978. This dataset was compiled in a geographic information system from 1:500,000 scale maps but has been greatly reduced in size here. The dark areas show areas deforested between 1975 and 1978.

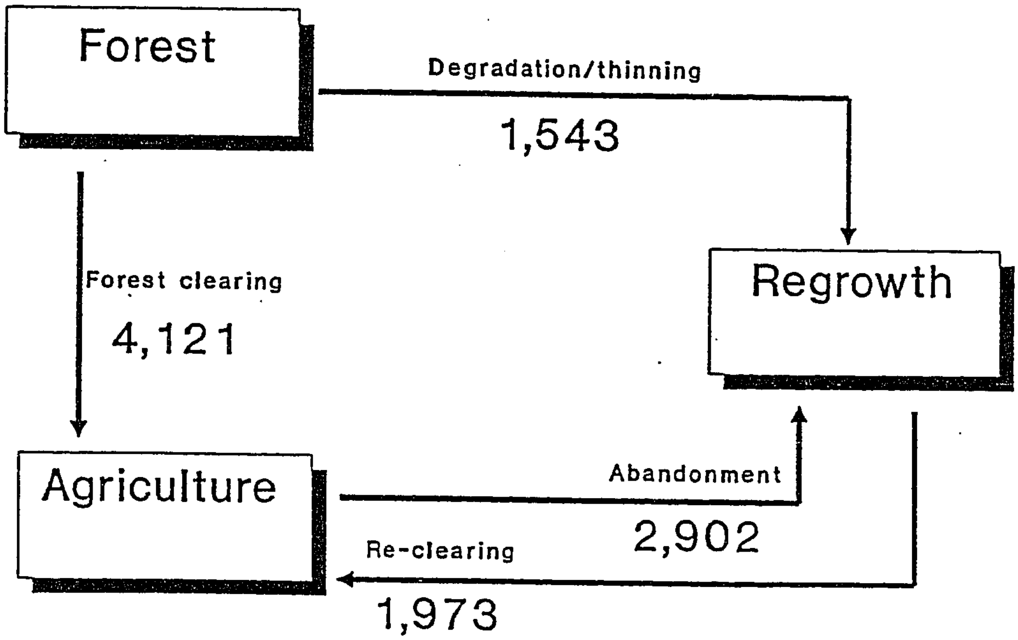

Figure 7.5. Land cover transformations in a test site in the Amazon (see Chapter 5) between 1986 and 1988. (Units are hectares per year.)

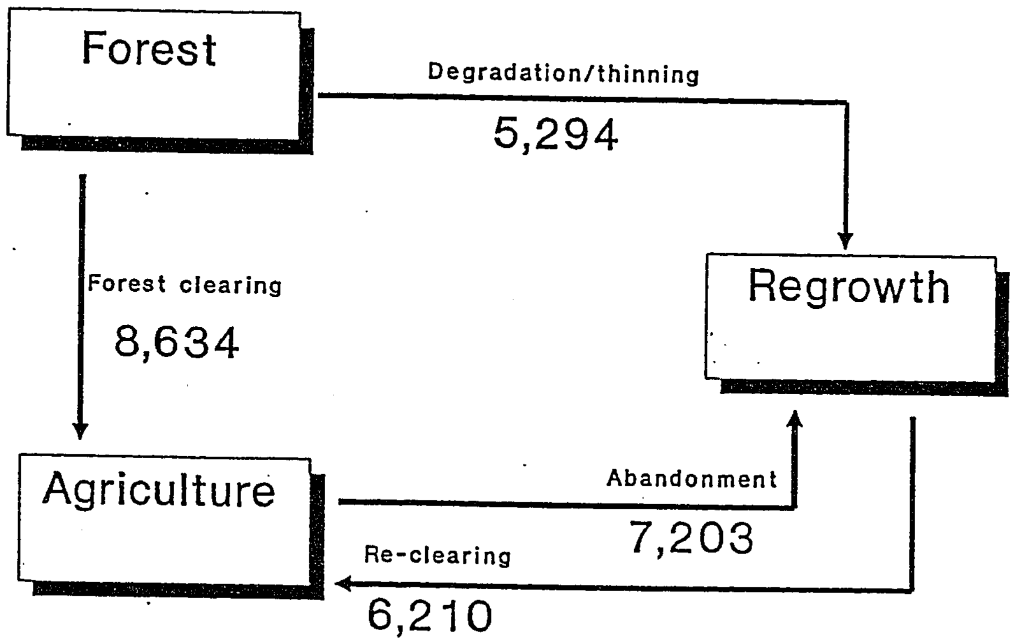

Figure 7.6. Land cover transformations in a test site in the Amazon (see Chapter 5) between 1988 and 1989. (Units are hectares per year.)

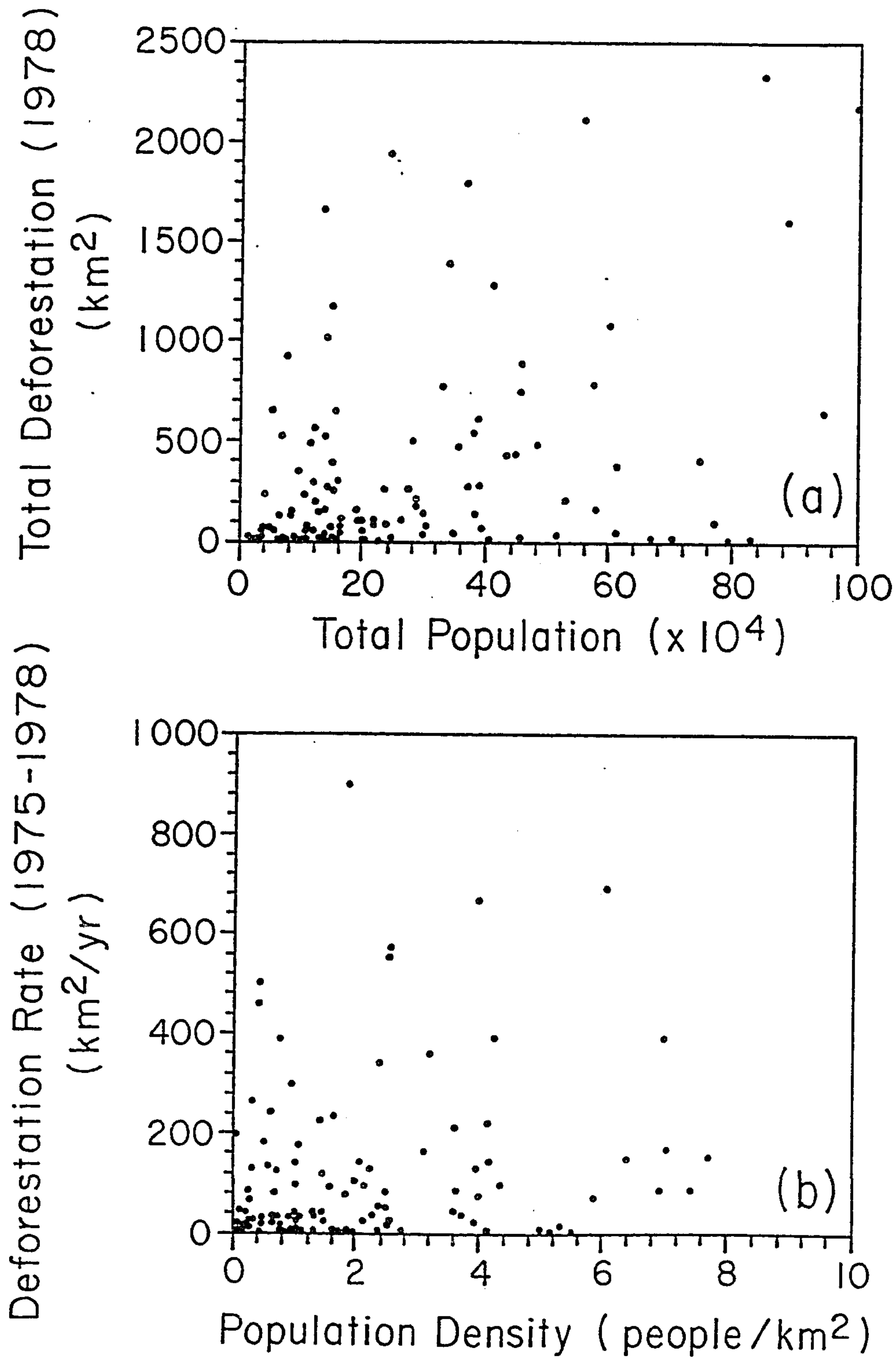

Figure 7.7. There appears to be no relationship between deforestation and population density. Scatter plots of population against total area deforested in 1978 (a) and population density against the deforestation rate in 1978 (b).

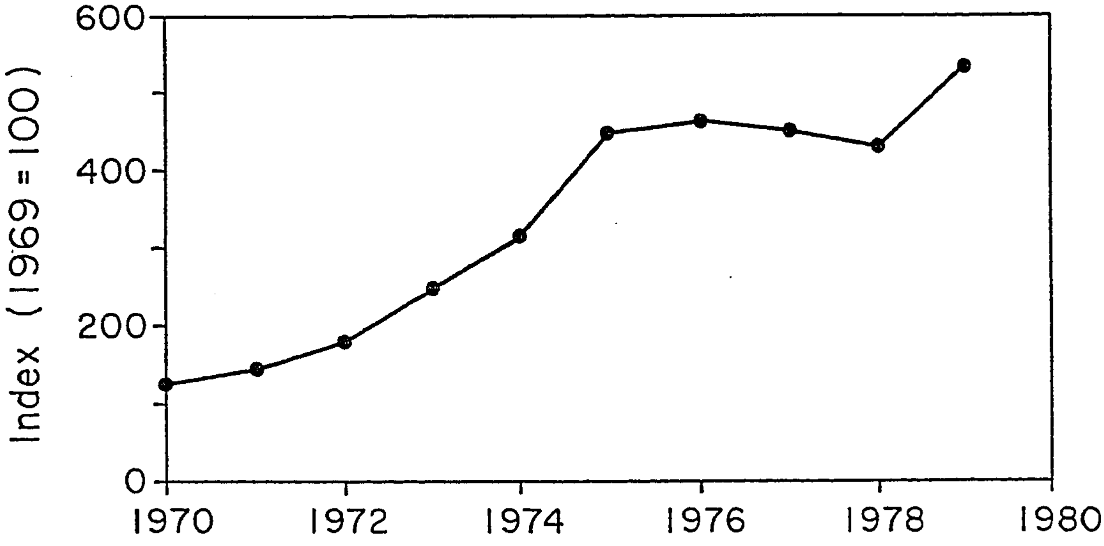

Figure 7.8. Change in the amount of crop credits provided to the agricultural sector in Brazil between 1970 and 1979.

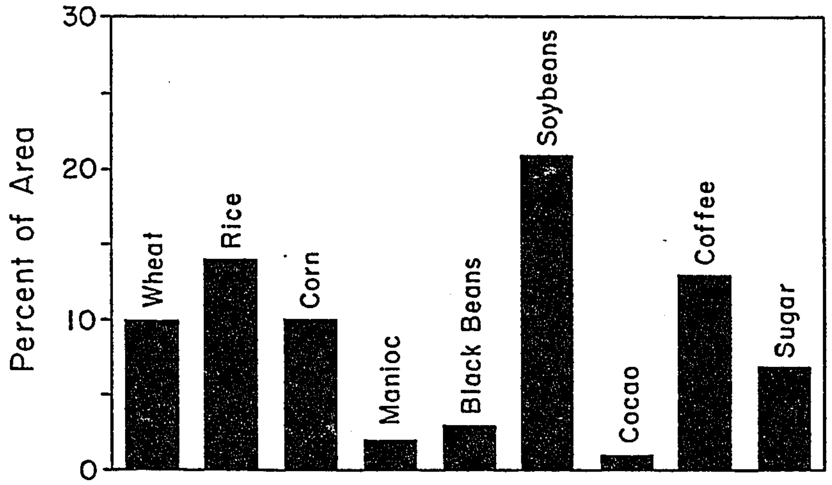

Figure 7.9. Allocation of crop credits in Brazil in 1978, as a percent of agricultural crop area.

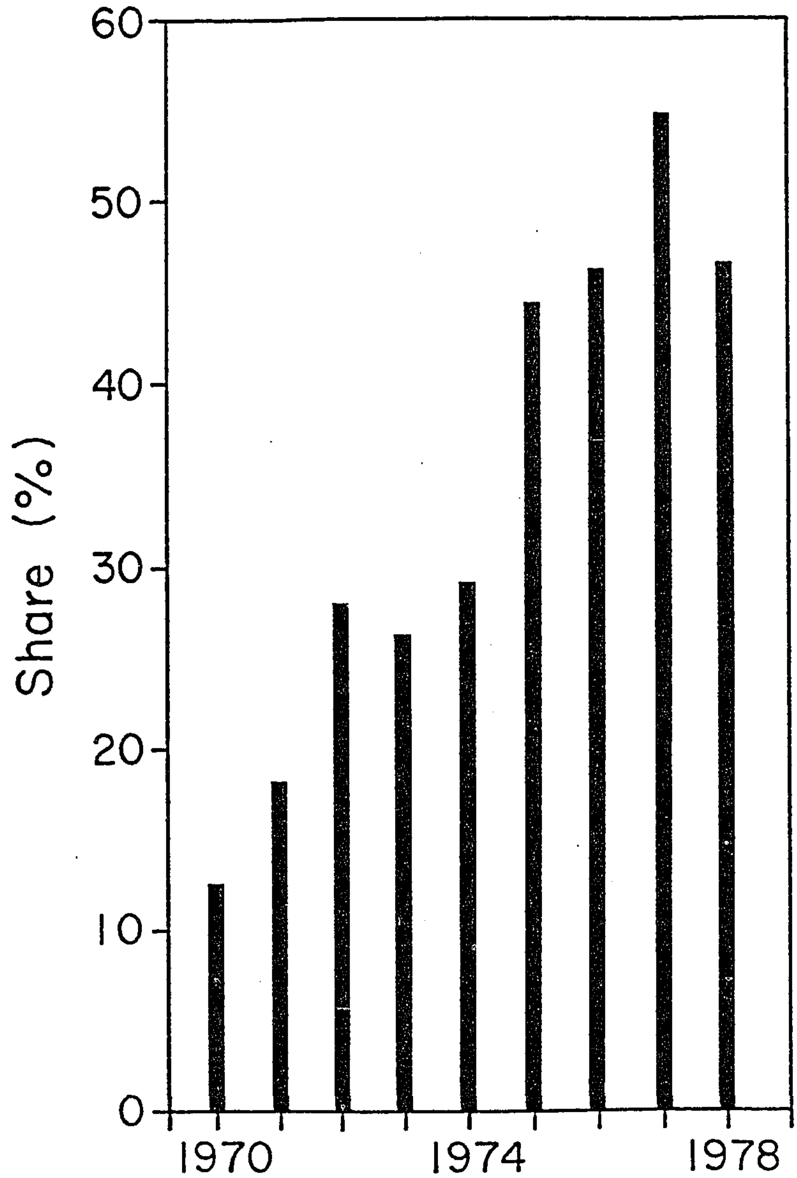

Figure 7.10. Brazil's share of the world soybean market from 1970 to 1978.

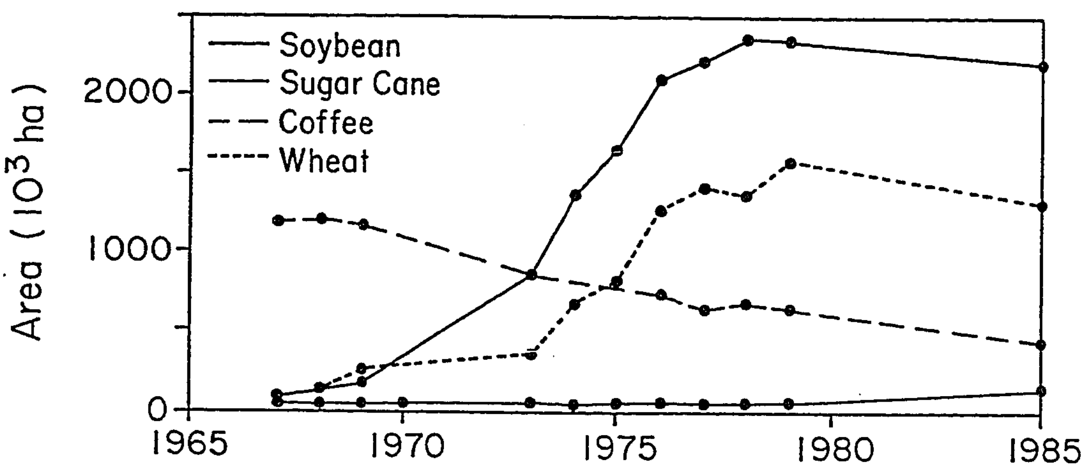

Figure 7.11. Change in area planted in major crops in Parana state between 1965 and 1985.

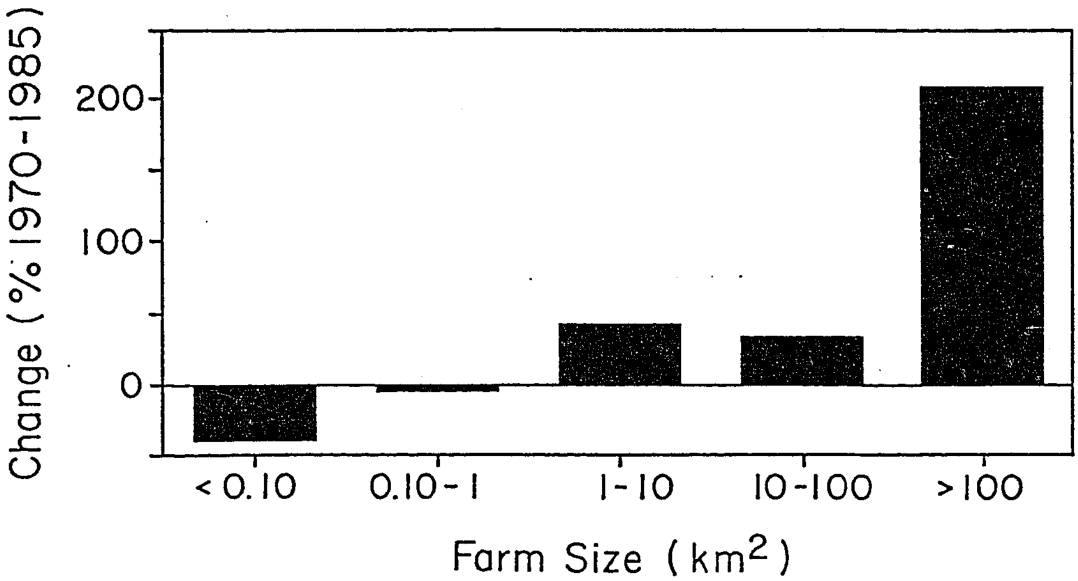

Figure 7.12. Change in the farm size distribution in Parana state between 1970 and 1985. Units are percent increase or decrease.

REFERENCES

Aber, J.D., J.M. Melillo, and C.A. McClaugherty. in press. Predicting long-term patterns of mass loss, nitrogen dynamics and soil organic matter formation from initial litter chemistry in forest ecosystems. Canadian Journal of Botany (in press).

Allen, J.C., and D.F. Barnes. 1985. The causes of deforestation in developing countries. Annals of the Association of American Geographers 75 (2) : 163-184.

Anderson, D. 1986. Declining tree stocks in African countries. World Development 14 (7) : 853-863.

Anderson, D., and R. Fishwick. 1984. Fuelwood Consumption and Deforestation in African Countries. Washington, D.C.: World Bank.

Andreae, M.O., E.V. Browell, M. Garstang, G.L. Gregory, R.C. Harriss, G.F. Hill, D.J. Jacob, M.C. Pereira, G.W. Sachse, A.W. Setzer, P.L. Silva Dias, R.W. Talbot, A.L. Torres, and S.C. Wofsy. 1988. Biomass-burning emissions and associated haze layers over Amazonia, J. Geophys. Res. 93:1509-1527.

Berry, J.K. 1987. Computer assisted map analysis: potential and pitfalls, Photogrammetric Engineering and Remote Sensing, 53(10):1405-1410.

Boden, T.A., P. Kanciruk, and M.P. Farrell. 1990. Trends '90: A Compendium of Data on Global Change. Carbon Dioxide Information Analysis Center, Oak Ridge National Laboratory, ORNL/CDIAC-36.

Bolle, H.-J., W. Seiler, B. Bolin. 1986. Other greenhouse gases and aerosols, In, B. Bolin, B.R. Doos, J. Jager, R.A. Warrick (eds.) The Greenhouse Effect, Climate Change, and Ecosystems, SCOPE 29, John Wiley and Sons, 541 pp.

Bolin, B. 1977. Changes of land biota and their importance for the carbon cycle, Science 196(4290):613-615

Bolin, B. 1984. Global biogeochemical cycles: studies of interaction and change - some views on the strategy of approach. In Moore, B. and M. Dastoor (ed) The Interaction of Global Biogeochemical Cycles, JPL Publications 18-24, Pasadena, CA, pp.25-51.

Blake, D.R. 1984. Increasing concentrations of atmospheric methane, 1979-1980. Ph.D thesis, University of California, Irvine.

Bracken, I. and C. Webster. 1989. Toward a typology of geographical information systems. International Journal of Geographic Information Systems, 3(2):137-152

Browder, J.O. 1988. Public policy and deforestation in the Brazilian Amazon. In Public Policies and the Misuse of Forest Resources. Edited by R. Repetto and M. Gillis. New York: Cambridge University Press.

Brown, S., and A.E. Lugo. 1982. The storage and production of organic matter in tropical forests and their role in the global carbon cycle. Biotropica 14(3):161-187.

Brown, S., and A.E. Lugo. 1984. Biomass of tropical forests: A new estimate based on volumes. Science 223:1290-1293.

Brown, S., and A.E. Lugo. 1990. Tropical secondary forests. J. Trop. Ecol. 6 : 1-32.

Brown, S., A.J.R. Gillespie, and A.E. Lugo. 1989. Biomass estimation methods for tropical forests with applications to forest inventory data. Forest Science, 35(4):881-902.

Bunker, S.G. 1984a. Modes of extraction, unequal exchange, and the progressive underdevelopment of an extreme periphery: the Brazilian Amazon, 1600-1980. American Journal of Sociology, 89(5):1017-1065.

Bunker, S.G. 1984b. Underdeveloping the Amazon: Extraction, Unequal Exchange, and the Failure of the Modern State. University of Illinois Press, Champaign.

Burrough, P.A. 1986. Principles of Geographic Information Systems for Land Resources Assessment, Oxford University Press, New York, 193 pp.

Buschbacher, R. 1986. Tropical deforestation and pasture development. BioScience 36 (1) : 22-28.

Buschbacher, R., C. Uhl, and A. S. Serrao. 1988. Abandoned pastures in eastern Amazonia. II. nutrient stocks in the soil and vegetation. Journal of Ecology 76 : 682-699.

Clements, F.E. 1916. Plant Succession. An Analysis of the Development of Vegetation. Carnegie Institute, Washington, D.C., 512 pp.

Cline-Cole, R.A., H.A.C. Main, and J.E. Nichol. 1990. On fuelwood consumption, population dynamics, and deforestation in Africa. World Development 18 : 513-527.

CNES. 1988. SPOT User's Handbook, SPOT Image Corporation, Reston, USA.

Colwell, R.N. 1983. Manual of Remote Sensing, American Society of Photogrammetry.

Comery, J.A. 1981. Elemental carbon deposition and flux from prescribed burning on a longleaf pine site in Florida. Masters thesis, University of Washington, Seattle.

Cross, A. 1990. AVHRR as a data source for a GIS: deforestation in Amazonia. IGARSS90 symposium, Washington, D.C.

Cross, A.M., J.J. Settle, N.A. Drake, and R.T.M. Paivinen. 1991. Subpixel measurement of tropical forest cover using AVHRR data. Int. Jour. Remote Sensing 12(5):1119-1129.

Crutzen, P.J. 1983. Atmospheric interactions - homogeneous gas reactions of C, N, and S containing compounds, In, Bolin, B. and R.B. Cook (eds.) The Major Biogeochemical Cycles and Their Interactions, SCOPE 21, John Wiley and Sons, 532 pp.

Crutzen, P.J. and M.O. Andreae. 1990. Biomass burning in the tropics: impact on atmospheric chemistry and biogeochemical cycles. Science 250:1669-1678.

Crutzen, P.J., L.E. Heidt, J.P. Krasnec, W.H. Pollock, and W. Seiler. 1979. Biomass burning as a source of the atmospheric gases CO, H_2, N_2O, NO, CH_3Cl and COS, Nature, 282:253-256.

Crutzen, P.J., A.C. Delany, J. Greenberg, P. Haagenson, L. Heidt, R. Lueb, W. Pollock, W. Seiler, A. Wartburg and P. Zimmerman. 1985. Tropospheric chemical composition measurements in Brazil during the dry season, J. Atmos. Chem., 2, 233-256.

Dale, V.H. 1990. Report of a Workshop on Using Remote Sensing to Estimate Land Use Change. Oak Ridge, TN: Environmental Sciences Division, Oak Ridge National Laboratory, publication 3397, ORNL/TM-11502.

Dale, V.H., R.A. Houghton, and A.S. Hall. 1991. Estimating the effects of land-use change on global atmospheric CO_2 concentrations. Canadian Journal of Forest Research 21 (1) : 87-90.

Detwiler, R.P., and C.A.S. Hall. 1988. Tropical forests and the global carbon cycle. Science 239 : 42-47.

Dickinson, R.E. 1981. Effects of tropical deforestation on climate. In Studies in Third World Societies. 515 pp. Publication 14, Department of Anthropology, College of William and Mary.

Dunn, R., R. Harrison, and J.C. White. 1990. Positional accuracy and measurement error in digital databases of land use: an empirical study. Int. J. Geographical Information Systems 4 (4) : 385-398.

Ehrlich, P.R., and A.H. Ehrlich. 1990. The Population Explosion. New York: Simon and Schuster.

Ehrlich, P.R., and J.P. Holdren. 1971. The impact of population growth. Science 171 : 1212-1217.

Ehrlich, P. R., and E. O. Wilson. 1991. Biodiversity studies: science and policy. Science 253 : 758-762.

Eiten, G., The cerrado vegetation of Brazil, Bot. Rev., 38, 201- 341, 1972.

Emanuel, W.R., B. Moore, and H.H. Shugart, 1984, Some aspects of understanding changes in the global carbon cycle, In: Moore, B., and Dastoor, M.N. (eds.), The Interaction of Global Chemical Cycles, National Aeronautics and Space Administration, JPL Publication 84-21

Emanuel, W.R., I. Fung, G.G. Killough Jr., B. Moore III, T.-H. Peng, 1985. Modeling the global carbon cycle and changes in atmospheric carbon dioxide levels. In, Trabalka, J.R. (ed) Atmospheric Carbon Dioxide and the Global Carbon Cycle, DOE/ER- 0239, U.S. Department of Energy, Washington, D.C.

ESRI. 1990. Introduction to Spatial Analysis: Spatial Manipulation and Analysis, and Understanding GIS: the ARC/INFO Method, Environmental Systems Research Institute, Inc., Redlands, California.

FAO. 1990. Interim Report on Forest Resources Assessment 1990 Project. Committee on Forestry, Tenth Session, Rome, Italy.

FAO. 1992. The Forest Resources of the Tropical Zone by Main Ecological Regions. Forest Resources Assessment 1990 Project, Food and Agriculture Organization, United Nations.

FAO/UNEP. 1981. Tropical Forest Resources Assessment Project. Forest Resources of Tropical America. FAO, Rome.

Fearnside, P.M. 1982. Deforestation in the Brazilian Amazon: how fast is it occurring? Interciencia 7 (2) : 82-88.

Fernside, P.M. 1983. Land use trends in the Brazilian Amazon region as factors in accelerating deforestation. Environmental Conservation 10(2):141-148.

Fernside, P., 1985. Brazil's Amazon forest and the global carbon problem, Interciencia 10(4): 179-186.

Fearnside, P.M. 1986. Spatial concentration of deforestation in the Brazilian Amazon. Ambio 15 (2) : 82-88.

Fernside, P.M., 1987a. Summary of progress in quantifying the potential contribution of Amazonian deforestation to the global carbon problem, In, Athie, Lovejoy, and Oyens (eds.), Proceedings of the Workshop on Biogeochemistry of Tropical Rainforests: Problems for Research, Universidade de Sao Paulo, CENA, Piracicaba, Sao Paulo, Brasil. 85 pp.

Fearnside, P.M. 1987b. Causes of deforestation in the Brazilian Amazon. In Dickinson, R.E. (ed.) The Geophysiology of Amazonia: Vegetation and Climate Interaction, Wiley - Interscience, New York, pp. 37-61.

Fernside, P.M. 1989. Burn quality prediction for simulation of the agricultural system of Brazil's Transamazon highway colonists. Turrialba 39(2):229-235.

Fearnside, P.M. 1990a. Deforestation in Brazilian Amazonia. In: G.M. Woodwell (ed), The Earth in Transition. Patterns and Processes of Biotic Impoverishment. Cambridge University Press. In Press.

Fearnside, P.M. 1990b. The rate and extent of deforestation in Brazilian Amazonia. Environmental Conservation 17:213-226.

Fearnside, P.M., A.T. Tardin, and L.G.M. Meira. 1990a. Deforestation rate in Brazilian Amazonia. Brasilia, Brazil: National Secretariat of Science and Technology.

Fearnside, P.M., A. Tardin, and L.G. Meira, 1990b. Deforestation in the Brazilian Amazon., National Secretariat of Science and Technology.

Field, C. and H.A. Mooney. 1986. The photosynthesis-nitrogen relationship in wild plants. In, T.J. Givinish, On the Economy of Plant Formation and Function. Cambridge University Press, New York.

Flint, E.P. and J.F. Richards. 1991. Historical analysis of changes in land use and carbon stock of vegetation in south and southeast Asia. Canadian Journal of Forest Research 21(1):91-110.

Fung, I.Y., C.J. Tucker, and K.C. Prentice, 1987. Application of advanced very high resolution radiometer vegetation index to study atmosphere-biosphere exchange of CO2. Journal of Geophysical Research, 92(D3):2999-3015.

Gash, J.H.C., and W.J. Shuttleworth. 1991. Tropical deforestation: albedo and the surface-energy balance. Climatic Change 19 (1-2) : 123-133.

Greenberg, J.P., P.P. Zimmerman, L.E. Heidt, and W. Pollock, 1984. Hydrocarbon and carbon monoxide emissions from biomass burnings in Brazil, Journal of Geophysical Research, 98:1350- 1354.

Goward, S.N., D.G. Dye, W. Dulaney, J. Yang. 1990. Critical assessment of the global vegetation index data product. In, Proceedings of the Workshop on the Use of Satellite-Derived Vegetation Indexes in Weather and Climate Prediction Models, Camp Springs, Md., February 26-27, 1990, U.S. Department of Commerce, National Oceanic and Atmospheric Administration.

Hall, F. G., D. B. Botkin, D. B. Strebel, K. D. Woods, and S. J. Goetz. 1991. Large-scale patterns of forest succession as determined by remote sensing. Ecology 72 (2) : 628-640.

Hao, W.M., M.H. Liu and P.J. Crutzen. 1990. Estimates of annual and regional releases of CO_2 and other trace gases to the atmosphere from fires in the tropics, based on the FAO statistics for the period 1975-1980. In, J.G. Goldamer (ed.) Fire in the Tropical Biota: Ecosystem Processes and Global Challenges. Ecological Studies, Vol. 84, Springer-Verlag, Berlin.

Harris, R.C., S.C. Wolfsy, M. Garstang, E.V. Browell, L.C.B. Molion, R.J. McNeal, J.M. Hoell Jr., R.J. Bendura, S.M. Beck, R.L. Navarro, J.T. Riley, and R.L. Snell. 1988. The Amazon boundary layer experiment (ABLE 2A): dry season 1985. Jour. Geophysical Research 93(D2):1351-1360

Hecht, S.B. 1983. Cattle ranching in the Eastern Amazon: environmental and social implications. In The Dilemma of Amazonian Development. Edited by E. Moran. Boulder: Westview Press.

Hecht, S.B. 1989. The Fate of the Forest. London: Verso.

Hecht, S.B. and A. Cockburn 1989. The Fate of the Forest, Verso, London. 266 pp.

Henderson-Sellers, A. 1987. Effects of change in land use on climate in the humid tropics. In, R.E. Dickinson (ed.) The Geophysiology of Amazonia, Vegetation and Climate Interactions. John Wiley and Sons, New York.

Henderson-Sellers, A. and V. Gornitz, 1984. Possible climatic impacts of land cover transformation, with particular emphasis on tropical deforestation. Climatic Change 6:231-256

Holben, B.N. and C.O. Justice, 1981. An examination of spectral band ratioing to reduce the topographic effect of on remotely sensed data. Int. J. Remote Sensing, 2, 115.

Holdridge, L. R. 1947. Determination of world formations from simple climatic data. Science 105: 367-368.

Holdridge, L. R. 1967. Life Zone Ecology. Tropical Science Center, San Jose, Costa Rica. 206 pp.

Houghton, R.A. 1986. Estimating changes in the carbon content of terrestrial ecosystems from historical data. In, J.R. Trabalka and D.E. Reichle (eds.), The Changing Carbon Cycle: A Global Analysis, Springer-Verlag, New York.

Houghton, R.A. 1991a. Releases of carbon to the atmosphere from degradation of forests in tropical Asia. Canadian Journal of Forest Research 21 (1) : 132-142.

Houghton, R.A. 1991b. Tropical deforestation and atmospheric carbon dioxide. Climatic Change 19 : 99-118.

Houghton, R.A. and D.L. Skole, 1990. Carbon, In. B.L. Turner (ed), The Earth Transformed by Human Action, Cambridge University Press.

Houghton, R.A., J.E. Hobbie, J.M. Melillo, B. Moore, B.J. Peterson, G.R. Shaver and G.M. Woodwell. 1983. Changes in the carbon content of terrestrial biota and soils between 1860 and 1980: a net release of CO_2 to the atmosphere. Ecol. Monogr. 53:235-262.

Houghton, R.A., W.H. Schlesinger, S. Brown, and J.F. Richards, 1985a. Carbon dioxide exchange between the atmosphere and terrestrial ecosystems. In, Trabalka, J.R. (ed) Atmospheric Carbon Dioxide and the Global Carbon Cycle, DOE/ER-0239, U.S. Department of Energy, Washington, D.C.

Houghton, R.A., R.D. Boone, J.M. Melillo, C.A. Palm, G.M. Woodwell, N. Myers, B. Moore, and D.L. Skole. 1985b. Net flux of CO_2 from tropical forests in 1980. Nature 316 (617-620)

Houghton, R.A., R.D. Boone, J.R. Fruci, J.E. Hobbie, J.M. Melillo, C.A. Palm, B.J. Peterson, G.R. Shaver, G.M. Woodwell, B. Moore, D.L. Skole, and N. Myers. 1987. The flux of carbon from terrestrial ecosystems to the atmosphere in 1980 due to changes in land use: Geographic distribution of the global flux. Tellus 39B:122-139.

Houghton, R.A., D.L. Skole, and D.S. Lefkowitz. 1991a. Changes in the landscape of Latin America between 1850 and 1985: II. a net release of CO_2 to the atmosphere. Journal of Forest Ecology and Management 38 : 173-199.

Houghton, R.A., D.S. Lefkowitz, and D.L. Skole. 1991b. Changes in the landscape of Latin America between 1850 and 1985 I. Progressive loss of forests. Forest Ecology and Management 38 : 143-172.

IBGE. 1960. Censo Agricola de 1960, VII recenseamento Geral do Brasil, Instituto Brasileiro de Geografia E Estatistica, Rio de Janeiro.

IBGE. 1970a. Censo Agropecuario, VIII Recenseamento Geral do Brasil, Instituto Brasileiro de Geografia E Estatistica, Rio de Janeiro.

IBGE. 1970b. Anuario Estatistico do Brasil - 1970b,Instituto Brasileiro do Geografia e Estatistica, Rio de Janeiro.

IBGE. 1970c. Censo Demografico, VIII Recenseamento Geral do Brasil, Instituto Brasileiro de Geografia E Estatistica, Rio de Janeiro.

IBGE. 1975. Anuario Estatistico do Brasil - 1975, Instituto Brasileiro do Geografia e Estatistica, Rio de Janeiro.

IBGE. 1979. Anuario Estatistico do Brasil - 1979, Instituto Brasileiro do Geografia e Estatistica), Rio de Janeiro.

IBGE 1980a. Censo Agropecuario - VII Recenseamento Geral do Brasil Instituto Brasileiro de Geografia E Estatistica, Rio de Janeiro.

IBGE. 1980b. Censo Agropecuario, IX Recenseamento Geral do Brasil, Instituto Brasileiro de Geografia E Estatistica, Rio de Janeiro.

IBGE. 1980c, Censo Demografico, IX Recenseamento Geral do Brasil, Instituto Brasileiro de Geografia E Estatistica, Rio de Janeiro.

IBGE. 1981. Anuario Estatistico do Brasil - 1981. Rio de Janeiro: Instituto Brasileiro de Geografia e Estatistica.

IBGE 1982a. Projecto Radambrasil, Amazonia Legal, Ministerio das Minas E Energia.

IBGE. 1982b. Synopse Preliminar do Censo Agropecuario, IX Recenseamento Geral do Brasil -1980, Fundacao Instituto Brasileiro de Geografia e Estatistica, Rio de Janeiro, Brasil.

IBGE. 1989. Anuario Estatistico do Brasil - 1989, Instituto Brasileiro do Geografia e Estatistica, Rio de Janeiro.

Instituto de Pesquisas Espaciais. 1989. Avaviacao da Alteracao da Coberta Florestal na Amazonia Legal Utilizando Sensoriamento Remoto Obital, Directoria de Sensoriamento Remoto, Sao Jose dos Campos.

INPE. 1992. Deforestation in Brazilian Amazonia. Instituto Nacional de Pesquisas Espaciais.

IPCC. 1992. Climate Change 1992: the Supplementary Report to the IPCC Scientific Assessment. Edited by J. T. Houghton, B. A. Callander and S. K. Varney. Intergovernmental Panel on Climate Change. Cambridge: Cambridge University Press.

John, D.M. 1973. Accumulation and decay of litter and net production of forest in tropical West Africa. Oikos 24:430-435.

Justice, C.O., J.R.G. Townshend, B.N. Holben, and C.J. Tucker. 1985. Analysis of the phenology of global vegetation using meteorological satellite data. International Journal of Remote Sensing 6 (8) : 1271-1318.

Kaufman, Y.J., A. Setzer, J. Justice, C.J. Tucker, M.G. Pereira, and I. Fung. 1990a. Remote sensing of biomass burning in the tropics. In Fire in the Tropical Biota. Edited by J. G. Goldammer. 371-399. Berlin: Springer-Verlag.

Kaufman, Y.J., C.J. Tucker, and I. Fung. 1990b. Remote sensing of biomass burning in the tropics. Journal of Geophysical Research 95 (D7) : 9927-9939.

Kauffmann, J.B., R.L. Sanford, E. Sampio, 1990c. Biomass burning in Brazilian tropical dry forest: carbon and nitrogen emissons, paper presented at the Chapman Conference on Biomass Burning, Atmospheric, Climatic, and BIospheric Implications, March 19-23, Williamsburg, VA. USA.

Keeling, C.D., R.B. Bacastow, A.F Carter, S.C. Piper, T.P. Whorf, M. Heimann, W.G. Mook, and H. Roeloffzen. 1989. A three-dimensional model of atmospheric CO_2 transport based on observed winds: 1. Analysis of observational data. In, D.H. Peterson (ed.) Aspects of Climate Variability in the Pacific and Western Americas, Geophysical Monograph 55:165-235

Keller, M., D. J. Jacob, S. C. Wofsy, and R. C. Harriss. 1991. Effects of tropical deforestation on global and regional atmospheric chemistry. Climatic Change 19 : 139-158.

Keyfits, N. 1991. Population and development within the ecosphere: one view of the literature. Population Index 57 (1)

Khalil, M.A.K., and R.A. Rasmussen, 1983. Sources, sinks, and seasonal cycles of atmospheric methane, Science, 224:54-56.

Kidwell, K.B., 1990. Global Vegetation Index Users Guide, National Environmental Satellite, Data, and Information Service, National Oceanic and Atmospheric Administration, Washington, D.C.

Kidwell, K.B. 1991. NOAA Polar Orbiter Data Users Guide. Washington, D.C.: National Environmental Satellite, Data, and Information Service, National Oceanic and Atmospheric Administration.

Kirchhoff, V.W.J.H, A.W. Setzer, M.C. Pereira, 1989. Biomass burning in Amazonia: seasonal effects on atmospheric O3 and CO, Geophysical Research Letters 16(5):469-472.

Klinge, H, W.A. Rodrigues, E. Brunig, and E.J. Fittkau, 1975 Biomass and structure of a central Amazonian rain forest. In, F.D. Golley and E. Medina (eds.) Tropical Ecological Systems: Trends in Terrestrial and Aquatic Research. Springer-Verlag, New York. 398 pp.

Koppen, W. 1936. Das geograpischa system der klimate. In, Koppen, W. and G. Geiger (eds.), Handbuch der Klimatologie, Vol. 1, Part C. Gebr. Borntraeger, Berlin.

Kuchler, A.W. 1949. A physiognomic classification of vegetation. Annals, Association of American Geographers, 39:201-210.

Lang, G.E. and D.H. Knight. 1979. Decay rates for tropical trees in Panama. Biotropica 11:316-317.

Lanly, J.P. 1982. Tropical Forest Resources. Food and Agricultural Organization of the United Nations, Rome. NTIS, 30.

Loveland, T.R., J.W. Merchant, D. Ohlen, and J.F. Brown. 1991. Development of a land-cover characteristics database for the Conterminous U.S. Photogrammetric Engineering and Remote Sensing, 11:1453-1463.

Maguire, D.J., M.F. Goodchild, and D.W. Rhind. 1991. Geographical Information Systems, Principles and Aapplications, John Wiley and Sons, New York.

Mahar, D.J. 1989. Government policies and deforestation in Brazil's Amazon region. Washington, D.C.: World Bank.

Malingreau, J.P. 1990. The contribution of remote sensing to the global monitoring of fires in tropical and subtropical ecosystems. In Fire in the Tropical Biota. Edited by J. G. Goldammer. Heidelberg: Springer-Verlag.

Malingreau, J.P. and C.J. Tucker. 1987. The contribution of AVHRR data for measuring and understanding global processes: large-scale deforestation in the Amazon basin. IGARSS '87 Symposium, Ann Arbor.

Malingreau, J.P. and C.J. Tucker. 1988. Large-scale deforestation in the southeastern Amazon basin of Brazil. Ambio 17 (1) : 49-55.

Malingreau, J.P. and C.J. Tucker, 1989. AVHRR for monitoring global tropical deforestation, Int. J. Remote Sensing, 10(4):855- 867.

Malingreau, J.P., C.J. Tucker, and N. Laporte. 1989. AVHRR for monitoring global tropical deforestation. International Journal of Remote Sensing 10 (4/5) : 621-626.

Marden dos Santos, J. 1987. Climate, natural vegetation, and soils in Amazonia: an overview. In, Dickinson, R.E. (ed.), The Geophysiology of Amazonia, Vegetation and Climate Interactions, John Wiley and Sons, New York.

Marland, G.R. and R. Rotty, 1984. Carbon dioxide emissions from fossil fuels: a procedure fro estimation and results for 1950- 1982, Tellus, 36B:232-261.

Marland, G., G.M. Rotty, and N.L. Treat, 1985, CO_2 from fossil fuel burnings global distribution of emissions, Tellus, 37B:243- 258.

Matson, P. A., P. M. Vitousek, and D. S. Schimel. 1989. Regional extrapolation of trace gas flux based on soils and ecosystems. In Exchange of Trace Gases between Terrestrial Ecosystems and the Atmosphere. Edited by M. O. Andreae and D. S. Schimel. 97-108. John Wiley and Sons Ltd.

Matthews, E., 1983. Global vegetation and land use: new high resolution data bases for climate studies. Journal of Climate and Applied Meteorology, 22(3):474-487.

Meentemeyer, V. 1978. Macroclimate and lignin control of decomposition. Ecology 63:621-626.

Melillo, J.M., J.D. Aber, and J.F. Mutore, 1982. Nitrogen and lignin control of hardwood leaf litter decomposition dynamics. Ecology, 63(3):621-626.

Melillo, J.M., C.A. Palm, R.A. Houghton, G.M. Woodwell, and N. Myeres, 1985. A comparison of two recent estimates of disturbance in tropical forests. Env. Conservation 12(1):37-40

Ministerio das Minas e Energia. No date. Projeto Radambrasil, Amazonia Legal, vegetation map of the Legal Amazon produced at 1:2,500,000 scale.

Moore, B., R.D. Boone, J.E. Hobbie, R.A. Houghton, J.M. Melillo, B.J. Peterson, G.R. Shaver, C.J. Vorosmarty and G.M. Woodwell. 1981. A simple model for analysis of the role of terrestrial ecosystems in the global carbon cycle, pp. 365-385. In: B. Bolin (ed.), SCOPE 16: Modelling the Global Carbon Budget. John Wiley and Sons, New York.

Moran, E.F., 1981. Developing the Amazon, Indiana University Press, Bloomington, 292 pp.

Moran, E.F. 1984. Colonization in the transamazon and Rondonia. In, M. Schmink and C.H. Wood (eds.), Frontier Expansion in Amazonia, University of Florida Press.

Mueller-Dombois, D. 1984. Classification and mapping of plant communities: a review with emphasis on tropical vegetation, In, Woodwell, G.M. (ed.) The Role of Terrestrial Vegetation in the Global Carbon Cycle: Measurement by Remote Sensing, SCOPE 23, John Wiley and Sons, Chichester.

Myers, N. 1980. Conservation of Tropical Moist Forests. National Research Council, Moran, E.F. 1981. Developing the Amazon. Bloomington: Indiana University U.P.

Myers, N. 1989. Deforestation Rates in Tropical Forests and Their Climatic Implications. Friends of the Earth, London.

Myers, N. 1991a. The world's forests and human populations: the environmental interconnections. In Population and Development Review. Edited by K. Davis and M. S. Berstam.

Myers, N. 1991b. Tropical forests: present status and future outlook. Climatic Change 19 : 3-32.

National Academy of Science, Washington, D.C.

Neftel, A., E. Moor, H. Oeschger. 1985. Evidence from polar ice cores for the increase in atmospheric CO_2 in the past two centuries. Nature 315:45-47.

Nelson, R., and B. Holben. 1986. Identifying deforestation in Brazil using multiresolution satellite data. International Journal of Remote Sensing 7 (3) : 429-448.

Nelson, R.F., D. Case, N. Horning, V. Anderson, and S. Pillai. 1987a. Continental land cover assessment using Landsat MSS data. Remote Sesning of Environment 21:61-81.

Nelson, R., N. Horning, and T.A. Stone. 1987b. Determining the rate of forest conversion in Mato Grosso, Brazil, using Landsat MSS and AVHRR data. International Journal of Remote Sensing 8 (12) : 1767-1784.

Olson, J.S., J.A. Watts, and L.J. Allison, 1983. Carbon in Live Vegetation of Major World Ecosystems, ORNL-5862, Oak Ridge National Laboratory, Oak Ridge, Tennessee, 164 pp.

Palm, C.A., R.A. Houghton, J.M. Melillo and D.L. Skole. 1986. Atmospheric carbon dioxide from deforestation in Southeast Asia. Biotropica 18:177-188.

Pereira da Cunha, R. 1989. Deforestation estimates through remote sensing: The state of the art in the Legal Amazonia. Pages 240-273, In, Amazonia: Facts, Problems, and Solutions. University of Sao Paulo, Sao Paulo, Brazil.

Peuquet, D.J., 1984. A conceptual framework and comparison of spatial data models. Cartographica 21(4):66-113.

Peuquet, D.J., 1988.Issues involved in selecting appropriate data models for global databases. In, H. Mounsey and R.F. Tomlinson (eds.) Building Databases for Global Science, Taylor and Francis, New York, 419 pp.

Pielke, R.A., G. Dalu, T.J. Lee, and T.G.F. Kittel. In press. Nonlinear influence of mesoscale landuse on weather and climate. J. Climate.

Pool, J.C., and S. Stamos. 1987. The ABC's of International Finance : Understanding the Trade and Debt Crisis. Lexington, MA: Lexington Books.

Post, W.M., T.-H. Peng, W.R. Emanuel, A.W. King, V.H. Dale, and D.L. DeAngelis. 1990. The global carbon cycle. American Scientist 78 : 310-326.

Reis, E.J., and S. Margulis. 1990. Economic perspectives on deforestation in Brazilian Amazon. Project Link Conference, Manilla, Phillipines.

Repetto, R. 1985. Population, resource pressures, and poverty. In The Global Possible: Resources, Development, and the New Century. Edited by R. Repetto. New Haven: Yale University Press.

Resende, E. 1973. As Rodovias e o Desenvolvimento do Brasil, Ministry of Transportation, Rio de Janeiro

Richards, J.F. 1984. Global patterns of land conversion. Environment 26 (9) : 6-38.

Richards, J.F., J.S. Olson, and R.M. Rotty. 1983. Development of a data base for carbon dioxide releases resulting from conversion of land to agricultural uses. ORAU/IEA-82-10(M), ORNL/TM-8801, Oak Ridge National Laboratories, Oak Ridge, Tennessee.

Rock, B.N., D.L. Skole, and B. Choudhury. 1992. Monitoring vegetation change using satellite data. In Vegetation Dynamics and Global Change. Edited by Shugart and Solomon. New York: Chapman and Hall.

Rudel, T.K. 1989. Population, development, and tropical deforestation: a cross national study. Rural Sociology 54 : 327-338.

Salati, E. 1987. The forest and the hydrological cycle. In The Geophysiology of Amazonia: Vegetation and Climate Interaction. Edited by R. E. Dickinson. 273-296. New York: Wiley - Interscience.

Salati, E. and P.B. Vose, 1984. Amazon basin: a system in equilibrium, Science 225:129-138.

Salati, E., and C.A. Nobre. 1991. Possible climatic impacts of tropical deforestation. Climatic Change 19 (1-2) : 177-196.

Santos, A. P. 1977. Uso de Dados do Landsat-1 na Implantacao, Controle e Acompanhamento de Projectos Agropecuarios no Sudoeste da Amazonia Legal. Sao Jose dos Campos: Instituto de Pesquisas Espaciais, INPE-1044TPT/065.

Santos, A.P. and E.M.L.M Novo. 1977. Uso de Dados do Landsat-1 na Implantacao, Controle e Acompanhamento de Projetos Agropecuarios no Sudoeste da Amazonia Legal. Instituto de Pesquisas Espaciais, INPE-1044-TPT/065, Sao Jose dos Campos, 183 pp.

Santos, A. P., G. V. Assuncao, and C. P. Santos Filho. 1979. Relatario das Altividades do Projecto IBDF/INPE (Subprojecto Desmatamento) Duranto o Ano de 1978. Sao Jose dos Campos: Instituto de Pesquisas Espaciais.

Sawyer, D.R. 1984. Frontier expansion and retraction in Brazil. In, M. Schmink and C.H. Wood (eds.), Frontier Expansion in Amazonia, University of Florida Press.

Seiler, W. 1984. Contribution of biological processes to the global budget of CH4 in the atmosphere, In, Klug, M.J. and C.A. Reddy (eds.) Current Perspectives in Microbial Ecology, American Society of Meteorology.

Seiler, W., and P.J. Crutzen. 1980. Estimates of gross and net fluxes of carbon between the biosphere and the atmosphere from biomass burning. Climatic Change 2:207-247.

Soule, M.E. 1991. Conservation: tactics for a constant crisis. Science 253:744-762.

Setzer, A.W. and M.C. Pereira. 1990. Amazon biomass burnings in 1987 and an estimate of their tropospheric emissions. Ambio 20(1):19-22.

Setzer, A.W., and M.C. Pereira. 1991. Amazonia biomass burnings in 1987 and an estimate of their tropospheric emissions. Ambio 20 (1) : 19-22.

Shukla, J., C. Nobre, and P. Sellers. 1990. Amazon deforestation and climate change. Science 247 : 1322-1325.

Siegenthaler, U. and H. Oeschger. 1987. Biospheric CO_2 emissions during the past 200 years reconstructed by deconvolution of ice core data. Tellus 39B:140-154.

Skole, D.L. in press. Data on global land cover change: acquisition, assessment, and analysis. In Global Land Use and Land Coevr Change. Edited by B. L. Turner. Boulder: UCAR/Office for Interdisciplinary Earth Studies.

Skole, D.L., B. Moore III, and W.H. Chomentowski, 1992. Global geographic information systems for vegetation change studies, In, A.M. Solomon (ed.), The Challenge of Modeling Global Biosphereic Change, International Institute for Applied Systems Analysis, Laxenburg, Austria (in press).

Skole, D.L., B. Moore, and W Chomentowski H. in press. Spatial analysis of land cover change and carbon flux associated with biomass burning in Brazil, 1970-1980. In Climate-Biosphere Interactions: Biogenic Emissions and Environmental Effects of Climate Change. Edited by R. Zepp. New York: John Wiley and Sons.

Skole, D.L., W.H. Chomentowski, and C.A. Nobre. submitted. Mapping deforestation in the Brazilian Amazon using a geographic information system. Ambio

Smith, N.J.H. 1981. Colonization lessons from a tropical forest, Science 214(4522):755-61

Smith, N.J.H. 1982. Rainforest Corridors: the Transamazon Colonization Scheme, University of California Press, Berkeley.

Smith, T.R., S. Menon, J.L. Star, and J.E. Estes, 1987. Requirements and principles for the implementation and construction of large-scale geographic information systems, International Journal of Geographical Information Systems, 1(1):13-32.

Soule. M.E. 1991. Conservation: tactics for a constant crisis. Science 253:744-750.

Stone, T., I.F. Brown, and G.M. Woodwell. 1991. Estimation, by remote sensing, of deforestation in central Rondonia, Brazil. Forest Ecology and Management 38 : 291-304.

Stone, T., and G.M. Woodwell. 1987. Analysis of forest and forest clearings in Amazonia with Landsat and shuttle imaging radar-A data. IGARRSS '87 symposium, Ann Arbor.

Stone, T.A., and P. Schlesinger. 1990. Monitoring deforestation in the tropics with NOAA AVHRR and Landsat data. International Symposium on Primary Data Acquisition, Manaus, Brazil.

Swift, M.J., O.W. Heal and J.M. Anderson. 1979. Decomposition in Terrestrial Ecosystems. Studies in Ecology Vol.5., University of California Press, Berkely.

Tans, P.P., I.Y. Fung, and T. Takahasi. 1990. Observational constraints of the global atmospheric CO_2 budget. Science 247 : 1431-1438.

Tardin, A.T., A.P. dos Santos, D.C. Lee, F.C.S. Maia, F.J. Mendoncza, G.V. Assunczio, J.E. Rodrigues, M. de Moura Abdon, R.A. Novacs, S.C. Chen, V. Duarte, and Y.E. Shimabukuro. 1979. Levantamento de areas do desmatamento na Amazonia Lefal atraves de imagens do satellite Landsat. Instituto Nacional de Pesquisas Espaciais. San Jose dos Campos, Brazil

Tardin, A.T., D.C.L. Lee, R.J.R. Santos, O.R. Ossis, M.P.S. Barbosa, M.L. Moreira, M.T. Pereira, D. Silva, and C.P. Santos Filho. 1980. Subprojecto Desmatamento. IBDF/CNPq -INPE, Instituto de Pesquisas Espaciais, Sao Jose dos Campos, Brasil.

Tardin, A.T., and R. Pereira da Cunha. 1990. Evaluation of deforestation in the Legal Amazon using Landsat-TM images. Sao Jose dos Campos, Brasil: Instituto de Pesquisas Espaciais.

Tarpley, J.D., S.R. Schneider, and R.L. Money. 1984. Global vegetation indices from NOAA-7 meteorological satellite. J. Climate appl. Met. 23:491.

Thornthwaite, C.W. 1948. An approach toward a rational classification of climate. Geographical Review, 38:55-94.

Townshend, J.R.G., and C.O. Justice. 1988. Selecting the spatial resolution of satellite sensors required for global monitoring of land transformations. International Journal of Remote Sensing 9 (2) : 187-236.

Townshend, J.R.G., and C.J. Tucker. 1984. Objective assessment of Advanced Very High Resolution Radiometer data for land cover mapping. International Journal of Remote Sensing 5 (2) : 497-504.

Townshend, J.R.G, C.O. Justice, V. Kalb. 1987. Characterization and classification of South American land cover types using satellite data, Int. Jour. Remote Sensing, 8:1189-1207.

Townshend, J., C. Justice, W. Li, C. Gurney, and J. McManus. 1990. Global land cover classification by remote sensing: present capabilities and future possibilities. Remote Sens. Environ. 35 : 243-255.

Tucker, R.P., and J.F. Richards. 1983. Global Deforestation and the Nineteenth Century World Economy. Durham: Duke U.P.

Tucker, C.J., B.N. Holben, and T.E. Goff. 1984. Intensive forest clearing in Rondonia, Brazil as detected by satellite remote sensing. Remote Sensing of the Environment 15 : 255-261.

Tucker, C.J., J.R.G. Townshend, and R.W. Goff. 1985. African land-cover classification using satellite data. Science 227 (4685) : 369-375.

Tucker, C.J., J.R.G. Townshend, T.E. Goff, and B.N. Holben. 1986. Continental and global scale remote sensing of land cover. In The Changing Carbon Cycle, a Global Analysis. Edited by J. R. Trabalka and D. E. Reichle. New York: Springer-Verlag.

Tucker, C.J., H.E. Dregne, and W.W. Newcomb 1991. Expansion and contraction of the Sahara desert from 1980 to 1990. Science 253: 299-301.

Turner, B.L., and W.B. Meyer. 1991. Land use and land cover in global environmental change: considerations for study. International Social Science Journal 43 (130) : 669-679.

Uhl, C. 1987. Factors controlling succession following slash-and-burn agriculture in Amazonia. Journal of Ecology 75 : 377-407.

Uhl, C. and R. Buschbacher. 1985. A disturbing synergism between cattle ranch burning practices and selective tree harvesting in the eastern Amazon. Biotropica 17:265-268.

Uhl, C., R.B. Buschbacher, and E.A.S. Serrao. 1988. Abandoned pastures in eastern Amazonia: I. patterns of plant succession. Journal of Ecology 76 : 663-681.

UNESCO 1973. International Classifcation and Mapping of Vegetation. UNESCO Ecology and Conservation Series 6, 93 pp.

Vitousek, P.M. 1982. Nutrient cycling and nutrient use efficiency. Am. Nat. 119:553-572.

Vitousek, P.M. and R.L. Sanford. 1986. Nutrient cycling in moist tropical forest, Annual Review of Ecology and Systematics 17:137- 167

Ward, D., A. Setzer, Y.J. Kaufman, R. Rasmussen, 1990. Characteristics of smoke emissions from biomass fires of the Amazon region - BASE-A Experiment, paper presented at the Chapman Conference on Global Biomass Burning: Atmospheric, Climatic and Biospheric Implications, March 19-23, 1990, Williamsburg, VA, USA.

Whittaker, R.H. 1978. Classification of Plant Communities, Junk Publishers, The Hague, 408 pp.

Whittaker, R.H. and G.E. Likens 1973. Carbon in the biota, In, Woodwell, G.M. and E.V. Pecan (eds.), Carbon and the Biosphere, U.S. Atomic Energy Commission, Washington, D.C.

Williams, M. 1989. Deforestation: past and present. Progress in Human Geography 13 : 176-208.

Williams, M., 1990a. Global deforestation. In, B.L. Turner (ed), The Earth Transformed by Human Action, Cambridge University Press.

Williams, M. 1990b. Forests. In The Earth as Transformed by Human Action. Edited by B. L. Turner, R. W. Clark, R. W. Kates, J. F. Richards, J. T. Mathews and W. B. Meyer. 179-201. Cambridge: Cambridge University Press.

Wilson, E.O. and F.M. Peter 1988. Biodiversity, National Academy Press, Washington, D.C.

Wilson, M.F. and A. Henderson-Sellers, 1985. A global archive of land cover and soils data for use in general circulation climate models. Journal of Climatology 5:119-143.

Wisniewski, J., and A.E. Lugo. 1992. Workshop Statement. Natural Sinks of CO2, Palmas del Mar, Puerto Rico.

Wood, C.H. and J. Wilson. 1984. The magnitude of migration to the Brazilian Frontier. In, M. Schmink and C.H. Wood (eds.), Frontier Expansion in Amazonia, University of Florida Press.

Woodwell, G.M., J.E. Hobbie, R.A. Houghton, J.M. Melillo, B.Moore, B.J. Peterson, G.R. Shaver, 1983. Global deforestation: contribution to atmospheric carbon dioxide, Science 222(4628):1081-1086

Woodwell, G.M., J.E. Hobbie, R.A. Houghton, J.M. Melillo, B. Moore, A.B. Park, B.J. Peterson, and J.R. Shaver. 1984. Measurement of changes in the vegetation of the earth by satellite imagery. In The Role of Terrestrial Vegetation in the Global Carbon Cycle: Measurement by Remote Sensing. Edited by G. M. Woodwell. New York: John Wiley and Sons.

Woodwell, G.M., R.A. Houghton, T.A. Stone, and A.B. Park. 1986. Changes in the area forests in Rondonia, Amazon Basin, measured by satellite imagery. In The Changing Carbon Cycle, A Global Analysis. Edited by J. R. Trabalka and D. E. Reichle. New York: Springer-Verlag.

Woodwell, G.M., R.A. Houghton, T.A. Stone, R.F. Nelson, and W. Kovalik. 1987. Deforestation in the tropics: New measurements in the Amazon Basin using Landsat and NOAA Advanced Very High Resolution Radiometer Imagery. Journal of Geophysical Research 92 : 2157-2163.

World Bank. 1982. Brazil:a Review of Agricultural Policies, a World Bank country study. World Bank, Washington, D.C.

World Bank. 1989. World Development Report. New York: Oxford U.P.

WRI. 1990. World Resources. A Guide to the Global Environment. Washington, D.C.: World Resources Institute.

APPENDIX 1

Total area deforested, the average annual deforestation rate (km^2 and $km^2\ yr^{-1}$), the percent change in deforested area, and the net flux of carbon (10^3 Mt yr^{-1}) for each municipio in the Brazilian Amazon.

	Total Cleared Area 1975	1978	Annual Rate	% Change	Net Flux
Maranhao					
GURUPI	312.700	938.938	208.746	200.3	4409
BAIAXADA OCIDENTAL MARANHENSE	92.660	531.570	146.30[illegible]	473.7	3091
SAO LUIS	124.680	196.082	23.801	57.3	504
BAIXADA ORIENTAL MARANHENSE	4.379	4.913	0.178	12.2	3
PINDARE	286.813	1028.042	247.076	258.4	5218
MEARIM	120.452	730.657	203.402	506.6	4308
ITAPECURU	68.093	279.186	70.364	310.0	1490
ALTO MUNIM	1.159	2.018	0.286	74.1	6
IMPERATRIZ	1629.131	6613.270	1661.380	305.9	34939
ALTO MEARIM E GRAJAU	93.848	378.214	94.789	303.0	1232
MEDIO MEARIM	160.626	316.429	51.934	97.0	1097
ALTO ITAPECURU	3.457	15.368	3.970	344.6	84
CHAPADAS DO SUL MARANHENSE	49.687	145.795	32.036	193.4	245
BIAXO BALSAS	0.0	10.375	3.458	0.0	22
PASTOS BONS	3.424	5.184	0.587	51.4	3
Goias					
EXTREMA NORTE GOIANO	2016.582	4070.635	684.684	101.9	13228
BAIXO ARAGUAIA GOIANO	1247.119	2284.431	345.771	83.2	2346
TOCANTINA DE PEDRO AFONSO	1.420	12.705	3.762	794.4	24
MEDIO TOCANTINS-ARAGUIA	371.062	2058.224	562.387	454.7	3558
SERRA GERAL DE GOIAS	156.489	436.246	93.252	178.8	653
ALTO TOCANTINS	142.492	371.874	76.460	161.0	495
Mato Grosso					
ARIPUANA	79.267	276.128	65.620	248.4	1389
ALTA FLORESTA	0.0	209.515	69.838		1479
RIO CLARO	571.032	1229.981	219.650	115.4	3846
PORTO DOS GAUCHOS	261.670	643.216	127.182	145.8	2692
DIAMANTINO	663.333	2164.550	500.406	226.3	5514

COLIDER	85.901	723.020	212.373	741.7	4498
SINOP	295.112	1440.935	381.941	388.3	7835
SANTA TEREZINHA	489.115	1152.660	221.182	135.7	3914
LUCIARA	377.316	1161.527	261.404	207.8	4823
SAO FELIX DO ARAGUIA	1317.989	2731.536	471.182	107.3	9680
NOBRES	115.369	513.672	132.768	345.2	1032
PARANATINGA	342.529	1064.129	240.533	210.7	2198
CANARANA	157.518	1410.370	417.617	795.4	2921
BARRA DO GARCAS	420.713	1590.759	390.015	278.1	2643
AGUA BOA	116.541	827.026	236.828	609.6	1544
NOVA XAVANTINA	56.245	628.241	190.665	1017.0	1243
CUIABA	28.735	778.314	249.860	2608.6	1629
NOVA BRASILANDIA	55.529	235.422	59.964	324.0	391
CHAPADA DOS GUIMARAES	74.862	347.930	91.023	364.8	593
ROSARIO OESTE	25.381	101.939	25.519	301.6	166
ACORIZAL	0.0	18.623	6.208		40
VARZEA GRANDE	0.0	95.329	31.776		207
NOSSA SENHORA DO LIVARAMENTO	0.0	17.872	5.957		40
SANTO ANTONIO DO LEVERGER	33.676	559.229	175.184	1560.6	1142
BARAO DE MELGACO	52.289	141.572	29.761	170.8	210
ITIQUIRA	18.783	916.467	299.228	4779.3	1951
PEDRA PRETA	87.353	364.114	92.254	316.8	601
POXOREO	6.221	496.956	163.579	7889.0	1066
DOM AQUINO	22.052	290.728	89.558	1218.4	584
JACIARA	11.413	261.748	83.445	2193.4	543
JUSCIMEIRA	2.768	127.774	41.669	4515.9	271
GENERAL CARNEIRO	0.0	247.154	82.385		537
TORIXOREU	5.047	122.733	39.229	2332.0	255
PONTE BRANCA	3.923	53.922	16.666	1274.6	108
ARAGUAINHA	0.0	20.445	6.815		44
ALTO ARAGUIA	101.011	487.652	128.880	382.8	840
TESOURO	0.0	64.978	21.659		141
GUIRATINGA	3.681	155.468	50.596	4123.7	330
ALTO GARCAS	97.566	523.327	141.920	436.4	925
RONDONOPOLIS	144.204	631.381	162.392	337.8	1054
POCONE	149.086	269.913	40.276	81.0	423
CACERES	290.848	680.466	129.873	134.0	887
PONTES E LACERDA	283.017	1008.379	241.787	256.3	1657
VILA BELA SANTISSIMA TRINDADE	566.892	1936.272	456.460	241.6	6193
ARENAPOLIS	375.257	1008.676	211.140	168.8	1461
NORTELANDIA	140.452	232.011	30.520	65.2	199
ALTO PARAGUAI	2.713	70.190	22.492	2487.0	146
BARRA DO BUGRES	1077.949	2090.917	337.656	94.0	3696
TANGARA DA SERRA	644.079	1013.308	123.077	57.3	1572
JAURU	214.294	691.204	158.970	222.5	1037
ARAPUTANGA	419.179	1004.468	195.096	139.6	1272
SALTO DO CEU	189.797	310.023	40.075	63.3	309
RIO BIANCO	416.096	581.798	55.234	39.8	361
MIRASOL D'OESTE	447.642	671.738	74.699	50.1	487
QUATRO MARCOS	397.552	733.439	111.962	84.5	722

Para

ORIXIMUNA	46.329	120.598	24.756	160.3	356
OBIDOS	38.188	136.238	32.683	256.8	683
ALENQUER	118.384	435.677	105.764	268.0	1405
MONTE ALEGRE	127.652	538.127	136.825	321.6	2780
ALMEIRIM	836.933	1377.627	180.232	64.6	3814
FARO	8.409	15.861	2.484	88.6	20
JURUTI	4.548	4.676	0.043	2.8	0
SANTAREM	1659.600	1907.925	82.775	15.0	1753
AVEIRO	57.882	145.263	29.127	151.0	616
ITAITUBA	25.925	275.573	83.216	963.0	1762
PRAINHA	201.894	879.610	225.906	335.7	4773
PORTO DE MOZ	5.739	56.800	17.020	889.6	358
FUROS	0.766	430.858	143.364	56134.1	3021
SENADOR JOSE PORFIRIO	5.552	126.544	40.331	2179.3	854
ALTAMIRA	89.102	475.277	128.725	433.4	2726
SAO FELIX DO XINGU	56.909	648.215	197.102	1039.0	4174
SANTANA DO ARAGUAIA	955.040	1653.981	232.980	73.2	4543
CONCEICAO DO ARAGUAIA	986.359	2973.444	662.362	201.5	12643
MARABA	369.061	1066.357	232.432	188.9	4923
SAO JOAO DO ARAGUAIA	610.141	1777.930	389.263	191.4	8219
ITUPIRANGA	18.194	301.845	94.550	1559.0	2002
BAGRE	1.022	121.435	40.138	11777.5	849
JACUNDA	7.566	250.696	81.043	3213.3	1710
TUCURUI	46.632	377.548	110.305	709.6	2336
SAO DOMINGOS DO CAPIM	1127.224	2782.879	551.885	146.9	11645
PARAGOMINAS	1937.324	4603.156	888.611	137.6	18802
VISEU	327.283	778.090	150.269	137.7	3181
OUREM	154.559	602.708	149.383	290.0	3164
CAPITAO POCO	358.799	764.786	135.329	113.2	2866
IRITUIA	501.376	744.389	81.005	48.5	1715
TOME-ACU	99.893	1270.008	390.038	1171.4	8236
ACARA	52.322	469.611	139.096	797.5	2946
BUJARU	42.215	105.669	21.151	150.3	448
MOJU	11.497	173.359	53.954	1407.8	1142
BAIAO	0.0	108.830	36.277		768
CAMETA	3.158	6.924	1.255	119.2	26
BELEM	46.415	304.746	86.110	556.6	1820
MOCAJUBA	1.133	2.517	0.461	122.0	9
IGARAPE-MIRI	7.489	77.793	23.435	938.8	496
ABAETETUBA	75.923	487.312	137.130	541.9	2901
BARCARENA	0.0	54.498	18.166		384
SALVATERRA	0.0	12.014	4.005		84
SOURE	0.0	41.997	13.999		296
SALGADO	37.972	286.987	83.005	655.8	1758
BRAGANTINA	306.170	994.479	229.437	224.8	4852

Rondonia					
PORTO VELHO	603.245	984.826	127.194	63.3	2689
ARIQUEMES	35.147	672.562	212.471	1813.5	4286
JI-PARANA	275.507	1980.887	568.460	619.0	12038
CACOAL	47.298	704.706	219.136	1389.9	4610
PIMENTA BUENO	90.162	644.415	184.751	614.7	3873
VILHENA	31.766	663.486	210.573	1988.7	4345
GUAJARA-MIRIM	454.324	701.335	82.337	54.4	1744
Roraima					
BOA VISTA	2.704	12.264	3.186	353.5	67
CARACARI	71.054	196.617	41.854	176.7	883
Amazonas					
SAO GABRIEL DA CACHOEIRA	5.015	9.081	1.355	81.1	28
SANTO ISABEL DO RIO NEGRO	10.933	68.592	19.220	527.4	407
JAPURA	7.502	9.862	0.787	31.5	16
SANTO ANTONIO DO ICA	9.407	14.259	1.617	51.6	34
SAO PAULO DE OLIVENCA	95.828	99.727	1.300	4.1	27
BENJAMIN CONSTANT	14.241	19.458	1.739	36.6	36
ATALAIA DO NORTE	0.0	4.501	1.500		31
IPIXUNA	142.117	157.900	5.261	11.1	111
EIRUNEPE	0.0	19.180	6.393		135
ENVIRA	21.711	62.887	13.725	189.6	290
JUTAI	9.785	17.094	2.436	74.7	51
FONTE BOA	25.574	30.393	1.606	18.8	34
JURUA	15.246	18.791	1.182	23.2	25
CARAURI	0.0	8.740	2.913		61
PAUINI	3.956	14.911	3.651	276.9	77
BOCA DO ACRE	13.717	99.296	28.526	623.9	604
MARAA	3.347	5.061	0.571	51.2	12
TAPAUA	0.0	2.278	0.759		16
LABREA	6.991	80.925	24.645	1057.5	522
BARCELOS	0.0	1.898	0.633		13
CODAJAS	11.623	13.821	0.732	18.9	15
ANDRI	1.083	4.513	1.143	316.5	24
MANACAPURU	6.368	29.386	7.673	361.5	162
CANUTAMA	0.088	14.440	4.784	16352.0	101
HUMAITA	2.913	21.520	6.202	638.8	131
MANICORE	55.382	76.837	7.152	38.7	151
BORBA	53.662	82.543	9.627	53.8	203
NOVA ARIPUANA	7.333	47.942	13.537	553.8	286
NOVO AIRAO	4.838	19.039	4.734	293.5	100
ITAPIRANGA	1.598	50.403	16.268	3053.7	339
URUCARA	11.362	12.359	0.332	8.8	7
NHAMUNDA	0.231	0.892	0.220	286.5	4
PARINTINS	12.204	30.922	6.239	153.4	132

BARREIRINHA	0.0	8.159	2.720		57
MAUES	13.203	34.678	7.159	162.7	151
NOVA OLINDA DO NORTE	5.522	24.621	6.366	345.9	134
AUTAZES	0.229	67.741	22.504	29480.2	476
CAREIRO	2.128	44.537	14.136	1993.0	299
ITACOATIARA	3.093	208.011	68.306	6624.5	1446
SILVES	36.020	127.350	30.443	253.6	644
MANAUS	298.504	674.939	125.478	126.1	2649
Amapa					
CALCOENE	5.385	10.330	1.648	91.8	34
NACAPA	177.792	198.437	6.881	11.6	145
NAZAGAO	0.0	22.307	7.436		157
Acre					
MANCIO LIMA	64.595	71.052	2.152	10.0	45
CRUZEIRO DO SUL	146.804	163.044	5.414	11.1	114
TARAUACA	35.038	154.788	39.917	341.8	845
FEIJO	34.468	99.508	21.680	188.7	459
MANDEL URBANO	3.911	28.741	8.277	634.8	175
SENA MADUREIRA	47.569	141.912	31.448	198.3	664
RIO BRANCO	464.812	964.465	166.551	107.5	3527
SENADOR GUIOMARD	81.490	201.487	39.999	147.3	847
PLACIDO DE CASTRO	14.698	63.212	16.171	330.1	342
XAPURI	148.244	387.768	79.841	161.6	1691
BRASILEIA	134.723	268.896	44.724	99.6	947
ASSIS BRASIL	3.277	5.030	0.585	53.5	12